

# **NANOPARTICULATE DRUG DELIVERY SYSTEM FOR TUBERCULOSIS**

A thesis submitted to Gujarat Technological University

for the Award of

**Doctor of Philosophy**

in

**PHARMACY**

BY

**Mr. Sujit Kumar Debnath**

[Enrolment No: 129990990008]



**GUJARAT TECHNOLOGICAL UNIVERSITY**

**AHMEDABAD**

**OCTOBER-2018**

# **NANOPARTICULATE DRUG DELIVERY SYSTEM FOR TUBERCULOSIS**

A thesis submitted to Gujarat Technological University

for the Award of

**Doctor of Philosophy**

in

**Pharmacy**

By

**Mr. Sujit Kumar Debnath**

[Enrolment No: 129990990008]

under supervision of

**Dr. S. Saisivam**



**GUJARAT TECHNOLOGICAL UNIVERSITY**

**AHMEDABAD**

**OCTOBER-2018**

**© Sujit Kumar Debnath**

# DECLARATION

I declare that the thesis entitled “**Nanoparticulate Drug Delivery System for Tuberculosis**” submitted by me for the degree of Doctor of Philosophy is the record of research work carried out by me during the period from 2012 to 2018 under the supervision of **Dr. S. Saisivam** and this has not formed the basis for the award of any degree, diploma, associateship, fellowship, titles in this or any other University or other institution of higher learning.

I further declare that the material obtained from other sources has been duly acknowledged in the thesis. I shall be solely responsible for any plagiarism or other irregularities, if noticed in the thesis.

Signature of the Research Scholar: ..... Date: .....

Name of Research Scholar: **Mr. Sujit Kumar Debnath**

Place: **Junagadh, Gujarat, India.**

# CERTIFICATE

I certify that the work incorporated in the thesis “**Nanoparticulate Drug Delivery System for Tuberculosis**” submitted by **Mr. Sujit Kumar Debnath** was carried out by the candidate under my supervision/guidance. To the best of my knowledge: (i) the candidate has not submitted the same research work to any other institution for any degree/diploma, Associateship, Fellowship or other similar titles (ii) the thesis submitted is a record of original research work done by the Research Scholar during the period of study under my supervision, and (iii) the thesis represents independent research work on the part of the Research Scholar.

Signature of Supervisor: ..... Date: .....

Name of Supervisor: **Dr. S. Saisivam**

Place: Junagadh, Gujarat, India

# Originality Report Certificate

It is certified that PhD Thesis titled “**Nanoparticulate Drug Delivery System for Tuberculosis**” by **Mr. Sujit Kumar Debnath** has been examined by us. We undertake the following:

- a. Thesis has significant new work / knowledge as compared already published or are under consideration to be published elsewhere. No sentence, equation, diagram, table, paragraph or section has been copied verbatim from previous work unless it is placed under quotation marks and duly referenced.
- b. The work presented is original and own work of the author (i.e. there is no plagiarism). No ideas, processes, results or words of others have been presented as Author own work.
- c. There is no fabrication of data or results which have been compiled / analysed.
- d. There is no falsification by manipulating research materials, equipment or processes, or changing or omitting data or results such that the research is not accurately represented in the research record.
- e. The thesis has been checked using “Turnitin” (copy of originality report attached) and found within limits as per GTU Plagiarism Policy and instructions issued from time to time (i.e. permitted similarity index  $\leq 25\%$ ).

Signature of the Research Scholar: ..... Date: .....

Name of Research Scholar: **Mr. Sujit Kumar Debnath**

Place: Junagadh, Gujarat, India

Signature of Supervisor: ..... Date: .....

Name of Supervisor: **Dr. S. Saisivam**

Place: Junagadh, Gujarat, India

---

ORIGINALITY REPORT

---

18%

SIMILARITY INDEX

8%

INTERNET SOURCES

14%

PUBLICATIONS

2%

STUDENT PAPERS

---

PRIMARY SOURCES

---

1	Sujit Kumar Debnath, Srinivasan Saisivam, Abdelwahab Omri. "PLGA Ethionamide Nanoparticles for Pulmonary Delivery: Development and in vivo evaluation of dry powder inhaler", Journal of Pharmaceutical and Biomedical Analysis, 2017 Publication	7%
2	<a href="http://www.ijddr.in">www.ijddr.in</a> Internet Source	3%
3	<a href="http://www.ncbi.nlm.nih.gov">www.ncbi.nlm.nih.gov</a> Internet Source	1%
4	Submitted to Gujarat Technological University Student Paper	1%
5	<a href="http://banglajol.info">banglajol.info</a> Internet Source	1%
6	<a href="http://www.archbronconeumol.org">www.archbronconeumol.org</a> Internet Source	1%
7	<a href="http://www.ipapharma.org">www.ipapharma.org</a> Internet Source	1%

---

8	S. Al-Qadi, A. Grenha, D. Carrión-Recio, B. Seijo, C. Remuñán-López. "Microencapsulated chitosan nanoparticles for pulmonary protein delivery: In vivo evaluation of insulin-loaded formulations", Journal of Controlled Release, 2012 Publication	1%
9	Pranab Jyoti Das, Paramita Paul, Biswajit Mukherjee, Bhaskar Mazumder et al. "Pulmonary Delivery of Voriconazole Loaded Nanoparticles Providing a Prolonged Drug Level in Lungs: A Promise for Treating Fungal Infection", Molecular Pharmaceutics, 2015 Publication	1%
10	<a href="http://services.aarc.org">services.aarc.org</a> Internet Source	1%
11	Sharma, Deepak Maheshwari, Dipika Philip. "Formulation and optimization of polymeric nanoparticles for intranasal delivery of lorazepam using B", BioMed Research International, Annual 2014 Issue Publication	1%
12	Submitted to University of West London Student Paper	1%

Exclude quotes On

Exclude matches < 1%

Exclude bibliography On



# **PhD Thesis Non-Exclusive License to**

## **GUJARAT TECHNOLOGICAL UNIVERSITY**

In consideration of being a PhD Research Scholar at GTU and in the interests of the facilitation of research at GTU and elsewhere, I, **Mr. Sujit Kumar Debnath** having Enrolment No. **129990990008** hereby grant a non-exclusive, royalty free and perpetual license to GTU on the following terms:

- a. GTU is permitted to archive, reproduce and distribute my thesis, in whole or in part, and/or my abstract, in whole or in part (referred to collectively as the “Work”) anywhere in the world, for non-commercial purposes, in all forms of media;
- b. GTU is permitted to authorize, sub-lease, sub-contract or procure any of the acts mentioned in paragraph (a);
- c. GTU is authorized to submit the Work at any National / International Library, under the authority of their “Thesis Non-Exclusive License”;
- d. The Universal Copyright Notice (©) shall appear on all copies made under the authority of this license;
- e. I undertake to submit my thesis, through my University, to any Library and Archives. Any abstract submitted with the thesis will be considered to form part of the thesis.
- f. I represent that my thesis is my original work, does not infringe any rights of others, including privacy rights, and that I have the right to make the grant conferred by this non-exclusive license.
- g. If third party copyrighted material was included in my thesis for which, under the terms of the Copyright Act, written permission from the copyright owners is required, I have obtained such permission from the copyright owners to do the acts mentioned in paragraph (a) above for the full term of copyright protection.

- h. I retain copyright ownership and moral rights in my thesis, and may deal with the copyright in my thesis, in any way consistent with rights granted by me to my University in this non-exclusive license.
- i. I further promise to inform any person to whom I may hereafter assign or license my copyright in my thesis of the rights granted by me to my University in this non-exclusive license.
- j. I am aware of and agree to accept the conditions and regulations of PhD including all policy matters related to authorship and plagiarism.

Signature of the Research Scholar:

Name of Research Scholar: **Mr. Sujit Kumar Debnath**

Date:..... Place: Junagadh, Gujarat, India

Signature of Supervisor:

Name of Supervisor: **Dr. S. Saisivam**

Date:..... Place: Junagadh, Gujarat, India

Seal:

# Thesis Approval Form

The viva-voce of the PhD Thesis submitted by **Mr. Sujit Kumar Debnath** (Enrolment No. 129990990008) entitled “**Nanoparticulate Drug Delivery System for Tuberculosis**” was conducted on .....(day and date) at Gujarat Technological University.

**(Please tick any one of the following option)**

☐ The performance of the candidate was satisfactory. We recommend that he/she be awarded the Ph D degree.

☐ Any further modifications in research work recommended by the panel after 3 months from the date of first viva-voce upon request of the Supervisor or request of Independent Research Scholar after which viva-voce can be re-conducted by the same panel again.

(briefly specify the modifications suggested by the panel)

☐ The performance of the candidate was unsatisfactory. We recommend that he/she should not be awarded the PhD degree.

(The panel must give justifications for rejecting the research work)

-----  
Name and Signature of Supervisor with Seal

-----  
1) (External Examiner 1) Name and Signature

-----  
2) (External Examiner 2) Name and Signature

-----  
3) (External Examiner 3) Name and Signature

## ABSTRACT

**Objective:** To formulate and characterize polymer loaded nanoparticles containing anti-tubercular drug and its administration as a dry powder inhaler that will reach lungs directly to give sustaining effect for the period of 24 hr.

**Method:** FTIR analysis was carried out to check the interaction between polymer, drug and inhalable grade lactose. Prothionamide nanoparticles were prepared by solvent evaporation method. Poly-lactic co-glycolic acid (75:25), a biodegradable polymer was used to coat Prothionamide. After some preliminary trials, 3<sup>3</sup> Box Behnken Design was employed to study the effect of three independent variables, i.e. drug-polymer ratio, concentration of surfactant, and organic phase volume, on three dependent variables like particle size, percentage drug entrapment (PDE), Polydispersibility index. Response surface curve and desirability factors helped in the selection of optimum formulation of PTH nanoparticles. Freeze dried nanoparticles and anhydrous inhalable grade lactose were mixed manually using geometrical dilution process to modify the nanoparticles in to dry powder inhaler and studied its mass median aerodynamic diameter (MMAD), stability and in-vitro release. One more formulation was prepared for Prothionamide with another biodegradable polymer named Chitosan. Chitosan/Tri polyphosphate nanoparticles containing Prothionamide were prepared by ionic gelation technique. Several process parameters like drug-polymer ratio, Chitosan-TPP ratio, TPP volume and stirring time were optimized. Chitosan nanoparticles containing PTH further modified to dry powder inhaler and studied the pharmacokinetic properties. Ethionamide loaded Poly lactic co-glycolic acid (50:50) nanoparticles were prepared by solvent evaporation method. Several process parameters were optimized to find suitable candidate for Dry powder inhaler. Dry powder inhaler further evaluated for mass median aerodynamic diameter, *in-vitro*, *in-vivo* and stability study.

**Result:** FTIR study revealed no interaction between the drug and other ingredients. Prothionamide loaded PLGA nanoparticles optimized through Box Behnken Design. Dependent parameters showed significant influence on the particles size and entrapment efficiency. Formulation was optimization with set criteria of maximum entrapment efficiency and minimum particle size, followed by higher desirability factor. Scanning electron microscopy (SEM) image showed spherical shape particle size of 205.6 nm.

43.52±0.81 % drug release was achieved in 24 hr using this DPI, but the concentration couldn't maintain above minimum inhibitory concentration (MIC) *in-vivo*. Hence, new formulation of PTH was prepared using Chitosan. Optimized Chitosan nanoparticles loaded with PTH showed more or less spherical in shape. DPI of Chitosan nanoparticles had MMAD of 1.76 µm with geometric standard deviation of 1.96. *In-vitro* release of DPI showed initial burst release of 22.04±1.94 % in 1 hr followed by 96.91±0.91 % up to 24 hr. As a result PTH concentration reached 4.56±0.31 µg/ml ( $C_{max}$ ) at  $T_{max}$  1 hr in lungs. AUC increased significantly when PTH was given in the form of nanoparticles. DPI of PTH nanoparticles maintained plasma concentration above the MIC for the period more than 12 hr, whereas pure PTH could maintain up to 3 hr. PTH nanoparticles reached the concentration of 0.39±0.06 µg/ml at 24 hr, which was lower than the MIC. Subsequently, Ethionamide nanoparticles were prepared by using PLGA (50:50). Optimized nanoparticles showed z-average value, zeta potential and PDI were 225.7 ± 6.4 nm, -6.9 ± 1.24 mV, and 0.216 ± 0.011 respectively. Percentage drug release-time profile of zero order kinetic showed highest correlation co-efficient ( $R^2$ ) of 0.992 in comparison of Higuchi, Peppas's models with  $R^2$  of 0.930 and 0.949 respectively. There was no significant changes occurred in the physical properties of nanoparticles during 6 month storage period. In the form of DPI, nanoparticles showed initial burst release of 9.23±1.15 % in first 1 hr and continued to release up to 95.17±3.59 % in 24 hr. This initial burst release helped to reach the ETH concentration to 2.64±0.07 µg/ml in lungs and ETH residency detected at 24 hr in lungs.

**Conclusion:** These results suggest that the DPI of optimized nanoparticles of Prothionamide and Ethionamide maintain the drug concentration above MIC for more than 12 hr. DPI administration daily basis may maintain drug concentration above MIC for 24 hr.

### **Keywords**

Tuberculosis; nanoparticles; Prothionamide; Ethionamide; PLGA; Chitosan; Dry powder inhaler.

# ACKNOWLEDGEMENT

*If you **WANT** to **SHINE** like a **SUN**. **FIRST** burn like a **SUN**.”*

- A.P.J Abdul Kalam

This is one quote of our former president of India, Dr. A. P. J. Abdel Kalam and inspires a lot to my life. Research is my dream and ultimate goal of life. To fulfil this dream, I started my journey as a Ph. D research scholar. The path never was smooth as day by day I faced new challenges to pursue this research activity. In this journey, I remember many people who helped me directly and indirectly to complete this task. With the blessing of god, I would like to acknowledge them who inspired me and play a vital role in my research work. Special thank also goes to GUJCOST for awarding MRP grant to boost my research activity.

Firstly, I would like to express my special appreciation and thanks to my esteemed guide Professor Dr. S. Saisivam, Principal N. R. Vekaria Institute of Pharmacy, Junagadh, Gujarat. You have been a tremendous mentor for me. I would like to thank you for your continuous encouragement in research and for allowing me to grow as a research scientist. Your advice on both research as well as on my career have been priceless. Fetching grant with your blessing is my utmost achievement in my life.

It was a great privilege to spend several years at N. R. Vekaria Institute of Pharmacy, Junagadh, Gujarat. I would like to bid special thanks to Mr. Nanjibhai Vekaria, Mr. Rameshbhai Vekaria (late) and Mr. Sureshbhai Vekaria, trusty of N. R. Vekaria Institute of Pharmacy, Junagadh, Gujarat for their liberty and permitting me to pursue research work at college and even at night time.

I am very much thankful and grateful to my doctoral progress committee members, Dr. Abhay Dharamsi, Professor and Dean, Faculty of Pharmacy, Parul University, Vadodara and Dr. Jolly Parikh Professor, Department of Pharmaceutics, A R College of Pharmacy, Vallabh Vidhyanagar for serving as my committee members even at hardship. I also want to thank you for letting my defence be an enjoyable moment, and for your brilliant comments and suggestions, thanks to you.

I am indebted to my colleague Dr. Lalji Baldaniya, Mr. Dillip Kumar Dash, Mr. Ashwin Agola, Mrs. Bina Aghera, Mr. Sunil Baile, and Mr. Sumit Chakraborty to support me during my research work. Their direct or indirect assists encourage me to pursue my work studiously.

My sincere gratitude to Dr. Abdel Omri, Professor, Laurentia University, Canada for showing his willingness to act as my international co-supervisor and providing his valuable insights, prompt, timely and helpful guidance throughout as well as for the unmatched support rendered at the time of publication of the articles.

I also thank to Dr. Rajesh K. S., Dr. Anil S. Solanki, Dr. R. D. Parmar, Dr. K. R. Patel, Dr. V. P. Patel, Dr. D. M. Patel, Dr. Anuj Garj and Dr. Sarika Sing who as examiners examined my research work during the research weeks and provided valuable ideas for betterment of my project.

In addition, I would like to give special thanks to Dr. Jayrajsinh sarvaiya, Assistant Professor, Gujarat Forensic Sciences University, Gandhinagar, Gujarat for his continuous and positive support in my research work.

I am grateful to Dr. Arkendu Chatterjee, Principal, Bengal College of Pharmaceutical Sciences and Research, Durgapur, West Bengal, for being extremely kind, ready to help nature and giving all necessary arrangement to conduct animal study.

I would like to convey my heartfelt thanks to all the staff members of N. R. Vekaria Institute of Pharmacy, Junagadh, Gujarat and Bengal College of Pharmaceutical Sciences and Research, Durgapur, West Bengal for their moral support and assistance at various stages of my research work.

I am immensely gratified to Evonik industries, Darmstadt, Germany for providing the gift sample of Resomer RG 755 S (PLGA 75:25) and RG 504 (PLGA 50:50), Kerry group, USA for providing inhalable grade Lactose anhydrous (INH 40 M 55.115), MIAT S. P. A. Milano, Italy for Mono-dose inhaler and nasal insufflators.

I am grateful to Dr. B. A. Gholakia (Professor and head), Dr. Umesh Kandalia (Associate Research Scientist), Dr. H. P. Gajera (Associate Professor), Dr. Yaymin K. Jadav (Research Associate) of Department of Biotechnology and nanotechnology, Junagadh,

Agriculture University for gifting some extra pure chemicals, expertise support for carrying out research with great success.

I am also thankful to Dr. V. J. Bhatiya (Professor and Head), Dr. J. B. Patel (Professor) of Main Oil Seed Research Station, Agriculture University, Junagadh, Gujarat for providing sophisticated infrastructure in the separation of nanoparticles.

I wish to express my sincere thanks to all publishers and referees who have published our research papers and also thankful to Gupta College of Technological Sciences, Asansol to make space for arranging oral presentation at the national seminar.

A special thanks to my family. Words cannot express how grateful I am to my mother, father, mother-in law, father-in-law (late), didibhai and jamaibabu for all of the sacrifices that you've made on my behalf. Your prayer was what sustained me thus far. I also thankful to my only son Smayan, as his smile face encourage me to work hard for his better future.

Last but not least, I would like to express appreciation to my beloved wife Mrs. Monalisha Debnath, Senior Research Fellow, Indian Institute of Technology, Kharagpur, West Bengal who spent sleepless nights with me during animal experiment and was always my support in each stage of my life.

Thanks for all your encouragement!

Sujit Kumar Debnath

Date:

Place: Junagadh, Gujarat, India



DEDICATED TO MY  
INSPIRING AND  
BELOVED FAMILY  
MEMBERS AND MY  
ESTEEMED GUIDE

# Table of Contents

Title Page .....	i
Declaration.....	iii
Certificate.....	iv
Originality Report Certificate .....	v
PhD Thesis Non-Exclusive License .....	viii
Thesis Approval Form .....	x
Abstract.....	xi
Acknowledgement .....	xiii
Table of Contents.....	xvii
List of Abbreviation.....	xxv
List of Symbols .....	xxviii
List of Figures .....	xxix
List of Tables .....	xxxix
List of Appendices .....	xxxiv

## **CHAPTER 1: Introduction .....1**

1.1. Definition of the problem .....	1
1.2. Aim of the research work.....	2
1.3. Objectives and scope of work .....	2
1.4. Rationale of the research work .....	3
1.4.1. Selection of disease .....	3
1.4.2. Selection of Anti-tubercular drug .....	3
1.4.3. Selection of dosage form.....	4
1.4.3.1. Nanoparticles .....	4
1.4.3.2. Biodegradable polymer.....	5
1.4.3.3. PLGA nanoparticles.....	5
1.4.3.4. Chitosan nanoparticles .....	6
1.4.4. Selection of route of administration.....	7
1.5. Hypothesis .....	7
1.6. Proposed plan of work .....	8
1.7. Outline of thesis .....	9

## **CHAPTER 2: Literature Review .....10**

2.1. Tuberculosis.....	10
------------------------	----

2.1.1. Types of tuberculosis .....	11
2.1.2. Symptoms.....	12
2.1.2.1. Symptoms of Pulmonary TB .....	13
2.1.2.2. Symptoms of Extra-pulmonary TB.....	13
2.1.2.3. Symptoms of lymph node TB .....	13
2.1.2.4. Symptoms of skeletal (bone and joint) TB .....	14
2.1.2.5. Symptoms of TB meningitis .....	14
2.1.2.6. Symptom of gastrointestinal, Kidneys or Abdominal TB .....	14
2.1.3. Diagnosis of tuberculosis .....	14
2.1.3.1. Active tuberculosis .....	14
2.1.3.2. Latent tuberculosis .....	15
2.1.4. Pathogenesis of tuberculosis .....	16
2.1.5. Life cycle of <i>Mycobacterium tuberculosis</i> .....	17
2.1.6. Current anti-tuberculosis drug therapy and its problem.....	17
2.1.7. Drug resistance.....	18
2.1.7.1. Types of drug resistance .....	18
2.1.7.2. Develop of drug resistance .....	19
2.1.7.3. Multi Drug-Resistant Tuberculosis (MDR-TB) .....	19
2.1.7.4. Extensively Drug-Resistant TB (XDR-TB).....	19
2.2. Anti-tubercular drug .....	19
2.2.1. Classification.....	20
2.2.2. Prothionamide Profile .....	21
2.2.2.1. Literature review on Prothionamide .....	23
2.2.2.2. Patent search on Prothionamide.....	24
2.2.3. Ethionamide Profile .....	26
2.2.3.1. Literature review on Ethionamide .....	28
2.3.3.2. Patent search on Ethionamide.....	29
2.3. Dosage form: nanoparticles .....	30
2.3.1. Advantages and disadvantages.....	32
2.3.2. Biodegradable polymer used in nanoparticles .....	32
2.3.2.1. Mechanism of degradation.....	32
2.3.2.2. Classification of biodegradable polymer .....	33
2.3.3. Residual solvent .....	43
2.3.3.1. Classification .....	43
2.3.3.2. Residual solvent analysis .....	45
2.4. Inhaled drug delivery system .....	45
2.4.1. Dry powder inhaler .....	46
2.4.2. Mean median aerodynamic diameter and its application.....	47
2.5. Pulmonary route of administration .....	51
2.5.1. Advantages and disadvantages.....	52
2.5.2. Drug deposition.....	52

2.5.3. Drug delivery devices .....	53
2.5.4. Structure of lungs .....	53
2.5.5. Factors affecting drug deposition in lungs .....	54
2.5.5.1. Particle Size and Shape.....	54
2.5.5.2. Airflow velocity .....	55
2.5.5.3. Airway geometry .....	55
2.5.5.4. Degree of humidity .....	55
2.5.5.5. Mechanisms for mucociliary clearance .....	55
<b>CHAPTER 3: Materials and Methods Pertaining to Prothionamide .....</b>	<b>58</b>
3.1. List of materials and equipments (Common for PTH & ETH formulation and estimation) .....	58
3.2. Excipients profile .....	60
3.2.1. Chitosan .....	60
3.2.2. Inhalable lactose anhydrous (INH 40 M 55.115).....	62
3.2.3. PLGA (75:25) .....	62
3.2.4. PLGA (50:50) .....	63
3.3. Identification of drug .....	64
3.3.1. Appearance.....	64
3.3.2. Melting point.....	65
3.3.3. Infrared absorption.....	65
3.3.4. UV spectrophotometric method .....	65
3.4. Analytical method.....	65
3.4.1. Estimation of Prothionamide using UV-Spectrophotometric method and its method validation.....	65
3.4.1.1. Preparation of pH 7.4 Phosphate buffer.....	65
3.4.1.2. Preparation of stock solution .....	66
3.4.1.3. Preparation of working standard solution for calibration curve .....	66
3.4.1.4. Method validation: Linearity .....	66
3.4.1.5. Limit of detection and limit of quantification.....	66
3.4.1.6. Analysis of tablet formulation .....	67
3.4.1.7. Accuracy .....	67
3.4.1.8. Precision.....	67
3.4.2. Preparation of standard curve of PTH in water-methanol system .....	68
3.4.2.1. Preparation of stock solution .....	68
3.4.2.2. Detection of maximum absorptivity .....	68
3.4.2.3. Construction of standard curve .....	68
3.4.3. Estimation of Prothionamide in rat plasma using HPLC method.....	69
3.4.3.1. Chromatography system and condition .....	69
3.4.3.2. Collection of plasma .....	69
3.4.3.3. Preparation of stock and diluted solution .....	69

3.4.3.4. Selection of detection wavelength .....	69
3.4.3.5. Construction of calibration plots.....	69
3.5. Formulation and characterization of DPI containing Prothionamide nanoparticles .....	70
3.5.1. Compatibility study .....	70
3.5.2. Preparation of PLGA-Prothionamide nanoparticles .....	70
3.5.2.1. Preparation of trial batch.....	70
3.5.2.1. Preparation of PLGA nanoparticles for Box-Behnken design.....	71
3.5.3. Experimental design.....	71
3.5.3.1. Determination of drug entrapment, drug load, process yield .....	73
3.5.3.2. Measurement of particle size, zeta potential and poly dispersibility index .....	73
3.5.3.3. Scanning electron microscopy (SEM) .....	73
3.5.3.4. Residual solvent analysis .....	74
3.5.3.5. Differential scanning calorimetry (DSC).....	74
3.5.4. Formulation of dry powder inhaler and characterization.....	74
3.5.4.1. Determination of MMAD using cascade impactor.....	75
3.5.4.2. <i>In-vitro</i> release study .....	75
3.5.4.3. Stability study .....	76
3.5.4.4. Design of DPI device and delivery dose calculation .....	76
3.5.5. <i>In-vivo</i> study.....	78
3.5.5.1. Animal .....	78
3.5.5.2. Anaesthetic dose and DPI administration.....	78
3.5.5.3. Dose calculation of Prothionamide for pulmonary delivery.....	78
3.5.5.4. Collection of sample and pharmacokinetic analysis.....	79
3.5.6. <i>In-vitro</i> anti tubercular activity .....	80
3.5.6.1. Preparation of 7H9 medium.....	80
3.5.6.2. Culture of <i>M. tuberculosis</i> in 7H9 medium .....	80
3.5.6.3. Culture of THP1 cell.....	80
3.5.6.4. Infection of THP1 cell .....	80
3.5.6.5. MTT assay .....	81
3.5.6.6. Drug and nanoparticles solution preparation .....	81
3.6. Formulation and characterization of DPI containing Prothionamide nanoparticles prepared by Chitosan .....	82
3.6.1. Compatibility study .....	82
3.6.2. Preparation of Prothionamide-Chitosan nanoparticles .....	82
3.6.3. Optimization and characterization of Prothionamide nanoparticles .....	82
3.6.3.1. Selection of strength-volume of acetic acid and TPP solution .....	83
3.6.3.2. Effect of stirring time.....	83
3.6.3.3. Effect of Chitosan and TPP ratio .....	83
3.6.3.4. Effect of PTH-Chitosan ratio.....	83
3.6.3.5. Effect of TPP solution volume.....	84
3.6.3.6. Scanning electron microscopy (SEM) .....	84
3.6.3.7. Differential scanning calorimetry (DSC).....	84

3.6.4. Formulation of dry powder inhaler and characterization.....	84
3.6.4.1. Determination of MMAD using cascade impactor.....	85
3.6.4.2. <i>In-vitro</i> release study .....	85
3.6.4.3. Stability study .....	85
3.6.4.4. Delivery dose calculation using modified device .....	86
3.6.5. <i>In-vivo</i> study.....	86
3.6.6. <i>In-vitro</i> anti-tubercular activity .....	87
3.6.7. Statistical analysis .....	87
<b>CHAPTER 4: Result and Discussion Pertaining to Prothionamide .....</b>	<b>88</b>
4.1. Identification of drug .....	88
4.2. Analytical methods .....	89
4.2.1. Estimation of Prothionamide using UV-Spectrophotometric method and its validation.....	89
4.2.1.1. Linearity.....	90
4.2.1.2. Limit of detection and limit of quantification.....	91
4.2.1.3. Analysis of tablet formulation .....	92
4.2.1.4. Accuracy .....	92
4.2.1.5. Precision.....	93
4.2.2. Preparation of standard curve for Prothionamide in water:methanol system .....	94
4.2.3. Estimation of Prothionamide in rat plasma using HPLC method.....	95
4.3. Formulation and characterization of DPI containing Prothionamide nanoparticles prepared by PLGA (75:25) .....	97
4.3.1. Compatibility study.....	97
4.3.2. Characterization of Prothionamide nanoparticles .....	98
4.3.2.1 Characterization of trial batch and optimization of sonication time.....	98
4.3.2.2. Characterization of Prothionamide nanoparticles prepared with Box Behnken design.....	98
4.3.3. Experimental design.....	100
4.3.3.1. Effect of independent variables on particle size .....	100
4.3.3.2. Effect of independent variables on entrapment efficiency .....	103
4.3.3.3. Effect of independent variables on polydispersiblity index .....	107
4.3.3.4. Search for Optimum nanoparticles of Prothionamide and its characterization.....	107
4.3.4. SEM analysis of system generated optimized nanoparticles .....	108
4.3.5. Residual solvent analysis .....	108
4.3.6. Differential scanning calorimetry (DSC).....	109
4.3.7. Formulation and characterization of dry powder inhaler.....	110
4.3.7.1. Determination of MMAD and geometric standard deviation.....	110
4.3.7.2. <i>In-vitro</i> release study .....	111
4.3.7.3. Stability study .....	113
4.3.8. Design of DPI and delivery dose calculation.....	113

4.3.9. <i>In-vivo</i> study.....	115
4.3.9.1. Dose calculation and its administration .....	115
4.3.9.2. Pharmacokinetic analysis.....	117
4.3.9.3. <i>In vitro- In vivo</i> correlation of DPI containing PP-DPI 2 .....	119
4.3. 10. <i>In-vitro</i> anti tubercular activity .....	120
4.4. Formulation and characterization of DPI containing Prothionamide nanoparticles prepared by Chitosan .....	121
4.4.1. Compatibility study .....	121
4.4.2. Characterization of Chitosan nanoparticles .....	122
4.4.2.1. Effect of stirring time.....	122
4.4.2.2. Effect of Chitosan-TPP ratio.....	123
4.4.2.3. Effect of PTH-Chitosan ratio .....	124
4.4.2.4. Optimization of TPP solution volume .....	125
4.4.2.5. Scanning electron microscopy (SEM) .....	125
4.4.2.6. Differential scanning calorimetry (DSC).....	126
4.4.3. Formulation and characterization of dry powder inhaler.....	126
4.4.3.1. Determination of MMAD and geometric standard deviation.....	127
4.4.3.2. <i>In-vitro</i> release study .....	128
4.4.3.3. Stability study .....	130
4.4.3.4. Delivery dose calculation using modified device .....	130
4.4.4. <i>In-vivo</i> study.....	131
4.4.4.1. Dose, DPI calculation and administration .....	131
4.4.4.2. Pharmacokinetic study .....	132
4.4.4.3. IVIVC of DPI containing PTH-Chitosan nanoparticles .....	134
4.4.5. <i>In-vitro</i> anti-tubercular activity .....	135
<b>CHAPTER 5: Method Pertaining to Ethionamide .....</b>	<b>136</b>
5.1. Identification of drugs.....	136
5.1.1. Appearance.....	136
5.1.2. Melting point.....	136
5.1.3. Chemical test.....	136
5.1.4. Infrared absorption .....	137
5.2. Analytical method.....	137
5.2.1. Estimation of Ethionamide using UV-Spectrophotometric method and its method validation.....	137
5.2.1.1. Preparation of stock solution .....	137
5.2.1.2. Determination of wavelength of maximum absorbance ( $\lambda_{\max}$ ).....	137
5.2.1.3. Linearity and range .....	137
5.2.1.4. Assay of Ethionamide in marketed tablet .....	138
5.2.1.5. Accuracy .....	138
5.2.1.6. Precision.....	138
5.2.2. Estimation of ETH in water-methanol system.....	138

5.2.2.1. Preparation of stock solution .....	139
5.2.2.2. Detection of maximum absorptivity .....	139
5.2.2.3. Construction of standard curve .....	139
5.2.3. Estimation of Ethionamide in rat plasma using HPLC method .....	139
5.2.3.1. Chromatography system and condition .....	139
5.2.3.2 Preparation of standard curve in rat plasma.....	139
5.3. Formulation and characterization of DPI containing Ethionamide nanoparticles prepared by PLGA (50:50) .....	140
5.3.1. Compatibility .....	140
5.3.2. Preparation of nanoparticles.....	140
5.3.3. Optimization and characterization of nanoparticles.....	141
5.3.3.1. Effect of ETH-PLGA ratio .....	141
5.3.3.2. Effect of surfactant concentration.....	141
5.3.3.3. Effect of organic phase composition .....	141
5.3.3.4. Scanning electron microscopy .....	141
5.3.3.5. Differential scanning calorimetry (DSC).....	142
5.3.3.6. Residual solvent analysis .....	142
5.3.4. Formulation of dry powder inhaler and its characterization .....	142
5.3.4.1. Determination of mass median aerodynamic diameter.....	142
5.3.4.2. <i>In-vitro</i> release study .....	143
5.3.4.3. Delivery dose calculation.....	143
5.3.4.4. Stability study .....	143
5.3.5. <i>In-vivo</i> study.....	143
5.3.6. <i>In vitro</i> anti-tubercular activity .....	144
5.3.7. Statistical analysis .....	144
<b>CHAPTER 6: Result and Discussion Pertaining to Ethionamide .....</b>	<b>145</b>
6.1. Identification of drug .....	145
6.2. Analytical methods .....	147
6.2.1. Estimation of Ethionamide using UV-Spectrophotscopy and its method validation.....	147
6.2.1.1. Determination of wavelength of maximum absorbance ( $\lambda_{\max}$ ).....	147
6.2.1.2. Linearity and range .....	147
6.2.1.3. Assay of Ethionamide in marketed tablet .....	149
6.2.1.4. Accuracy .....	150
6.2.1.5. Precision.....	150
6.2.2. Preparation of standard curve of ETH in water-methanol system .....	151
6.2.3. Estimation of Ethionamide in rat plasma using HPLC method .....	152
6.3. Formulation and Characterization of DPI containing Ethionamide nanoparticles prepared by PLGA (50:50) .....	153
6.3.1. Compatibility study.....	153
6.3.2. Optimization and characterization of ETH nanoparticles.....	154



6.3.2.1. Effect of ETH-PLGA ratio .....	155
6.3.2.2. Effect of surfactant concentration.....	155
6.3.2.3. Effect of organic phase composition .....	156
6.3.2.4. SEM analysis .....	156
6.3.2.5. Differential scanning calorimetry (DSC).....	157
6.3.2.6. Residual solvent analysis .....	158
6.3.3. Formulation and characterization of dry powder inhaler.....	159
6.3.3.1. Determination of MMAD and geometric standard deviation.....	160
6.3.3.2. <i>In-vitro</i> release study .....	161
6.3.3.3. Delivery dose calculation.....	162
6.3.3.4. Stability study .....	162
6.3.4. <i>In-vivo</i> study.....	163
6.3.4.1. Dose, DPI calculation and administration .....	163
6.3.4.2. Pharmacokinetic analysis.....	164
6.3.4.3. <i>In-vivo-in vitro</i> correlation of EP-DPI2 .....	167
6.3.5. <i>In-vitro</i> anti tubercular activity .....	168
<b>CHAPTER 7: Summary and Conclusion .....</b>	<b>169</b>
7.1. Summary of the work .....	169
7.1.1. With respect to PP-DPI 2 contained PTH-PLGA nanoparticles.....	169
7.1.2. With respect to PC-DPI 4 contained PTH-Chitosan nanoparticles.....	170
7.1.3. With respect to EP-DPI 2 contained ETH-PLGA (50:50) nanoparticles.....	171
7.2. Achievements with respect to the objectives .....	171
7.3. Major contribution and practical implications of the work to society.....	172
7.4. Recommendation for future research.....	172
7.5. Conclusion .....	173
<b>References.....</b>	<b>174</b>
<b>Bibliography .....</b>	<b>187</b>
<b>Appendix.....</b>	<b>197</b>
<b>List of Publications .....</b>	<b>200</b>

## List of Abbreviation

Sr. No	Abbreviation	Full form
1.	AIDS	Acquired Immunodeficiency Syndrome
2.	ANOVA	Analysis of variance
3.	API	Active Pharmaceutical Ingredients
4.	approx.	Approximately
5.	ATD	Anti-Tubercular Drug
6.	ATDS	Antitubercular drugs
7.	AUC	Area under curve
8.	BCS	Biopharmaceutical classification system
9.	BP	British Pharmacopoeia
10.	BSA	Bovine serum albumin
11.	CF	Cystic fibrosis
12.	CFU	Colony forming unit
13.	CLANI	Canadian List of Acceptable Non-medicinal Ingredients
14.	Cm	Centimetre
15.	CMC	Critical Micelle concentration
16.	Conc.	Concentration
17.	COPD	chronic obstructive pulmonary disease
18.	DNA	Deoxyribonucleic acid
19.	DCM	Dichloromethane
20.	DDA	Degree of deacetylation
21.	DILI	Drug Induce Liver Injury
22.	DPI	Dry Powder Inhaler
23.	DLW	Dry lung weight
24.	DOTS	Directly Observed Treatment Short Course
25.	DR	Drug Resistance
26.	DSC	Differential Scanning Calorimetry
27.	ETH	Ethionamide
28.	FDA	Food and drug administration
29.	FPF	fine particle fraction
30.	FTIR	Fourier transform infrared spectroscopy
31.	Gm	Gram
32.	GMP	Good manufacturing practice
33.	GRAS	Generally recognized as safe
34.	GSD	Geometric standard deviation
35.	HSGC	Headspace gas chromatography
36.	HPLC	High performance liquid chromatography
37.	Hr	Hour
38.	ICH	International conference on harmonization
39.	IFR	inspiratory flow rate
40.	IGRA	Interferon- $\gamma$ release assays
41.	INH	Isoniazide

Sr. No	Abbreviation	Full form
42.	IP	Indian Pharmacopoeia
43.	IPCS	International Program on Chemical Safety
44.	IUPAC	International Union of Pure and Applied Chemistry
45.	JP	Japan Pharmacopoeia
46.	KV	Kilovolt
47.	Lab	Laboratory
48.	LMW	Low molecular weight
49.	LOD	Limit of detection
50.	LOQ	Limit of quantification
51.	LTD	Limited
52.	<i>M. tuberculosis</i>	<i>Mycobacterium tuberculosis</i>
53.	MDI	metered-dose inhaler
54.	MDR	Multi Drug Resistance
55.	MIC	Minimum inhibitory concentration
56.	Min	Minutes
57.	ml	Millilitre
58.	MMAD	Mean Median Aerodynamic Diameter
59.	MRSA	Methicillin-resistant Staphylococcus aureus (MRSA)
60.	mV	Milli volt
61.	NM	Nanometer
62.	NP	Nanoparticle
63.	NPs	Nanoparticles
64.	PBS	Phosphate Buffer Solution
65.	PDE	Percentage drug entrapment
66.	PDI	Poly dispersibility index
67.	Mg	Milligram
68.	PGA	Poly glycolic acid
69.	PhEur	European Pharmacopoeia
70.	PIV	Pulmonary intravascular volume
71.	PLA	Poly lactic acid
72.	PLGA	Poly lactic co-glycolic acid or polylactide-coglycolide
73.	PPM	Parts per million
74.	PTH	Prothionamide
75.	PVA	Polyvinyl alcohol
76.	PVT	Private
77.	ODS	Octadecyl-silica
78.	OSHA	Occupational Safety and Health Administration
79.	RBC	Red blood cells
80.	RF	Repairable fraction
81.	RH	Relative humidity
82.	RNA	Ribonucleic acid
83.	RP	Reverse Phase

<b>Sr. No</b>	<b>Abbreviation</b>	<b>Full form</b>
84.	RPM	Revolution per minutes
85.	RSD	Relative standard deviation
86.	SD	Standard deviation
87.	SFD	spray freeze drying
88.	SEAR	South East Asia Region
89.	SLF	Simulated lungs fluid
90.	SPE	Solid phase extraction
91.	TB	Tuberculosis
92.	TCA	Trichloroacetic acid
93.	TDI	tolerable daily intake
94.	TFF	thin film freezing
95.	TM	Trade mark
96.	TPP	Sodium tripolyphosphate
97.	UK	United Kingdom
98.	USA	United State of America
99.	USP-NF	United State Pharmacopoeia National Formulary
100.	UV	Ultra violet
101.	VBC	viable bacterial count
102.	WST	Water-soluble tetrazolium
103.	WHO	World Health Organization
104.	XMDR	Extremely Drug Resistance
105.	ZP	zeta potential

## List of Symbols

Sr. No.	Symbol	Meaning
1.	%	Percentage
2.	$\pm$	Positive or negative
3.	$^{\circ}\text{C}$	Degree Celsius
4.	$\lambda_{\text{max}}$	Wave length of maximum absorption
5.	$\text{m}^2$	Square of length in meter
6.	$\mu\text{g}$	Microgram
7.	$\mu\text{m}$	Micrometer
8.	$\mu\text{l}$	Micro litre
9.	pH	Negative logarithm of hydrogen ion concentration
10.	l	Litre
11.	M	Mole
12.	n	No of sample
13.	®	Registered
14.	w/v	Weight by volume
15.	v/v	Volume by volume
16.	kg	Kilogram
17.	i.e.	It is
18.	$C_T$	Targeted drug concentration
19.	$V_L$	Lungs volume
20.	$K_E$	Elimination rate constant
21.	$T_D$	Duration of action
22.	$T_{\text{max}}$	Time required to reach maximum concentration
23.	$R^2$	Regression correlation coefficient
24.	P	Probability
25.	$\bar{x} \pm s$	Mean $\pm$ Standard deviation
26.	<	Less than
27.	i.d.	Internal diameter
28.	$\sim$	more or less
29.	$\approx$	Approximately
30.	w/o/w	water-in-oil-in-water
31.	$0-\infty$	Zero to infinitive

## List of Figures

Figure 2. 1: Symptoms and stages of tuberculosis.....	13
Figure 2. 2: M. Tuberculosis (stained red) in sputum.....	15
Figure 2. 3: Mantoux tuberculin skin test .....	15
Figure 2. 4: Spreading of tuberculosis from one person to another person through fine respiratory droplets .....	16
Figure 2. 5: Infection cycle of M. Tuberculosis .....	17
Figure 3. 1: Pulmonary administration for human: (A) Monodose nasal insufflators, (B) Monodose inhaler .....	77
Figure 3. 2: Penn-Century Dry Powder Insufflator™ Model DP-4.....	77
Figure 4. 1: FTIR of Pure Prothionamide .....	88
Figure 4. 2: Overlay UV spectra of PTH at different concentrations .....	90
Figure 4. 3: Calibration curve of PTH in pH 7.4 .....	91
Figure 4. 4: Standard curve of Prothionamide in Water-Methanol system .....	95
Figure 4. 5: Linear curve of Prothionamide using HPLC.....	96
Figure 4. 6: HPLC Chromatogram of PTH (5 µg/ml) and ETH (5 µg/ml) .....	96
Figure 4. 7: FTIR of pure Prothionamide and physical mixture of Prothionamide, PLGA(75:25) and inhalable grade lactose.....	97
Figure 4. 8: Effect of polymer amount and organic phase volume on particle size .....	102
Figure 4. 9: Effect of surfactant concentration and polymer amount on particles size .....	103
Figure 4. 10: Effect of Surfactant concentration and organic phase on particle size .....	103
Figure 4. 11: Effect of polymer amount and organic phase volume on percentage drug entrapment .....	105
Figure 4. 12: Effect of surfactant concentration and polymer amount on percentage drug entrapment .....	106
Figure 4. 13: Effect of organic phase volume and surfactant concentration on percentage drug entrapment .....	106
Figure 4. 14: SEM image of optimized freeze dried nanoparticles (OP) .....	108
Figure 4. 15: GC chromatograms of (a) pure DCM, (b) optimized PLGA-PTH nanoparticles (OP) .....	109
Figure 4. 16: DSC Thermogram of (a) Prothionamide, (b) PLGA (75:25) polymer, (c) Optimized PTH-PLGA nanoparticles (OP) .....	109

Figure 4. 17: Snapshot of calculated aerodynamic particle size determination.....	111
Figure 4. 18: Release profile of PP-DPI 2 in simulated lung fluid.....	113
Figure 4. 19: Modified design of dry powder inhaler delivery device .....	114
Figure 4. 20: Lung's tissue (A) & Plasma (B) distribution of PP-DPI2 and PL-DPI 4.....	118
Figure 4. 21: IVIVC of DPI containing PP-DPI 2 .....	119
Figure 4. 22: FTIR of pure PTH (a) and physical mixture of PTH, Chitosan, Inhalable grade lactose (b).....	121
Figure 4. 23: SEM image of Chitosan-PTH nanoparticles (OPB).....	125
Figure 4. 24: DSC thermogram of (a) PTH, (b) Chitosan polymer, (c) PTH-Chitosan nanoparticles (OPB).....	126
Figure 4. 25: Snapshot of aerodynamic determination from web site .....	128
Figure 4. 26: <i>In-vitro</i> dissolution profile of CP-DPI 4 .....	130
Figure 4. 27: Lungs (A) & Plasma (B) distribution of PC-DPI 4 & PL-DPI4 .....	134
Figure 4. 28: IVIVC of PC-DPI4.....	135
Figure 6. 1: FTIR of Pure Ethionamide .....	146
Figure 6. 2: Determination of $\lambda_{\max}$ for Ethionamide in pH 7.4.....	147
Figure 6. 3: Calibration curve of Ethionamide at pH 7.4. ....	148
Figure 6. 4: Standard curve of Ethionamide in water-methanol system.....	152
Figure 6. 5: Linear curve of Ethionamide using HPLC .....	153
Figure 6. 6: FTIR of pure ETH (a) and physical mixture of ETH, PLGA (50:50), Inhalable grade lactose (b).....	154
Figure 6. 7: SEM image of optimized freeze dried nanoparticles (EPS1) at 19.99KX.....	157
Figure 6. 8: DSC thermogram of pure ETH (a), PLGA (50:50) (b), optimized nanoparticles of ETH-PLGA (EPS1) (c).....	157
Figure 6. 9: GC chromatograms of (a) pure Acetone, (b) pure DCM and (c) optimized PLGA-ETH nanoparticles (EPS1) .....	159
Figure 6. 10: Snapshot of aerodynamic determination from web site .....	160
Figure 6. 11: Lungs (A) & plasma (B) distribution of EP-DPI2 & EL-DPI5.....	166
Figure 6. 12: IVIVC of EP-DPI2 .....	167

## List of Tables

Table 2. 1: Symptoms of TB.....	12
Table 2. 2: List of anti- tubercular drug with mechanism of action .....	20
Table 2. 3: Properties of Prothionamide .....	21
Table 2. 4: List of patents related to Prothionamide .....	25
Table 2. 5: Properties of Ethionamide .....	26
Table 2. 6: List of patents related to Ethionamide .....	30
Table 2. 7: List of biodegradable polymer based on origin .....	33
Table 2. 8: Chitosan-based drug delivery systems with drugs and method.....	35
Table 2. 9: Class 1 solvents in pharmaceutical products .....	43
Table 2. 10: Class 2 solvents in pharmaceutical products .....	44
Table 2. 11: Class 3 solvents in pharmaceutical products .....	45
Table 2. 12: Solvents for which no adequate toxicological data was found.....	45
Table 3. 1: List of materials used in this project.....	58
Table 3. 2: List of apparatus used in this project.....	59
Table 3. 3: List of equipments used in this project.....	59
Table 3. 4: Excipient's profile of Chitosan.....	61
Table 3. 5: Excipient's profile of inhalable lactose anhydrous.....	62
Table 3. 6: Excipient's profile of PLGA (75:25).....	63
Table 3. 7: Excipient's profile of PLGA.....	63
Table 3. 8: Adopted variables and their levels in Box-Behnken design.....	71
Table 3. 9: Box Behnken experimental design. ....	72
Table 3. 10: Composition of simulated lung fluid .....	76
Table 3. 11. Drug solution and nanoparticles solution preparation .....	81
Table 4. 1: Test for physical properties of Prothionamide .....	88
Table 4. 2: Major peaks observed and reported for Prothionamide in IR spectra .....	89
Table 4. 3. Absorbance of different concentration of PTH in pH 7.4 .....	90
Table 4. 4: Determination of limit of detection and limit of quantification .....	91
Table 4. 5: Assay of marketed product of Prothionamide .....	92
Table 4. 6: Data for accuracy .....	93
Table 4. 7: Intra-day & Inter-day precision for three different concentrations of PTH.....	93
Table 4. 8: Standard curve of PTH in water-methanol .....	94



Table 4. 9: Calibration data of PTH using HPLC .....	95
Table 4. 10: Comparison of FTIR date between pure PTH with physical mixture .....	97
Table 4. 11: Sonication time optimization.....	98
Table 4. 12: Box-Behnken experimental design.....	99
Table 4. 13: Physico-chemical evaluation parameters.....	99
Table 4. 14: Selection of model for conduction ANOVA analysis .....	100
Table 4. 15: ANOVA analysis of particles size.....	101
Table 4. 16: Analysis of variance .....	101
Table 4. 17: Selection of model for ANOVA analysis .....	104
Table 4. 18: ANOVA analysis for response surface.....	104
Table 4. 19: Characterization of optimized batch (OP).....	107
Table 4. 20: Optimization of dry powder inhaler .....	110
Table 4. 21: Drug deposition in different chamber of impactor from PP-DPI 2 .....	110
Table 4. 22: <i>In-vitro</i> release study data of optimized batch (PP-DPI 2) in simulated lung fluid.....	112
Table 4. 23: Stability study of PP-DPI 2 .....	113
Table 4. 24: Delivery dose calculation of modified DPI device.....	114
Table 4. 25: Dose administration of Optimized DPI (PP-DPI2) in rat .....	115
Table 4. 26: Dose administration of DPI containing pure PTH (PL-DPI 4) in rat .....	116
Table 4. 27: Lungs tissue and plasma distribution of PTH from DPI .....	117
Table 4. 28: Pharmacokinetic parameters of PTH in plasma and lungs .....	119
Table 4. 29: Comparison between <i>in-vitro</i> release and <i>in-vivo</i> diffusion.....	119
Table 4. 30: Absorbance and cell viability of Pure Prothionamide and Prothionamide-PLGA nanoparticles in MTT assay .....	120
Table 4. 31: Comparison of FTIR date between pure PTH with physical mixture .....	122
Table 4. 32: Effect of stirring time on Chitosan-PTH nanoparticles (1:1) .....	123
Table 4. 33: Effect of Chitosan & TPP ratio on nanoparticles .....	123
Table 4. 34: Effect of PTH:Chitosan ratio on nanoparticles.....	124
Table 4. 35: Effect of TPP solution volume contain 16 mg TPP .....	125
Table 4. 36: Optimization of dry powder inhaler .....	127
Table 4. 37: Amount of drug determination in different stage in cascade impactor .....	128
Table 4. 38: Release study of PTH from chitosan nanoparticles loaded DPI (PC-DPI 4) .....	129
Table 4. 39: Stability study of PC-DPI4 .....	130
Table 4. 40: Delivery dose of PC-DPI4 calculation of modified DPI device.....	131

Table 4. 41: Dose and equivalent DPI calculation.....	132
Table 4. 42: Lung's tissue and plasma distribution of PC-DPI4 and PL-DPI4 .....	132
Table 4. 43: Pharmacokinetic evaluation.....	133
Table 4. 44: Comparison between <i>in vitro</i> release and <i>in vivo</i> drug diffusion for PC-DPI4 .....	134
Table 4. 45: Absorbance and cell viability of pure Prothionamide and Prothionamide-Chitosan nanoparticles in MTT assay.....	135
Table 6. 1: Test for physical properties of Ethionamide.....	145
Table 6. 2: Major peaks observed and reported for Ethionamide in IR spectra .....	146
Table 6. 3: Absorbance of different concentration of ETH in pH 7.4 .....	148
Table 6. 4: Determination of limit of detection and limit of quantification .....	149
Table 6. 5: Assay of marketed tablet for Ethionamide .....	149
Table 6. 6: Recovery studies on marketed formulations .....	150
Table 6. 7: Intra-day & Inter-day precision for three different concentrations of ETH ...	150
Table 6. 8: Standard curve of ETH in water-methanol (9:1) .....	151
Table 6. 9: Calibration data of ETH using HPLC.....	152
Table 6. 10: Comparison of principle peaks between pure ETH with physical mixture...	154
Table 6. 11: Influence of ETH-PLGA ratio on nanoparticles.....	155
Table 6. 12: Effect of surfactant concentration on nanoparticles .....	156
Table 6. 13: Effect of DCM-acetone ratio on the nanoparticles .....	156
Table 6. 14: Flow property analysis of different composition of DPI.....	159
Table 6. 15: Deposition of drug in different chamber of cascade impactor for EP-DPI 2	160
Table 6. 16: <i>In-vitro</i> release profile of EP- DPI 2 .....	161
Table 6. 17: Delivery dose for EP- DPI 2.....	162
Table 6. 18: Stability study of DPI .....	162
Table 6. 19: Dose administration of EP-DPI2 in rat.....	163
Table 6. 20: Dose administration of EL-DPI5 containing pure ETH in rat.....	164
Table 6. 21: Lung's tissue and plasma distribution of ETH from DPI.....	165
Table 6. 22: Pharmacokinetic evaluation.....	165
Table 6. 23: IVIVC of DPI containing ETH-PLGA (50:50) nanoparticles.....	167
Table 6. 24: Absorbance and cell viability of Ethionamide in MTT assay .....	168

## **List of Appendices**

Appendix A: Certificate of approval from institutional animal ethical committee

Appendix B: Residual solvent analysis of PLGA-PTH nanoparticles (OP)

Appendix C: Residual solvent analysis of PLGA-ETH nanoparticles (EPS1)

# CHAPTER 1: Introduction

## 1.1. Definition of the problem

Tuberculosis (TB) continues to be a major worldwide epidemic with approximately one-third of the world population infected with *Mycobacterium tuberculosis* [1]. According to the World Health Organization (WHO) South-East Asia Region (SEAR) report, one fourth of the world population accounts for 38 % morbidity and 39 % mortality of the global burden of tuberculosis [2]. Along with increasing the incidence of drug resistance (DR), multi drug resistance (MDR) and extremely drug resistance (XMDR) in tuberculosis represents a continuous challenge to the clinician and researcher since tuberculosis first detected [3]. In the treatment of tuberculosis, first line Anti-tubercular drugs (ATD) are normally used for several months. These ATDs are distributed throughout the body; hence high doses are required for the drugs to be effective. These doses often result in unwanted side effects and development of drug resistance, multi drug resistance & extreme multi drug resistant tuberculosis. In that situation, second line anti tubercular drug is used. Prothionamide (PTH) and Ethionamide (ETH) are belong to this category, has good clinical efficacy against *Mycobacterium tuberculosis*, but poor tolerable because of considerable gastrointestinal adverse effect, such as nausea, vomiting, anorexia, a metallic taste and abdominal pain. These side effects prohibit this drug from being used as a first line therapy [4]. Prothionamide (PTH)/ Ethionamide (ETH) used to administer repeatedly due to its short half life of 2-3 hr [5]. Lungs are mainly affected by the *M. Tuberculosis* in pulmonary tuberculosis, whereas drug reaches to lungs is very less from oral conventional dosage form. As no new molecules have been developed in the recent decades, all these problems can be resolved by using a novel drug delivery approach with currently available drugs (PTH/ETH).

## 1.2. Aim of the research work

The aim of the present investigation is to design and optimize nanoparticles containing anti-tubercular drug in the form of dry powder inhaler that can reach to lungs through pulmonary route and give sustained effect for the period of 24 hr in the lungs, which is mainly affected by *Mycobacterium tuberculosis*.

## 1.3. Objectives and scope of work

The overall objectives of the research are summarized as

- To prepare and optimize nanoparticles using biodegradable polymers containing anti-tubercular drug that can sustain the drug release for the period of 24 hr.
- To make suitable for pulmonary administration, modify the optimized nanoparticles in the form of dry powder inhaler (DPI).
- To target the drug directly to lungs by administer the optimised DPI through pulmonary route.
- To avoid gastro intestinal side effect like excessive abdominal pain associated with anti-tubercular drug.
- To reduce drug induce liver injury (DILI), which generally occurred due to repeated high dose administration.
- To reduce systemic toxicity, by decreasing the concentration of drug in plasma.
- To estimate drug concentration in lungs and plasma after administering the optimized DPI through pulmonary route.

### Scope of the research work

Dry powder inhaler containing nanoparticles of ATD can be effective in the management of Pulmonary Tuberculosis, as it reach directly to lungs and give the local effect on the *M. tuberculosis*. Due to nanosize, its absorption will be more and DILI will be prevented by administered lesser dose. Dry powder inhaler of Prothionamide and Ethionamide planned for 24 hr, that prevent the miss dose, along with reduces the chance of drug resistance.

## 1.4. Rationale of the research work

### 1.4.1. Selection of disease

Tuberculosis (TB) becomes leading bacterial infection disease. Tuberculosis is a common and often deadly infectious disease caused by various strains of mycobacterium, usually *Mycobacterium tuberculosis*. It becomes deadly disease due to drug resistance, which generally developed in a couple of months, weeks, day or hours. This resistance mainly developed due to non availability of drug, discontinuation or patient noncompliance. Tuberculosis usually attacks the lungs but can also affect other parts of the body. It is spread through the air. This disease has been considered to be a disease of poverty for many years with quite rare occurrence in the developed countries. Recently more people in the developed world are contracting tuberculosis because their immune systems are compromised by immunosuppressive drugs, substance abuse, or AIDS [6]. Although potential pharmacotherapy being available for more than 50 years, but also the long term treatment and the pill burden can hamper patient lifestyle [7]. In recent history, however, poor compliance with the prolonged and complicated chemotherapeutic regimens currently used to treat the disease [1].

### 1.4.2. Selection of Anti-tubercular drug

Drugs such as Isoniazid (INH) and Rifampicin have historically been successful in the treatment of tuberculosis infections. Resistance to frontline therapeutics results in treatment of patients with “second-line” agents [1]. Thioamides, Prothionamide (PTH) and Ethionamide (ETH) are very potent bactericidal drugs. Due to poor water solubility and first pass metabolism [8], both the drugs shows low bioavailability, a lot of difficulties in the process of designing the pharmaceutical formulation and poor tolerability [9]. Poor tolerability because of considerable gastrointestinal adverse effects, such as nausea, vomiting, anorexia, a metallic taste and abdominal pain, prohibits these drugs from being used as a first-line therapy [4]. Due to these problems, both PTH and ETH often administered with meals to reduce gastrointestinal intolerance. Biological half life of PTH is 2 hr and ETH is 2.5 hr [5]. As a result, these drugs used to administer repeatedly 2 to 4 times a day to maintain drug concentration above minimum inhibitory concentration that increases gastrointestinal side effects. These drugs present in blood mainly in the unbound form [10], which leads to systemic toxicity.

### **1.4.3. Selection of dosage form**

#### **1.4.3.1. Nanoparticles**

Development of new drug molecules is expensive and time consuming. Hence, improving safety efficacy ratio of old drugs is achieved by individualizing drug therapy, dose titration, therapeutic drug monitoring and developing drug delivery system [11]. Over the past couple of decades, the field of drug delivery has been revolutionized with the advent of nanoparticles, wherein these particles act as inert carriers for drugs and genes to target cells or tissues. This has resulted in significant improvement in methods to induce drug accumulation in target tissues with subsequent reduction in non-specific effects, a major limitation encountered in conventional therapies for chronic conditions [12]. Patient noncompliance to current tuberculosis (TB) therapy owing to multidrug administration daily leads to treatment failure and emergence of multidrug resistant and extensively drug resistant TB. To avoid the frequent dosing, application of nanotechnology is the only viable solution by virtue of sustained release of drugs. Nanoparticulate drug delivery systems offer numerous advantages over conventional dosage forms, including improved efficacy, reduced toxicity and improved patient compliance. Nanoparticles can also be utilized in the form of carriers in drug delivery. Other potential advantages of the system include the possibility of selecting various routes of dosing, reduction in drug dosage/adverse effects/drug interactions, targeting drug resistant and latent bacteria etc [13]. The nanoparticulate formulations have been known to increase the oral bioavailability of drugs due to their specialized uptake mechanisms and because they bypass hepatic first-pass metabolism. Liposomes, microparticles, nanoparticles and solid lipid nanoparticles are very good carriers for the pulmonary system [14]. ATD loaded nanoparticles may improve the drug efficacy by keeping the drug concentration above minimum inhibitory concentration (MIC) for a longer period of time and enhance the bactericidal effect of drug [8]. Nanotechnology employs engineered materials or devices with the smallest functional organization on the nanometer scale (1–1000 nm) that are able to interact with biological systems at molecular level. Thus, they may stimulate, respond and interact with target cells and tissues in order to induce desired physiological responses while minimizing undesirable side effects [15]. Nanoparticles have unique physicochemical properties such as, ultra small size, large surface area to mass ratio and high reactivity which are different from bulk materials of the same composition. These

properties can be used to overcome some of the limitations found in traditional therapeutic and diagnostic agents [16]. The increased surface area offered by small particles makes these exceedingly effective for targeted drug delivery [17]. Materials on a nanometer scale have unique physicochemical properties that are due to their small size, surface area, chemical composition, surface structure, solubility, and shape; these properties have thus far been utilized in various fields including drug delivery. [18]

#### **1.4.3.2. Biodegradable polymer**

Polymers are one of the most omnipresent classes of materials in the medical industry and in our society. One such drawback is the persistence of the nanoparticles system in the body long after the therapeutic effect of the delivered drug has been realized. This has led to the development of biodegradable nanoparticles [12]. Micro and nanospheres fabricated from a biodegradable polymer for drug delivery systems have become increasingly important owing to the fact that such systems enable controlled drug release at desired sites [19]. Since they occur in nature, materials of both plant and animal origin are often presumed to exhibit enhanced compatibility with human hosts, the ability to exhibit bioactivity, and to undergo biodegradation. As such, natural nanomaterials and particulate materials can exhibit these characteristics in situations where synthetic materials have not met clinical expectations [20]. Worldwide many researchers are exploring the potential use of biodegradable polymeric as carriers for a wide range of therapeutic applications. Broadly, biodegradable polymers can be classified into natural or synthetic [21]. Biodegradable polymers release drugs by a combination of polymer degradation and drug diffusion [22].

#### **1.4.3.3. PLGA nanoparticles**

Poly (D, L-lactide-co-glycolide) (PLGA) is a copolymer of poly lactic acid (PLA) and poly glycolic acid (PGA). It is currently considered the best biomaterial available for drug delivery with respect to design and performance [21]. Among the different polymers developed to formulate polymeric nanoparticles, PLGA has attracted considerable attention due to its attractive properties: (i) protection of drug from degradation, (ii) possibility to modify surface properties to provide stealthness and/or better interaction with biological materials [23]. PLGA is a sustained release carrier and used in targeted drug delivery [24]. Its polymer chains undergoes bulk degradation and this degradation generally occurs at a



uniform rate throughout the PLGA matrix [25]. The lactide/glycolide polymers chains are cleaved by hydrolysis into natural metabolites (lactic and glycolic acids), which are eliminated from the body by the citric acid cycle [26]. PLGA nanoparticles able to entrap both water soluble and water-insoluble molecules. This polymer extensively used for the delivery of drugs, genetic materials and proteins to cultured cells and experimental animals. These nano-particulate systems are rapidly endocytosed by cells followed by release of their therapeutic payload by both passive diffusion and slow matrix degradation [12]. Given all these exquisite properties, it has been approved by Food and Drug Administration in USA and European Medical Agency for use in parenteral drug delivery systems [17]. PLGA is stable under the ultrasonic insonification than monomolecular layers of lipids or surfactants, and can act as ligand for targeted imaging and a drug carrier in targeted drug delivery system [27]. PLGA-based porous nanoparticles can be very helpful to optimize the therapeutic efficiency of medical treatments and to reduce serious side effects. The porous nanoparticles systems also exhibit much better flow and aerosolization efficiency during pulmonary administration when compared to nonporous nanoparticles [17].

#### **1.4.3.4. Chitosan nanoparticles**

Chitosan, a polycationic polymer comprised mainly of glucosamine units, is a N-deacetylated derivative of chitin [28]. Compared to other natural polymers, chitosan has positive charge [29]. This positive charge is very important in chitosan drug delivery systems as it plays a very important role in mucoadhesion (adhesion to the mucosal surface) [30]. It has emerged as a promising material with unmatched properties including biocompatible, biodegradable, non-toxic [31]. In the medical field, chitosan has been developed not only as artificial skin and a wound healing accelerator, but also as a new physiological material due to its antitumor, immune enhancing, and antimicrobial properties [32]. So far, Chitosan has been utilized in various fields of pharmaceutical technology, including the formulation of controlled release dosage forms, such as tablets, gels, microspheres and nanoparticles as mucoadhesive and/or permeation enhancing excipients for oral, nasal, ocular and buccal drug delivery and in non-viral gene delivery [33].

#### 1.4.4. Selection of route of administration

Tuberculosis usually attacks the lungs but can also affect other parts of the body. Bacteria named *Mycobacterium* enter into respiratory system as aerosol droplets. These bacteria non-specifically phagocytosed by alveolar macrophages that process the bacterial antigens and present them to lymphocytes. Then, the number of bacteria increase gradually by killing the host cell and spread all over the lungs [7]. Kanamycin, Amikacin, Capreomycin and different types of fluoroquinolones are available in injectable form and rest of other second line ATDs are available for oral administration. Injections are generally used for tuberculosis treatment, it is led to inconvenience to patients that need long term challenges [9]. Oral therapy using the currently employed anti-tubercular drugs (ATDs) is still being associated with a number of significant drawbacks. After oral administration, only a small fraction of the anti-tubercular drugs reach alveoli which are the desired site of drug action. The development of a tubercular vaccine has different array of challenges. More than 80% of TB cases are of pulmonary TB alone and high drug doses are required to be administered because only a small fraction of the total dose reaches the lungs after oral administration [34]. Even this small fraction is cleared rapidly due to short biological half life [14]. In contrast, pulmonary tuberculosis remains the commonest form of this disease and the development of methods for delivering ATDs directly to the lungs via the respiratory route is a rational therapeutic goal [14]. TB drug to the lungs include the possibility of reduced systemic toxicity, as well as achieving higher drug concentration at the main site of infection [35]. The increasing incidence of drug resistance in pulmonary tuberculosis represents a continuous challenge to the clinician and researcher [3]. So using nanoparticles by pulmonary delivery the above problem can be overcome. This route has numerous advantages like high solute permeability, large absorption surface area, limited proteolytic activity, and non-invasiveness. DPI particles which have a size ranged between 1  $\mu\text{m}$  and 5  $\mu\text{m}$  could be efficiently deposited in lung tissues [36]. Inhaled powders work locally in the lung as a common site of action; lower doses are needed to achieve the same therapeutic effect as the oral doses [37].

#### 1.5. Hypothesis

It was hypothesized that nanoparticles containing ATD in the form of dry powder inhaler would improve the management of tuberculosis because of

- Better absorption due to small size of particles.
- Reduced dose dependent toxicity like drug induces liver toxicity commonly associated with ATD.
- Reduced drug resistance by minimizing the frequent administration of drug.
- Increased drug availability at the targeted site of lungs, which is mainly affected by tuberculosis in a form of dry powder inhaler.
- Reduced the systemic toxicity by controlling the release of drug from polymeric nanoparticles.
- Persistence of drug at lungs for longer period of time.

### 1.6. Proposed plan of work

In the present investigation, an attempt was made to design and formulate nanoparticles of Prothionamide/ Ethionamide. These prepared nanoparticles further modified into dry powder inhaler to made suitable for pulmonary administration. These work categorized in the following heads

- Literature review
- Preformulation studies like Selection of polymer, drug, dosage form, method of preparation.
- Analytical method development for the estimation of selected drug of Prothionamide and Ethionamide.
- Formulation, optimization and characterization of Prothionamide nanoparticles using biodegradable polymer.
- In the similar way formulation, optimization and characterization of Ethionamide nanoparticles.
- Conversion of nanoparticles to dry powder inhaler for make suitable for pulmonary delivery.
- In-vitro study of the optimized dry powder inhaler in the simulated lungs fluids.
- In-vivo study of the optimized dry powder inhaler using rat.
- Stability studies as per ICH guideline.

## **1.7. Outline of thesis**

The thesis contain the research work has been divided into major seven chapters. The first chapter of introduction includes brief background, definition of the problem, aim, objectives, rationale, hypothesis, proposed plan of work. Chapter 2 presents literature review on various aspects related with the work including the description about disease, available therapies, challenges associated with them, approaches to overcome them, formulation, route of administration, targeted delivery to desired site and brief profile of the components used in the final formulation. Chapter 3 deals with the description of experimental work performed for the investigations including analytical method development, validation, formulation development, optimization and their evaluation related to Prothionamide. Chapter 4 includes results obtained with the experiments performed and detailed discussions related to Prothionamide. Different materials and similar method adopted for Ethionamide in its identification, formulation and characterization, are described in Chapter 5 and its result and discussion are mentioned in chapter 6. Chapter 7 finally presents the summary of the work and conclusion of the thesis.

## CHAPTER 2: Literature Review

### 2.1. Tuberculosis

Tuberculosis (TB) is a highly contagious persistent infection caused by *Mycobacterium tuberculosis* and *Mycobacterium bovis*. This disease has highest mortality rate than any other infectious disease. *Mycobacterium tuberculosis* is an acid-fast bacillus and intracellular pathogen, which has developed numerous strategies to avoid being killed by macrophages [38]. Robert Koch in 1882 was awarded “Nobel Prize” for this remarkable discovery. In 1993, World Health Organization (WHO) declared tuberculosis as global emergency. It is a major infectious burden worldwide and statistical estimated continue to worsen with each passing year. Worldwide, one-third of the population is infected due to this disease and of these, 8 to 10 million develop active disease, along with 2 million die each year. As a result, it serve as world’s second most common cause of death after HIV/AIDS [39]. Although TB treatments exist for couple of decades, but poor patient compliance and drug resistance pose a great challenge to treat this disease worldwide. Hence, a polymeric nano-drug delivery system for anti-TB drugs was developed that could enable entry, targeting, sustained release for longer periods and engulf of the antibiotics in the cells, hence reducing the dose frequency and simultaneously improving patient compliance [40]. The treatment schedule poses several problems that can result in therapeutic failure as mentioned below

- Daily administration of multiple anti-tubercular drugs (ATD) is frequently associated with patient non-compliance.
- Frontline ATDs are hepatotoxic and at least in some patient they fail to eradicate persistent bacilli.

- Directly Observed Treatment, Short course (DOTS) programme has not been completely successful till dated in solving the problem of patient non-compliance.
- Most of the patients fail or not able to adhere to multidrug therapy daily for such a longer period.

Bacillus Calmette Guerin (BCG) is currently available as vaccines for TB. This vaccines suffers from several demerits such as variable efficacy in different populations, limited success against pulmonary TB that accounts for most of the disease burden and short term immunity [41]. Mycobacterium more frequently attacks the lungs. Along with, it can attack any part of the body, like the kidney, lymphatic system, central nervous system (meningitis), circulatory system (military tuberculosis), genitourinary system, joints, and bones [38].

The success and failure rate to treat tuberculosis depends on various factors like

- (a) Patient compliance to the treatment taken,
- (b) Malnutrition,
- (c) Smoking,
- (d) Coexisting diseases like HIV,
- (e) Inadequate supervision by health care staffs.

### 2.1.1. Types of tuberculosis

Tuberculosis (TB) can be classified in different way. Based on the activity of bacteria, two main types are active and latent tuberculosis. In active TB, the disease shows symptoms and can be transmitted to other people. Whereas, latent disease is another type where the person is infected with *Mycobacterium tuberculosis*, but the bacteria are not able to produce symptoms due to the body's immune system suppressing the bacterial growth and spread. In the stage of latent TB, people cannot transfer *Mycobacterium tuberculosis* to others unless the immune system fails. The failure causes reactivation of bacterial growth that trans into active TB so the person becomes contagious.

Tuberculosis also can be classified based on sit of action. Tuberculosis may infect any part of the body. In active state, tuberculosis most commonly involves the lungs known as

pulmonary tuberculosis. It is also known as disseminated or miliary TB, refers to all the different types of TB other than pulmonary TB. Generally it is the types of TB that do not affect the lungs. In 15–20 % of active cases, the infection spreads outside the lungs, causing other kinds of TB. These are collectively denoted as "extra-pulmonary tuberculosis". Extra-pulmonary TB occurs frequently in persons with immunosuppressed problem and children. 50% cases occurred with the patient having HIV. The extra-pulmonary infection sites include the pleura (tuberculous pleurisy), the central nervous system (tuberculous meningitis), the lymphatic system (scrofula of the neck), the genitourinary system (urogenital tuberculosis), and the bones and joints (Pott disease of the spine), among others. Spread to lymph nodes is the most common. After few times, an ulcer may occur nearby the infected lymph nodes. This is painless, slowly enlarging and has an appearance of "wash leather"[42]. Gradually it spreads to the bones, which is known as "osseous tuberculosis", a form of Osteomyelitis. Disseminated tuberculosis is another form, where 90 % of cases are more serious in widespread. This active form is known as miliary tuberculosis. Miliary TB currently covers about 10 % of extra-pulmonary cases. Extra-pulmonary TB may coexist with pulmonary TB.

### 2.1.2. Symptoms

Latent TB is usually asymptomatic in primary infection but in few cases it shows non-specific symptoms. In reactivation, the symptoms may include cough that produced mucopurulent sputum, occasional hemoptysis and chest pain [7]. The symptoms of TB vary (Table 2.1) based on the type of TB: that is part of the body has been infected. It is very difficult to diagnose TB just from the symptoms, as these symptoms can often be the symptoms of another disease. So to diagnose TB it is always necessary to do at least one TB test. Coughing up blood can be a symptom of TB [43].

**Table 2. 1: Symptoms of TB**

Latent TB	Active TB
anorexia, fatigue, weakness, weight loss and low-grade fever	weakness or feeling very tired, losing weight without trying, lack of appetite, chills, fever (a high temperature of 38°C or above) and night sweats

### 2.1.2.1. Symptoms of Pulmonary TB

The specific symptom of pulmonary TB is bad cough that persist more than three weeks. Pain in the chest and coughing up blood or phlegm from deep inside the lungs are some other symptoms of this TB.

### 2.1.2.2. Symptoms of Extra-pulmonary TB

The general symptoms of extrapulmonary TB are the same as for pulmonary TB. There are some specific symptoms relating to the particular site or sites in the body that are infected, which are depicted as below (Figure 2.1)[44].

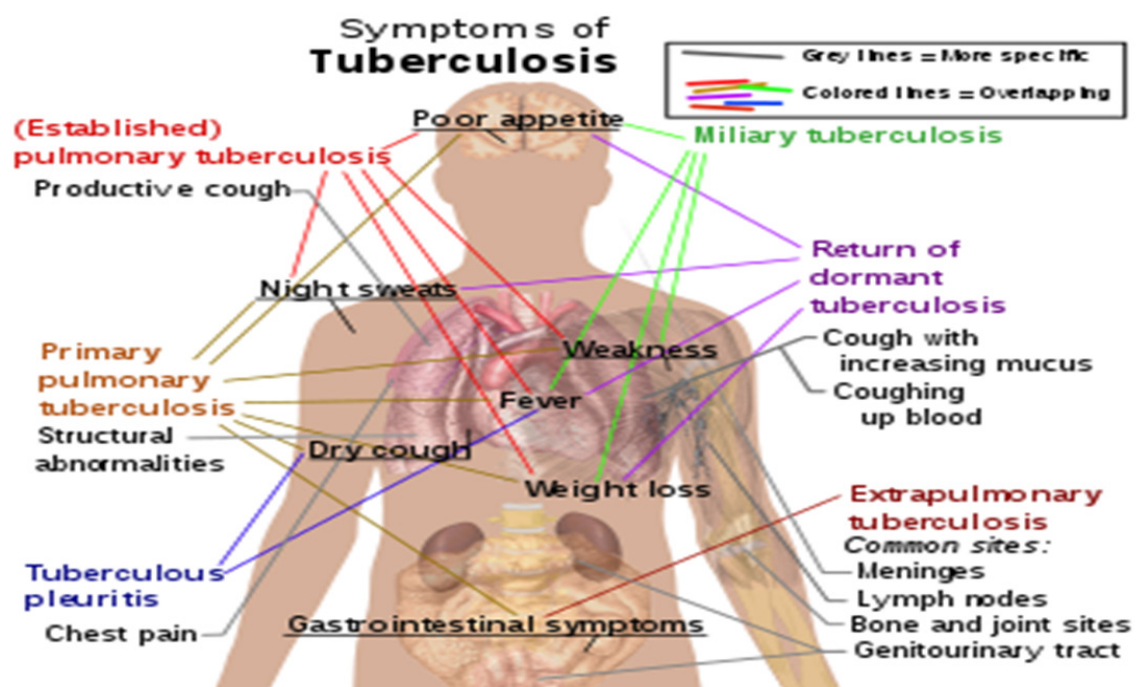


**Figure 2. 1: Symptoms and stages of tuberculosis**

### 2.1.2.3. Symptoms of lymph node TB

The only symptoms of TB lymphadenitis may be painless and slowly enlarging lymph nodes. In many time, general TB symptoms are not observed in this type. In the neck area, this type of TB is occurs. This type of TB frequently named as Scrofula or TB adenitis. It a can also develop in the groin area [43].



#### **2.1.2.4. Symptoms of skeletal (bone and joint) TB**

The most common and preliminary symptom of bone TB is pain, but its savouriness depends on the extent of infection. Curving of bone or joint, and loss of movement are the general symptom of this TB. This infected bone gradually weakened and may fracture easily. Spinal TB/ TB Spondylitis or Pott Disease is the example of this type. Due to this disease, back pain is occurred, which is known as the common symptom of this disease[43].

#### **2.1.2.5. Symptoms of TB meningitis**

There is significant difference between the symptoms of TB meningitis and classic meningitis. Initially, the symptom starts with vague, results in aches and pains. This symptoms further progress to fever and discomfort. It persists for 2 to 8 weeks. Afterward, it shows the more advance symptoms like vomiting, severe headache, a dislike of lights, neck stiffness and seizures occur [43].

#### **2.1.2.6. Symptom of gastrointestinal, Kidneys or Abdominal TB**

Abdominal pain, diarrhoea, and bleeding from the anus or rectum are the symptoms of abdominal TB. TB in the kidneys can cause blood in your urine [43].

### **2.1.3. Diagnosis of tuberculosis**

#### **2.1.3.1. Active tuberculosis**

Sometimes, diagnosing of active tuberculosis is difficult on the basis of signs and symptoms of disease. Diagnosis of TB is needed if lung disease or associated symptoms lasting longer for more than two weeks. Chest X-ray and multiple sputum cultures for acid-fast bacilli are used for the initial evaluation. Interferon- $\gamma$  release assays (IGRA) and tuberculin skin tests are also used for the same purpose. Accurate diagnosis of TB is carried out by identifying *M. tuberculosis* in a clinical sample (Figure 2. 2) (e.g., sputum, pus, or a tissue biopsy). But, the main demerit of this test is due to slow-growing organism that can take time to grow 2-6 weeks for blood or sputum culture. Nucleic acid amplification tests and adenosine deaminase testing are used for rapid diagnosis of TB. Blood tests to detect antibodies are not specific or sensitive test to detect TB, hence they are not recommended [44].

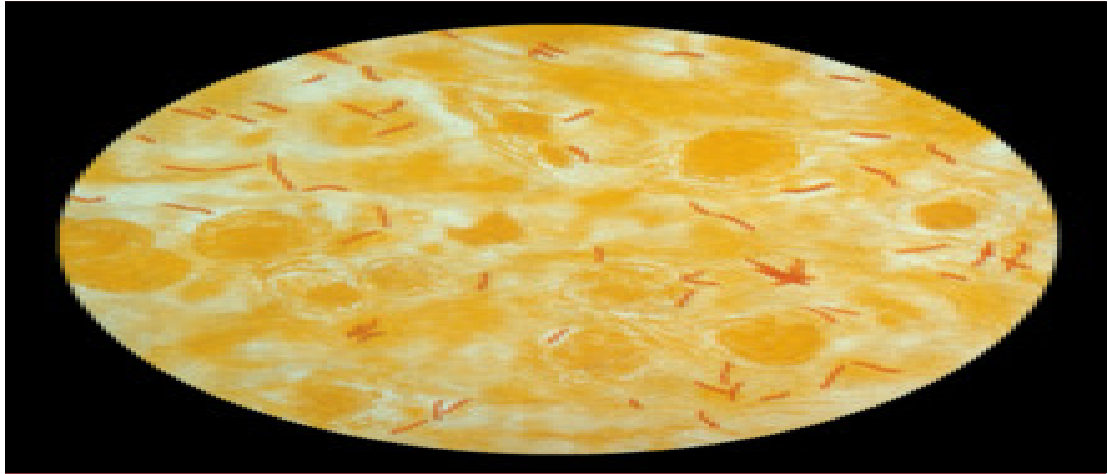


**Figure 2. 2: M. Tuberculosis (stained red) in sputum**

### **2.1.3.2. Latent tuberculosis**

The Mantoux tuberculin skin test is frequently used for screening people having high risk of tuberculosis. But, those who have been immunized previously may show false-positive test result. The test may be falsely negative in those with sarcoidosis, Hodgkin's lymphoma, malnutrition, and most notably, active tuberculosis. IGRA test for blood sample are recommended in those who are positive to the Mantoux test. These are not affected by immunization or environmental mycobacteria, so they generate fewer false-positive results. However, they are affected by *M. szulgai*, *M. marinum*, and *M. kansasii*. IGRA is less sensitive than the skin test when used alone. It may increase sensitivity when used in addition to the skin test (Figure 2. 3) [44].



**Figure 2. 3: Mantoux tuberculin skin test**

#### 2.1.4. Pathogenesis of tuberculosis

The infectious bacilli are inhaled as droplets from the atmosphere; hence tuberculosis is an airborne disease. The bacteria are phagocytised by the alveolar macro-phage of the lungs. In the interaction of mycobacterium components with macrophage receptors, chemokines and cytokines are formed, which serve as infection signals. These signals result in migration of monocyte derived macrophages and dendritic cells from the blood stream to the site of infection in the lung. The dendritic cells that engulf bacteria then mature and migrate to the lymph nodes. Once there, CD4 and CD8 T cells are primed against mycobacterial antigens. Primed T cells expand and migrate back to the focus of infection in the lungs, probably in response to mediators produced by infected cells. This phenomenon of cell migration towards the infection focus culminates in the formation of a granuloma, the hallmark of TB. The granuloma is formed by T cells, macrophages, B cells, dendritic cells, endothelial and epithelial cells, among others in a proportion that varies with its age. This granuloma prevents the spreading of bacilli resident within macrophages and generates an immune. Micro-environment which facilitates the interaction between cytokines secreted by macrophages and T cells. However, the granuloma also provides housing for *M. Tuberculosis* during a long period of time. The latent bacilli can be later released if the cytokine balance is broken, triggering disease reactivation [45].

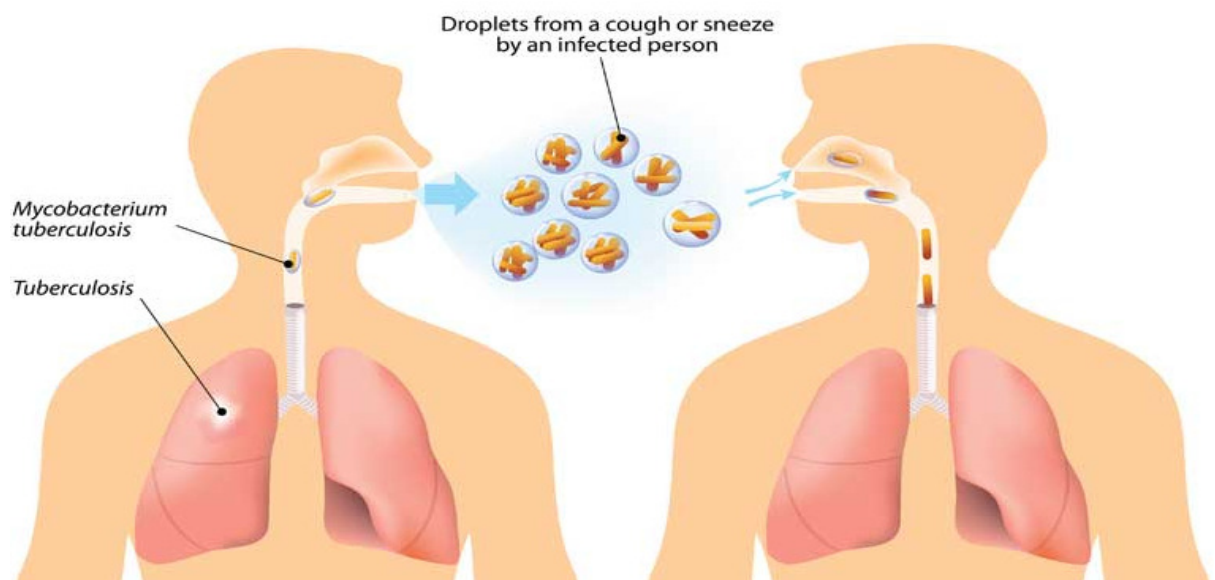


**Figure 2. 4: Spreading of tuberculosis from one person to another person through fine respiratory droplets**

### 2.1.5. Life cycle of *Mycobacterium tuberculosis*

As describe previously, tuberculosis occurs due to inhalation of air bone bacilli of *M. tuberculosis* and a single bacterium may be enough to initiate an infection (Figure-2.5). Firstly, *M. Tuberculosis* reaches the alveolar space of the human lung, and then this bacterium is phagocytised by alveolar macrophages. Afterward this bacterium helps in invasion of the epithelial layer in the human lung. Macrophages are not able to kill the bacterium but, they can push it into lymph nodes with the help of dendritic cells. As a result, an inflammatory response is started and mononuclear cells are recruited to the site of infections [46].

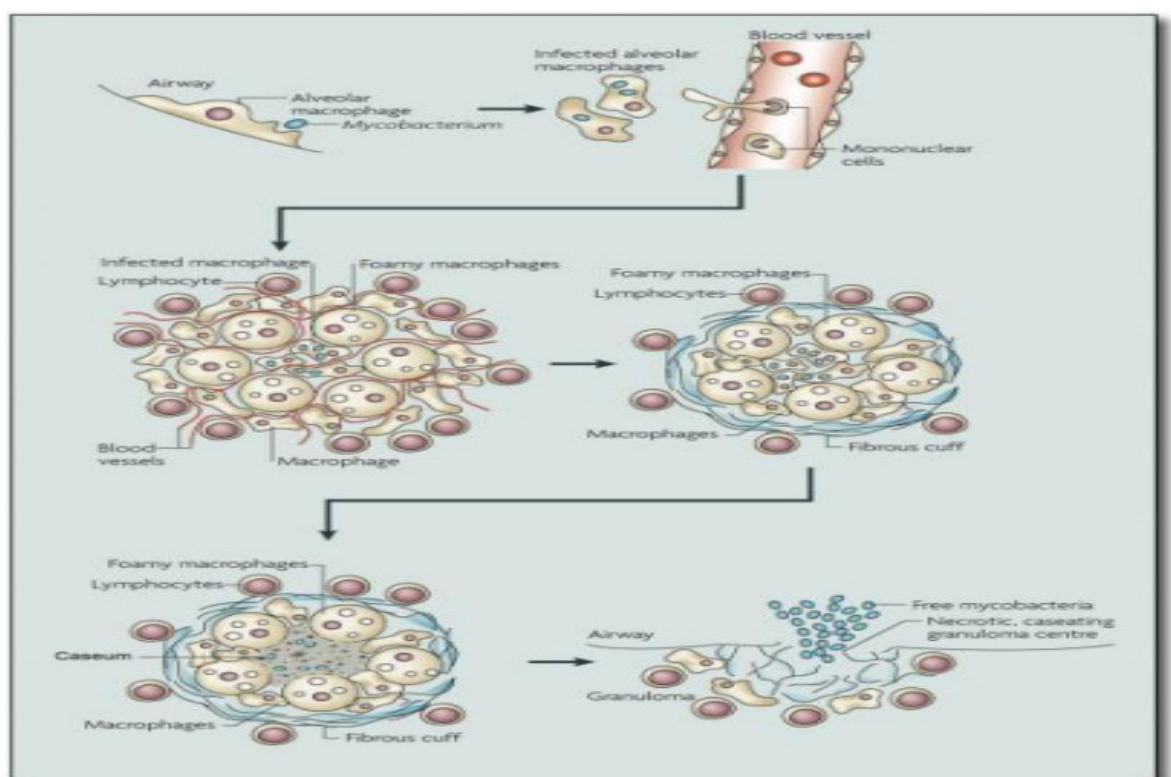


**Figure 2. 5: Infection cycle of M. Tuberculosis**

### 2.1.6. Current anti-tuberculosis drug therapy and its problem

There are several major problems associated with the currently available TB treatment [47]:

- The duration and complexity often resulting in non-adherence and leading to emergence of resistance and continuous spread of the disease.
- Adverse events in response to anti-TB drugs.

- Some drugs for drug resistant TB are not available everywhere and are less effective more toxic, and require longer use.
- Co-infection of TB and HIV, where their combined treatment involves a high pill count with associated adherence problems, overlapping toxicity profiles, drugs interaction and risk of immune reconstitution syndrome.
- Prophylactic therapy of latent TB (TB infection without symptoms) is also associated with problems.

### **2.1.7. Drug resistance**

Daily dosing of anti-tubercular drug for prolonged periods is known to cause non-compliance and treatment failure which in turn leads to Multi drug resistant tuberculosis (MDR-TB) and extensively drug resistant tuberculosis (XDR-TB) [8]. Across all geographical regions surveyed, 10 % of MDR cases were XDR, thus posing the threat of an untreatable global epidemic [48]. The overall success rate for XDR-TB in a recent meta-analysis was reported as 44 % [49]. It is very much difficult to comply with the full course of anti-tuberculosis therapy and inclusion of all drugs included in the multiple-drug regimen. Missed doses increase the chances of treatment failure which further develop in drug resistance to the anti-tuberculosis regimen [4]. Treatment of MDR-TB continues for several months on the basis of susceptibility testing. As without this information it is impossible to treat such patients. It is recommended to treat patient with suspected MDR-TB, and the patient should be started on streptomycin, Isoniazid, Rifampicin, Ethambutol, Pyrazinamide, and Cycloserine until receive the result of laboratory susceptibility testing [50].

#### **2.1.7.1. Types of drug resistance**

There are two types of drug resistance: Primary and secondary.

- Primary resistance refers to the fact that the organisms transmitted were resistant to one or more anti tubercular drugs (ATD).
- Secondary resistance means that new resistance developed as a result of inadequate drug treatment.

There are different types of bacterial mechanisms of drug resistance like barrier mechanisms, degrading or inactivating enzymes, and genetic drug target modification. Another important mechanism of TB drugs resistance is due to endogenous chromosomal

mutation and not to acquired resistance from an exogenous genetic source such as plasmids.

#### **2.1.7.2. Develop of drug resistance**

Degree of naturally occurring resistance to anti tubercular drug (ATD) varies from drug to drug. Cavities contain approximately  $10^8$ - $10^9$  bacilli. Hence, there is a significantly higher risk of naturally resistant organisms being present in cavity TB. It is recommended to prescribe multi drug therapy for TB disease in naturally resistant organisms. Secondary resistance to a particular drug is unlikely to occur within two months [14]. Effective regimen should continue until achieving a cure to prevent the development of secondary resistance.

#### **2.1.7.3. Multi Drug-Resistant Tuberculosis (MDR-TB)**

This is one form of tuberculosis (TB) defined by resistance to at least two first-line anti-tuberculosis drugs. Inadequate or inconsistent treatment has allowed MDR-TB to emerge and spread quickly. The treatment for drug-resistant TB takes almost two or more years and, in addition, the treatment is so complex, expensive, and toxic that creates numerous problems in MDR-TB patients. Sometimes, treatment of MDR-TB consists of second-line drugs [5]. But, many second-line drugs are lethal and have harsh side effects.

#### **2.1.7.4. Extensively Drug-Resistant TB (XDR-TB)**

XDR-TB poses a major risk to public health. This is more brutal form of MDR-TB and is characterized by resistance to any fluoroquinolone and at least one of the three injectable second-line drugs. This makes resistance XDR-TB treatment extremely problematic. Around 70 % of XDR-TB patients died within a month of diagnosis. According to WHO's estimation, 5 % of MRD-TB cases are XDR-TB [38].

### **2.2. Anti-tubercular drug**

Remarkable progress has been made in the last 50 years since the introduction of Streptomycin in 1947 for the treatment of tuberculosis. In the late 1970s, TB appeared to be fading away from being a major public health problem at least in the developed countries [51]. Its full therapeutics potential could be utilized only after 1952 when Isoniazide was produced to accompany it. The discovery of Ethambutol in 1961, Rifampin

in 1962, and redefinition of the role of Pyrazinamide has changed the strategies in the chemotherapy of tuberculosis [52].

### 2.2.1. Classification

Since 1970 the efficacy of short course (6-9 months) and domiciliary utility the anti-TB drugs can be divided into (Table 2. 2) [52]:

- First line: These drugs have high anti-tubercular efficacy as well as low toxicity; are used routinely. Examples: Isoniazide, Rifampicin, Pyrazinamide, Ethambutol, Streptomycin.
- Second line: These drugs have either low anti-tubercular efficiency or high toxicity or both; are used in special circumstances only. Example: Thiacetazone, Paraaminosalicylic acid, Prothionamide, Kanamycin, Ethionamide etc.

**Table 2. 2: List of anti- tubercular drug with mechanism of action**

Type of Drug	Name of Drug	Mode of action [53]
<b>First generation</b>	Isoniazide	Inhibit the synthesis of mycolic acid.
	Rifampicin	Inhibit DNA dependent RNA synthesis.
	Pyrazinamide	Inhibit the synthesis of mycolic acid.
	Ethambutol	Inhibit arabinogalactan synthesis and interfere with mycolic acid incorporation in micobacterial cell wall.
	Streptomycin	It is essentially suppressing the growth of the bacillus by inhibiting their protein synthesis.
<b>Second Generation</b>	Thiacetazone	It is tuberculostatic.
	Para amino salicylic acid	It is tuberculostatic used in combination therapy to inhibit the development of resistant strains of the tubercle bacillus to other concurrently used drugs.
	Ethionamide	It suppresses the multiplication of human strains of <i>Mycobacterium tuberculosis</i> and is used for the treatment of tuberculosis resistant to first-line drugs.
	Prothionamide	Prothionamide inhibits peptide synthesis. It is active against mycobacteria species. Bacteriostatic against
	Cycloserine	It is a chemical analogue of D-alanine: inhibits bacterial cell wall synthesis by inactivating the enzymes which recemize L-alanine and link two D-alanine residues.
	Kanamycin	Act by inhibiting the protein synthesis in <i>M. tuberculosis</i> .
	Amikacin	
	Capreomycin	
	Viomycin	

<b>Other Drugs</b>	Ciprofloxacin	Penetrate to cells and kill M. lodged in macrophages.
	Ofloxacin	
	Clarithromycin	Act by inhibiting the protein synthesis in M. <i>Tuberculosis</i> .
	Azithromycin	
	Rifabutin	Inhibit DNA dependent RNA synthesis.
	Terizidone	Inhibiting cell wall synthesis
	Clofazimine	Bind to mycobacterial DNA leading to disruption of the cell cycle.
	Thioridazone	Inhibit bacterial efflux pumps also inhibits the replication of phagocytosed MRSA, causes bacterial lysis.
	Imipenem	Inhibition of cell wall synthesis
	Amoxycillin-clavulanate	Inactivation of the enzyme prevents the formation of a cross-link of two linear peptidoglycan strands, inhibiting the third and last stage of bacterial cell wall synthesis.

### 2.2.2. Prothionamide Profile

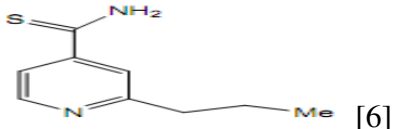
PTH is a thioisonicotinamide or thioamide derivative with antibacterial activity against mycobacteria like *Mycobacterium tuberculosis* and *Mycobacterium leprae* [54]. PTH has been used for more than 30 years in the treatment of patients with drug-resistant TB [55]. PTH is used as a bacteriostate at the concentration of 0.5 µg/ml and this drug has crystallinity, poor water solubility and low bioavailability. Prothionamide was first marketed in Germany in the 1970s but registered in the framework of posterior registration process in Germany in 2005 and approved by the German Federal Institute for Drugs and Medical Devices for the following indications [56]:

- Treatment of all forms and stages of pulmonary and extrapulmonary TB as second-line drug;
- Treatment of diseases caused by ubiquitous (atypical) mycobacteria;
- Treatment of leprosy in the context of modified therapy regimens.

**Table 2. 3: Properties of Prothionamide**

SR. NO	PROPERTIES	CHARACTER
1	Synonym	Prothionamide, Ektebin; Tubex; Peteha; Trevintix, $C_9H_{12}N_2S$ [57]



2	Structure	
3	Name	2-Propylpyridine-4-carbothionamide[58]
4	State	Solid [59]
5	Molecular Weight	180.3[59]
6	Melting range	142-145°C[60]
7	Solubility	Soluble in methanol, Acetic acid, ethanol. Practical insoluble in water. [60]
8	Appearance	Yellow crystals or crystalline solid [60]
9	Taste	Unpleasant sulfurous taste
10	Log p	2.22[61]
11	Pka	Acidic -8.19, Basic-7.25 [61]
12	Absorption	The drug is readily absorbed in the GIT after oral administration.[62]
13	Distribution	Almost not bind to plasma protein. Vd-93 L. [10]
14	Metabolism	Metabolized into Prothionamide sulphoxide (T1/2 = 2 hr.) [63]
15	Excretion	Mainly eliminated through urine as unchanged drug.[64]
16	Elimination half life	1.5 to 2.1 hr.[64]
17	MIC	0.5-2 µg/ml[65]
18	Mild Side effect	Gastrointestinal side effect, aundice-like reactions, hepatitis, skin rashes [62]
19	Serious side effect	Sleepiness, Headache, Insomnia, Depression, Paresthesias [62]
20	Mechanism of action	Protionamide inhibits peptide synthesis. It is active against mycobacteria species. Bacteriostatic agents.[66]
21	Derivative	Prothionamide s-oxide[67]
22	BCS class	Class II
23	Thermo labile	No
24	Dose for adult	15-20 mg/kg. should not exceed 1g/day.[62]

25	Dose for Pediatrics	10-15 mg/kg. should not exceed 750 mg/day.[62]
26	Food	Can be taken before or after food intake [62]
27	HIV patients	Can be given to HIV patients
28	Storage	Glass, Polyethylene, Polypropylene container, at room temperature
29	Formulation available in Market	Film coated tablet, Capsule

### 2.2.2.1. Literature review on Prothionamide

- ❖ Baartels H *et al* (1998) [16] developed a simple high performance liquid chromatography (HPLC) method that can determine the PTH in human serum. Initially serum was treated with trichloroacetic acid (TCA) followed by centrifugation and neutralization with  $\text{NaHCO}_3$ . PTH was separated by Kromasil 100 C4 column (acetonitrile–sodium tetraborate buffer pH 8–dibutylamine) and determined photometrically at 291 nm. The lower limit of quantification (LOQ) was 27 mg/ l and linearity was observed up to 15 mg/ l.
- ❖ Lee HW *et al* (2009) [17] evaluated the pharmacokinetics of Prothionamide (PTH) in South Korean patients having multi drug resistant tuberculosis and also investigated whether difference in body mass index could explain observed difference in PTH disposition. In this study seventeen patients were selected. All the patients had MDR-TB. They are treated in combination with PTH, Cycloserine, Ofloxacin, Para amino salicylic acid and Streptomycin or Kanamycin for at 2 weeks. They calculated the mean AUC for 0-12 hr was  $11.0 \pm 3.7$   $\mu\text{hr/ml}$ . The  $T_{\text{max}}$  and  $t_{1/2}$  were 3.6 hr and 2.7 hr respectively. They found no significant difference in PTH disposition in patients.
- ❖ Kumar PM *et al* (2011) [21] developed stability indicating RP HPLC method to determine PTH in pure and pharmaceutical dosage form. C18 column (250 x 4.6 mm), 5  $\mu\text{m}$  with mobile phase methanol-buffer (0.02 M  $\text{KH}_2\text{PO}_4$ ) solution in the ratio 85:15 and pH 4.5, flow rate 1 ml/min was used. The retention time of PTH was 4.8 min and showed good liner relationship in the concentration range 200-1200  $\mu\text{g/ml}$ .

- ❖ Lee JK *et al* (2012) [9] prepared solid dispersion of PTH using polymer complex through spray drying and improved dissolution property. They perform SEM analysis and confirmed that PTH changed to amorphous from crystalline form due to nano size. Fourier transform infrared spectroscopy (FT-IR) was used to analyze chemical changes of solid dispersion. They demonstrated that the solid dispersion of Prothionamide with poly(N-vinylpyrrolidone) improved the dissolution rate.

#### 2.2.2.2. Patent search on Prothionamide

- ❖ **FR2091338 (A5):** The invention relates to a novel process for the preparation of 2-ethylisonicotinonitrile and 2-propyl (n)-isonicotinonitrile, the final step in the process of obtaining Ethionamide and Prothionamide. Methods for the preparation of 2-ethyl thioisonicotinamide and 2-propyl (n)-thioisonicotinamide are also known. However, the process of the invention makes it possible to significantly reduce the number of passes and to obtain high yields of final products. This process offers the twofold advantage of giving the final intermediates, i.e., 2-ethylisonicotinonitrile and 2-propyl (n)-isonicotinonitrile with approximately total conversion, so that they are ready to be transformed without any loss into the desired final products, and to form them from a compound which is easily obtained by a series of reactions easy to perform [68].
- ❖ **UA69394 (U):** A method for treating tuberculosis of the lungs with the advanced resistance of mycobacteria towards antituberculous drugs within the intensive phase of chemotherapy provides for the daily use of five antituberculous drugs at the average daily doses, including those drugs of line I-II (primary agents) that are still effective against mycobacteria according to sensitivity assay with additional back-up drugs. In addition, 2-3 primary drugs to which mycobacteria are resistant are included into the treatment regimen: Pirasinamide and/or Etambutol and/or Prothionamide and/or PASA [69].

There are some other patents also been available for Prothionamide and mentioned in Table 2.4 [70].

**Table 2. 4: List of patents related to Prothionamide**

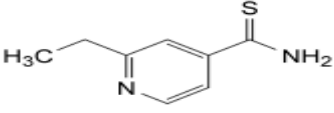
Name of database	Application no	Patent no	Title	Date of filing
EPO	SU198029426 87 19800618	SU92263 5 (A1)	Method of determination of Prothionamide in drugs	23/04/1982
	SU198335847 64 19830310	SU11137 20 (A1)	Prothionamide determination method	10/03/1983
	GB197400353 99 19740812	GB14269 96 (A)	Pharmaceutical compositions	12/08/1974
	RU201101495 43 20111206	RU24725 12 (C1)	Antituberculous composition and method for preparing it	06/12/2011
	RU201101287 58 20110712	RU20111 28758(A)	Pharmaceutical anti-tuberculosis combined composition	12/07/2011
	RU200801477 37 20081203	RU20081 47737(A)	Combined antituberculous drug and method for preparing thereof	03/12/2008
	CN200612003 13 20060404	CN18572 19 (A)	Slow released medicine prepn containing antituberculous	04/04/2006
	RU200501048 07 20050224	RU22804 51 (C1)	Pharmaceutical composition possessing antituberculosis effect	24/02/2005
	RU200301376 22 20031229	RU22475 60 (C1)	Composite formulation with antituberculous activity	29/12/2003
	RU200001185 52 20000714	RU21669 42 (C1)	Pharmaceutical composition showing antituberculosis effect and method of its preparing	14/07/2000
	DE198939112 63 19890407	DE39112 63 (A1)	Combination products	07/04/1989

### 2.2.3. Ethionamide Profile

Ethionamide (ETH) is an isonicotinic acid derivative of thioamide class. It shows activity against *M. tuberculosis*, *M. bovis* and *M. semegmatis*. It is also active against *M. leprae* [6]. It is an important second-line drug used in the treatment of drug-resistant tuberculosis. ETH is an efficacious, relatively non-toxic and cheap, and easily available drug, which has been in use since the 1960s [50]. It first received U.S. FDA approval in 1965, and is approved for the treatment of active TB resistant to Isoniazid or Rifampicin, or where the patient is intolerant of other drugs [56]. ETH acts on intracellular and extracellular bacilli [71]. These bacilli grow within human macrophages. Drug resistant mycobacterium are increasingly common in different parts of the world and are fuelled with spread of Acquired Immunodeficiency Syndrome (AIDS), as a result of this second line antimicrobial agents such as Ethionamide are being used much more frequently [72]. The MIC of ETH for *M. tuberculosis* is 0.5µg/ml. At the usual doses, Ethionamide is bacteriostatic [73]. Well-recognised adverse effects of Ethionamide are hepatotoxicity and nervous system effects similar to that of Isoniazid. Hypothyroidism, although a known adverse effect, is described as rare [4]. Ethionamide (ETA) is a bacteriostatic, isonicotinic acid derived antituberculosis agent. It is used in combination for the treatment of clinical tuberculosis that has failed to respond to adequate first-line therapy [74]. ETH is a structural analogue of Isoniazid. Both compounds are known to inhibit mycolic acid biosynthesis. The structural similarity and existence of cross-resistant phenotypes suggested that these two drugs share a common molecular target [50]. Resistance to Ethionamide is due to genetic alterations in EthA. *M. tuberculosis* strains that are resistant to isoniazid due to alterations in the *katG* gene (catalase/peroxidase enzyme) remain sensitive to Ethionamide [71]. The usual dose is 250 to 500 mg two to four times per day. The daily dose is limited by gastrointestinal toxicity. The elimination half-life in humans is approximately 2 to 3 hr [5].

**Table 2. 5: Properties of Ethionamide**

SR. NO	PROPERTIES	CHARACTER
1	Synonym	Ethinamide, ethinamid, ethionamidum, etionamide[75]

2	Structure	 [76]
3	IUPAC Name	<i>2-ethylpyridine-4-carbothioamide</i>
4	State	Solid [77]
5	Molecular Weight	166.243[77]
6	Melting range	158-164 °C [76]
7	Solubility	Practically insoluble in water, soluble in methanol [76]
8	Appearance	Yellow, crystalline powder [76]
9	Taste	Metallic taste [71]
10	Log p	1.33 [78]
11	pKa	4.49 [79]
12	Absorption	Bioavailability approximately 80 %
13	Distribution	Vd-93.5 liter [10], Approximately 30 % bound to proteins [71].
14	Metabolism	Metabolite-Ethionamide sulphoxide, 2-ethyl-4-amidopyridine [80], [81] .
15	Excretion	Less than 1 % of the oral dose is excreted through urine in unchanged form [74].
16	Elimination half life	2 to 3 hours [35],[82]
17	Minimum Inhibitory concentration	0.25 µg/ml [5], [83]
18	Mild Side effect	Gastrointestinal side effect [83]
19	Serious side effect	Hepatotoxicity, Neurotoxicity, Cardiovascular effect, Endocrine effect, Skin reaction [71] Hypothyroidism [4].
20	Derivative	Ethionamides-oxide, 2-ethyl-4-cyanopyridine, 2-ethyl-4-amidopyridine, 2-ethyl-4-carboxypyridine, 2-ethyl-4-hydroxymethylpyridine [84].
21	Mechanism of action	Inhibit protein synthesis, preventing mycolic acid biosynthesis and affecting the bacterial cell membrane [71].
22	BCS class	3/1[85]

23	Food effect	No interaction with food, orange juice [74].
24	Dose for adult	15-20 mg /Kg daily as single dose. Max dose: 1gm daily [71]. 250-500 mg 2-4 times per day.[5]
25	Dose for Child	10-20 mg/kg daily as a single dose. Max dose: 750 mg [86][86][86][86][86]
26	HIV Patients	Can be given to HIV patients [4]
27	Thermo labile	No
28	Storage	Preserve in air-tight containers at less than 40°C, preferably between 15 to 30°C [77].
29	Formulation available in Market	Tablet

### 2.2.3.1. Literature review on Ethionamide

- ❖ Kumar G *et al* (2010) [8] mentioned that the sustained release nano-formulations of second line ATD drugs can help in reducing their dosing frequency and improve patient's compliance in multi-drug resistant tuberculosis (MDR TB). Ethionamide-loaded nanoparticles were administered orally to mice at two different doses and the control group received free (un-encapsulated) Ethionamide. They investigated the pharmacokinetics and tissues distribution of Ethionamide. Ethionamide-loaded PLGA nanoparticles produced sustained release of Ethionamide for 6 days in plasma against 6 hr for free Ethionamide.
- ❖ Mahmood A *et al* (2009) [72] assessed the pharmacokinetics of Ethionamide in the local population of healthy human subjects. Serum samples were taken from each of the selected subject at different time intervals. These samples were analyzed by using RP HPLC with C18 column and UV detector set at 291 nm. The mobile phase was consisted of 0.02 M disodium hydrogen phosphate and acetonitrile (75:25) and delivered at a rate of 1.5 ml/min. They found the  $C_{max}$  of  $1.941 \pm 1.487$   $\mu$ g/ml and  $T_{max}$  of  $1.75 \pm 1.487$  hr. Calculated AUC was  $8.745 \pm 0.536$ . The elimination half life ( $t_{1/2}$ ) was found as  $1.995 \pm 1.157$  hr. A 20-gauge venous cannula was inserted into a forearm for the collection of blood samples. 3 ml blood samples were collected before dosing (zero time) and at 0.5, 1.0, 1.5, 2.0, 2.5, 3.0, 4.0, 6.0, 8.0, 12.0 and 24.0 hours after Ethionamide tablet administration.

- ❖ Walash *et al* (2004) [87] developed a fluorimetric method for the determination of Ethionamide in pharmaceutical preparations and biological fluids (urine and plasma). The proposed method is based on the study of the quantitative quenching effect of Ethionamide on the native fluorescence of eosin in acidic medium due to complex formation. The results obtained were in good agreement with the official methods.
- ❖ Peloquin CA *et al* (1991) [88] employed a solid phase extraction method to estimate Ethionamide in human serum using HPLC. Octadecyl SPE column were used in this work. They remove serum constituents from the column with water and eluted ETH with methanol. Samples were allowing evaporate and reconstituted with mobile phase. Author demonstrated that the method was reproducible with recovery of 64 % in comate to liquid-liquid extraction method.

#### 2.3.3.2. Patent search on Ethionamide

- ❖ **CN104473897 (A):** The invention provides a preparation method of an Ethionamide tablet, which comprises the following steps: preparing a solid dispersion, and preparing the Ethionamide tablet by a dry granulation / tableting process or powder direct tableting process. The dissolution test on the Ethionamide tablet indicates that more than 75 % of Ethionamide can be dissolved out within 45 minutes, and thus, the Ethionamide tablet is beneficial to absorption and bioavailability of the organisms and can enhance the antiphthisic treatment effect.
- ❖ **UA76005 (C2):** The invention relates to the medicine, namely to phthisiatry. The method for treating the patients with the chronic tuberculosis of the lungs consists in 12-month course of drug therapy. Within the first six months of the treatment, Etambutol, Pyrasinamide, Cyprofloxacin, Kanamycin, Etionamide are prescribed at mean daily doses. In addition, within the first two months of the treatment, Clarytromycin and Omeprasol are given. Within the last six months of the treatment, Etambutol, Pyrasinamide, and Cyprofloxacin are prescribed at mean daily doses [89].



There are some other patent granted related to Ethionamide that are mentioned herewith

**Table 2. 6: List of patents related to Ethionamide**

Name of database	Application no	Patent no	Title	Date of filing
EPO	US201314426543 20130906	US2015246126 (A1)	Magnetodynamic activation of 13c-acyl Isoniazid and Isoniazid and Ethionamide derivatives [68].	09-03-2015
	US201313760605 20130206	US20153150415 (A1)	Rationally improved Isoniazid and Ethionamide derivatives and activity through selective isotopic substitution [90].	13-06-2013
	US20070306333 20070704	US2011136823 (A1)	Compounds having a potentiating effect on the activity of Ethionamide and uses thereof [91].	09-06-2011
	FR19710016539 19710507	FR2091338	2-ethyl and 2-propyl isonicotinonitrile - intermediates for Ethionamide and Prothionamide [68].	14-01-1972
	FR20040004636 20040430	FR2861745 (A1)	Selecting compounds that inhibit the mycobacterial EthR repressor, useful in treatment of tuberculosis and leprosy, improve efficiency of conversion of Ethionamide to its active form [92].	06-05-2005

### 2.3. Dosage form: nanoparticles

In 1981, Gregoriadis described drug targeting using novel drug delivery system as ‘old drug in new clothes’. The concept of designing targeted delivery system has been originated from the Paul Ehrlich, who was a microbiologist, proposed the idea of drug delivery in the form of magic bullet [93]. Nanoparticles have become an important area of research in the field of drug delivery because they have the ability to deliver a wide range of drug to different areas of the body at appropriate times. Over the past couple of decades, the field of drug delivery has been revolutionized with the advent of nanoparticles, wherein these particles act as inert carriers for drugs and genes to target cells or tissues [12]. The use of controlled release system has certain advantages over the conventional dosage

forms, as they can minimize side effects, prolong the efficacy of the drug release rate and can reduce the frequency of administration of the drug [16].

An essential requirement of modern drug therapy is the controlled delivery of a drug their desire site of action in the body with an optimal concentration versus time profile. One evergreen attempt to achieve this goal is the development of colloidal drug carriers known as nanoparticles, chiefly because of their small particle size. Nanoparticles are solid colloidal particles with diameters ranging from 1-1000 nm. They consist of macromolecular materials in which the active ingredient is dissolved, entrapped, encapsulated and adsorbed or chemically attached [94].

Polymeric nanoparticles are of especial interest from the pharmaceutical point of view.

- First they are more stable in the gastrointestinal tract than other colloidal carriers, such as liposome, and also able to protect encapsulated drugs from gastrointestinal environment. Consequently, it has already been extensively shown that nano-encapsulation of peptides and protein colloidal particles protect them against the harsh environment of the gastrointestinal tract, and enhance their transmucosal transport [34].
- Second, the use of various polymeric materials enable the modulation of physicochemical characteristics (e.g. hydrophobicity, zeta potential), drug release properties (e.g. delayed, prolonged, triggered), and biological behaviour (e.g. targeting, bio-adhesion, improved cellular uptake) of nanoparticles.
- Finally, the particle surface can be modified by adsorption or chemical grafting of certain molecules such as poly(ethylene glycol) (PEG), poloxamers, and bioactive molecules (lectins, invasins etc). Moreover, their submicron size and their large specific surface area favour their absorption compared to larger carriers.
- Polymeric nanoparticles (NPs) have been an exciting approach for lung delivery due to their ability to enter intracellular compartments and escape macrophages phagocytosis. Furthermore, they provide the possibility of achieving high drug loading capacity, sustained release, enhanced drug stability and absorption, as well as targeted deposition [95].

### **2.3.1. Advantages and disadvantages**

The advantages of nanotechnology are as follows:

- (i) Increased bioavailability (quick dissolution; improved penetration through membranes);
- (ii) Lower doses;
- (iii) Lower toxicity;
- (iv) Targeted bio-distribution;
- (v) Reduction of influence of food on variability;
- (vi) Quicker development of formulations.

A great problem is the insufficiently investigated possible toxicity of nanoparticles. The toxicity is dependent on the shape and surface properties of nanoparticles, because both can influence nanoparticle-cell interactions as well as the rate of penetration to cells. Among the various nanoparticles forms nano-tubes were found to be one of the most toxic nanoparticle shapes [96].

### **2.3.2. Biodegradable polymer used in nanoparticles**

Use of biodegradable polymers for biomedical applications has increased in recent decades due to their biocompatibility, biodegradability, flexibility, and minimal side effects. The main advantage of biodegradable polymers is that the products of degradation are not toxic or are completely eliminated from the body by natural metabolic pathways with minimal side effects. These degradation products define the biocompatibility of a polymer. For example, poly(lactic-co-glycolic acid) (PLGA), poly(glycolic acid) (PGA) and poly(lactic acid) (PLA) have been approved by the US Food and Drug Administration (FDA) for certain medical applications, because their products of degradation are eliminated from the body in the form of carbon dioxide and water [97]. The most important biomedical goal of biodegradable polymeric materials is the development of matrices to control the release of drugs into specific sites in the body. Classification of biodegradable polymers is mainly restricted to their origin.

#### **2.3.2.1. Mechanism of degradation**

The mechanisms of degradation for different polymers depend on the chemistry, molecular weight and morphology of each type of polymer and environmental factors such as pH or

temperature also play an important role. Degradation occurs mainly by hydrolysis, oxidation or enzymatic reaction [97]. The stability of the polymeric material affects its efficiency. Therefore, knowledge about its mechanisms of degradation is crucial to select a polymer for specific applications. The most important mechanisms of polymeric degradation are Hydrolytic degradation, oxidation, and enzymatic degradation. Polymer with hydrolysable backbones is susceptible to hydrolytic biodegradation under particular conditions. Water is initially absorbed into the sample, followed by polymer molecular weight reduction throughout the sample. As soon as a critical molecular weight is reached, the polymer starts to diffuse from the surface and finally a combination of water diffusing into the polymer structure and polymer erosion on the surface causes complete degradation. The inflammatory response of cells like leukocytes and macrophages produces reactive oxygen species such as nitric oxide, hydrogen peroxide, or superoxide. These free radicals produced react with the polymer and are transferred to different regions of the polymer chain; and finally, cleavage of the polymeric chain at the free radical site forms shorter segments. Enzymatic degradation mechanism follows surface erosion, in that the polymers lose material from the surface because the enzyme cannot penetrate into the polymer. The enzymatic hydrolysis of chitosan-grafted PEG and chitosan nanoparticles has been studied.

### 2.3.2.2. Classification of biodegradable polymer

Biodegradable polymer can be classified in the several ways. Here, it has been classified based on the origin [97].

**Table 2. 7: List of biodegradable polymer based on origin**

Sl. No	Origin	Sub classification	Examples
1	Synthetic	i) Hydrolyzable backbones Polyesters	Poly(glycolic acid) Poly (lactic acid) Poly (Caprolactone) Poly(lactic-co-glycolic acid) Poly(butylenes succinate) Poly(trimethylene carbonate) Poly(p-dioxanone) Poly(butylenes terephthalate)
		ii) Poly(ester amide)s	Hybrane S1200
		iii) Polyurethanes	Degrapol
		iv) Polyanhydrides	Poly[bis(hydroxyethyl) terephthalate-ethyl]

			orthophosphorylate/ terephthaloyl chloride]
		v) Poly(ortho esters)	Poly(ortho esters) I Poly(ortho esters) II Poly(ortho esters) III Poly(ortho esters) IV
		vi) Poly(alkyl cyanoacrylates)	Poly(butyl cyanoacrylate)
		vii) Polyether	Poly(ethylene glycol)
		viii) Poly(amino acids)	Tyrosine derived polycarbonate
2	Semi synthetic	Microbial polyesters	Poly ( $\beta$ -hydroxyalkanoate)s Poly (hydroxybutyrate) Poly(hydroxybutyrate-co- hydroxyvalerate)
3	Natural	<b>Protein</b>	
		i) Animal source	Collagen
		ii) Vegetable source	Gluten
		<b>Polysaccharides</b>	
		i) Animal source	Chitosan Hyaluronate
		ii) Vegetable source	Cellulose Alginate Starch

**A) CHITOSAN NANOPARTICLES:** Chitosan, poly [ $\beta$ -(1-4)-linked-2-amino-2-deoxy-D-glucose], is a polycationic polymer [98]. It is a semi crystalline polysaccharide constituted by N-glucosamine and N-acetyl-glucosamine units and is prepared by the N-deacetylation of chitin [99]. Chitin, next to cellulose, is the second most abundant polysaccharide in nature and is widely found in the exoskeletons of crustacean and insects as well as in the cell walls of fungi and algae. Chitosan has numerous applications in pharmaceutical systems and medicine. It has been reported that Chitosan has antioxidant and anti-inflammatory properties [28]. Chitosan derived from chitin has emerged as a promising material with unmatched properties including biocompatible, biodegradable, modifiable, mucoadhesive, antimicrobial, tumor cells recognition, and sustained release of loaded therapeutics [31]. It is a linear polyamine containing a number of free amine groups that are readily available for cross-linking, its cationic nature allows for ionic cross-linking with multivalent anions, it has muco-adhesive character, which increases residual time at the site of absorption. It avoids the use of hazardous organic solvents while fabricating particles since it is soluble in aqueous acidic solution [46]. Low molecular weight (LMW) Chitosan nanoparticles have attracted considerable attention as colloidal

drug carriers, but when applied to intravascular drug delivery, they are easy to be removed from circulation by the reticuloendothelial system, which limits their applications as long-circulating or target-specific carriers. Erythrocytes have a long circulation time in the blood, but they are sometimes not suitable for loading and releasing of drug directly [100]. Chitosan with an average degree of deacetylation and a characteristic polycationic character is generally soluble at acidic pH conditions, with aqueous acetic acid as the most commonly used solvent [101]. Chitosan also exhibits other interesting properties, namely availability of reactive functional groups for chemical modifications, hydrophilicity, mechanical stability, regenerability, and ease of preparation in different geometrical configurations suitable for a chosen biotransformation. In addition, Chitosan is an inexpensive material enabling to prepare low-cost carriers for large scale applications [102]. Chitosan based drug delivery systems containing different drugs were prepared that are reported in Table 2.8 [29].

**Table 2. 8: Chitosan-based drug delivery systems with drugs and method**

Type of dosage form	Method of preparation	Drug
Tablets	Matrix	Diclofenac sodium, Pentoxifylline, Salicylic acid, Theophylline
	Coating	Propranolol HCl
Capsules	Capsule shell	Insulin, 5-Amino salicylic acid
Microspheres / Microparticles	Emulsion cross-linking	Theophylline, Cisplatin, Pentazocine, Phenobarbitone, Theophylline, Insulin, 5-Fluorouracil, Diclofenac sodium, Griseofulvin, Aspirin, Diphtheria toxoid, Pamidronate, Suberoylbisphosphonate, Mitoxantrone, Progesterone
	Coacervation / precipitation	Prednisolone, Interleukin-2, Propranolol-HCl
	spray-drying	Cimetidine, Famotidine, Nizatidine, Vitamin D-2, Diclofenac sodium, Ketoprofen, Metoclopramide-HCl, Bovine serum albumin, Ampicillin, Cetylpyridinium chloride, Oxytetracycline, Betamethasone
	Ionic gelation	Felodipine
	Sieving method	Clozapine
Nanoparticles	emulsion-droplet coalescence	Gadopentetic acid
	coacervation/precipitation	DNA, doxorubicin
Nanoparticles	ionic gelation	Insulin, Ricin, Bovine serum albumin,

		Cyclosporin A
	reverse micellar method	Doxorubicin
Beads	Coacervation / precipitation	Adriamycin, Nifedipine, Bovine serum albumin, Salbutamol sulfate, Lidocaine-HCl, Riboflavin
	Solution casting	Isosorbide dinitrate, Chlorhexidine gluconate, Trypsin, Granulocyte-macrophage colony-stimulating factor, Acyclovir, Riboflavine, Testosterone, Progesterone, Beta-Oestradiol
Gel	cross-linking	Chlorpheniramine maleate, Aspirin, Theophylline, Caffeine, Lidocaine-HCl, Hydrocortisone acetate, 5-Fluorouracil

Chitosan is an attractive material for intranasal drug delivery because of its low immunogenicity [43]. It has been used as a film coating material, as an excipient in direct compression tablets, as a tablet disintegrant for improvement of drug dissolution, and for controlling drug release in oral formulations [44]. Chitosan is a nontoxic polymer that has been used in biomedical fields in the forms of sutures, wound coverings, and as artificial skin [45].

### Literature review on Chitosan

- ❖ Fernandez A *et al* (2014) [103] prepared hard gelatine capsules containing Indapamide and Lisinopril loaded chitosan nanoparticles to improve oral bioavailability. The mucoadhesive characteristics of Chitosan nanoparticles will prolong the residence time in contact with the intestinal membrane thereby increasing its oral bioavailability. Author developed simultaneous method of both the drug using HPLC.
- ❖ Elmizadeh H *et al* (2013) [98] prepared chitosan nanoparticles of Tacrine by spontaneous emulsification method. Optimization was carried out through Box-Behnken statistical design. Magnetic nanoparticles were prepared using this optimized method by incorporating Fe<sub>3</sub>O<sub>4</sub> and found the average particle size of 33.63 to 77.87 nm.
- ❖ Anbarasan B *et al* (2013) [16] prepared chitosan-tripolyphosphate nanoparticles of Chloroquine by ionic cross gelation techniques with different ration of drug and polymer. Maximum entrapment efficiency of 92.87 % was achieved with drug-polymer

ratio of 1:6. 85.13 % release was achieved within 24 hr from the optimized formulation.

- ❖ Pospiskova K *et al* (2013) [102] prepared two large scale magnetic chitosan nanoparticles. Both magnetic chitosan derivatives were used as carriers for immobilization of two important enzyme namely lipase and  $\beta$ -galactosidase. Prepared microparticles by microwave assisted synthesis were very stable for 28 days without loss of activity. On the other hand these enzymes immobilized on chitosan microparticles with entrapped magnetite retained more than 90 % of activity during the same time period.
- ❖ Nesalin JAJ *et al* (2012) [104] prepared Zidovudine loaded nanoparticles by ionic gelation of chitosan with tripolyphosphate. Chitosan nanoparticles produced with particle size in the range of 342-468 nm and zeta potential 20.4 to 37.08 mV. Entrapment efficiency increased with increasing polymer amount. All the prepared batches followed first order and provide sustained release for the period of 24 hr.
- ❖ Subbaih R *et al* (2012) [31] prepared hepatitis B virus antigen loaded with chitosan nanoparticles and studied for controlled intranasal delivery. By loading 380 and 760  $\mu$ l hepatitis B antigen, spherical nanoparticles of  $143\pm33$ ,  $259\pm47$  nm with highest loading efficiency and capacity of 90-93 % and 96-97 % respectively. In vitro drug release analysis ensured cumulative drug release of 93 % in 43 days. *In-vivo* immunological study was performed for 6-8 weeks on old female mice and concluded the efficiency of nanoparticles for antigen is highly stable and better than standard.
- ❖ Singh A *et al* (2011) [94] formulated Losartan potassium loaded nanoparticles by ionic cross gelation techniques. Optimized batch showed zero order release kinetics and provide sustained release over the period of 24 hr with highest entrapment efficiency of 87.5 %.
- ❖ Tsao CT *et al* (2011) [99] studied the acid depolymerisation of Chitosan. They found the depolymerisation rate increase with elevated temperatures and high concentration of acid but no other structural changes was observed. Rouleaux formation was observed when erythrocytes contracted with low molecular weight Chitosan that was



due to interference of negative charge cell membrane through its polycationic properties. Kinetic study revealed that the complex salt formed by amine on chitosan and acetic acid acted as catalyst.

- ❖ Tan Q *et al* (2011) [28] prepared quercetin loaded lecithin-Chitosan nanoparticles for topical delivery. Tocopheryl propylene glycol succinate was used as a surfactant. The mean particles size found 95.3 nm with entrapment efficiency and drug loading for quercetin were 48.5 % and 2.45 % respectively. Author demonstrated higher permeation ability and significantly increased accumulation of quercetin in the skin, when given in the nanoparticles form in comparison to quercetin solution.
- ❖ Shan C *et al* (2010) [105] developed a novel glucose biosensor based on immobilization of glucose oxidase in thin films of Chitosan containing grapheme and gold nanoparticles. Prepared film showed good electro catalytical activity against  $H_2O_2$  and  $O_2$ . The wide linear response and good reproducibility were obtained. This film showed prominent electrochemical response to glucose.
- ❖ Deng QY *et al* (2006) [106] prepared Chitosan nanoparticles loaded with lysozyme by ionic gelation techniques. Author found the entrapment efficiency increase first then decreased upon increasing molecular weight, TPP content. They also demonstrated the lysozyme release rate increased with decreasing the amount of lysozyme, molecular weight or content of Chitosan and increasing the amount of TPP.
- ❖ Zheng Y *et al* (2006) [107] prepared Chitosan- Glycyrrhetic acid nanoparticles by mixing positive charged of Chitosan and negative charged Glycyeehetic acid at room temperature. These nanoparticles were stable at pH ranging from 4.0 to 7.0. Encapsulation was increased from 55.5 to 88.1 % with increasing the weight ratio of Chitosan-Glycyrrhetic acid. Simultaneously loading capacity of nanoparticles decreased from 7.3 to 6.4 %. With a specific condition the nanoparticles particles size achieve of 298 nm with polydispersibility index of 0.04.

**B) PLGA NANOPARTICLES:** Biodegradable polymers such as poly(D,L-lactic-co-glycolic acid) or PLGA, a biocompatible and non-toxic polymer, has been intensely studied in the field of novel drug delivery system [108]. PLGA-based nanotechnology has

gained tremendous interest in medical applications such as sustained drug release, drug delivery, diagnostics and treatment [109]. Polylactide (PLA) and its copolymers that contain glycolide have been approved by the US food and drug administration (FDA). Drawback of polymeric nanoparticles is the persistence of the nanoparticles system in the body long after the therapeutic effect of the delivered drug has been realized. This has led to the development of biodegradable nanoparticles, particularly comprised of the polymer polylactide-coglycolide (PLGA), where the particle matrix degrades slowly *in vivo* and the by-products like lactic and glycolic acid are easily metabolized and excreted [12]. Hence, PLGA is an ideal choice for drug delivery because of its unique properties including biocompatibility, bioavailability and variable degradation kinetics, stability and extended drug release over other carriers such as liposome [109]. PLGA has been widely explored for preparation of polymeric nanoparticles and is well reported for mucoadhesive properties, and enhanced entrapment efficiencies [110]. These NPs have a number of appealing features: their hydrophobic core is capable of carrying highly insoluble drugs with high loading capacity, while their hydrophilic shell provides steric protection and functional groups for surface modification. PLGA was selected for the hydrophobic core due to its biodegradable nature and ability to encapsulate high amounts of hydrophobic drugs [111].

### Literature review on PLGA nanoparticles

- ❖ Sharma D *et al* (2014) [110] prepared Lorazepam loaded PLGA nanoparticles (50:50) using nano-precipitation method and investigated the effect of process variable on the response using Box-Behnken design. Effect of four independent factors like polymer, drug, surfactant and aqueous/organic ratio was studied on particle size and PDE. Optimized nanoparticles were nearly spherical with z-average value of 167-318 nm, PDI below 0.441 and zeta potential of -18.4 mV.
- ❖ Jain DS *et al* (2014) [112] prepared PLGA (50:50) nanoparticles containing Temozolomide using solvent diffusion method and characterized for particle size and morphology. Dialysis membrane was used to study the diffusion and the drug estimation was carried out by developed and validated UV-spectrophotometric method. 20 mg drug equivalent nanoparticles dispersed 1 ml dispersion medium and filled in to dialysis bag and then suspending in 500 ml of dissolution medium with 100 rpm. Pure

drug diffuse out in 2 hr whereas PLGA coated nanoparticles continue the release up to 120 hr.

- ❖ Mozafari M *et al* (2013) [113] studied the ability of sodium chloride (NaCl) and different percentages of a water-soluble form of natural vitamin E, on the formation of PLGA nanoparticles. They mentioned PLGA is a potential carrier for drug delivery. They shown average particle size decrease with increasing the percentage of natural vitamin E. They achieved average size of the PLGA particles of <100 nm using 0.26 w/v % vitamin E. Additionally NaCl helped PLGA to form smaller particles.
- ❖ Manoochchri S *et al* (2013) [114] prepared PLGA (50:50) nanoparticles of Docetaxel by emulsification evaporation method. Prepared nanoparticles were surface conjugated with human serum albumin and this was confirmed by Fourier transform infrared spectrum and nuclear magnetic resonance. PLGA nanoparticles were prepared of 199 nm with zeta potential of -11.07 mV. For drug release patterns of prepared nanoparticles dialysis technique was adopted.
- ❖ Bhatnagar P *et al* (2013) [115] encapsulated Bromelain with PLGA and used another coating materials that is acidic pH resistive polymer, Eudragit, in order to provide stability against degradation in the acidic pH. Authors performed the physiochemical characterization of particles and studied the proteolytic activity and structure integrity of Bromelain after encapsulation. A comparative study was carried out between BR-PLGA and free Bromelain to demonstrate their antitumor efficacy *in vitro* and *in vivo*. The particles were in the range of  $145.6 \pm 9.85$  nm with entrapment efficiency of  $48 \pm 4.81$  %. *In vitro* release kinetics Bromelain from nanoparticles followed Higuchi model. Coated nanoparticles also showed 40% reduction in burst release at acidic pH.
- ❖ Ilyas A *et al* (2013) [17] mentioned porous PLGA nanoparticles and their use as controlled release vehicles are a novel approach. Bovine serum albumin (BSA) loaded PLGA nanoparticles were prepared by water-in-oil-in-water (w/o/w) double emulsion method. Specifically, PLGA nanoparticles were prepared using chloroform and polyvinyl alcohol, and freeze drying was employed for the phase separation to obtain the nanoparticles. The porous nanoparticles were prepared through the salt-leaching process where sodium bicarbonate was used as an extractable porogen. *In vitro* drug

release behaviour of porous and nonporous nanoparticles was monitored over a period of 30 days. Several characterizations like laser scattering, zeta potential analysis, and scanning electron microscopy were carried out. The drug loading efficiencies for BSA in porous and nonporous PLGA nanoparticles were 65.50 % and 77.59 %, respectively. BSA released from PLGA porous and non-porous nanoparticles were measured to be 87.41 % and 59.91 %, respectively after 30 days.

- ❖ Hussein AS *et al* (2012) [116] prepared Linamarin-loaded PLGA nanoparticles by the double emulsion solvent evaporation technique. Two different grade polymer like PLGA (50:50) and PLGA (85:15) were used. Nanoparticles were spherical in shape. Average particle size (< 190 nm), drug entrapment efficiency (50–52 %) and zeta potentials (–25 to –30 mV) were determined. All prepared NPs showed controlled biphasic release profile. Polymer degradation was investigated and finally concluded that the polymer biocompatibility as well as safety.
- ❖ Averineni R *et al* (2012) [117] formulated PLGA nanoparticles of Paclitaxel by solvent evaporation techniques and evaluated for physicochemical parameters, *in-vitro* anti tumour activity and *in-vivo* pharmacokinetic studies in rats. Particle size of optimized nanoparticles was found to be less than 200 nm. Maximum entrapment efficiency was shown in polymer-drug ratio of 20:1. *In vitro* drug release exhibited biphasic pattern with initial burst release followed by slow and continuous release for 15 days.
- ❖ Derakhshandeh K *et al* (2011) [118] studied the uptake and transport of 9-nitrocamptothecin (9-NC) (anticancer agent) across CACO-2 cell monolayers in free and PLGA loaded drug form. Nanoparticles were prepared by nano-precipitation method with particle size of 110-950 nm. Author demonstrated that CACO-2 cell uptake and transport of encapsulated 9-nitrocamptothecin was significantly affected by the carrier's diameter and incubation time.
- ❖ Bojat V *et al* (2011) [119] prepared Paclitaxel loaded into PLGA nanoparticles using nano-precipitation method. Paclitaxel encapsulation efficacy and *in vitro* release study were carried out. Cytotoxic activity and cell accumulation of nanosomal formulation of Paclitaxel was studied on multi-resistant cell line Jurkat WT (cells of human T-

limphoblastic leucosis). PLGA-Paclitaxel nanoparticles showed 90-98 % encapsulation efficacy, higher cell accumulation and cytotoxic activity.

- ❖ Boitumelo S *et al* (2010) [18] evaluated the effects of PLGA nanoparticles for *in vitro* and *in vivo* and compared its size with industrial nanoparticles of zinc oxide, ferrous oxide, and fumed silica. An *in vitro* cytotoxicity study was conducted to assess the cell viability following exposure to PLGA nanoparticles. Viability was determined by means of a WST assay, wherein cell viability of greater than 75 % was observed for PLGA-amorphous fumed silica particles and ferrous oxide, but was significantly reduced for zinc oxide particles. *In-vivo* toxicity assays were performed but no significant change was observed in the tissues of mice. After 7 days of administration, the particles were detectable in different organ of mice.
- ❖ Jain S *et al* (2010) [120] prepared cyclosporine-A loaded PLGA nanoparticles with a diameter < 200 nm. Various process variables like homogenization / sonication, choice of suitable stabilizer and its concentration were optimized to achieve maximum drug loading and desired particle size. A step wise freeze drying cycle was developed and suitable lyoprotectants were screened for long term shelf storage of the formulation in dried form. Accelerated stability testing was also carried out to determine the change in physicochemical characteristics of the nanoparticles during storage. Nanoparticles were successfully prepared with high encapsulation efficiency (> 85 % w/w) and low particle size (163 nm) using 2 % w/v PVA as surfactant with probe sonication technique. No significant changes were observed after 3 months accelerated storage conditions. Author concluded that the developed formulation is a potential delivery vehicle for cyclosporin A.
- ❖ Mainardes RM *et al* (2005) [26] designed spherical nano-particulate drug carriers made of PLGA with controlled size. Praziquantel is a hydrophobic molecule and was entrapped into the nanoparticles with theoretical loading varying from 10 to 30 % w/w. The effects of sonication time, PLGA content, surfactant content and organic solvent evaporation rate on the size distribution were investigated after preparing nanoparticles prepared by emulsion-solvent evaporation method. The results showed these effects have a significant influence on size distribution of the nanoparticles.

### 2.3.3. Residual solvent

Residual solvents, or organic volatile impurities, are a potential toxic risk of pharmaceutical products and have been a concern of manufacturers for many years [121]. In pharmaceuticals, residual solvents are defined as organic volatile chemicals that are used in the manufacture of drug substances or excipients, or drug products. Several processes are adopted to remove this solvent from preparation, excipients. But, these solvents are not completely removed using these techniques. Hence, the safety of products should be checked at the stage of final products [122]. As a result, International Conference of Harmonization (ICH) introduced this key area named "Residual Solvent" in its guideline. Acceptable levels of many solvents are included in this guidance mainly in Q3C(R5) 2011 [121]. The guideline recommends use of less toxic solvents and describes levels considered to be toxicologically acceptable for some residual solvents [123]. Solvent like Dichloromethane significantly increases the chances of lung and liver tumours as well as benign mammary tumours in tested mice [124].

#### 2.3.3.1. Classification

The term "tolerable daily intake" (TDI) is used by the International Program on Chemical Safety (IPCS) to describe exposure limits of toxic chemicals and "acceptable daily intake" (ADI) is used by the World Health Organization (WHO) and other national and international health authorities and institutes. The new term "permitted daily exposure" is defined in the present guideline as a pharmaceutically acceptable intake of residual solvents. After critical review, ICH classified these solvents into three main classes like:

**Class 1 (solvents to be avoided):** Known human carcinogens, strongly suspected human carcinogens, and environmental hazards (Table 2. 9).

**Table 2. 9: Class 1 solvents in pharmaceutical products**

Solvent	Concentration limit (ppm)	Concern
Benzene	2	Carcinogen
Carbon tetrachloride	4	Toxic and environmental hazard
1,2-Dichloroethane	5	Toxic
1,1-Dichloroethene	8	Toxic
1,1,1-Trichloroethane	1500	Environmental hazard

**Class 2 (solvents to be limited):** Non-genotoxic animal carcinogens or possible causative agents of other irreversible toxicity such as neurotoxicity or teratogenicity. Solvents suspected of other significant but reversible toxicities (Table 2. 10).

**Table 2. 10: Class 2 solvents in pharmaceutical products**

Solvent	Permitted daily exposure (mg/day)	Concentration limit (ppm)
Acetonitrile	4.1	410
Chlorobenzene	3.6	360
Chloroform	0.6	60
Cumene	0.7	70
Cyclohexane	38.8	3880
1,2-Dichloroethene	18.7	1870
Dichloromethane	6.0	600
1,2-Dimethoxyethane	1.0	100
N,N-Dimethylacetamide	10.9	1090
N,N-Dimethylformamide	8.8	880
1,4-Dioxane	3.8	380
2-Ethoxyethanol	1.6	160
Ethyleneglycol	6.2	620
Formamide	2.2	220
Hexane	2.9	290
Methanol	30.0	3000
2-Methoxyethanol	0.5	50
Methylbutyl ketone	0.5	50
Methylcyclohexane	11.8	1180
N-Methylpyrrolidone	5.3	530
Nitromethane	0.5	50
Pyridine	2.0	200
Sulfolane	1.6	160
Tetrahydrofuran	7.2	720
Tetralin	1.0	100
Toluene	8.9	890
1,1,2-Trichloroethene	0.8	80
Xylene	21.7	2170

**Class 3 (solvent with low toxicity):** Solvents with low toxic potential to man; no health-based exposure limit is needed. Class 3 solvents have permitted daily exposure of 50 mg or more per day (Table 2. 11). These solvent should be limited by GMP or other quality based requirements.

**Table 2. 11: Class 3 solvents in pharmaceutical products**

Acetic acid	Acetone	Anisole	1-Butanol
2-Butanol	Butyl acetate	tert-Butylmethyl ether	Dimethyl sulfoxide
Ethanol	Ethyl acetate	Ethyl ether	Ethyl formate
Formic acid	Heptane	Isobutyl acetate	Isopropyl acetate
Methyl acetate	3-Methyl-1-butanol	Methylethyl ketone	Methylisobutyl ketone
Pentane	2-Methyl-1-propanol	1-Pentanol	1-Propanol
2-Propanol	Propyl acetate		

**Special class - Solvents for which no adequate toxicological data was found:** The following solvents (Table 2. 12) may also be of interest to manufacturers of excipients, drug substances, or drug products. However, no adequate toxicological data on which to base a PDE was found. Manufacturers should supply justification for residual levels of these solvents in pharmaceutical products.

**Table 2. 12: Solvents for which no adequate toxicological data was found**

1,1-Diethoxypropane	1,1-Dimethoxymethane	2,2-Dimethoxypropane
Isooctane	Isopropyl ether	Methylisopropyl ketone
Methyltetrahydrofuran	Petroleum ether	Trichloroacetic acid
Trifluoroacetic acid		

### 2.3.3.2. Residual solvent analysis

Residual solvents are typically determined using chromatographic techniques such as gas chromatography. Generally reported method in the pharmacopoeias should be used for determining levels of residual solvents as described. Otherwise the most appropriate validated analytical procedure can use [123]. Headspace gas chromatography (HS-GC) method has been used for the determination of residual solvents in pharmaceutical compounds [125].

## 2.4. Inhaled drug delivery system

Inhalation therapy is widely employed to deliver drugs to treat respiratory diseases [126]. Treating respiratory diseases with inhalers requires delivering sufficient drug to the lungs to bring about a therapeutic response [127]. Inhaled drug delivery systems can be divided into 3 principal categories: metered-dose inhalers (MDIs), DPIs, and nebulizers. Each class bears its own unique strengths and weaknesses. This classification is based on the physical states of dispersed-phase and continuous medium. Each class also differentiate on the basis



of metering, means of dispersion, or design. Nebulizers are distinctly different from both MDIs and DPIs, as the drug is dissolved or suspended in a polar liquid, usually water. Nebulizers are used mostly in hospital and ambulatory care settings and are not typically used for chronic-disease management because they are larger and less convenient, and the aerosol is delivered continuously over an extended period of time. MDIs and DPIs are bolus drug delivery devices that contain solid drug, suspended or dissolved in a non-polar volatile propellant or in a dry powder mix (DPI) that is fluidized when the patient inhales [127].

#### **2.4.1. Dry powder inhaler**

Dry powder inhalers (DPIs) are more sophisticated dosage form for respiratory drug delivery and play an important role in delivering medicinal aerosols. Their most common application is the transport of drugs to the bronchioles [128]. Respiratory maladies like asthma, COPD and Tuberculosis, where the benefits of delivering drugs to the lungs is more rather than other body organ as the drug is targeted directly to lungs the infected part. It can start acting much quicker (clearly an important advantage during an asthma attack) and it avoids flooding the rest of the body with the drug, which is wasteful and potentially harmful [61]. DPIs are usually preferred due to suitable behaviour in terms of stability and bioavailability of active ingredient, compared to the liquid counterparts and easy to manufacture [34],[95].

The rationale for this delivery approach includes a more targeted and localized delivery to the diseased site with reduced systemic exposure, potentially leading to decreased adverse side effects [129]. DPIs are one-phase system of solid particle blends. Formulation should be considered based on number of drugs, dose of drug, target area in the lung and patients compliance. Mostly the drug is micronized to 2-5 micrometer and blended with carrier particles usually lactose of particle size 30-60 micrometer or pure drug processed to improve flow property, and prevent aggregation to improve powder aerosolization [130]. The development of DPIs has been motivated by the desire for alternatives to MDIs, to reduce emission of ozone-depleting and greenhouse gases (chlorofluorocarbons and hydrofluoroalkanes, respectively). Generally these are used as propellants (Maintain internal pressure inside the aerosol container), and to facilitate the delivery of macromolecules and products of biotechnology [127].

### Advantages of DPI

- Environmental sustainability, propellant-free design
- Little or no patient coordination required
- Formulation stability

### Disadvantages of DPI

- Deposition efficiency dependent on patient's inspiratory airflow
- Potential for dose uniformity problems
- Development and manufacture more complex/expensive

### 2.4.2. Mean median aerodynamic diameter and its application

Aerodynamic particle size has a significant impact on the regional lung deposition. Its influence on the aerosol distribution along the airways can be understood by considering both the deposition mechanisms and airway geometry [131]. The size and shape of particles are primordial factors that control their deposition in the lungs. This size called as mass Median Aerodynamic Diameter (MMAD). MMAD defined as the diameter of a particle in which 50 % of the aerosol mass is greater and the other 50 % is smaller. Depending on their size and shape, the particles can be deposited by means of four mechanisms:

- **IMPACTION:** This is the physical phenomenon. Here, the aerosol particles tend to continue on a path when they travel through the airway, instead of conforming to the curves of the respiratory tract. Particles bearing higher momentum are affected by centrifugal force results in suddenly changes direction, colliding with the airway wall. This is mainly occurs in the first 10 bronchial generations due to high air speed and turbulent flow. Particle size larger than 10  $\mu\text{m}$  mainly affects due to this phenomenon, which are mostly retained in the oropharyngeal region, especially if the drug is administered by dry powder inhalers (DPI) or metered-dose inhalers (MDI).
- **INTERCEPTION:** This is another phenomenon mainly happens in case of fibres. Due to elongated shape, fibres are deposited on the airway wall as soon as they come in contact.
- **SEDIMENTATION:** In this physical phenomenon, particles (sufficient mass) are deposited due to the force of gravity when they remain in the airway for a sufficient length

of time. This is mainly seen in the last 5 bronchial generations, where the air speed is slow. Hence, the residence time of the particles is longer.

- **SUSPENSION:** In this phenomenon, aerosol particles move irregularly in the airways from one place to another. This happens as a result of the Brownian diffusion of particles with an MMAD smaller than 0.5  $\mu\text{m}$  when they reach the alveolar spaces, where the air speed is practically zero. These particles are not deposited in the respiratory track and are excluded out during exhalation.

- ❖ Okuda T *et al* (2015) [132] used two types of biodegradable polycation (PAsp(DET) homopolymer and PEG-PAsp(DET) copolymer) as vectors for inhalable dry gene powders prepared by spray freeze drying (SFD). The prepared dry gene powders had spherical and porous structures with particle size of 5-10  $\mu\text{m}$ . *In-vitro* inhalation study was carried out using Andersen cascade impactor. Inhalation performance of dry powders could markedly improve on the addition of L-leucine.

- ❖ Lindert S *et al* (2014) [133] mentioned aerosol administration through pulmonary route is affected by the anatomy of the upper airways and the inhalation pattern and these parameter changes on age. Considering this aspect, different upper airway models that representing the geometries of adults and preschool children, and a conventional induction port (as per specification of European Pharmacopeia) were used for *in vitro* testing of dry powder inhalers with single dosed capsules (Cyclohaler®, Handihaler® and Spinhaler®). Deposition of particles was measured at steady flow rates of 30 and 60 l/min for the Handihaler®/Spinhaler® and 30, 60 and 75 l/min for the Cyclohaler®. The inhalation volume was set at 1 litre. For the Cyclohaler®, the *in vitro* testing was supplemented by a paediatric inhalation profile. Slight differences of pulmonary deposition between the idealized adult (11 % – 15 %) and paediatric (9 %–11 %) upper airway model were observed for the Cyclohaler®.

- ❖ Demoly P *et al* (2014) [134] clarified the complex inter-relationships between inhaler design and resistance, inspiratory flow rate (IFR), FPF, lung deposition and clinical outcomes, as a better understanding may result in a better choice of DPI for individual patients. Aerodynamic particle size distribution, the inspiratory

manoeuvre, airway geometry and the three basic principles that determine the site and extent of deposition: inertial impaction, sedimentation and diffusion.

- ❖ Wang YB *et al* (2014) [129] studied on *in vitro* and *in vivo* performance of an amorphous formulation prepared by thin film freezing (TFF) and a crystalline micronized formulation produced by milling was compared for Tacrolimus. When emitted from a Miat ® monodose inhaler, TFF-processed TAC formulations exhibited a fine particle fraction (FPF) of 83.3 % and a mass median aerodynamic diameter (MMAD) of 2.26 µm. Single-dose 24 hr pharmacokinetic studies in rats demonstrated that the TAC formulation prepared by TFF exhibited higher pulmonary bioavailability with a prolonged retention time in the lung, possibly due to decreased clearance (e.g., macrophage phagocytosis), compared to the micronized TAC formulation. Additionally, TFF formulation generated a lower systemic TAC concentration with smaller variability than the micronized formulation following inhalation, potentially leading to reduced side effects related to the drug in systemic circulation.
- ❖ Sinha B *et al* (2012) [135] prepared Poly-lactide-co-glycolide nanoparticles (207–605 nm) containing voriconazole (VNPs) were developed using a multiple-emulsification technique and were also made porous during preparation in presence of an effervescent mixture for improved pulmonary delivery. Pulmonary deposition of the particles was studied using a customized inhalation chamber. VNPs had a maximum of 30 % (w/w) drug loading and a zeta potential (ZP) value around –20 mV. In the initial 2 hr, 20 % of the drug was released from VNPs, followed by sustained release for 15 days. Porous particles had a lower mass median aerodynamic diameter (MMAD) than nonporous particles. Porous particles produced the highest initial drug deposition (~120 µg/g of tissue).
- ❖ Sinha B *et al* (2012) [136] designed a dry powder inhaler (DPI) for delivery of dry powder and a nose-only inhalation chamber for small animals that can be used with nebuliser/DPI. The inhalation chamber was made with a polypropylene-rectangular box and centrifuge tubes. DPI was made of a polypropylene tube. Micronized Voriconazole and Voriconazole solution were used for DPI and nebulizer, respectively, for both *in vitro* and *in vivo* studies. *In vitro* drug deposition from

nebulizer was found to be 11–26 % w/w and that from DPI was 42 to 57 % w/w depending on experimental set up. Uniform deposition across all the inhalation ports was observed irrespective of the methods. Repairable fraction (RF) varied from 34 to 73 % in case of nebulizer and from 47 to 54 % in case of DPI. *In vivo* deposition of Voriconazole in lungs was found to be 80–130 µg/g from DPI and 40–68 µg/g from nebulizer.

- ❖ Geller DE *et al* (2011) [137] mentioned PulmoSphere™ technology is an emulsion-based spray-drying process that enables the production of light porous particle, dry-powder formulations, which exhibit improved flow and dispersion from passive dry powder inhalers. They explored the fundamental characteristics of PulmoSphere technology, focusing on the development of a dry powder formulation of Tobramycin for the treatment of chronic pulmonary *Pseudomonas aeruginosa* infection in cystic fibrosis (CF) patients.
- ❖ Murthy TEGK *et al* (2010) [73] developed DPI for Triotropium Bromide with a view to treat broncho spasm associated with chronic obstructive pulmonary disease (COPD). The formulations were prepared with different grades of Lactose monohydrate like Lactohale 300, Sorbolac 400, Inhalac 230, Respitose SV003, DCL 11 and Flowlac 100 and evaluated for physical appearance, average fill weight per capsule, content uniformity, uniformity of delivered dose, emitted dose. The influence of composition of DPI and overages on performance of DPI was studied. The better fine particle fraction was obtained from the DPIs formulated with 10:90 ratio of fine lactose (Lactohale 300): coarsely lactose (Respitose SV003) and having 20 % w/w overages.
- ❖ Westerman EM *et al* (2007) [138] mentioned DPI may be an alternative to nebulisation of drugs in the treatment of chest infections in CF patients. Ten CF-patients, chronically infected with *P. aeruginosa*, participated in a randomised cross over study. Patients inhaled Colistin sulphomethate as 25 mg dry powder (Twincer®) or as 158 mg nebulised solution (Ventstream® nebuliser, PortaNeb® compressor) on two visits to the outpatient clinic. Pulmonary function tests were performed before, 5 and 30 min after inhalation. Serum samples were drawn prior to each dose and at 15, 45, 90, 150, 210, 330 min after inhalation. The DPI was well tolerated by the patients

and no significant reduction in FEV1 was observed. Relative bioavailability of DPI to nebulisation was 140 % based on actual dose and 270 % based on drug dose label claim.

- ❖ Muttill P *et al* (2007) [139] prepared microparticles containing large payloads of two anti-tuberculosis (TB) drugs and evaluated for the suitability as a dry powder inhalation targeting alveolar macrophages. Microparticles were administered to mice using an in-house inhalation apparatus or by intra-tracheal instillation. Drugs in solution were administered orally and by intra-cardiac injection. Microparticles having drug content ~50 % (w/w), particle size ~5 µm and satisfactory aerosol characteristics (median mass aerodynamic diameter, MMAD= 3.57 µm; geometric standard deviation, GSD= 1.41 µm; fine particle fraction, FPF<4.6 µm = 78.91 ± 8.4%) were obtained in yields of >60 %. About 70 % of the payload was released *in vitro* in 10 days. Microparticles targeted macrophages and not epithelial cells on inhalation. Drug concentrations in macrophages were ~20 times higher when microparticles were inhaled rather than drug solutions administered.

## 2.5. Pulmonary route of administration

The pulmonary route is a potent non-invasive route for systemic and local delivery. The aerosolized formulation not only affects locally its main site of action but also avoids remaining in circulation for a long period of time in peripheral blood [109]. The pulmonary administration of therapeutic macromolecules for systemic delivery is receiving a great deal of attention on account of the promising anatomical features of the lung; particularly its large absorptive epithelial surface area. The development of adequate delivery systems has become an important issue, with the fundamental requirement that inhaled particles must possess appropriate aerodynamic properties to reach the deep lung [140]. Therapeutic macromolecules (i.e. peptides and proteins) are prone to intestinal enzymatic degradation and exhibit poor membrane permeability due to their hydrophilicity and large size. This is the explanation for their usual administration as injectable formulations, which causes patient's pain and discomfort. Thus, these molecules are good candidates for non-invasive administration through mucosal routes, such as the pulmonary. Lungs are ideally suited for this purpose as they are characterized by large absorptive surface area, high vascularization and thin blood–alveolar barrier which, together, facilitate macromolecule transport into

systemic circulation. When compared to the oral route, lungs have become more enticing for drug delivery due to the absence of hepatic first pass-effect and low enzymatic activity. Besides, the possible targeted drug delivery to the lungs is an attractive therapeutic approach that may result in reduced administered dose, as well as reduced drug side effects [95].

### **2.5.1. Advantages and disadvantages**

This has resulted in significant improvement in methods to induce drug accumulation in target tissues with subsequent reduction in non-specific effects, a major limitation encountered in conventional therapies for chronic conditions [12]. The potential advantages of direct delivery of the TB drug to the lungs include the possibility of reduced systemic toxicity, as well as achieving higher drug concentration at the main site of infection [141]. Direct drug administration to the lungs via inhalation offers several theoretical advantages over systemic delivery, including the possibility of regional drug delivery to the lungs and airways with lower doses and fewer systemic side effects, avoiding first-pass metabolism of the drug in the liver and the use of a non-invasive “needle-free” delivery system. The alveolar surface also provides a large surface area for rapid systemic absorption of drugs [128].

### **2.5.2. Drug deposition**

The anatomy and physiology of pulmonary tract offers enhanced drug absorption through inhalation drug delivery system. Since, the delivery system delivers the drug as a fine particle to the respiratory tract in the large pulmonary surface area (more than 100 m<sup>2</sup>) and the smaller epithelium layer of thickness 0.2–1 µm. Pulmonary delivery is more attractive for systemic delivery since this region is rich in blood supply and allows fast absorption (high solute permeability) and fast onset of drug action. Drug particles with 2-5 µm size are suitable for topical delivery and less than 2 µm particle size is required for systemic effects. In contrast, particles smaller than 0.5 µm may not deposit at all, since they move by Brownian motion and settle very slowly. Moreover they are inefficient as a 0.5 µm sphere, which delivers only 0.1 % of the mass that carries into the lungs. Further if particles are very small it will be exhaled [13]. The optimal size range for the DPI formulation is 1-5 µm. Particles with 5 µm deposit in the bronchial region of the respiratory tract and particle size of 1-3 µm range reaches the alveoli [130].

### **2.5.3. Drug delivery devices**

Inhaler device has major influence on the performance of the dosage form. Inhalers are small hand-held devices where medicine is released as spray into the mouth, from a small canister and reaches the lung directly. Like a skin ointment, inhalers can be likened to a lung ointment for the windpipes. The drug-blend is filled in hard gelatine / hydroxyl propyl methyl cellulose capsules of suitable size and dispersed through suitable inhaler device. The selection of inhalation devices depends upon the formulation and capacity to handle the device by the patient. Pre-metered formulation contains previously measured doses or unit doses (e.g. single or multiple doses in blisters, capsules, or other cavities) that are consequently inserted into the device by the patient before use. Thereafter, the dose may be inhaled directly from the pre-metered unit or it may be transferred to a chamber before being inhaled by the patient. Device-metered DPIs have an internal reservoir containing sufficient formulation for multiple doses that are metered by the device itself during actuation by the patient. Several devices are available in the market for aerosolization and each device is unique in its own way of delivering drug. The devices are made as pre-metered or device metered dry powder inhaler and both can be driven by patient inspiration alone or with some type of power-assistance. Differentiation of device design causes variation in performance based on the capacity of patients' inspiratory flow rate [130].

### **2.5.4. Structure of lungs**

Lungs are tremendous sponges of blood that also act as enormous filters that purify the air we breathe. The respiratory tract is especially designed, both anatomically and functionally, so that air can reach the most distal areas of the lungs in the cleanest possible condition. Nasal hairs, nasal turbinate, vocal chords, the cilia of the bronchial epithelium, the sneeze and cough reflexes, etc., all contribute to this filtering process. Most of the occasions it worked properly [142].

Various levels of airways in the lungs can generally be categorized into two parts: the conducting zone and the respiratory zone. The conducting zone consists of the first 16 generations of airways. This zone begins with trachea (generation 0), which divides into the two main bronchi. These two main bronchi further subdivide into smaller bronchi that enter into two left and three right lobes. Inside each lobe, the bronchi continue to undergo further division to form new generations of smaller calibre airways, the bronchioles. The



conducting zone ends with terminal bronchioles (generation 16), the smallest airways devoid of alveoli. The airways in the conducting zone do not participate in gas exchange. Their main function is to allow the bulk flow of air to move into and out of the lungs during each breath. The respiratory zone is the region where gas exchange occurs. It starts at the respiratory bronchioles (generation 17). These bronchioles further divide into additional respiratory bronchioles. This branching process continues through alveolar ducts and terminates in the alveolar sacs (generation 23) [131].

From the trachea to the alveolar sacs, two pronounced physical changes occur in the airways. First, the airway calibre decreases as the airways branch. For example, the trachea diameter (1.8 cm) is considerably larger than alveolar diameter (0.04 cm). This narrowing of airways allows adequate penetration of the air into the lower airways for a given expansion of the lungs. Second, the cross-sectional area of the airways increases during each division due to an increase in the number of the airways. The total surface area increases moderately over the levels of airways between the trachea and the terminal bronchiole (from 2.5 to 180 cm<sup>2</sup>). However, from the terminal bronchiole to the alveolar sac, the cross-sectional area increases dramatically (from 180 to 10,000 cm<sup>2</sup>), resulting in a significant decrease in the air flow velocity and promoting extensive and efficient diffusional gas exchange between the alveolar space and blood in the pulmonary capillaries. These changes in the air flow velocity and surface area have a significant effect on drug deposition in the lungs and systemic absorption of the inhaled drug, as explained below [131].

#### **2.5.5. Factors affecting drug deposition in lungs**

There are several factors are affecting the drug deposition in the different region of the lungs are mentioned as follow [81]:

##### **2.5.5.1. Particle Size and Shape**

It can generally be considered that particles with an MMAD higher than 10µm are deposited in the oropharynx, those measuring between 5 and 10µm in the central airways and those from 0.5 to 5 µm in the small airways and alveoli. Therefore, it is better to use particles with an MMAD between 0.5 to 5 µm in respiratory treatment. This is also being known as breathable fraction of an aerosol.

**2.5.5.2. Airflow velocity**

Particles are transported through the airway by an air current; their trajectories are affected by its characteristics. The air flow in the lungs is determined by the tidal volume and respiratory rate. Particles deposition increases for any size particle as the inspiratory flow increases. A minimal inspiratory flow is necessary to drag the particles toward the interior of the bronchial tree.

**2.5.5.3. Airway geometry**

The probabilities of particle deposition by impaction increase when the particles themselves are larger, the inspiratory airflow is greater, the angle separating the two branches is wider and the airway is narrower. In pathologies such as chronic bronchitis or asthma, which may alter the lung architecture with the appearance of bronchoconstriction, inflammation or secretion accumulation, the deposition of aerosolized drugs is modified.

**2.5.5.4. Degree of humidity**

The particles of aerosolized drugs can be hygroscopic to a greater or lesser extent. Hygroscopicity is the property of some substances to absorb and exhale humidity depending on the setting in which they are found. This means that they can get larger or smaller in size upon entering into the airway, with the consequent modification in the deposition pattern compared to what was initially expected. The diameter that a particle reaches after hygroscopic growth depends on its initial diameter, the intrinsic properties of the particle, and the environmental conditions in the airways. The mole fraction of water vapour contained in the airway has been demonstrated to be an important factor related with the increase in the MMAD of the aerosol particles.

**2.5.5.5. Mechanisms for mucociliary clearance**

Once deposited in the airways, the particles can be carried by the mucociliary system, degraded or absorbed into the systemic circulation or the lymph ducts. The first of these mechanisms is found in the conducting airways (from the trachea to the terminal bronchioles), which have ciliated epithelium that are covered by two layers of mucus: a low-viscosity periciliary layer, or sol, and a thicker layer that covers the former, or gel. This biphasic layer of mucus protects the epithelium from dehydration, helping to humidify the air and providing a protective barrier by trapping inhaled particles. The

insoluble particles are trapped by the gel and they are moved toward the pharyngolaryngeal region by the movements of the ciliated epithelium, where it is either coughed up or swallowed. The clearance speed depends on the number of ciliated cells and the cilia beat frequency, and it may be affected by factors that influence the function of the cilia or the quantity or quality of the mucus.

- ❖ Paranjpe M *et al* (2014) [143] mentioned the pulmonary route, owing to a noninvasive method of drug administration, for both local and systemic delivery of an active pharmaceutical ingredient (API) forms an ideal environment for APIs acting on pulmonary diseases and disorders.
- ❖ Sung JC *et al* (2009) [144] formulated PA-824, a Nitroimidazopyran with promise for the treatment of tuberculosis, for efficient aerosol delivery to the lungs in a dry powder porous particle form. The physical, aerodynamic, and chemical properties of the dry powder were stable at room temperature for 6 months and under refrigerated conditions for at least 1 year. Pharmacokinetic parameters were determined in guinea pigs after the pulmonary administration of the PA-824 powder formulation at three doses (20, 40, and 60 mg/kg of body weight) and compared to those after the intravenous (20 mg/kg) and oral (40 mg/kg) delivery of the drug. Animals dosed by the pulmonary route showed drug loads that remained locally in the lungs for 32 hr postexposure, whereas those given the drug orally cleared the drug more rapidly.
- ❖ Mansour HM *et al* (2009) [145] mentioned the lung is an attractive target for drug delivery due to non-invasive administration via inhalation aerosols, avoidance of first pass metabolism, direct delivery to the site of action for the treatment of respiratory diseases, and the availability of a huge surface area for local drug action and systemic absorption of drug. Colloidal carriers (i.e., nano-carrier systems) in pulmonary drug delivery offer many advantages such as the potential to achieve relatively uniform distribution of drug dose among the alveoli, achievement of improved solubility of the drug from its own aqueous solubility, a sustained drug release which consequently reduces dosing frequency, improves patient compliance, decreases incidence of side effects, and the potential of drug internalization by cells.

- ❖ Garcia CL *et al* (2006) [81] studied the efficiency of Rifampicin-loaded polymeric microspheres (RPLGA) delivered to guinea pigs infected with *Mycobacterium tuberculosis* (H37Rv) was compared with a daily dose of nebulised Rifampicin suspension. Drug and polymer treated multiple dose groups exhibited significantly lower wet lung weights than untreated animals. Spleen wet weights and viable bacterial counts (VBCs) were much lower for drug microsphere treated animals than for all other groups.
- ❖ Putte BPV *et al* (2005) [146] mentioned that isolated lung perfusion (ILuP) is an experimental surgical technique for the treatment of pulmonary metastases. They demonstrated a wide range in drug lung levels in phase-I trials. That might be due to the variance of lung size and pulmonary intravascular volume (PIV). Therefore, they developed AMETHOD to assess PIV and investigated the relation of PIV and dry lung weight (DLW). Thirty-two rats of 555G8 and 199G5 g underwent left ILuP two, four and eight minutes. Venous effluent was analyzed for haemoglobin, red blood cells (RBC), leucocytes, platelets, albumin and creatinine. PIV was calculated by dividing the product of perfusate volume and post-ILuP parameter by the difference between post-ILuP and pre-ILuP parameter. No significant differences in PIV for all perfusion times were noted between the different variables ( $P=0.14$ ). Based on haemoglobin ( $P<0.0009$ ), RBC ( $P=0.006$ ), leucocytes ( $P=0.0003$ ), platelets ( $P=0.017$ ) and creatinine ( $P=0.003$ ) analysis, PIV was significantly smaller in rats of 199 g while PIV/DLW ratio was not significantly different.
- ❖ Rabbani NR *et al* (2005) [82] mentioned pulmonary drug delivery is an attractive, convenient and effective route for the administration of therapeutic macromolecules, such as gene therapy agents and proteins and peptides, as well as systemically acting drugs, including hormones.

## CHAPTER 3: Materials and Methods Pertaining to Prothionamide

### 3.1. List of materials and equipments (Common for PTH & ETH formulation and estimation)

**Table 3. 1: List of materials used in this project**

SR. NO	NAME	OBTAINED FROM
1.	Prothionamide	Yarrow Chem products, Mumbai
2.	Ethionamide	Shiro Pharma Chem. Pvt Ltd, Navi Mumbai
3.	Chitosan (>75% deacetylation) Himedia	Gift sample from Department of Biotechnology, Agriculture University, Junagadh
4.	Sodium Tripolyphosphate (Sigma Aldrich)	
5.	PLGA (75:25)	Gifted by Evonik Industries, Darmstadt, Germany
6.	PLGA (50:50)	
7.	Inhalable Lactose Anhydrous	Kerry Ingredients, USA
8.	Poloxamer P 188	Gifted by BASF, Mumbai
9.	Ketamine	Instrumentation India Pvt. Ltd., Kolkata
10.	Xylazine	
11.	Poly vinyl alcohol	Yarrow Chem products, Mumbai
12.	Acetronitile (HPLC grade)	Merck Specialties Pvt. Ltd, Merck Millipore, Mumbai
13.	Calcium chloride dihydrate	
14.	Dichloromethane	
15.	Glacial acetic acid	

SR. NO	NAME	OBTAINED FROM
16.	Acetone	Merck Specialties Pvt. Ltd, Merck Millipore, Mumbai
17.	Magnesium chloride (hexahydrate)	
18.	Potassium chloride	
19.	Potassium dihydrogen phosphate	
20.	Sodium acetate (trihydrate)	
21.	Sodium chloride	
22.	Sodium citrate dihydrate	
23.	Sodium hydrogen carbonate	
24.	Sodium hydroxide	
25.	Sodium phosphate monobasic monohydrate	
26.	Sodium sulfate (anhydrous)	

**Table 3. 2: List of apparatus used in this project**

SR. NO	NAME OF APPARATUS	MANUFACTURED BY
1.	Mono-dose inhaler	Obtained as gift sample from MIAT S. P. A. Milano, Italy
2.	Nasal insufflators	

**Table 3. 3: List of equipments used in this project**

SR. NO	NAME OF INSTRUMENT	MANUFACTURED BY
1.	Probe Sonicator Power variation 0-100 %	BANDELIN electronic GmbH & Co. KG, Berlin Germany
2.	Vortex Mixture- CM101	Remi Elektrotechnik Ltd, Thane
3.	UV spectrophotometry-1800	Shimadzu Corporation, Kyoto, Japan

SR. NO	NAME OF INSTRUMENT	MANUFACTURED BY
4.	High performance liquid chromatography with C18 Column (Phenomenex)	Shimadzu Corporation, Kyoto, Japan
5.	Magnetic stirrer with hot plate	Macro Scientific work, 10A/UA, Jawahar Road, Delhi
6.	Centrifuge, C-24 PLUS Rotor no15, 18000 rpm, Cap: 12 X15	Remi Elektrotechnik Ltd, Thane
7.	FTIR	Perkin Elmer (Massachusetts, USA)
8.	Lyophilizer, OPR-FDU-7003-70°C with automatic vacuum	Operon, Korea
9.	Particle size analyzer	Zetatrak, Microtrak Inc. Toronto
10.	Particle size analyzer	Malvern, UK
11.	Eight Stage Cascade impactor	Thermo Fisher Scientific, USA
12.	Dissolution apparatus	Labard Instruchem Private Limited, Kolkata
13.	Stability chamber	
14.	Gas chromatography with head space	Auto System XL, Perkin Elmer, Japan
15.	Scanning Electron microscope with SE detector, EVO-18	Carl Zesis, Germany
16.	Melting point apparatus	Sunsim India Pvt. Ltd, New Delhi

## 3.2. Excipients profile

### 3.2.1. Chitosan

Chitosan / kartesean/ is a linear polysaccharide composed of randomly distributed  $\beta$ -(1 $\rightarrow$ 4)-linked D-glucosamine (deacetylated unit) and N-acetyl-D-glucosamine (acetylated unit). It is made by treating the chitin shells of shrimp and other crustaceans with an alkaline substance, like sodium hydroxide [147].

**Table 3. 4: Excipient's profile of Chitosan**

Product name	Chitosan
Non-sproprietary name	Chitosan
Appearance	Chitosan occurs as odourless, white or creamy-white powder or flakes. Fiber formation is quite common during precipitation and the chitosan may look 'cottonlike'.
Chemical formula	Poly-b-(1,4)-2-Amino-2-deoxy-D-glucose
Molecular weight	Chitosan is commercially available in several types and grades that vary in molecular weight by 10,000–1,000,000, and vary in degree of deacetylation and viscosity
Synonyms	2-Amino-2-deoxy-(1,4)-b-D-glucopyranan; chitosani hydrochloridum; deacetylated chitin; deacetylchitin; b-1,4-poly-D-glucosamine; poly-D-glucosamine; poly-(1,4-b-D-glucopyranosamine).
Solubility	Sparingly soluble in water; practically insoluble in ethanol (95%), other organic solvents, and neutral or alkali solutions at pH above approximately 6.5. Chitosan dissolves readily in dilute and concentrated solutions of acid.
Application	Coating agent; disintegrant; film-forming agent; mucoadhesive; tablet binder; viscosity increasing agent.
Viscosity	A wide range of viscosity types is commercially available. Owing to its high molecular weight and linear, un branched structure, chitosan is an excellent viscosity-enhancing agent in an acidic environment. It acts as a pseudo-plastic material, exhibiting a decrease in viscosity with increasing rates of shear.
Stability and storage Condition	Chitosan powder is a stable material at room temperature, although it is hygroscopic after drying. Chitosan should be stored in a tightly closed container in a cool, dry place.
Incompatibility	Chitosan is incompatible with strong oxidizing agents.
Safety	Chitosan is being investigated widely for use as an excipient in oral and other pharmaceutical formulations. It is also used in cosmetics. Chitosan is generally regarded as a nontoxic and non-irritant material. It is biocompatible with both healthy and infected skin. Chitosan has been shown to be biodegradable.
Regulatory status	Chitosan is registered as a food supplement in some countries



**3.2.2. Inhalable lactose anhydrous (INH 40 M 55.115)**

Lactose is a disaccharide molecule; a sugar composed of galactose and glucose that is found in milk. Lactose makes up around 2–8 % of milk (by weight). The name comes from “lac” (gen. lactis), the Latin word for milk, plus the -ose ending used to name sugars [149],[148].

**Table 3. 5: Excipient’s profile of inhalable lactose anhydrous**

Product name	Lactose
Non-proprietary name	BP: Anhydrous Lactose JP: Anhydrous Lactose PhEur: Lactose, Anhydrous USP-NF: Anhydrous Lactose
Appearance	Lactose occurs as white to off-white crystalline particles or powder. It is odourless and slightly sweet-tasting.
Chemical formula	$C_{12}H_{22}O_{11}$
Molecular weight	342.30
Synonyms	D-glucose,4-O-, beta-D-galactopyranosyl; D-glucose,4-O-, beta-D-galactopyranosyl Lactose anhydrous; Inhalac; inhalation lactose; Lactohale; Respitose
Melting point	202.8°C
Solubility	Soluble in water; sparingly soluble in ethanol (95 %) and ether; 40 gm/100mL at 25°C for typical Sheffield Pharmaceutical Ingredients products
Application	Diluents; dry powder inhaler carrier
Stability and storage condition	Inhalation lactose should be stored in a well-closed container in a cool, dry place.
Incompatibility	Lactose is a reducing sugar. Typical reactions include the Maillard reaction with either primary or secondary amines
Safety	Lactose is widely used in pharmaceutical formulations as diluents in oral capsule and tablet formulations, and has a history of being used in dry powder inhaler formulations.
Regulatory status	GRAS listed. Included in the FDA Inactive Ingredients Database (inhalation preparations). Included in non-parenteral and parenteral medicines licensed in the UK, which refer to lactose monohydrate in general

**3.2.3. PLGA (75:25)**

PLGA or poly(lactic-co-glycolic acid) is a copolymer which is used in a host of Food and Drug Administration (FDA) approved therapeutic devices, owing to its biodegradability and biocompatibility. PLGA is synthesized by means of ring-opening co-polymerization of

two different monomers, the cyclic dimers (1,4-dioxane-2,5-diones) of glycolic acid and lactic acid [149].

**Table 3. 6: Excipient's profile of PLGA (75:25)**

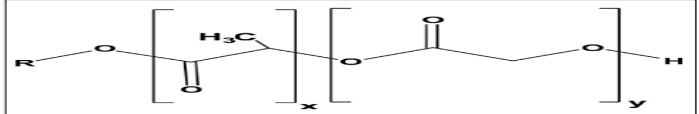
Product name	Poly(D,L-lactide-co-glycolide)
Non-proprietary name	Resomer RG 755S
Appearance	White to off-white solid
Chemical formula	$-(C_6H_8O_4)_x(C_4H_4O_4)_y)_n-$
Molecular weight	90,000-150,000 [150]
Synonyms	Poly(DI-Lactide-Co-Glycolide)
Melting point	45-90 °C
Flowability	Free flowing
Solubility	Soluble in Acetone , chloroform and Dichloromethane etc
Application	Polymer used to coat both hydrophilic and lipophilic drug
Viscosity	0.50 - 0.70 dl/gm
Stability and storage Condition	Store at 4-8 °C. Protect from moisture. Microspheres may be handled under nitrogen or other inert gas for best stability. Microspheres may be frozen / desiccated for long-term storage. Keep container tightly closed in a dry and well-ventilated place. Store in cool place. Store under inert gas. Moisture sensitive [151].
Incompatibility	Compatible with both hydrophilic and lipophilic drugs.
Safety	The application of biodegradable polymers in dental implants, nasal drug deliveries, contraceptive devices, immunology, gene, transdermal, ophthalmic and veterinary applications, as well as, the sterilization of biodegradable based formulations and regulatory considerations for product filing [21].
Regulatory status	Approved by US food and drug administration (FDA)

### 3.2.4. PLGA (50:50)

The forms of PLGA are usually identified by the monomer's ratio used. PLGA 50:50 is most frequently used in nanotechnology, identifies a copolymer whose composition is 50% lactic acid and 50% glycolic acid [152].

**Table 3. 7: Excipient's profile of PLGA**

Product name	Poly(D,L-lactide-co-glycolide)
Non-proprietary name	Resomer, RG 504

Appearance	White to off-white solid
Chemical formula	 $-(C_6H_8O_4)_x(C_4H_4O_4)_y-$
Molecular weight	48 kDa
Synonyms	Poly(DL-Lactide-Co-Glycolide)
Melting point	45-90°C
Flowability	Free flowing
Solubility	Water solubility is 0.32 % w/w. Soluble in chlorinated solvent, Acetone, chloroform and Dichloromethane etc
Application	Polymer used to coat both hydrophilic and lipophilic drug
Viscosity	45-60+ dl/g
Stability and storage Condition	Store at 4-8°C. Protect from moisture. Microspheres may be handled under nitrogen or other inert gas for best stability. Microspheres may be frozen / desiccated for long-term storage. Keep container tightly closed in a dry and well-ventilated place. Store in cool place. Store under inert gas. Moisture sensitive [151].
Incompatibility	Compatible with both hydrophilic and lipophilic drugs
Safety	The application of biodegradable polymers in dental implants, nasal drug deliveries, contraceptive devices, immunology, gene, transdermal, ophthalmic and veterinary applications, as well as, the sterilization of biodegradable based formulations and regulatory considerations for product filing [21].
Regulatory status	Approved by US food and drug administration (FDA)

### 3.3. Identification of drug

Before starting the product development, preliminary preformulation is the identification test of the procured drug to verify and ensure its purity. Identification of drug sample in the present investigations was based on its appearance, solubility, melting point and was confirmed by Fourier-transform infrared (FTIR) spectroscopic determination of various functional groups.

#### 3.3.1. Appearance

The procured drug sample was visually observed for its colour and was compared with the reported appearance of the drug.

### **3.3.2. Melting point**

Melting point is another most important identification test for solid substance. Generally, all the solid drugs have sharp or narrow range of melting point. Hence, it was determined for the sample by capillary method using melting point apparatus (Sunsim, India). After sealing one side, small amount of sample was filled in the capillary tube and placed in the melting point apparatus. The temperature at which the substance started to convert into liquid was recorded.

### **3.3.3. Infrared absorption**

The qualitative aspects of infrared spectroscopy are one of the most powerful attributes of this diverse and versatile analytical technique [153]. It is an important complementary tool for the solid-state characterization of pharmaceutical solids. The drugs were triturated with potassium bromide (1:20) in a glass mortar pestle to produce fine and uniform mixture. After preparing pellets, samples were placed on sample disc in the sample compartment. Sample was scanned at transmission mode in the range of 4000 to 600  $\text{cm}^{-1}$ . IR spectrum obtained was checked for functional group.

### **3.3.4. UV spectrophotometric method**

Maximum absorptivity is one of the unique properties of drug at respective solvent. 0.002 % w/v solution of Prothionamide was prepared in ethanol (95 %) and examined in the range of 230 nm to 350 nm according to IP.

## **3.4. Analytical method**

### **3.4.1. Estimation of Prothionamide using UV-Spectrophotometric method and its method validation**

#### **3.4.1.1. Preparation of pH 7.4 Phosphate buffer**

6.805 gm of Potassium dihydrogen phosphate and 1.564 gm of Sodium hydroxide were dissolved in sufficient quantity of water to produce 1000 ml. Finally pH was adjusted to 7.4 by drop wise addition of 0.5 M sodium hydroxide solution.

**3.4.1.2. Preparation of stock solution**

100 mg of Prothionamide (PTH) was weighed accurately and transferred to 100 ml volumetric flask. This sample was mixed vigorously with 50 ml of pH 7.4 phosphate buffer followed by sonication for 20 min. Finally volume was made up to 100 ml with pH 7.4 phosphate buffer to make 1000 µg/ml stock solution (S1). 1 ml of this solution was further diluted to 10 ml with same solvent to obtain 100 µg/ml stock solutions (S2).

**3.4.1.3. Preparation of working standard solution for calibration curve**

The standard stock solution or S2 (100 µg/ml) was further diluted with pH 7.4 phosphate to prepare working standard solution. Appropriate aliquots of the solution (0.4, 0.8, 1.2, 1.6 and 2.0 ml) were pipetted out into 10 ml validated volumetric flasks and made up to mark with pH 7.4 phosphate buffer. The diluted solutions were vortexed and then used for further analysis. pH 7.4 phosphate buffer was used as blank. The absorption maximum was determined by scanning the different diluted solutions at 200 to 400 nm in UV-double beam spectrophotometer. Repetition was made for five times and recorded the observations. The calibration curve was plotted between concentrations and absorbances.

**3.4.1.4. Method validation: Linearity**

The methods were validated according to ICH guidelines of Q2B (2005) in terms of linearity, sensitivity, precision and accuracy for each analyte. Linearity denotes the ability of the method to provide results directly proportional to the concentration of substance in question within a given application range [154]. The method linearity was assessed by linear regression analysis using the least-squares methods for the average points of three authentic calibration curves, at concentrations of 4, 8, 12, 16 and 20 µg/ml. Five point linear curve was prepared by plotting concentration (µg/ml) vs absorbance and correlation co-efficient was calculated.

**3.4.1.5. Limit of detection and limit of quantification**

The limit of detection (LOD) is defined as the lowest concentration of a substance that an analytical process can reliably distinguished from the absence of that substance but not necessarily quantified under the stated experimental conditions [155]. The limit of quantification (LOQ) is defined as the lowest concentration of standard curve that can able

to measure with acceptable accuracy, precision and variability (ICH guideline Q2B, 2005). The LOD and LOQ were calculated as

$$\text{LOD} = 3.3 \frac{\text{SD}}{\text{S}} \dots\dots\dots(1)$$

$$\text{LOQ} = 10 \frac{\text{SD}}{\text{S}} \dots\dots\dots(2)$$

where, S = slope of the linearity curve, SD = standard deviation of y-intercept

#### **3.4.1.6. Analysis of tablet formulation**

20 marketed tablets of Prothionamide (Protomid, Macleods Pharmaceuticals Ltd.) were weighed and ground to fine powder; amount equal to 10 mg of Prothionamide was taken in 100 ml of volumetric flask and the volume was made up to mark with pH 7.4 phosphate buffer. The flask was sonicated further for 20 min to solubilise the drug present in tablet powder. After sonication, filtration was done through Whatman filter paper No. 41. Filtrate was collected and further diluted with pH 7.4 phosphate buffer to get the final concentrations of drug in the working range. The absorbance of final diluted solution was observed at  $\lambda_{\text{max}}$ .

#### **3.4.1.7. Accuracy**

Accuracy is defined as the closeness of result that obtained near to its true value. It is often expressed as percentage recovery by analyzing known added amounts of analyte [156]. It is also can be expressed as the percent of recovered amount by assay from a known added amount. For its measurement, data from nine determinations over three concentration levels was chosen [157] at lower, intermediate and higher concentration, prepared from stock solutions followed by analysis the same. Here, recovery study was conducted at three different levels (80 %, 100 % and 120 %) [158] to assess accuracy.

#### **3.4.1.8. Precision**

Precision is the degree of repeatability of an analytical method under normal operational conditions [159]. Repeatability was calculated by taking different levels of concentrations, prepared from pure drug stock solution and analyzed. Intermediate precision was calculated by taking the variations of inter-day and intra-day response. Respective concentrations from stock solution in triplicates were prepared three different times in a

day and studied for intraday (n=9) and inter-day variation (n=15). The relative standard deviation in percentage (% RSD) of the estimated concentrations from the regression equation was taken as precision.

### **3.4.2. Preparation of standard curve of PTH in water-methanol system**

UV-spectrophotometric method for the estimation of PTH at pH 7.4 phosphate buffer is able to detect the un-entrapped/free PTH concentration in solution. In some situation like, stability study, delivery dose calculation, estimation of entrapped PTH is difficult as PTH coated with polymer. Lots of time will be taken to extract the PTH from nanoparticles using the pH 7.4 phosphate buffer. Therefore, alternate method was needed to extract drug from polymer coated nanoparticles. As PTH is soluble in methanol, combination solvent system of water-methanol (8:2) was used to detect this drug. Hence, separate standard curve was prepared in this solvent system.

#### **3.4.2.1. Preparation of stock solution**

10 mg of PTH was transferred into a 100 ml volumetric flask. 20 ml of Methanol was added into this drug to dissolve it completely. Volume was made up to mark with distilled water to prepare 100 µg/ml (S3).

#### **3.4.2.2. Detection of maximum absorptivity**

From the stock solution (S3), 1.0 ml of PTH solution was transferred to 10 ml volumetric flask and the volume was adjusted to the mark with same solvent to obtain 10 µg/ml. The wavelength of maximum absorptivity of PTH in specific media (water-methanol in 8:2 ratio) was determined by scanning the diluted solutions in the range of 200-400 nm.

#### **3.4.2.3. Construction of standard curve**

1, 1.5, 2, 2.5, 3, 3.5 and 4 ml of the above stock solution (S3) were transferred into 10 ml volumetric flask. The volume was made up to mark with combination solvent of water-methanol in the ratio of 8:2 to prepare 10, 15, 20, 25, 30, 35, 40 µg/ml solutions. These seven solutions were used to construct standard curve. Replication was made for three times.

### **3.4.3. Estimation of Prothionamide in rat plasma using HPLC method**

#### **3.4.3.1. Chromatography system and condition**

Analysis was performed with a Shimadzu (Japan) RP HPLC equipped with an SPD-10A UV–visible detector, Phenomenex ODS analytical column (250 mm × 4 mm internal diameter, 5 µm Particles). The mobile phase was a mixture of Water and Acetonitrile in the ratio of 70:30 (v/v). The flow rate was 1.0 ml/min and all the spectrums were monitored at 290 nm using Ethionamide as internal standard [55].

#### **3.4.3.2. Collection of plasma**

1 ml of blood sample was collected in to 2 ml micro centrifuge tube containing Sod-EDTA (1.5 mg). Centrifuge the blood sample at 3000 rpm for 10 min. 300 µl supernatant was collected using hand pipette attached with micro tip.

#### **3.4.3.3. Preparation of stock and diluted solution**

Weighed accurately 10 mg of Prothionamide and transferred into 100 ml volumetric flasks. 30 ml of HPLC grade Acetonitrile was added, and the mixture was sonicated to dissolve the drug and finally volume of this solution was made up with HPLC grade water (100 µg/ml) (S4). Prepared stock solution was filtered through 0.22 µm nylon membrane filter and then sonicated for degassing [155]. The stock solution was stored at 4 °C and protected from light [160].

#### **3.4.3.4. Selection of detection wavelength**

The UV spectrum of diluted solutions of various concentrations of PTH in mobile phase was recorded using UV spectrophotometer (Shimadzu-1800). The wavelength of maximum absorbance was recorded for the estimation of PTH.

#### **3.4.3.5. Construction of calibration plots**

Eight working standard solutions for calibration curve were prepared by adding 1, 5, 10, 50, 100, 150, 200, 250 µl of the aliquots from the stock solution (S4) with 200 µl of blank rat plasma and finally diluted up to 1 ml with mobile phase followed by vortex for 30 sec. The concentration of the prepared solution were 0.1, 0.5, 1, 5, 10, 15, 20, 25 µg/ml respectively. Thereafter, 90 µl of 30% trichloroacetic acid was added and vortexed the



mixture for 5 min. Centrifuged the resulted solution at 8000 rpm for 10 min. Sample solutions were filtered through 0.2  $\mu\text{m}$  cellulose nitrate (Whatman®) filter paper. 20  $\mu\text{l}$  of each solution was injected into the HPLC system to get the chromatograms. The peak area and retention time were recorded. Linearity curve was constructed by plotting concentration on X-axis and peak areas on Y-axis and regression equations were computed.

### **3.5. Formulation and characterization of DPI containing Prothionamide nanoparticles prepared by PLGA (75:25)**

#### **3.5.1. Compatibility study**

FTIR analysis was performed to study the chemical interaction between Prothionamide and PLGA using Perkin Elmer (Massachusetts, USA). FTIR spectra was recorded at room temperature to verify alteration in frequency and intensity of bands of pure drug in presence of excipients [161]. Two samples were run, one for Prothionamide and another for the physical mixture of Prothionamide, anhydrous inhalable grade lactose and PLGA. The samples were scanned in the IR range from 400 to 4000  $\text{cm}^{-1}$ .

#### **3.5.2. Preparation of PLGA-Prothionamide nanoparticles**

##### **3.5.2.1. Preparation of trial batch**

PLGA nanoparticles were prepared by solvent evaporation technique as reported earlier [26]. Initially, PVA concentration was kept at its saturated solubility of 3 % w/v in 20 ml. PTH (5 mg) and PLGA (5 mg) were dissolved in 2 ml of Dichloromethane (DCM). Organic solution added drop wise in to aqueous solution and probe sonicated for 20 min over ice bath. Organic solvent was evaporated for 12 hr under magnetic stirrer. Trial batche was prepared and check the suitability of adopted method. Sonication time influences more in the particle size and size distribution of nanoparticles. That's why six different formulations were prepared with varying sonication time, where PLGA, PTH, PVA amount and DCM volume were kept constant.

### 3.5.2.1. Preparation of PLGA nanoparticles for Box-Behnken design

PLGA and PTH were dissolved in common solvent of Dichloromethane and further transferred to 10 ml Polyvinyl alcohol solution followed by vortexing for 10 min. Micro-emulsion was formed when sonicated over the ice bath. The prepared emulsion kept on magnetic stirrer at room temperature for 2 hr to evaporate Dichloromethane. The nanoparticles were recovered by ultracentrifugation at 18000 rpm for 25 min at temp of  $-4^{\circ}\text{C}$  followed by single wash with distilled water. Freeze dried the prepared suspension using Mannitol 2 % w/v as cryoprotectant. In this process primary drying was carried out at  $-20^{\circ}\text{C}$  and secondary drying was carried out at  $-60^{\circ}\text{C}$ .

### 3.5.3. Experimental design

From the preliminary trials, a  $3^3$  Box-Behnken Design was employed to study the effect of independent variables on the dependent variables using design expert software [162]. Three independent variables were polymer amount ( $X_1$ ), concentration of surfactant in % w/v ( $X_2$ ), and organic phase volume in ml ( $X_3$ ). Before implementing the Box-Behnken design, dissolution was carried out for the trial batches and no significant differences was found. On the other hand, three dependent variables were particle size ( $Y_1$ ), percentage drug entrapment (PDE) ( $Y_2$ ), Polydispersibility index (PDI) ( $Y_3$ ). Effects of independent variables were studied at three different levels (Table 3. 8). Literature review also supported for the selection of dependent variables as particle size, percentage drug entrapment and polydispersibility index [163],[164],[165],[166],[167].

**Table 3. 8: Adopted variables and their levels in Box-Behnken design**

Independent variables / Factor	Levels		
	-1	0	1
$X_1$ = Polymer amount (mg)	1:1	1:3	1:5
$X_2$ = Surfactant Concentration (% w/v)	0.25	0.75	1.25
$X_3$ = Organic Phase volume (ml)	2	4	6
Dependent variables / Response	Constraints		
$Y_1$ = Particle size (nm)	Minimum		
$Y_2$ = Percentage drug entrapment (% w/w)	Maximum		
$Y_3$ = Poly dispersibility index	Minimum		

Equal molar drug and polymer is able to prepare the nanoparticles successfully. Hence, lower level of polymer amount was fixed as 25 mg and the upper limit was 125 mg due to

restriction of surfactant solution of 10 ml. PVA was used as surfactant to prepare emulsion and the lower limit for it was selected as its critical micelle concentration (CMC) of 0.25 % w/v. Solubility and viscosity of surfactant solution increases rapidly after CMC. That's why the upper limit of PVA concentration was chosen as five times of CMC means 1.25 % w/v. 125 mg of PLGA and 25 mg of PTH would able to dissolve successfully in 4 ml of DCM, hence 4 ml was chosen as lower limit of Factor X<sub>3</sub>. Due to volume restriction, upper limit of organic phase volume was chosen as 6 ml. The experiment design matrix generated by the software is shown in Table 3.9.

**Table 3. 9: Box Behnken experimental design.**

Formulation code	Factor X <sub>1</sub> (Polymer amount in mg)	Factor X <sub>2</sub> (Surfactant Concentration in % w/w)	Factor X <sub>3</sub> (Organic Phase volume in ml)
1	125	1.25	4
2	125	0.25	4
3	75	1.25	2
4	125	0.75	6
5	125	0.75	2
6	25	0.25	4
7	75	0.25	2
8	75	0.25	6
9	25	0.75	6
10	75	0.75	4
11	25	1.25	4
12	75	0.75	4
13	75	0.75	4
14	25	0.75	2
15	75	1.25	6

The polynomial equation can be used to draw conclusions after considering the magnitude of coefficient and the mathematical sign it carries, i.e. positive or negative [168]. The PTH-PLGA nanoparticles were prepared with different independent variable at different levels and response, particle size, PDE and PDI were obtained. The data was substituted to design expert software and polynomial equations were obtained. The polynomial regression results were expressed using 3-D graphs and contour plots. The non-linear quadratic model generated by the design was:

$Y = A_0 + A_1X_1 + A_2X_2 + A_3X_3 + A_4X_1X_2 + A_5X_2X_3 + A_6X_1X_3 + A_7X_1^2 + A_8X_2^2 + A_9X_3^2$ ,  
in which Y is the measured response of the dependent variables associated with each factor-level combination; A<sub>0</sub>-A<sub>9</sub> are the regression coefficients of the respective variables

and their interaction terms computed from the observed experimental values of Y; and  $X_1$ ,  $X_2$ ,  $X_3$  are the coded levels of independent variables. The term  $X_1$ ,  $X_2$  and  $X_3$  represent the interaction and quadratic terms respectively. The effect of independent variables on dependent variables was investigated through 3-D surface and contour plots [110]. Finally, the optimum formulation was selected based on the desirability factors.

### 3.5.3.1. Determination of drug entrapment, drug load, process yield

Free drug was estimated from supernatant obtained after centrifugation and estimated by UV-spectrophotometric method as mentioned in section 3.4.1. PDE, drug load and process yield in percentage were carried out as mention as follow [106],[112], [169].

$$\text{Drug Entrapment (\% w/w)} = \left( \frac{\text{Total weight of drug - untrapped drug weight}}{\text{Total weight of drug taken}} \right) \times 100 \quad \dots\dots\dots 1$$

$$\text{Drug Load (\% w/w)} = \left( \frac{\text{Total weight of drug - untrapped drug weight}}{\text{Total amount of polymer}} \right) \times 100 \quad \dots\dots\dots 2$$

$$\text{Process yield (\% w/w)} = \left( \frac{\text{Total weight of nanoparticles}}{\text{Weight of drug + polymer + cryoprotectant}} \right) \times 100 \quad \dots\dots\dots 3$$

### 3.5.3.2. Measurement of particle size, zeta potential and poly dispersibility index

Average particle size and Poly Dispersity Index (PDI) of the prepared nanoparticles were determined by laser dynamic light scattering using Zetatract, Microtrac Inc. USA. The PDI value indicates the particle size distribution of nanoparticles in a given sample. Higher value of PDI indicates the distribution of NPs with capricious size range due to aggregates results in low homogeneity. Zeta potential indicates the surface charge on the particles and was measured to determine the stability of nanoparticles in the suspension [110].

### 3.5.3.3. Scanning electron microscopy (SEM)

The shape and surface morphology of the nanoparticles were examined for the optimized batch by Scanning Electron Microscopy (Karl Zesis with SE detector, EVO-18). The samples were sputter-coated with gold and observed for morphology at an acceleration voltage of 7.0 kV with highest magnification of 19.99 KX.

#### **3.5.3.4. Residual solvent analysis**

Organic solvents are routinely applied during synthesis of drug substance, excipients or during drug product formation. They are not desirable in the final product, mainly because of their toxicity, influence on the quality of crystals of the drug substance and their odour or taste, which can be unpleasant for patients [170]. Here, PLGA is water insoluble polymer. Its copolymer is frequently dissolved in lipophilic solvent of dichloromethane (DCM) prior to mixing with drug aqueous solution [124]. DCM listed as class 2 solvent in ICH guideline. Hence, residual solvent study was conducted. Pure DCM and dried nanoparticles set in a closed vessel until the volatile components reach equilibrium between the sample and the gas volume above, i. e. the so called “headspace”. An aliquot of the headspace is sampled and introduced into gas chromatographic column for analysis. In this analysis, nitrogen as carrier gas was used with a flow rate of 1 ml/min. The analytical time was set at 15 min. Rising the temperature was carried out at 10 °C per min up to 240 °C for 15 min.

#### **3.5.3.5. Differential scanning calorimetry (DSC)**

Differential Scanning Calorimetry (DSC) is a thermoanalytical technique that is used to demonstrate the energy phenomena produced during heating or cooling of a substance (or a mixture of substances) and to determine the changes in enthalpy and specific heat and the temperatures at which these occur [171]. DSC-60 instrument from Shimadzu Corporation, Kyoto, Japan was used for this study. Approximately 5-10 mg of samples (pure PTH, PLGA polymer and PTH-PLGA nanoparticles) were placed in aluminium pans and were crimped followed by heating at a scanning rate of 20 °C/min from 20 °C to 250 °C [117]. Aluminium pan containing same quantity of Indium was used as reference. Both the sample and reference are maintained the same temperature throughout the experiment.

#### **3.5.4. Formulation of dry powder inhaler and characterization**

Prothionamide nanoparticles and anhydrous inhalable lactose were mixed manually by geometrical dilution process. Bulk and tapped density were carried out in each stage upon addition of lactose. Optimization of dry power inhaler was carried out based on the excellent flow property. Zeta size and potential were carried out to check the stability of nanoparticles in the form of DPI. Similarly DPI of pure drug also carried out by diluting the pure PTH with inhalable grade lactose.

**3.5.4.1. Determination of MMAD using cascade impactor**

Aerodynamic diameter of a particle controls its deposition in pulmonary tract. MMAD represents aerodynamic diameter below which 50 % particles remain. MMAD of the optimized dry powder inhaler was determined using an eight stage cascade impactor. Effective cut off diameter for each impactor stage were calibrated by manufacturer and stated as follow: stage zero (9  $\mu\text{m}$ ); stage one (5.8 $\mu\text{m}$ ); stage two (4.7  $\mu\text{m}$ ); stage 3 (3.3  $\mu\text{m}$ ); stage 4(2.1  $\mu\text{m}$ ); stage 5 (1.1  $\mu\text{m}$ ); stage 6 (0.7  $\mu\text{m}$ ); stage 7 (0.4  $\mu\text{m}$ ). Firstly DPIs were passed through the cascade impactor with a flow rate of 28.3 l/min. Thereafter, the content of each chamber by dissolving in water-methanol (8:2) and determined the PTH content at 287.40 nm (section 3.4.2). These values were inserted into the MMAD CALCULATOR to obtain MMAD and geometric standard deviation (GSD) [136]. Fine particle fraction (particles < 5  $\mu\text{m}$ ) is representative of those particles that have a high probability of penetrating into the deep lung. Size of stage 2 in cascade apparatus is 4.7  $\mu\text{m}$ . Hence, percentage deposition from stage 2 to filter was calculated as fine particle fraction. Extra fine (<1.0 $\mu\text{m}$ ) particles improve peripheral lung deposition and that inhalers with flow rate-independent fine particle fraction produce a more consistent delivered dose to the lungs [134]. Chamber 6 contains 0.7  $\mu\text{m}$  pore size. Hence, percentage deposition in stage 6, 7, and filter was calculated to find the extra fine fraction. Amount deposited in each chamber was calculated and sum of each deposition was the emitted dose.

**3.5.4.2. *In-vitro* release study**

5 mg PTH equivalent DPIs were dispersed in 2 ml of simulated lungs fluid (SLF) [172] and subsequently filled in dialysis bag (12,000 molecular weight cut off). Composition of simulated lung fluid is given in Table 3. 10. To avoid floating, the drug filled bag was tied over the glass plate and kept at the bottom of the dissolution chamber. *In-vitro* release study was carried out in 1l SLF maintained at 37  $\pm$ 0.5°C with a paddle speed of 100 rpm [173]. 10 ml of dissolution fluid was withdrawn at each hour up to 24 hr and replaced with fresh SLF.

**Table 3. 10: Composition of simulated lung fluid**

Sl. No	Component	Quantity (gm/l)
1	Magnesium chloride (hexahydrate)	0.2033
2	Sodium chloride	6.0193
3	Potassium chloride	0.2982
4	Sodium sulfate (anhydrous)	0.0710
5	Calcium chloride dehydrate	0.3676
6	Sodium acetate (trihydrate)	0.9526
7	Sodium hydrogen carbonate (NaHCO <sub>3</sub> )	2.6043
8	Sodium citrate dehydrate	0.0970
9	Sodium phosphate monobasic monohydrate	0.1420
<b>Properties</b>		
1	pH	7.4

#### 3.5.4.3. Stability study

Stability study was carried out as per the ICH guideline Q1A (R2). Paraffin tape was used to seal cryoprotectant vials contained freshly prepared DPI of PTH nanoparticles. These vials were kept in stability chamber and maintained at  $25 \pm 2$  °C &  $60 \pm 5$  % RH. The nanoparticles were analyzed for the period of 6 months [174]–[175]. Zeta size, zeta potential, PDI, drug entrapment and drug release were carried out to check the stability of dry powder inhaler of PTH nanoparticles.

#### 3.5.4.4. Design of DPI device and delivery dose calculation

Development of pharmaceuticals for inhalation is a particular challenge, as it involves the preparation of a formulation and the selection of a device for aerosol dispersion. Most DPIs contain micronized drug blended with larger carrier particles, which prevents aggregation and helps flow. The dispersion of a dry powder aerosol is conducted from a static powder bed. To generate the aerosol, the particles have to be moved. When the patient activates the DPI and inhales, airflow through the device creates shear and turbulence; air is introduced into the powder bed and the static powder blend is fluidized and enters the patient's airways [127]. Mono-dose inhaler and nasal insufflators were

obtained as a gift sample from MIAT S. P. A. Milano, Italy for this project. But these devices are helpful for the DPI delivery in human but not for rodent (Figure 3. 1). Hence, it is highly required to design a delivery device for effective delivery of dry powder inhaler for rat (selected animal). Penn Century marketed different device model for individual animal like mice, rat, guinea pig etc [176]. Specimen of the delivery device reported is shown in Figure 3. 2. With same feature, delivery device was designed for intra tracheal or intranasal use in rat. Application of this device also reported in literature [177].

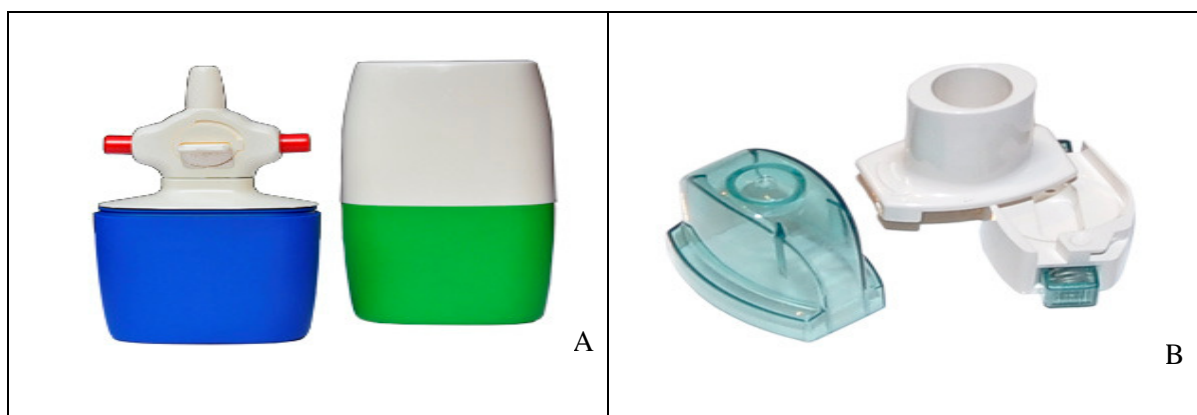


**Figure 3. 1: Pulmonary administration for human: (A) Monodose nasal insufflators, (B) Monodose inhaler**

After design, the efficiency of the delivery device checked by spraying the optimized DPI. Total content of the DPI was segregated in three parts and sprayed. Cleaned the needle and syringe with 10 ml of water-methanol solvent in 8:2 ratio. This solution was stirred for 20 min under magnetic stirrer followed by filtration. The filtrate was estimated for PTH content under UV-spectrophotometer. From this percentage dose delivery, fine particle fraction, extra fine particle fraction and emitted dose were calculated.

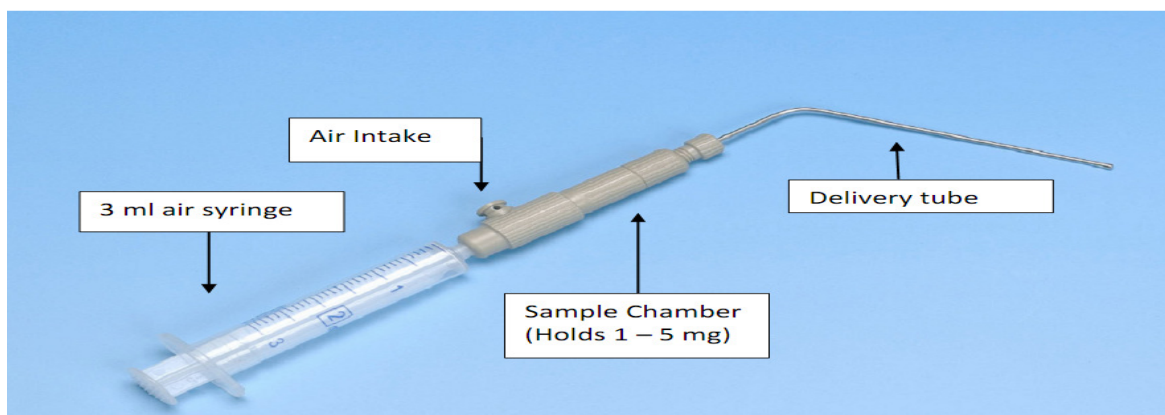


**Figure 3. 2: Penn-Century Dry Powder Insufflator™ Model DP-4**



### **3.5.5. *In-vivo* study**

All animal experiments were approved and performed in accordance with the guidelines of institutional animal ethical committee of Bengal College of Pharmaceutical Sciences and Research, Durgapur, West Bengal (Registration No: 1799/PO/ Ere/15/S/CPCSEA under CPCSEA, India).

#### **3.5.5.1. Animal**

Wistar rats (*Rattus norvegicus*) (4-6 month old & average weight 200-250 g) of both sexes were used to study the pharmacokinetic parameters of PTH in the form of DPI. The rats were housed for 12 hr light/dark cycle with free availability of food and water. Rats were divided into two groups: Group I treated with DPI of Prothionamide-PLGA nanoparticles and group II treated with pure Prothionamide [178]. In each group, 18 animals were selected. In each study time, three animals were sacrificed after 1<sup>st</sup>, 2<sup>nd</sup>, 3<sup>rd</sup>, 6<sup>th</sup>, 12<sup>th</sup>, 24<sup>th</sup> hr of drug administration. The carcasses were disposed through pollution control board and as per norms after experimentation.

#### **3.5.5.2. Anaesthetic dose and DPI administration**

Ketamine at the dose of 80 mg/kg was given to rat, that body weight less than 0.23 kg and the dose strength increased to 100 mg/kg in higher weight of rat. Similarly xylazine at the dose level of 10 mg/kg under the rat weight of 0.230 kg and this dose increased to 15 mg/kg for higher weight of rat. Two different drug solutions were prepared for Ketamine (1000 mg in 25ml) and Xylazine (200 mg in 25 ml). Depending upon body weight, calculated dose administered to the respective rat. Dry powder inhaler delivery device was designed with little modified as described previously [132]. Tongue was gently pulled outside and placed the DPI device in the trachea and sprayed the DPI.

#### **3.5.5.3. Dose calculation of Prothionamide for pulmonary delivery**

**i) DOSE CALCULATION OF PROTHIONAMIDE FOR HUMAN:** Target concentration of Prothionamide is 2 mg/l or 2 µg/ml (MIC= 0.5 µg/ml) [55],[56]. Human lungs volume (4.341 l) [174] was used to calculate the human dose of Prothionamide for pulmonary administration. Dose has been categorized in two parts: One is initial dose and another is maintenance dose.

$$\text{Initial dose} = C_T * V_L = 2 * 4.341 = 8.682 \text{ mg}$$

Where  $C_T$  is the targeted drug concentration and  $V_L$  is the lungs volume. Elimination half life of Prothionamide is 2 hr [64].

$$\text{Maintenance dose} = C_T * V_L * K_E * T_D = 4.341 * 2 * 0.3465 * 24$$

Where,  $K_E$  is elimination rate constant ( $0.693/2=0.3465 \text{ hr}^{-1}$ ) and  $T_D$  is duration of action (24 hr). As initial and maintenance dose will be release together, one correction is needed to calculate the dose, that is  $T_D - T_{\max} = 24 - 1 = 23 \text{ hr}$ . Where,  $T_{\max}$  of time required to reach maximum concentration for Prothionamide is 1hr.

$$\text{Corrected dose} = C_T * V_L * K_E * (T_D - T_{\max}) = 4.341 * 2 * 0.3465 * 23 = 69.19 \text{ mg.}$$

$$\text{Total dose} = \text{Initial dose} + \text{maintenance dose} = 8.68 + 69.19 = 77.87 \approx 78 \text{ mg}$$

**ii) DOSE CALCULATION OF PROTHIONAMIDE FOR RAT:** Dose calculation for rat was carried out with equivalent surface and weight with no observed adverse effect as reported previously [178]. Normal Human body weight is 70 kg. 70 kg body weight required 78 mg of dose. Hence, Prothionamide dose in human is  $78/70 = 1.1 \text{ mg/kg}$  body weight. Dose conversion factor from human to rat is 7 [179].

$$\text{So Rat dose} = 1.1 * 7 = 7.7 \text{ mg/kg.}$$

#### **3.5.5.4. Collection of sample and pharmacokinetic analysis**

After administration, three separate studies were performed. 1 ml blood was withdrawn from the tail vein of rat to check the bio-distribution of PTH at 1, 2, 3, 6, 12 & 24 hr. 1.5 mg of sodium EDTA was added to the 1 ml of blood and centrifuged at 3000 rpm for 10 min. Supernatant was collected using Pasteur pipette attached with micro tip. Each sample was added to 60  $\mu\text{l}$  of 30 % trichloroacetic acid, the mixture was immediately mixed by vortex mixer for 5 min followed by centrifugation at 8000 rpm for 10 min. With this supernatant 90  $\mu\text{l}$  of 1 M  $\text{NaHCO}_3$  solution was mixed and vortexed for 5 minutes followed by centrifugation for 10 min at 8000 rpm. Samples were analyzed by HPLC.

By sacrificing the animal at the specified time interval, un-diffused drug was extracted into the lavage of phosphate buffer from the isolated lungs as per modified method of Chougule M et al (2007) [175] and Lombry C et al (2002) [180]. To check the lung's tissue

distribution, lungs and trachea portion were homogenized with 10 ml of PBS solution and 1 ml of methanol, followed by vortexing for 5 min. 30 % trichloroacetic acid was added to each sample for deprotenization. After neutralization with sodium bi carbonate, each sample was centrifuged for 10 min at 8000 rpm. Supernatant containing Prothionamide was estimated by HPLC as described previously.

### **3.5.6. *In-vitro* anti tubercular activity**

#### **3.5.6.1. Preparation of 7H9 medium**

Firstly 2.35 grams of 7H9 was suspended in 450 ml distilled water. 1 ml of glycerol was added to the above solution. The above solution was further heated to dissolve the medium completely. Afterward, sterilization was carried out in autoclave at 15 lbs pressure (121°C) for 10 min. Finally, cooled the medium to 45°C or below and aseptically add contents of 1 vial of Middlebrook ADC Growth Supplement (FD019).

#### **3.5.6.2. Culture of *M. tuberculosis* in 7H9 medium**

Culture of *M. tuberculosis* was grown in 7H9 (Hi-media) broth supplemented with Middlebrook OADC enrichment containing 0.05% (v/v) Tween 80 to avoid clumping at 37°C. Further the growth of bacteria was carried out in 96-well plates to their exponential phase growth of an optical density of 0.15 corresponding to 10<sup>8</sup>CFU/ml.

#### **3.5.6.3. Culture of THP1 cell**

RPMI 1640 medium was used with 2 mM L-glutamine adjusted to contain 1.5 g/l sodium bicarbonate, 4.5 g/l glucose, 10 mM HEPES and 1.0 mM sodium pyruvate and fetal bovine serum, 10 %. Prior to the addition of the vial contents, the culture vessel containing the complete growth medium was placed into the incubator for at least 15 minutes to allow the medium to reach its normal pH (7.0 to 7.6). The vial contents were transferred to a centrifuge tube containing 9 ml complete growth medium and spin at approximately 125xg for 5 to 7 min. Cell pellet was re-suspended with the recommended complete growth medium and dispensed into the appropriate number of culture flasks. The culture was incubated at 37°C in a COD incubator.

#### **3.5.6.4. Infection of THP1 cell**

THP1 cells were infected with tubercle bacilli at a ratio of 10 to 20 bacilli per cell. 0.1 ml of the mycobacterium culture was added to 10 ml of RPMI 1640 medium. The

macrophages were allowed to phagocytize the bacteria for 4 hr at 37 °C, and the number of intracellular organisms was determined by lysing the macrophages with 0.25 % (w/v) of sodium dodecyl sulfate (SDS). After incubation, infected cells were washed four times to remove extracellular bacilli. Infected cells were finally resuspended ( $2 \times 10^5$  cells/ml) in RPMI medium supplemented with 10 % fetal bovine serum (Hyclone), 2 mM L-glutamine and pyruvate and dispensed in 96 well plate.

### 3.5.6.5. MTT assay

Cells were seeded in a 96-well flat-bottom microtiter plate at a density of  $1 \times 10^4$  cells/well and allowed to adhere for 24 hr at 37 °C in a CO<sub>2</sub> incubator. After 24 hr of incubation, culture medium was replaced with a fresh medium. Cells were then treated with various concentrations of the desired compound for 24 hr at 37 °C in a CO<sub>2</sub> incubator. Subsequently, 20 µl of MTT working solution (5 mg/ml in phosphate buffer solution) was added to each well and the plate was incubated for 4 hr at 37 °C in a CO<sub>2</sub> incubator. Supernatant solution was withdrawn and formed formazan crystals were solubilized by adding 20 µl of DMSO per well for 30 min at 37 °C in a CO<sub>2</sub> incubator. The intensity of the dissolved formazan crystals was detected at (purple colour) 590 nm. Percentage cell viability was carried out using the following formula.

<b>Percentage cell viability</b>	=	$\frac{\text{Absorbance of sample} - \text{absorbance of SC}}{\text{Absorbance of GC} - \text{Absorbance of SC}} \times 100$
----------------------------------	---	--

Where, SC-Sterile control contained only media; GC-Growth control contain bacteria infected cell without growth inhibitor.

### 3.5.6.6. Drug and nanoparticles solution preparation

The solution of drugs or drug containing nanoparticles were dissolved using DMSO of 2.5% [181].

**Table 3. 11. Drug solution and nanoparticles solution preparation**

5 mg drug or drug equivalent to 78.40mg of <b>PTH-PLGA nanoparticles</b> in 50 ml (100 µg/ml) (38.96 mg of drug present in 610.9 mg of nanoparticles)				
10ml to 100 ml (10 µg/ml)				
<b>Dilution made</b>	0.8 ml to 10 ml (0.8 µg/ml)	1 ml to 10 ml (1 µg/ml)	1.2ml to 10 ml (1.2 µg/ml)	1.4 ml to 10 ml (1.4 µg/ml)
50 µl	0.04	0.05	0.06	0.07
Above 50 µl nanoparticles suspension was added to 50 µl bacteria infected RPMI 1640 medium and final volume was 100 µl in each well				
<b>Concentration prepared (µg/ml)</b>	0.4	0.5	0.6	0.7

### **3.6. Formulation and characterization of DPI containing Prothionamide nanoparticles prepared by Chitosan**

#### **3.6.1. Compatibility study**

Fourier transform infrared spectroscopy (FTIR) analysis was performed to check the absence of chemical interaction between Prothionamide, inhalable anhydrous Lactose and Chitosan using Perkin Elmer (Massachusetts, USA). Two samples were run separately for pure Prothionamide and physical mixture of Prothionamide, inhalable anhydrous Lactose and Chitosan. The samples were scanned in the IR range from 400 to 4000  $\text{cm}^{-1}$ .

#### **3.6.2. Preparation of Prothionamide-Chitosan nanoparticles**

Chitosan/TPP nanoparticles were prepared using ionic gelation technique with minor modification as reported [95]; [182]. Briefly, Chitosan (5 mg/ml) was dissolved in aqueous solution of Acetic acid under magnetic stirring at room temp. Prothionamide was dispersed in the above Chitosan solution with constant stirring. Aqueous solution of TPP (as cross linking agent) was added drop wise using syringe needle size 24G into the above Chitosan solution containing PTH with continuous stirring. The stirring was continued for specified period of time. The resultant nano-suspension was centrifuged at 18,000 rpm (revolution per minutes) for 30 min followed by one time washing with distilled water. Excessive heat is produced during the centrifugation process, hence to stabilize the nanoparticles  $-4^{\circ}\text{C}$  was maintained during centrifugation. Several process parameters like stirring time, chitosan-TPP ratio, chitosan-PTH ratio and TPP solution volumes were optimized to achieve suitable nanoparticles for the formulation of dry powder inhaler.

#### **3.6.3. Optimization and characterization of Prothionamide nanoparticles**

Percentage Drug Entrapment (PDE) of PTH in nanoparticles was determined by separating the nanoparticles from the aqueous medium by ultracentrifugation at 18000 rpm for 30 min. The amount of free PTH in the supernatant was measured by UV-Spectrophotometry at 288 nm. Other evaluation parameters were calculated as reported previously [183]. Zeta potential indicates the surface charge on the particles and was measured to determine the stability of nanoparticles in the suspension [110]. PDI value indicates the particle size distribution of nanoparticles in a given sample. Higher value of PDI indicates the distribution of nanoparticles with variable size range which results in the

formation of aggregates and could result in low stability of particle suspension and low homogeneity. The zeta size, zeta potential and Poly Dispersibility Index (PDI) were determined using Zetasizer (Malvern, UK) as mentioned earlier [110].

#### **3.6.3.1. Selection of strength-volume of acetic acid and TPP solution**

Chitosan dissolves completely in acidic media. Different percentage of Acetic acid solution [99],[104], [184] was reported in the formulation of Chitosan nanoparticles. As Prothionamide and Chitosan both dissolve in Acetic acid, its percentage was selected as 1 % v/v. Initially, Acetic acid and TPP solution volume was selected as 10 ml and 5 ml respectively [185].

#### **3.6.3.2. Effect of stirring time**

Stirring time plays a vital role to obtain uniform PTH nanoparticles. So stirring time was changed by keeping all other process parameters (Chitosan-TPP ratio of 6:1, TPP solution volume of 5 ml, Chitosan-PTH weight ratio of 50:50) constant. The influence of stirring time on the average particles size, zeta potential and PDE were studied in four stirring time at 15, 30, 45 and 60 min [95], [182], [186], [187], [188]. Based on smaller particle size and higher PDE, optimized formulation had been chosen.

#### **3.6.3.3. Effect of Chitosan and TPP ratio**

PTH nanoparticles were further optimized for Chitosan-TPP ratio. During this optimization, other process parameters were kept constant. From literature, [186]; [189] four new ratios like 5:1, 4:1, 3:1, and 2:1 were selected. Nanoparticles were prepared by using these ratios and compared with 6:1 ratio for optimizing stirring time. Acetic acid and TPP solution volume was maintained 10 ml and 5 ml respectively. Nanoparticles were prepared using this ratio and studied its influence on nanoparticles.

#### **3.6.3.4. Effect of PTH-Chitosan ratio**

PTH-Chitosan ratio was optimized accordingly, where all other process parameters remained constant. Four different formulations were prepared by changing the amount (60, 70, 80 and 90 mg) of Chitosan with fixed amount of PTH and also checked the influence of Chitosan amount on PDE and particles size. As the volume of 1 % v/v Acetic acid was

restricted to 10 ml, maximum 90 mg of Chitosan could incorporate. Hence, the PTH-Chitosan ratio 1:1.2, 1:1.4, 1:1.6 and 1:1.8 were prepared and compared with 1:1.

#### **3.6.3.5. Effect of TPP solution volume**

Volume of TPP and Chitosan solution play a great role in the drug entrapment and uniform particle size distribution. So, finally volume of TPP solution was increased from 5 ml to 10 ml (with constant TPP amount) to check its effect on the physicochemical properties of PTH-chitosan nanoparticles.

#### **3.6.3.6. Scanning electron microscopy (SEM)**

The shape and surface morphology of the Prothionamide nanoparticles were examined by Scanning Electron Microscopy (Karl Zesis with SE detector, EVO-18). The samples were sputter-coated with gold and observed for morphology at an acceleration voltage of 7.0 kV with highest magnification of 19.99 KX.

#### **3.6.3.7. Differential scanning calorimetry (DSC)**

DSC is widely used to characterize the thermal behaviour of various materials, such as melting and crystallization behaviours [190]. The temperature was calibrated with indium in a nitrogen atmosphere. About 5 mg PTH was weighed very accurately. The temperature was controlled within the range of 20-250°C, with a heating rate was 20°C. Similar procedure also followed for chitosan polymer and PTH-chitosan nanoparticles as mentioned in 3.5.3.5.

#### **3.6.4. Formulation of dry powder inhaler and characterization**

Initially, flow property of PTH nanoparticles was determined. To increase the flow property, PTH nanoparticles and anhydrous inhalable grade lactose were mixed (1:0.5, 1:1, 1:1.5 etc.) manually using geometrical dilution process. Angle of repose, Carr's index and Hausner ratio were carried out in each stage of addition of inhalable grade lactose [191]. Optimization of dry powder inhaler was carried out based on the excellent flow property. Optimized formulation was further characterized for the zeta size and potential to check the changes of nanoparticles in the form of DPI.

**3.6.4.1. Determination of MMAD using cascade impactor**

Mass median aerodynamic diameter (MMAD) represents aerodynamic diameter below which 50 % particles remain. Aerodynamic diameter of a particle controls its deposition in pulmonary tract. MMAD of the optimized dry powder inhaler was determined using an eight stage cascade impactor [136]. Firstly, DPIs were flowed through the cascade impactor with a flow rate of 28.3 l/min. After deposition of DPI, Prothionamide content was determined in each chamber by UV-spectrophotometer at 287.40 nm using water-methanol ratio of 8:2. Estimated drug content in each chamber were inserted into the “MMAD CALCULATOR” to obtain MMAD and geometric standard deviation (GSD). Thereafter, fine particle fraction, extra fine particle and emitted dose was calculated as mentioned in section 3.5.4.1.

**3.6.4.2. *In-vitro* release study**

5 mg PTH equivalent dry powder inhaler was dispersed in 2 ml of simulated lung fluid (SLF) [172] and filled in dialysis bag (Himedia labs, Mumbai, 12,000 molecular weight cut off) afterward. To avoid floating, the drug filled bag was tied over the glass plate and kept at the bottom of the dissolution chamber. *In-vitro* release study was carried out in 1 litre SLF [172] and temperature maintained at  $37 \pm 0.5$  °C with a paddle speed of 100 rpm [173]. 10 ml of dissolution fluid was withdrawn at specific time interval up to 24 hr and replaced with fresh SLF. The *in-vitro* release data was analyzed for zero order, Higuchi and Korsmeyer-Peppas's models. Based on the correlation co-efficient ( $R^2$ ) best fitted model was selected.

**3.6.4.3. Stability study**

Stability study was carried out as per the ICH guideline Q1A (R2). Paraffin tap was used to seal cryoprotectant vials, contained freshly prepared dry powder inhaler of Prothionamide nanoparticles. These vials were kept in stability chamber and maintained at temperature and relative humidity of  $25 \pm 2$ °C,  $60 \pm 5$ % respectively. The nanoparticles were analyzed for 6 months with a frequency of 1.5 month for first 3 months and next on 6<sup>th</sup> month [192]; [193]. Zeta size, zeta potential, PDI, drug entrapment and drug release were carried out to check the stability of dry powder inhaler of Prothionamide nanoparticles.



**3.6.4.4. Delivery dose calculation using modified device**

Modified delivery device was used here for PDI administration to rat mentioned in section 3.5.4.4. DPI was sprayed through modified delivery device in three divided form. After spray, needle and syringe were cleaned with water-methanol in the ratio of 8:2. Prothionamide content was estimated by UV-spectrophotometric method and finally percentage delivery dose was calculated.

**3.6.5. *In-vivo* study**

All animal experiments were approved and performed in accordance with the guidelines of institutional animal ethical committee of Bengal College of Pharmaceutical Sciences and Research, Durgapur, West Bengal (Registration No:1799/PO/Ere/15/S/CPCSEA under CPCSEA, India). Wistar rats both sex (4-6 months old & average weight 200-250 gm) were used to study the pharmacokinetic parameters of Prothionamide in the form of DPI. The rats were housed in a 12 hr light/dark cycle with food and water available. Human lungs volume, that is 4.341 l [174] was used to calculate the human dose of Prothionamide for pulmonary administration. Targeted concentration was chosen as 2 µg/ml to maintain the plasma concentration above minimum inhibitory concentration (MIC) for the period of 24 hr. Dose was divided as loading and maintenance dose. Equivalent dose calculation for rat had been carried out from the human dose (section 3.5.5.3). Dose calculation for rat was carried out with equivalent surface and weight with no observed adverse effect with 7.7 mg/kg body weight [178], [179]. Mono-dose inhaler and nasal insufflators were obtained to administer drug to pulmonary route, but this device was suitable for the human use not for animal administration. So, dry powder inhaler delivery device was designed with little modified as described previously [132]. Firstly 1 ml of blood was withdrawn from the tail vein of rat to check the bio-distribution of PTH at the time interval of 1, 2, 3, 6, 12 & 24 hr. By sacrificing the animal at the specified time interval, un-diffused drug was extracted into the lavage of phosphate buffer from the isolated lungs as per modified method of Chougule M et al (2007) [175] and Lombry C et al (2002) [180]. Thereafter, these lungs and trachea were homogenized with 10 ml of PBS solution and 1ml methanol. 60 µl of 30 % Trichloroacetic acid was added in each sample for deprotenization. After vortexed for 5 min, these samples were centrifuged at 8000 rpm for 10 min. With the supernatant, 1 molar sodium bi-carbonate was added to neutralize the sample and followed

by vortexed for 5 min. These samples were centrifuged again at 8000 rpm for 10 min. Supernatant containing Prothionamide was estimated using HPLC.

#### **3.6.6. *In-vitro* anti-tubercular activity**

*In-vitro* anti-tubercular activity was carried out as mentioned in section 3.5.6. Concentration ranges for PTH loaded Chitosan nanoparticles was 0.4-0.7 µg/ml.

#### **3.6.7. Statistical analysis**

The data were expressed as the mean of three experiments  $\pm$  standard deviation (S.D.) and were analysis by one-way analysis of variance (ANOVA) for repeated measurements and differences were considered to be significant at a level of  $P < 0.05$ .

# CHAPTER 4: Result and Discussion Pertaining to Prothionamide

## 4.1. Identification of drug

Identification of the procured drug sample and ensuring its purity is a prerequisite before proceeding with the formulation development.

- The identification tests and the inferences for the drug sample based on its appearance, and melting point determination are summarized in Table 4. 1.

**Table 4. 1: Test for physical properties of Prothionamide**

Parameters	Observations	Reported [55]	Inference
Appearance	Yellow powder	Yellow, crystalline powder	Complies
Melting point	143 ± 1° C	142-145°C	Complies

- Various functional groups present in the powder drug sample were determined by fourier-transform infrared (FTIR) spectroscopic and compared with the standard spectra of Prothionamide for confirmation. The observed IR spectra of PTH are shown in Figure 4.1.

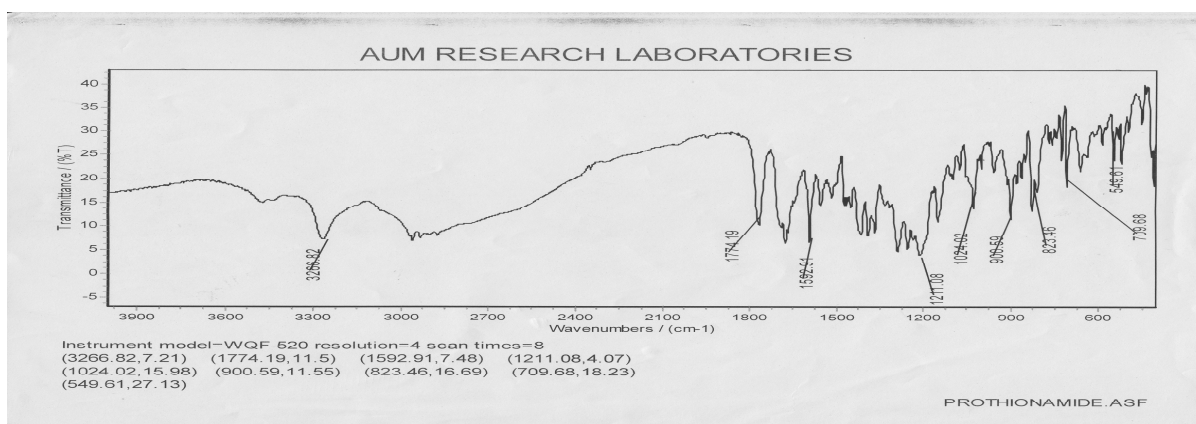


**Figure 4. 1: FTIR of Pure Prothionamide**

Strong peak of C=S was detected at  $1024.02\text{ cm}^{-1}$ . Wide peak of  $3266.82\text{ cm}^{-1}$  was due to N-H stretching [194]. All other major IR peaks observed for Prothionamide molecule is summarized in Table 4.2.

**Table 4. 2: Major peaks observed and reported for Prothionamide in IR spectra**

Principle Peak ( $\text{cm}^{-1}$ ) Pure Drug	Functional Group	Principle Peak ( $\text{cm}^{-1}$ ) Pure Drug	Functional Group
823.46	N-H wag	1211.08	C-N stretching
900.59	=C-H bending	1592.91	C-C=C stretch in ring
1024.02	C=S Stretching	3266.82	N-H stretch

➤ 0.002 % w/v solution of Prothionamide was prepared in ethanol and scanned in the range of 230 nm to 350 nm. The absorption maximum was found at 291 nm with absorbance of  $0.780 \pm 0.001$ . This spectroscopy data compiled the official identification test for Prothionamide according to IP.

Based on physical properties, IR spectra and UV- Spectrophotometric data, it was confirmed that the procured powder sample was Prothionamide and the sample can be used for further process.

## 4.2. Analytical methods

### 4.2.1. Estimation of Prothionamide using UV-Spectrophotometric method and its validation

Previous literature survey suggested the existence of HPLC method of Prothionamide estimation using NS-4000 [9], Eurobond RP18 [171], Kromasil 100 C4 column [54]. Kumar and Sreeramulu (2011) reported stability indicating RP-HPLC with Shimadzu LC-20AT series [58]. Thin layer chromatography was reported by GPHF-Minilab in 2010 [195]. No UV spectrophotometric method is available for the estimation of Prothionamide formulation. So, it was felt necessary to develop a UV spectrophotometric method where no complexing agent, no harmful chemicals, no extraction, derivatization, or evaporation step, are involved.

#### 4.2.1.1. Linearity

Different concentrations of Prothionamide solutions were prepared in pH 7.4. The overlay spectra of PTH at different concentrations are shown in Figure 4.2. Prothionamide showed maximum absorptivity at  $\lambda_{\max}$  at 288 nm.

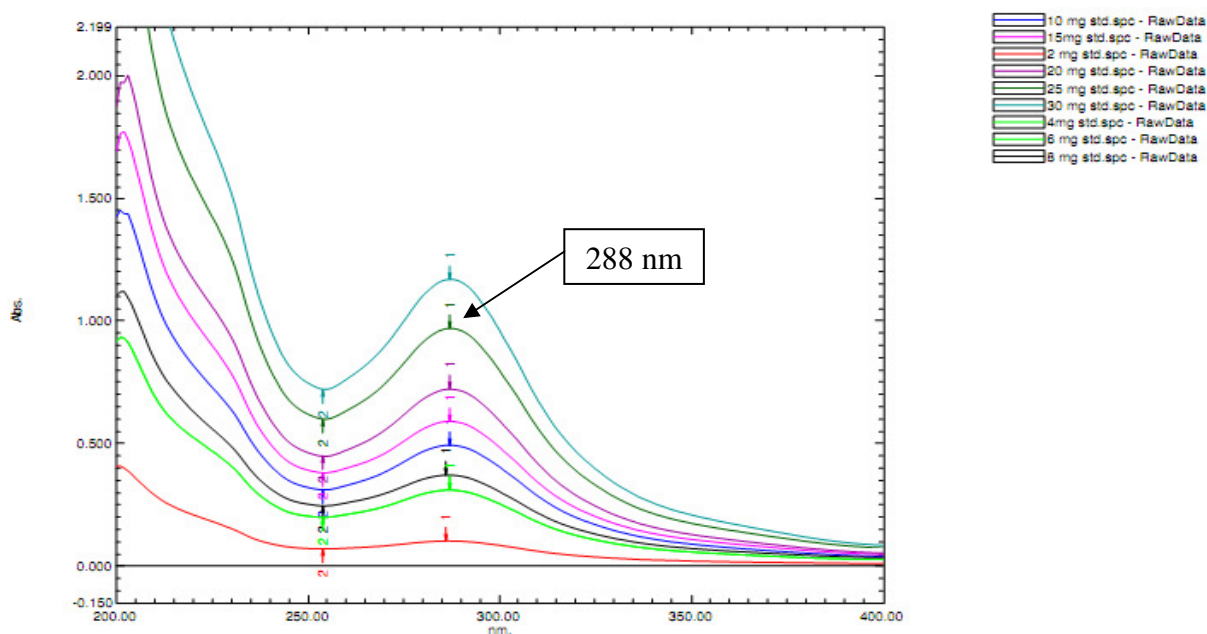


**Figure 4. 2: Overlay UV spectra of PTH at different concentrations**

Hence, five Point calibration curve data was constructed in the range of 4 to 20  $\mu\text{g/ml}$ , using UV-spectrophotometer (UV-1800, Shimadzu). Absorbance of different concentrations of diluted solutions is shown in Table 4.3 and calibration curve is shown in Figure 4.3.

**Table 4. 3. Absorbance of different concentration of PTH in pH 7.4**

Conc. ( $\mu\text{g/ml}$ )	Absorbance			
	Trial 1	Trial 2	Trial 3	Average <sup>‡</sup>
4	0.206	0.212	0.204	$0.207 \pm 0.0041$
8	0.401	0.398	0.398	$0.399 \pm 0.0017$
12	0.602	0.597	0.599	$0.599 \pm 0.0025$
16	0.809	0.809	0.812	$0.810 \pm 0.0017$
20	1.001	0.984	1.011	$0.999 \pm 0.0136$
Equation	$y=0.05x+0.004$	$y = 0.048x+0.013$	$y = 0.050x-0.002$	$y=0.049x + 0.004$
$R^2$	0.999	0.999	0.999	0.999

<sup>‡</sup>Mean of three data  $\pm$  Standard deviation

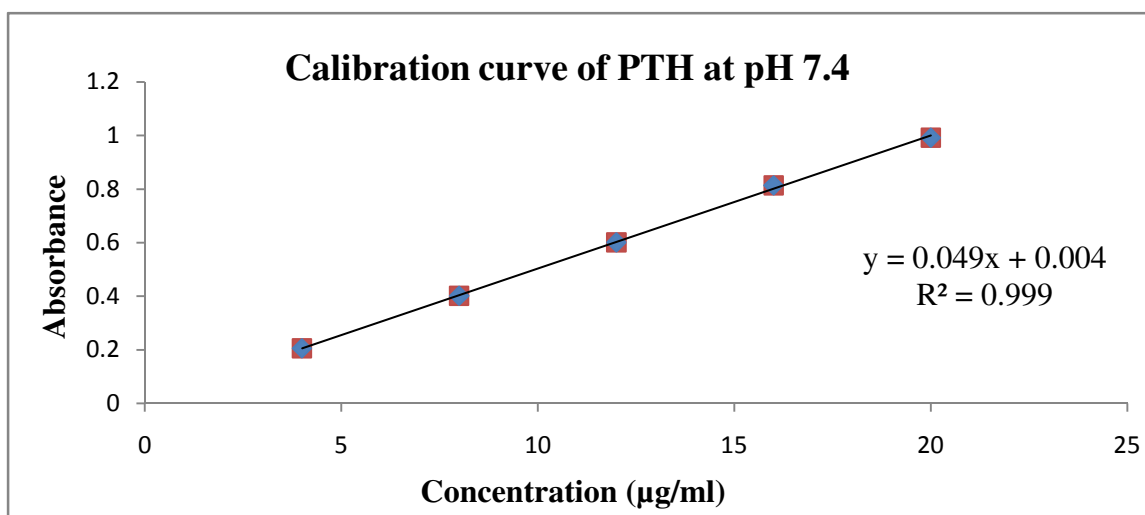


**Figure 4. 3: Calibration curve of PTH in pH 7.4**

The linear regression equation obtained by the proposed method using three authentic calibration curves was,  $y = 0.049x + 0.004$ , where “y” represents the absorbance, and “x” represents Prothionamide concentration in µg/ml. The correlation coefficient (0.999) of regression was found almost equal to 1 in the range of 4-20 µg/ml which states that the method was linear to the concentration versus absorbance. This correlation coefficient demonstrates the good quality of the calibration curve, as lower the dispersion of the set of points, lower the uncertainty of the estimated regression coefficients [154].

#### 4.2.1.2. Limit of detection and limit of quantification

Intercept value of all the calibration curves are taken from Table 4.4 and calculated the standard deviation of this y-intercept. Slope of the linear curve was used to calculate the limit of detection (LOD) and limit of quantification (LOQ) [196],[197]. LOD and LOQ for PTH were found to be 0.397µg/ml and 1.204µg/ml respectively, indicating that the proposed UV method is highly sensitive.

**Table 4. 4: Determination of limit of detection and limit of quantification**

y-intercept				Slope	LOD (µg/ml)	LOQ (µg/ml)
Trial 1	Trial 2	Trial 3	SD			
0.004	0.013	0.002	0.0059	0.049	0.397	1.204

#### 4.2.1.3. Analysis of tablet formulation

Assay value of Prothionamide in tablet formulations is ranged from  $98.40 \pm 0.91$  to  $99.80 \pm 1.56$  % (Table 4.5). In all the cases relative standard deviation were within the limit [198]. Assay values of formulation were same as label claim. Powder samples contained drug with other excipients; but no interference of excipients was observed in the determination of Prothionamide. Percentage relative standard deviation (% RSD) in all the case was found to be within the limit.

**Table 4. 5: Assay of marketed product of Prothionamide**

Label claim	Conc. prepared (µg/ml)	Absorbance	Conc. Recovered	Amount found mg/tab	% Label claim	Mean % label claim <sup>‡</sup>	% RSD
250	10	0.491	9.82	245.50	98.20	98.40±0.91	0.925
		0.487	9.74	243.50	97.40		
		0.478	9.96	249.00	99.60		
	15	0.741	14.82	247.00	98.80	99.80±1.56	1.563
		0.765	15.30	255.00	102.00		
		0.739	14.78	246.50	98.60		
	20	0.982	19.64	245.50	98.20	98.87±0.62	0.627
		0.987	19.74	246.75	98.70		
		0.997	19.94	249.25	99.70		
Over all mean percentage label claim: 99.02±1.32							1.04

<sup>‡</sup>Values are mean of three data  $\pm$  standard deviation

#### 4.2.1.4. Accuracy

Accuracy of the method was studied by recovery experiments [199]. The percentage recovery for the standard analysis and reference analysis method for all the three concentration levels ranged from  $97.55 \pm 0.36$  to  $98.60 \pm 0.84$  % with confidence interval ranging from 0.34 to 0.85 (Table 4.6). The accuracy of the method was found to be good with the overall % RSD for recovery at 80 %, 100 % and 120 % levels were all within the limits. This indicates that the proposed method was found to be accurate.

**Table 4. 6: Data for accuracy**

Conc. level	Sl. No	Pure drug solution	Formulation solution	Amount added (µg/ml)	Amt. recover	Percentage recover	Mean percentage recovered <sup>‡</sup>	% RSD
80%	1	10ml of 10µg/ml	10 ml of 8µg/ml	20ml of 9 µg/ml	8.74	97.11	97.55±0.36	0.39
	2				8.82	98.00		
	3				8.78	97.55		
100%	1		11 ml of 10µg/ml	20ml of 10 µg/ml	9.76	97.60	98.00±0.33	0.34
	2				9.80	98.00		
	3				9.84	98.40		
120%	1		12 ml of 12µg/ml	20ml of 11 µg/ml	10.72	97.46	98.60±0.84	0.85
	2				10.94	99.45		
	3				10.88	98.90		
Over all mean percentage recovery							98.05±0.75	0.53

<sup>‡</sup>Values are mean of three data  $\pm$  standard deviation

#### 4.2.1.5. Precision

The precision of analytical procedure expresses closeness of agreement (degree of scatter) between a series of measurements obtained from multiple sampling of the same homogenous sample under prescribed conditions [156].

**Table 4. 7: Intra-day & Inter-day precision for three different concentrations of PTH**

Conc ( $\mu\text{g/ml}$ )	Intra Day						Inter Day	
	Day-1		Day-2		Day-3			
	Repeatability <sup>‡</sup> ( $n=9$ )	% RSD	Repeatability <sup>‡</sup> ( $n=3$ )	% RSD	Repeatability <sup>‡</sup> ( $n=3$ )	% RSD	Repeatability <sup>‡</sup> ( $n=15$ )	% RSD
5	0.246 $\pm$ 0.002	0.81	0.255 $\pm$ 0.002	0.63	0.255 $\pm$ 0.001	0.31	0.249 $\pm$ 0.005	1.88
10	0.486 $\pm$ 0.006	1.21	0.489 $\pm$ 0.006	1.15	0.498 $\pm$ 0.005	1.04	0.489 $\pm$ 0.007	1.49
15	0.747 $\pm$ 0.008	1.08	0.753 $\pm$ 0.008	1.09	0.745 $\pm$ 0.01	1.27	0.748 $\pm$ 0.009	1.18

<sup>‡</sup>Values are mean  $\pm$  standard deviation; n= No of sample analysed

The intra-day and inter-day precision study (Table 4. 7) of the developed method confirmed adequate sample stability and method reliability where all the RSDs were  $< 2\%$  [198]. Hence the proposed method was found to be precise.



UV-Spectrophotometric methods were developed for Prothionamide (PTH) which can be conveniently employed for routine analysis in pharmaceutical dosage forms and will eliminate unnecessary tedious sample preparations. The standard error, standard deviation, and coefficient of variance were obtained for Prothionamide was satisfactorily low.

#### 4.2.2. Preparation of standard curve for Prothionamide in water:methanol system

Previous UV estimation method is useful for estimation of drug in the solution. The extraction of drug from nanoparticles is difficult due to polymer coating. Hence, alternate standard curve was constructed in water-methanol system. The wavelength of maximum absorptivity ( $\lambda_{\max}$ ) of Prothionamide in water- methanol (8:2) was found as 287.40 nm. Diluted the stock solutions with same solvent and replicated absorbance reading three times (Table 4. 8).

**Table 4. 8: Standard curve of PTH in water-methanol**

Conc. ( $\mu\text{g/ml}$ )	Absorbance			
	Trial 1	Trial 2	Trial 3	Average <sup>‡</sup>
10	0.271	0.269	0.268	0.269 $\pm$ 0.002
15	0.379	0.378	0.378	0.378 $\pm$ 0.001
20	0.511	0.511	0.513	0.512 $\pm$ 0.001
25	0.64	0.636	0.636	0.637 $\pm$ 0.002
30	0.77	0.773	0.773	0.772 $\pm$ 0.002
35	0.902	0.901	0.901	0.901 $\pm$ 0.001
40	1.026	1.03	1.03	1.029 $\pm$ 0.002
Regression equation	$y = 0.025x + 0.005$	$y = 0.025x + 0.001$	$y = 0.025x + 0.001$	$y = 0.025x + 0.002$
$R^2$	0.999	0.999	0.999	0.999

<sup>‡</sup>Values are mean of three data  $\pm$  standard deviation

Individually, all the curves were analysed and found the  $R^2$  value as 0.999. Average of three data was used to construct the standard curve of PTH in a solvent of water-methanol system (8:2).

Standard curve showed the regression equation of  $y = 0.025x + 0.002$  with regression coefficient of 0.999. Figure 4.4 shows the standard curve of Prothionamide.

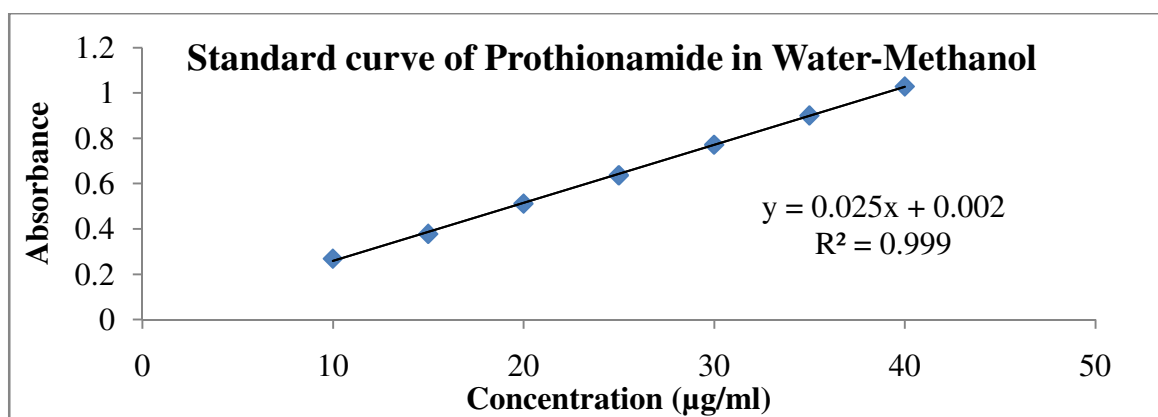


**Figure 4. 4: Standard curve of Prothionamide in Water-Methanol system**

#### 4.2.3. Estimation of Prothionamide in rat plasma using HPLC method

Mobile phase was composed of HPLC grade Water and Acetonitrile in the ratio of 70:30 (v/v). The flow rate was 1 ml/min. Dilution made in concentrated Prothionamide solution (100 µg/ml) (S4) with mobile phase and scanned by UV-visible spectrophotometry (Shimadzu, Japan; 1800) in the range 200–400 nm to detect  $\lambda_{\max}$  for Prothionamide estimation. PTH showed the maximum absorptivity at 290 nm.

**Table 4. 9: Calibration data of PTH using HPLC**

PTH Conc. (µg/ml)	Trial 1	Trial 2	Trial 3	Average <sup>‡</sup>
	Area [mV.s]	Area [mV.s]	Area [mV.s]	Area [mV.s]
0.1	4.02	23.127	17.501	14.893±9.82
0.5	58.66	77.549	71.781	69.33±9.68
1	126.96	145.945	139.631	137.512±9.67
5	685.832	705.311	698.150	696.431±9.85
10	1357.511	1363.297	1342.754	1354.521±10.59
15	2001.294	2016.270	2023.893	2013.819±11.49
20	2749.718	2761.871	2749.034	2753.541±7.22
25	3405.872	3408.537	3389.601	3401.337±10.25
Regression Equation	y = 136.6x-9.658	y = 136.1x+9.602	y = 135.7x + 3.896	y = 136.1x+1.280
R <sup>2</sup>	0.999	0.999	0.999	0.999

<sup>‡</sup>Values are mean of three data ± standard deviation

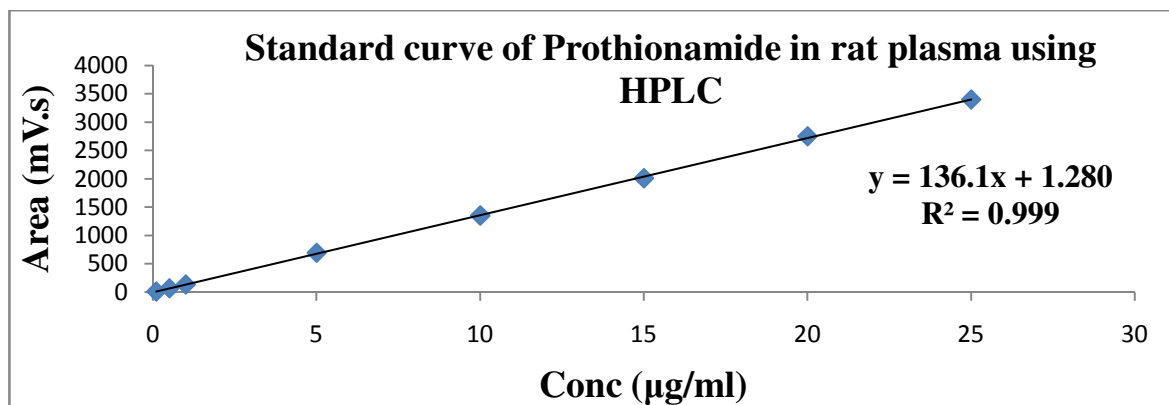


**Figure 4. 5: Linear curve of Prothionamide using HPLC**

Afterward diluted solutions of different concentration were injected directly into HPLC and the responses (peak area) were recorded at 290 nm. C18-Phenomenex (250 mm × 4mm i.d., 5 µm particles) was used to analyse PTH [88]. The linear regression equation obtained by the proposed method using three authentic calibration curves was (Table 4.9),  $y = 136.1x + 1.280$ , where “y” represents the peak area in the chromatogram, and “x” represents Prothionamide concentration in µg/ml.

The correlation coefficient (0.999) of regression was found almost equal to 1 in the range of 0.1-25 µg/ml which states that the method was linear to the concentration versus peak area responses. Calibration curve is shown in Figure 4.5.

The retention time for PTH was found to be 9.50 min, whereas internal standard of Ethionamide was detected at 4.90 (Figure 4. 6). No interference from mobile phase or baseline disturbance observed in the chromatogram. Therefore, 290 nm is the most appropriate wavelength for the analysis of PTH with suitable sensitivity.

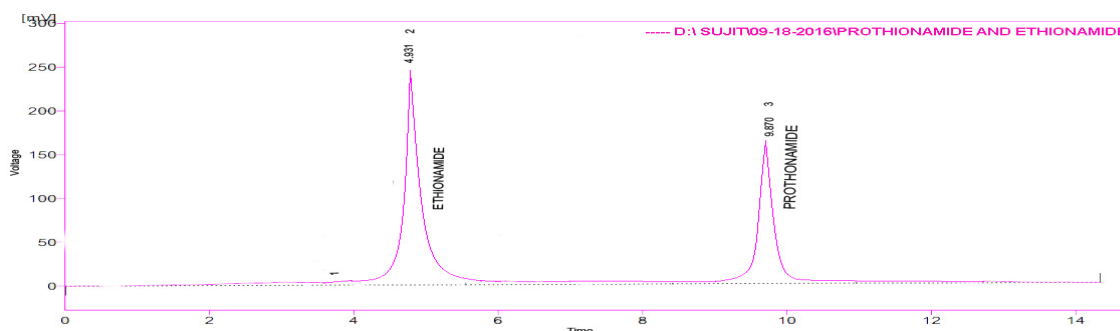


**Figure 4. 6: HPLC Chromatogram of PTH (5 µg/ml) and ETH (5 µg/ml)**

### 4.3. Formulation and characterization of DPI containing Prothionamide nanoparticles prepared by PLGA (75:25)

#### 4.3.1. Compatibility study

Major principle peak of aromatic stretching, C-N stretching, C=S stretching, =C-H bending were observed for pure Prothionamide at 1592.91, 1211.08, 1024.02 and 900.59  $\text{cm}^{-1}$  respectively. Same functional group peaks were observed in physical mixture of PTH, PLGA and inhalable grade anhydrous lactose at 1604.48, 1223.13, 1027.50, and 889.0  $\text{cm}^{-1}$  respectively.

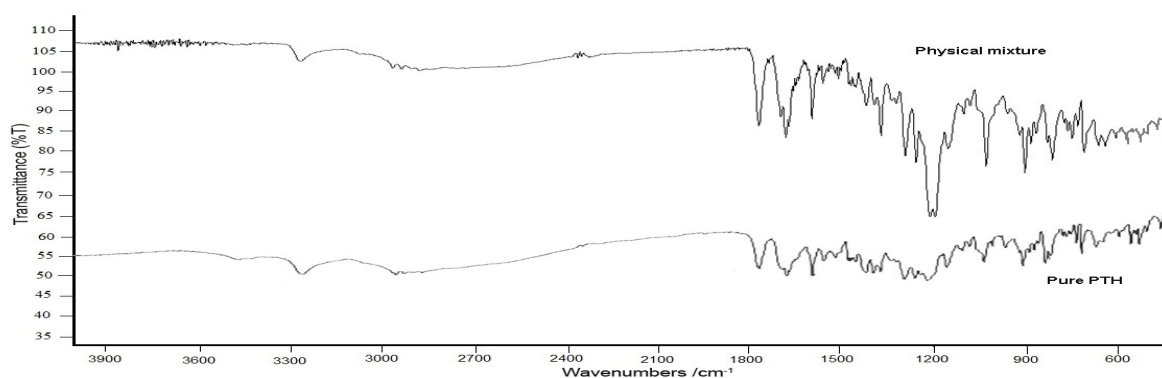


**Figure 4. 7: FTIR of pure Prothionamide and physical mixture of Prothionamide, PLGA(75:25) and inhalable grade lactose**

FTIR spectra (Figure 4.7) confirmed the absence of chemical interaction by maintaining the integrity of principle peaks and comparisons of these peaks are shown in Table 4.10.

**Table 4. 10: Comparison of FTIR data between pure PTH with physical mixture**

Principle Peak( $\text{cm}^{-1}$ ) Pure Drug/ Physical Mixture	Functional Group	Principle Peak ( $\text{cm}^{-1}$ ) Pure Drug/ Physical Mixture	Functional Group
823.46/825.77	N-H wag	1211.08/1223.13	C-N stretching
900.59/899.0	=C-H bending	1592.91/1604.48	C-C=C stretch in ring
1024.02/1027.50	C=S Stretching	3266.82/3270.52	N-H stretch

### 4.3.2. Characterization of Prothionamide nanoparticles

#### 4.3.2.1 Characterization of trial batch and optimization of sonication time

PLGA nanoparticles containing PTH were prepared at 1:1 ratio (PTH:PLGA) by solvent evaporation technique. PVA solution (3% w/v) was used. Drug entrapment was found to be 18.40 % and the particle size distribution was wide which was reflecting in PDI value (6.1 in ST 5). On the other hand, more than 90 % drug got released within 10 hr. Low drug entrapment and rapid drug release was due to the insufficient amount of PLGA.

Increasing the sonication time, reduced the particle size with increased PDI value. More PDI signifies the wide distribution of particles size that can be seen for ST5, ST6 (Table 4. 11). Whereas 100 % distribution of particles with least PDI value of 0.0813 was observed in ST2 batch. ST4 batch also showed the 100 % distribution of particles with PDI of 0.3. But correlation between distribution particle sizes with average particle size is more significant in ST2. Hence, in further formulation, the sonication time was fixed for 5 min.

**Table 4. 11: Sonication time optimization**

Formula code	Sonication Time (min)	Particle size & Size Distribution (nm)		Average Particle size (nm)	Polydispersity Index
ST1	1	4165	100%	4586.64	0.854
ST2	5	2724	100 %	2842.53	0.0813
ST3	10	5440	27.4 %	3587.58	0.2089
		2644	72.6 %		
ST4	15	2408	100 %	2845.37	0.3000
ST5	20	5020	71.5 %	4091.72	6.10
		1844	11.4 %		
		205	17.1 %		
ST 6	25	4830	62.5	3662.13	6.0
		1819	22.9		
		206	14.6		

#### 4.3.2.2. Characterization of Prothionamide nanoparticles prepared with Box Behnken design

Un-entrapped drug was calculated from supernatant after centrifugation by UV-spectrophotometric method as mentioned in section 4.2.1. Entrapment efficiency was calculated from it and found in the range of 55.31-81.56 % (Table 4.12). After freeze drying, nanoparticles were dispersed in water and determined their particle size using Zetatracs,

Microtrac Inc. USA. In all formulations, zeta potential values were within  $\pm 5$  mV. Hence, no significant relation was established between PDI and independent variables.

**Table 4. 12: Box-Behnken experimental design**

Formula code	Factor 1 X <sub>1</sub> :Polymer Amount (mg)	Factor 2 X <sub>2</sub> :Surfactant Concentration (% w/v)	Factor 3 X <sub>3</sub> :Organic Phase volume (ml)	Response 1 Y <sub>1</sub> : Particle Size (nm)	Response 2 Y <sub>2</sub> : Drug Entrapment (% w/w)	Response 3 Y <sub>3</sub> : PDI
1	125	1.25	4	295	64.17	0.607
2	125	0.25	4	314	77.15	1.363
3	75	1.25	2	285	74.39	1.696
4	125	0.75	6	510	69.39	0.964
5	125	0.75	2	265	81.56	1.456
6	25	0.25	4	296	75.43	2.248
7	75	0.25	2	275	74.36	2.095
8	75	0.25	6	390	79.02	0.816
9	25	0.75	6	286	71.79	1.192
10	75	0.75	4	294	71.11	0.652
11	25	1.25	4	224	58.99	1.787
12	75	0.75	4	297	74.29	1.547
13	75	0.75	4	308	72.58	0.827
14	25	0.75	2	411	69.06	0.715
15	75	1.25	6	291	55.31	1.125

PTH nanoparticles were further evaluated for drug load and process yield (Table 4.13). These values were found to be in the range of 12.83-75.43 % and 62.67-92.33 % respectively. Drug loading and PDE values were found to be increasing with increased the polymer amount and vice versa.

**Table 4. 13: Physico-chemical evaluation parameters**

Formulation code	Polymer used (mg)	Nanoparticles weight (mg)	Drug load (% w/w)	Process yield (% w/w)	Zeta Potential (mV)
1	125	266.4	12.83	76.11	4.28
2	125	273.9	15.43	78.26	5.04
3	75	259.2	24.80	86.40	3.33
4	125	282.4	13.88	80.69	1.65
5	125	312.5	16.31	89.29	1.28
6	25	213.0	75.43	85.20	2.73
7	75	260.2	24.79	86.73	3.61
8	75	277.0	26.34	92.33	3.17

9	25	227.9	71.80	91.16	3.98
10	75	206.7	23.70	68.90	-0.53
11	25	221.2	58.99	88.48	-3
12	75	188.0	24.77	62.67	1.49
13	75	242.9	24.19	80.97	-3.35
14	25	218.8	69.06	87.52	-2.49
15	75	241.2	18.44	80.40	-1.78

### 4.3.3. Experimental design

In this study, a fifteen-run, three factors and three levels Box-Behnken design was employed to construct polynomial models for the optimization process. This design was suitable for investigating the quadratic response surface and constructing a second order polynomial model using Design-Expert software (Trial Version 7.1.6, Stat-Ease Inc., MN) [162]. The design consisted of replicated centre points and a set of points lying at the midpoints of each edge of the multidimensional cube, which defined the region of interest used to evaluate the main effects, interaction effects, and quadratic effects of the formulation ingredients, and to optimize the formulation [192]. After filling the data, system suggested quadratic model to be followed for further analysis.

#### 4.3.3.1. Effect of independent variables on particle size

Particle size varied from 224 (Formulation 11) to 510 nm (formulation 4). In quadratic model significant correlation was established between adjusted and predicted  $R^2$  values (Table 4.14).

**Table 4. 14: Selection of model for conduction ANOVA analysis**

Source	Sequential p-value	Lack of Fit p-value	Adjusted R-Squared	Predicted R-Squared	System discussion
Linear	0.4296	0.0090	-0.00029	-0.67	-
2FI	0.0179	0.0197	0.584059	-0.21042	-
<b>Quadratic</b>	<b>&lt; 0.0001</b>	<b>0.9550</b>	<b>0.99496</b>	<b>0.992817</b>	<b>Suggested</b>
Cubic	0.9550	-	0.988995	-	-

Hence, system suggested quadratic model used to conduct analysis of variances (ANOVA) to check the influence of independent variables on particle size. Polymer amount plays an important role in controlling particle size along with release of drug from the matrix.

**Table 4. 15: ANOVA analysis of particles size**

Source	Sum of Squares	Df	Mean Square	F Value	p-value Prob > F	System suggestion
Model	68998.52	9	7666.502	308.0979	< 0.0001	Significant
X <sub>1</sub> -Polymer amount	3486.125	1	3486.125	140.0988	< 0.0001	-
X <sub>2</sub> -Surfactant Concentration	4050	1	4050	162.7595	< 0.0001	-
X <sub>3</sub> -Organic Phase volume	7260.125	1	7260.125	291.7666	< 0.0001	-
X <sub>1</sub> X <sub>2</sub>	702.25	1	702.25	28.2217	0.0032	-
X <sub>1</sub> X <sub>3</sub>	34225	1	34225	1375.419	< 0.0001	-
X <sub>2</sub> X <sub>3</sub>	2970.25	1	2970.25	119.367	0.0001	-
X <sub>1</sub> <sup>2</sup>	1501.641	1	1501.641	60.34726	0.0006	-
X <sub>2</sub> <sup>2</sup>	5215.41	1	5215.41	209.5945	< 0.0001	-
X <sub>3</sub> <sup>2</sup>	8566.256	1	8566.256	344.2568	< 0.0001	-
Residual	124.4167	5	24.88333	-	-	-
Lack of Fit	15.75	3	5.25	0.096626	0.9550	not significant
Pure Error	108.6667	2	54.33333	-	-	-

The analysis of variance (ANOVA) quadratic regression model demonstrated that the model F-value of 308.10 implied the model was significant due to very low probability ( $P < 0.0001$ ) [200]. In this case X<sub>1</sub>, X<sub>2</sub>, X<sub>3</sub>, X<sub>1</sub>X<sub>2</sub>, X<sub>1</sub>X<sub>3</sub>, X<sub>2</sub>X<sub>3</sub>, X<sub>1</sub><sup>2</sup>, X<sub>2</sub><sup>2</sup>, X<sub>3</sub><sup>2</sup> were significant model terms as values of "Prob > F" was less than 0.05 (Table 4.15). The positive value before a factor in the regression equation indicates that the response increases with the factor and vice versa [192].

The effect of average particle size was explained by the following quadratic equation:

$$\text{Particle Size (Y}_1\text{)} = + 299.67 + 20.87X_1 - 22.50X_2 + 30.13X_3 + 13.25X_1X_2 + 92.50X_1X_3 - 27.25X_2X_3 + 20.17X_1^2 - 37.58X_2^2 + 48.17X_3^2 \dots\dots\dots 1$$

**Table 4. 16: Analysis of variance**

Std. Dev.	4.99		R-Squared	0.9982
Mean	316.0667		Adjusted R-Squared	0.9950
C.V. %	1.578249		Predicted R-Squared	0.9928
PRESS	496.5		Adequate Precision	70.189



The "Predicted R-Squared" of 0.9928 is in reasonable agreement with the "Adjusted R-Squared" of 0.9950. "Adequate Precision" measures the signal to noise ratio. Adequate precision value was 70.189 (required more than 4) indicates an adequate signal (Table 4.16). This model can be used to navigate the design space.

Three dimensional (3-D) surface and contour plots for the obtained responses were drawn based on the model polynomial functions to assess the change of the response surface [201]. Different response surface curves (Figure 4.8, 4.9, 4.10) were obtained to establish the effect of independent variables on particle size. X1, X2 and X3 had the significant effect on the particle size, as the coefficient values were more. In Figure 4.8, the effect of polymer amount and organic phase volume on particle size (Y1) was studied when surfactant concentration was kept constant. The result showed that the particle size rapidly increased as the polymer amount (X1) increased. This was mainly occurred due to formation of more viscous solution. This action also detected in the following plot: The red dot in the 3D plot elaborated in the contour plot. The sky colour region bears the lower particle size and the size is increased in the region of green, yellow, red respectively.

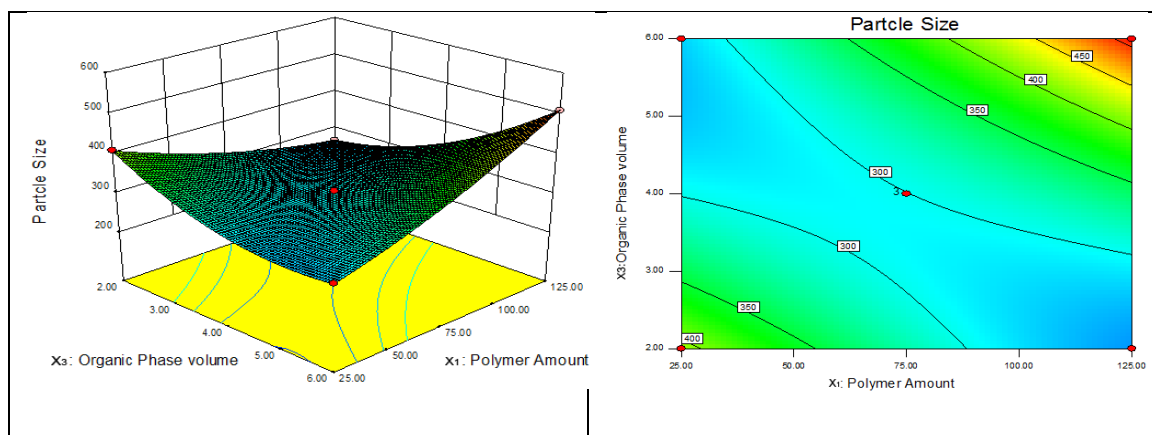


**Figure 4. 8: Effect of polymer amount and organic phase volume on particle size**

Increasing the surfactant concentration with fixed organic phase volume decreased particle size shown in Figure 4.9. Combination effects were seen in the changes of polymer amount and surfactant concentration. In the way of blue region particles size were decreased and that was occurred due to increasing surfactant concentration and decreasing polymer amount. Changes of blue to sky or green, results in increasing particle size.

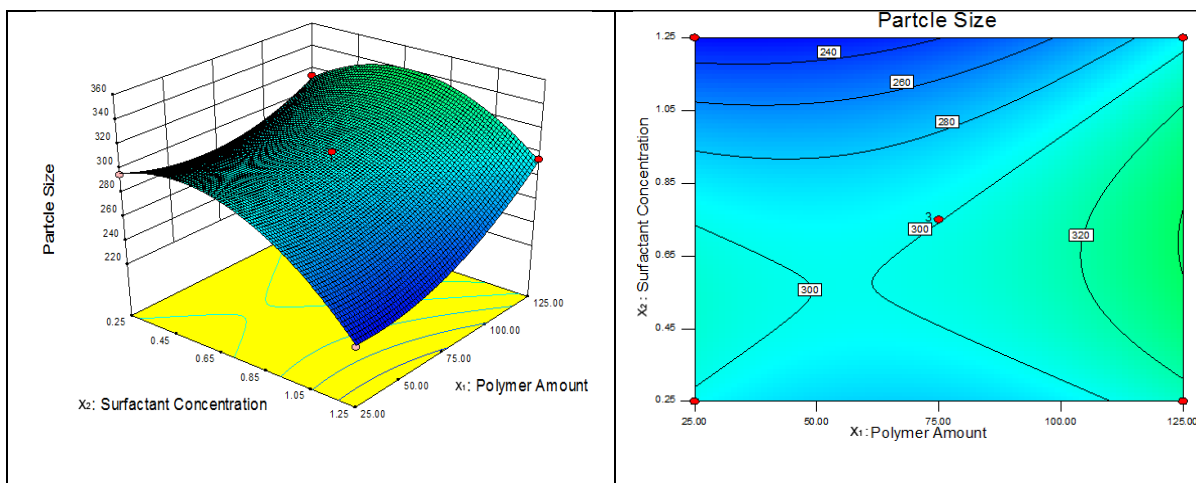


**Figure 4. 9: Effect of surfactant concentration and polymer amount on particles size**

In Figure 4.10, particle size was significantly increased by the increasing organic phase volume. Mainardes RM et al (2005) [26] reported particle size of PLGA nanoparticles decreased with increasing organic phase volume. But here opposite effect was seen. This signifies that the drug molecular structure also influence the formation of nanoparticles. Contour plot is defined as the geometric illustration of a response obtained by plotting one independent variable against another, holding the magnitude of response and other variables as constant [195]. These are two dimensional representations of the responses for the selected factors. As discussed earlier, blue region signifies lower particles size and these particles size increase in the green area.

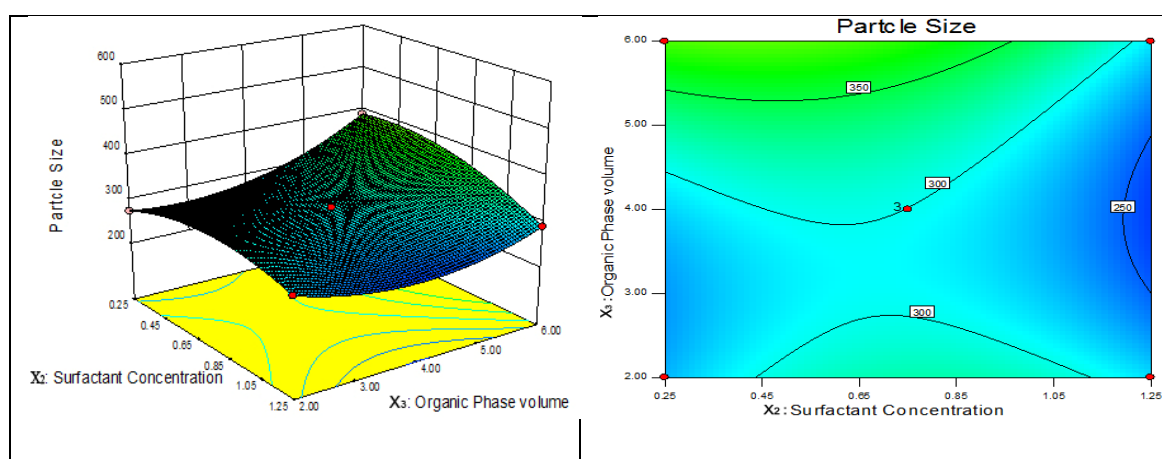


**Figure 4. 10: Effect of Surfactant concentration and organic phase on particle size**

#### 4.3.3.2. Effect of independent variables on entrapment efficiency

Percentage drug entrapment varies from 55.31 % (Formulation 15) to 81.56 % (Formulation 5) for various factors level combinations. System suggested quadratic model was selected due

to maximum correlation between adjusted and predicted  $R^2$  values shown in Table 4. 17. The "Predicted R-Squared" of 0.8477 was in reasonable agreement with the "Adjusted R-Squared" of 0.9579. The analysis of variance (ANOVA) quadratic regression model demonstrated that the model F-value of 36.38 implied the model was significant due to very low probability ( $P < 0.05$ ) with the confidence interval of 95 %.

**Table 4. 17: Selection of model for ANOVA analysis**

Source	Sequential p-value	Lack of Fit p-value	Adjusted R-Squared	Predicted R-Squared	System decision
Linear	0.0095	0.0764	0.5327	0.2297	-
2FI	0.0044	0.2289	0.8644	0.6548	-
Quadratic	0.0314	0.5668	0.9579	0.8477	Suggested
Cubic	0.5668	-	0.9549	-	-

The Model F-value of 36.38 implied the model was significant.  $X_1$ ,  $X_2$ ,  $X_3$ ,  $X_1X_3$ ,  $X_2X_3$ , and  $X_{22}$  were significant model terms (Table 4.18).

**Table 4. 18: ANOVA analysis for response surface**

Source	Sum of Squares	Df	Mean Square	F Value	p-value Prob > F	System suggestion
Model	714.8167	9	79.42407	36.37744	0.0005	Significant
$X_1$ -Polymer amount	36.125	1	36.125	16.5458	0.0097	-
$X_2$ -Surfactant concentration	351.125	1	351.125	160.8206	< 0.0001	-
$X_3$ -Organic phase volume	72	1	72	32.9771	0.0022	-
$X_1X_2$	2.25	1	2.25	1.030534	0.3566	-
$X_1X_3$	64	1	64	29.31298	0.0029	-
$X_2X_3$	144	1	144	65.9542	0.0005	-
$X_1^2$	1.852564	1	1.852564	0.848503	0.3992	-
$X_2^2$	38.00641	1	38.00641	17.40752	0.0087	-
$X_3^2$	4.00641	1	4.00641	1.834997	0.2335	-
Residual	10.91667	5	2.183333	-	-	-
Lack of Fit	6.25	3	2.083333	0.892857	0.5668	Not significant
Pure Error	4.666667	2	2.333333	-	-	-

The effect of average particle size was explained by the following quadratic equation:  
 Percentage drug entrapment =  $+72.67 + 2.13X_1 - 6.63X_2 - 3.00X_3 + 0.75X_1X_2 - 4.00X_1X_3 - 6.00X_2X_3 - 0.71X_1^2 - 3.21X_2^2 + 1.04X_3^2$  .....2

There was little influence of  $X_1$ ,  $X_2$  &  $X_3$  on the PDE that was revealed due to low coefficient value. Different response surface curve was obtained to establish the effect of independent variables on percentage drug entrapment (Figure 4.11, 4.12, 4.13). Red zone signifies more drug entrapment in respect of yellow zone. Change of colour from yellow to green signifies the decrease in percentage drug entrapment.

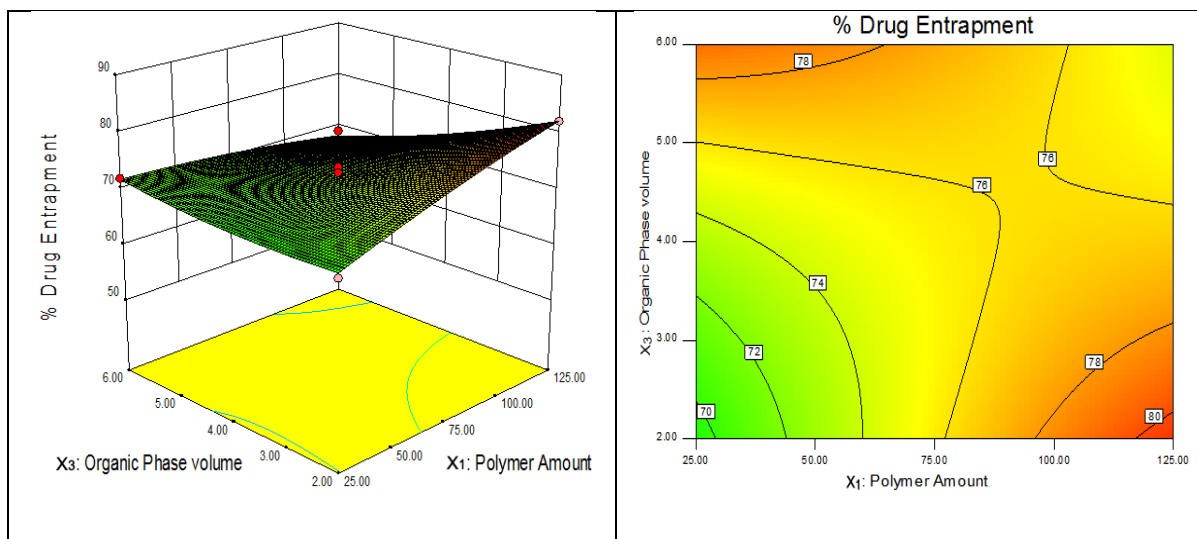


**Figure 4. 11: Effect of polymer amount and organic phase volume on percentage drug entrapment**

The effect of varying amount of polymer amount and organic phase volume on the percentage drug entrapment was studied when surfactant concentration was constant (Figure 4.11). In equation 2, coefficient of  $X_1$  was  $+^ve 2.13$ . Hence, percentage drug entrapment ( $Y_2$ ) was increased with increasing the polymer amount ( $X_1$ ). This is mainly occurred due to more bond formation between lipophilic drugs with lipophilic polymer. But due to low coefficient value the influence of polymer amount on response  $Y_2$  was less. In combination of higher polymer amount-lower organic phase volume and lower polymer amount-higher organic phase volumes denoted as the red area means of higher PDE value.

In Figure 4.12, influence of polymer amount and surfactant concentration studied with constant value of organic phase volume on PDE. Due to negative sign before the coefficient of  $X_2$  inverse effect was seen between PDE and surfactant concentration. That means PDE values was decreased with increasing the surfactant concentration that supported by the literature [26]. But the influence of surfactant concentration was less due to low coefficient value. Red zone was detected in the combination of higher polymer amount and lower

surfactant concentration. Decreasing the polymer amount and increasing surfactant amount the plot turns into green means lower PDE value.

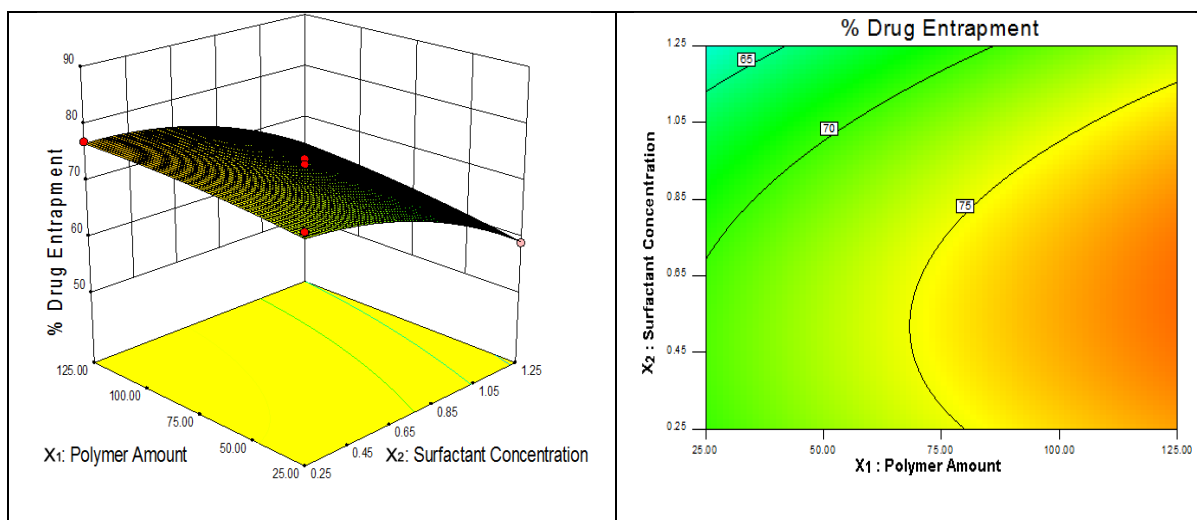


**Figure 4.12: Effect of surfactant concentration and polymer amount on percentage drug entrapment**

Influence of organic phase volume and surfactant concentration was studied on PDE shown in Figure 4.13. Due to negative coefficient of  $X_3$ , inverse relationship was established between PDE and DCM volume. Means drug entrapment increased with decreasing DCM volume and vice-versa. This signifies that the percentage drug entrapment increased with drug concentration in the organic phase [192]. The interaction term ( $X_1X_2$ ,  $X_1X_3$ ,  $X_2X_1$ ,  $X_1^2$ ,  $X_2^2$ , and  $X_3^2$ ) showed the PDE changed when two variables were changed simultaneously. The PDE values decreases in the order of yellow > green > sky > blue.

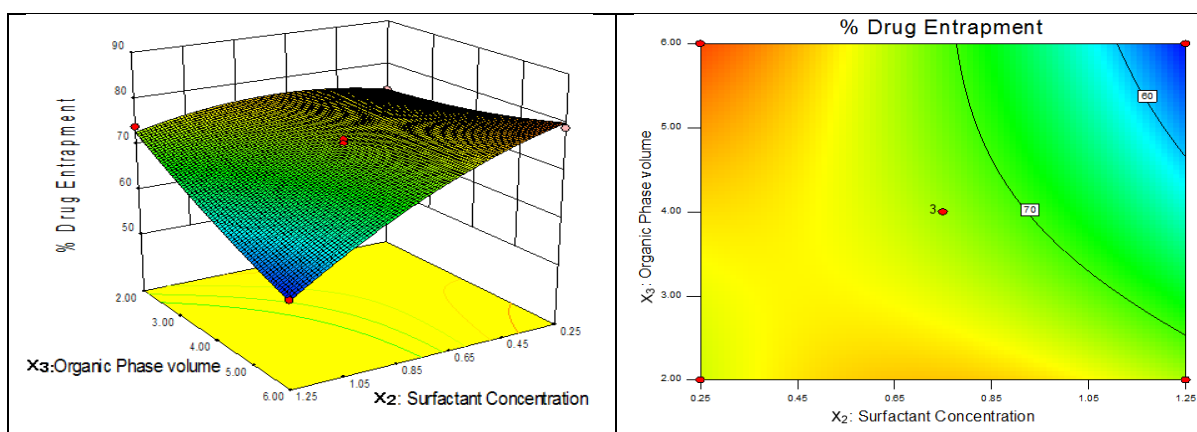


**Figure 4.13: Effect of organic phase volume and surfactant concentration on percentage drug entrapment**

#### 4.3.3.3. Effect of independent variables on polydispersibility index

No significant correlations were established between independent variables with polydispersibility index. The value of zeta potential of all the batches was in the range of  $\pm 5$  mV. Due to aggregation of particles PDI value was found to be in the range of 0.607 (formulation 1) to 2.248 (formulation 6).

#### 4.3.3.4. Search for Optimum nanoparticles of Prothionamide and its characterization

Formulation optimization was carried out to find the levels of the variable that affect the chosen responses and determine the levels of the variable from which a robust product with high quality characteristics may be produced. All the measured responses that may affect the quality of the product were taken into consideration during the optimization [202]. No significance co-relation was established with poly dispersibility index. Hence, particle size and percentage drug entrapment had been taken under consideration for the selection of optimized batch (OP). Formulation was optimized with set criteria of maximum entrapment efficiency and minimum particle size, followed by higher disability factor. Optimized formulation (OP) contained 25 mg of PTH, 125 mg of PLGA, 0.36 % PVA and 2 ml of DCM volume. System suggested optimized formulation was prepared with particle size, PDE and DPI of  $310 \pm 12$  nm,  $80.08 \pm 0.26$  % and  $0.386 \pm 0.13$  respectively. Practical values have reasonable agreement with the predicted values. Other evaluation parameters are shown in Table 4.19.

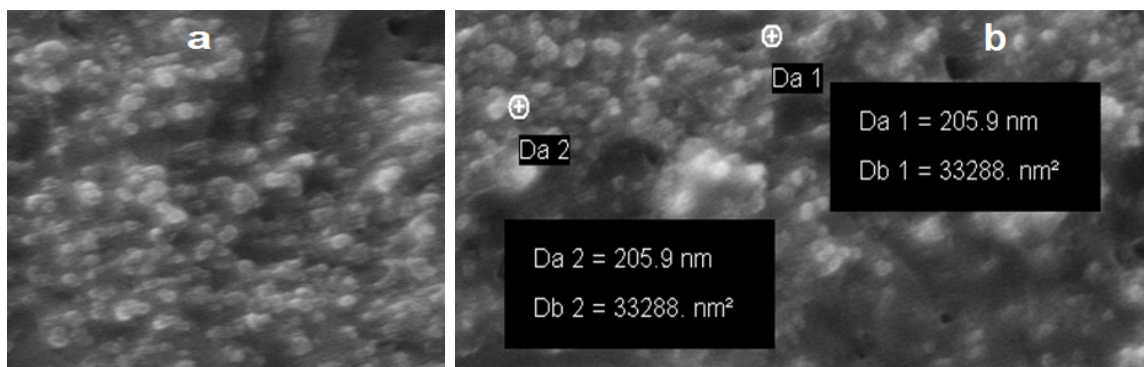
**Table 4. 19: Characterization of optimized batch (OP)**

Composition of optimized batch (OP)		Response		Prediction	Practical value <sup>‡</sup>
PLGA -125 mg		Particle Size (nm)		229.35	310 ± 12
PVA – 0.36 %		% Drug Entrapment		79.58	80.08 ± 0.26
DCM- 2mL		PDI		Not analyzed	0.386 ± 0.13
Other evaluation parameters					
Drug used (mg)	Cryoprotectant (% w/v)	nanoparticles weight <sup>‡</sup> (mg)	Drug content <sup>‡</sup> (% w/w)	Process yield <sup>‡</sup> (% w/w)	Zeta potential <sup>‡</sup> (mV)
25	2	0.316±6.33	6.33±0.08	90.44±1.81	6.11±0.11

<sup>‡</sup>Values are mean of three data  $\pm$  standard deviation

#### 4.3.4. SEM analysis of system generated optimized nanoparticles

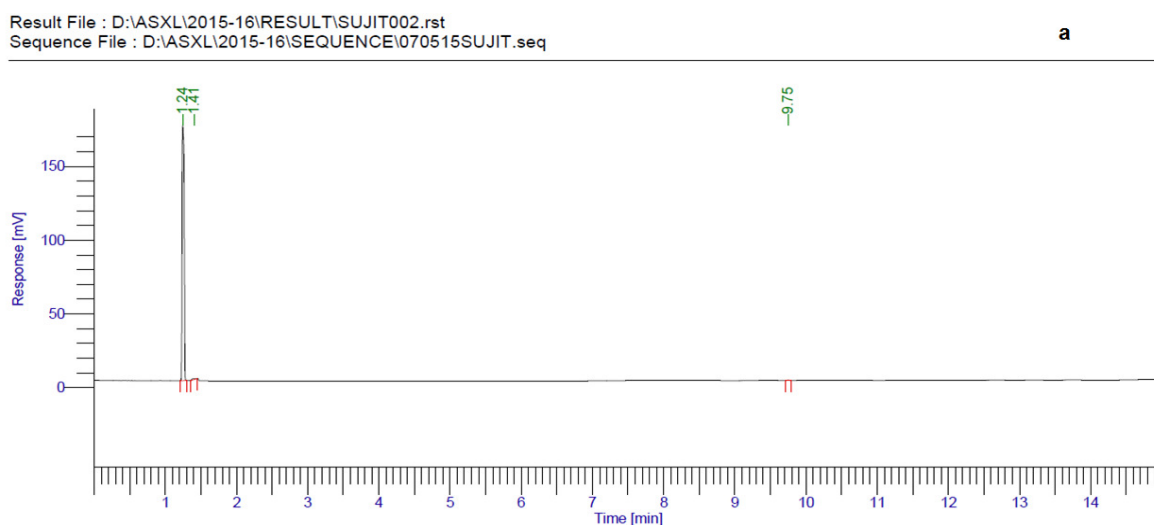
SEM images (Figure 4. 14) showed that the optimized Prothionamide nanoparticles (OP batch) were spherical in shape. Most of the particle size was of 205.9 nm, which are suitable for the inhalation formulation.



**Figure 4. 14: SEM image of optimized freeze dried nanoparticles (OP)**

#### 4.3.5. Residual solvent analysis

ICH has recommended the permissible amount of such compounds in pharmaceutical formulations for the safety of the human being or patient [122]. DCM is a controlled organic solvent which may cause severe syndromes after inhalation, oral administration or skin contact [124]. In the present study, freeze dried nanoparticles (OP) tested for residual solvent of DCM and found 0.11 ppm (Appendix B). Figure 4.15 shows the chromatogram of pure DCM (a) and PLGA nanoparticles sample (b). Principle peak of DCM detected at 1.24 min in Figure 4. 15 (a) and same can be seen in Figure 4.15 (b) at 1.25min.





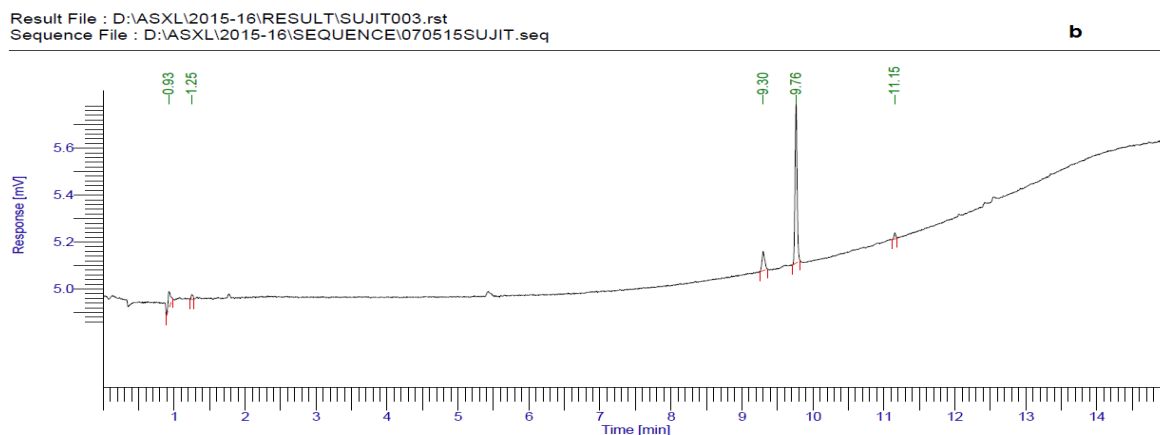


**Figure 4. 15: GC chromatograms of (a) pure DCM, (b) optimized PLGA-PTH nanoparticles (OP)**

#### 4.3.6. Differential scanning calorimetry (DSC)

DSC allows a rapid evaluation of possible incompatibilities by revealing changes in the appearance, shift or disappearance of melting or other endothermic and/or exothermic processes, and/or variations in the corresponding enthalpies reactions [203]. Figure 4.16 DSC curves of pure PTH (a), PLGA (75:25) (b), and nanoparticles of PTH-PLGA (OP)(c). As seen in the DSC thermograph, PLGA (75:25) showed a glass transition state at 46.52°C means this polymer in the amorphous state. Similar peak also seen in the nanoparticles means no changes occurred in PLGA during formation of nanoparticles. On the other hand, Pure PTH showed characteristic endothermic sharp peak at 144.32°C due to its crystalline form [204]. Same peak also seen in the nanoparticles at 143.11°C, but this time the peak was little wide means its crystal form turns into amorphous form due to incorporation in the PLGA coat.

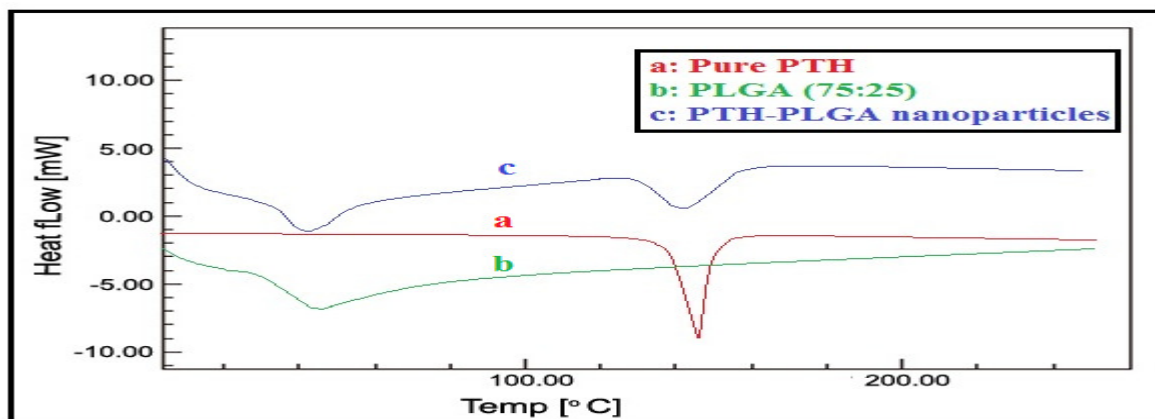


**Figure 4. 16: DSC Thermogram of (a) Prothionamide, (b) PLGA (75:25) polymer, (c) Optimized PTH-PLGA nanoparticles (OP)**



#### 4.3.7. Formulation and characterization of dry powder inhaler

Different proportion of anhydrous lactose was added to the optimized Prothionamide nanoparticles by physical geometric mixture. In each addition angle of repose, Carr's index and Hausner ratio were determined (Table 4. 20). Upon addition of anhydrous lactose, these values were decreased initially but increased afterward. PP-DPI 2 showed excellent flow property in 1:1 proportion of Prothionamide nanoparticles and lactose.

**Table 4. 20: Optimization of dry powder inhaler**

Formulation code	Nanoparticles: Anhydrous lactose	Angle of repose <sup>‡</sup>	Carr's index <sup>‡</sup>	Hausner ratio <sup>‡</sup>
PP-DPI 1	1.0:0.5	33.68 ± 1.34	11.12 ± 0.41	1.13 ± 0.001
PP-DPI 2	1.0:1.0	27.41 ± 0.73	8.13 ± 1.92	1.09 ± 0.02
PP-DPI 3	1.0:1.5	32.86 ± 2.38	12.08 ± 1.81	1.14 ± 0.02
PP-DPI 4	1.0:2.0	34.98 ± 0.41	13.54 ± 1.80	1.16 ± 0.02

<sup>‡</sup>Values are mean of three data ± standard deviation

Similarly DPI of pure PTH also prepared by blend the inhalable grade lactose with pure PTH. Optimum DPI found for the pure PTH- lactose (PL-DPI 4) in the ratio of 1:4.

##### 4.3.7.1. Determination of MMAD and geometric standard deviation

The size and shape of particles are the main parameters that determine their deposition in the different parts of lungs. Aerodynamic particle size in range of 0.5-5 µm can reach to the small airways and alveoli [142]. Each chamber cleaned carefully and calculated the content of PTH in each chamber by UV-spectrophotometric method using water-methanol solvent of 8:2 (Table 4. 21).

**Table 4. 21: Drug deposition in different chamber of impactor from PP-DPI 2**

Stage	micron	Absorbance	Conc. (µg/ml)	dilution factor	amount(µg)	amount(mg)	Percentage deposition
0	9	0.162	6.4	10	64	0.064	0.64
1	5.8	0.578	23.04	10	230.4	0.2304	2.304
2	4.7	0.691	27.56	10	275.6	0.2756	2.756
3	3.3	0.224	8.88	100	888	0.888	8.88
4	2.1	0.49	19.52	100	1952	1.952	19.52
5	1.1	0.839	33.48	100	3348	3.348	33.48
6	0.7	0.468	18.64	100	1864	1.864	18.64
7	0.4	0.398	15.84	20	316.8	0.3168	3.168
Filter	n/a	0.261	10.36	20	207.2	0.2072	2.072

Flow Rate:		28.3 L/min
Cut off Diameter		
Impactor Stage	(microns)	Drug Collected
Stage 0	9	0.064
Stage 1	5.8	0.2304
Stage 2	4.7	0.2756
Stage 3	3.3	0.888
Stage 4	2.1	1.952
Stage 5	1.1	3.348
Stage 6	0.7	1.864
Stage 7	0.4	0.3168
Filter	n/a	0.2072
MMAD:	1.69	microns
GSD:	1.95	

**Figure 4. 17: Snapshot of calculated aerodynamic particle size determination**

Amount obtained in each chamber placed in MMAD calculator available in official web site of Anderson cascade impactor is represented in Figure 4.17. Prepared DPI of Prothionamide nanoparticles showed aerodynamic particle size of 1.69  $\mu\text{m}$  and geometric standard deviation as 1.95. This signifies that the prepared DPIs can reach deeply to lungs. Fine particle fraction, extra fine particle fraction and emitted dose were 76.88 %, 23.88 % and 91.46 % respectively.

#### 4.3.7.2. *In-vitro* release study

The optimized Prothionamide nanoparticles loaded DPI (PP-DPI 2) was subjected for *in-vitro* drug release behaviour. Simulated lungs fluid was used as dissolution medium for evaluating the release pattern of Prothionamide from PLGA nanoparticles. The optimized Prothionamide-PLGA nanoparticles showed initial burst release of  $20 \pm 1.08\%$  in 1 hr followed by sustained drug release up to  $43.52 \pm 0.81\%$  in 24 hr (Figure 4.18). The initial burst release will help to reach the desired plasma concentration in lungs, and the sustained release will help to maintain the PTH dose for prolong period of time. The *in-vitro* release data was analyzed through zero order, Higuchi, Peppas models and obtained correlation co-efficient ( $R^2$ ) were 0.982, 0.966, and 0.933 respectively (Table 4. 22). Hence, the release best fitted with zero order kinetics.

**Table 4. 22: *In-vitro* release study data of optimized batch (PP-DPI 2) in simulated lung fluid**

Zero order		Higuchi Plot		Peppas	
Time (hr)	% Cumulative drug release <sup>‡</sup>	Square route of time (hr)	% Cumulative drug release <sup>‡</sup>	Log time (hr)	log % CDR
1	20.00±1.08	1.00	20.00±1.08	0.00	1.30
2	24.69±0.41	1.41	24.69±0.41	0.30	1.39
3	25.75±0.41	1.73	25.75±0.41	0.48	1.41
4	26.00±0.42	2.00	26.00±0.42	0.60	1.42
5	27.07±0.42	2.24	27.07±0.42	0.70	1.43
6	27.33±0.43	2.45	27.33±0.43	0.78	1.44
7	28.00±0.43	2.65	28.00±0.43	0.85	1.45
8	29.09±0.43	2.83	29.09±0.43	0.90	1.46
9	29.77±0.03	3.00	29.77±0.03	0.95	1.47
10	31.27±0.74	3.16	31.27±0.74	1.00	1.50
11	31.97±0.04	3.32	31.97±0.04	1.04	1.50
12	32.26±0.04	3.46	32.26±0.04	1.08	1.51
13	32.96±0.37	3.61	32.96±0.37	1.11	1.52
14	33.67±0.38	3.74	33.67±0.38	1.15	1.53
15	33.97±0.38	3.87	33.97±0.38	1.18	1.53
16	35.91±1.05	4.00	35.91±1.05	1.20	1.56
17	37.86±0.02	4.12	37.86±0.02	1.23	1.58
18	38.19±0.39	4.24	38.19±0.39	1.26	1.58
19	39.34±0.42	4.36	39.34±0.42	1.28	1.59
20	39.69±0.41	4.47	39.69±0.41	1.30	1.60
21	40.03±0.02	4.58	40.03±0.02	1.32	1.60
22	40.78±0.40	4.69	40.78±0.40	1.34	1.61
23	41.53±0.39	4.80	41.53±0.39	1.36	1.62
24	43.52±0.81	4.90	43.52±0.81	1.38	1.64
$R^2 = 0.982$		$R^2 = 0.966$		$R^2 = 0.933$	

<sup>‡</sup>Values are mean of three data ± standard deviation

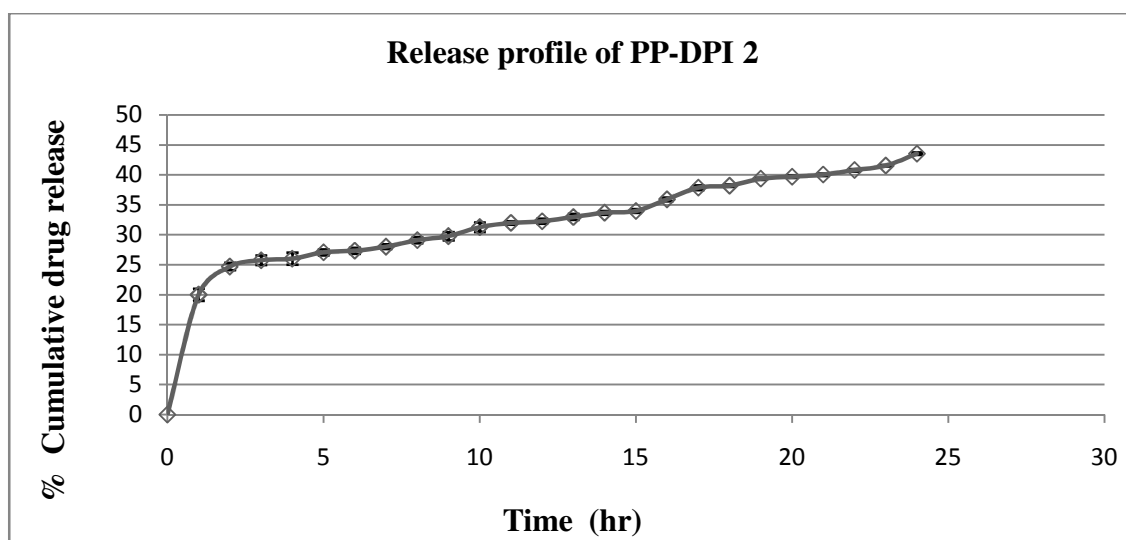


**Figure 4. 18: Release profile of PP-DPI 2 in simulated lung fluid**

#### 4.3.7.3. Stability study

Various literatures reported the instability of nanoparticles during storage. Six months stability study revealed no clumping or aggregation of particles. Zeta size, PDI, and drug release demonstrated that the dry powder inhaler was stable during stress testing (Table 4. 23).

**Table 4. 23: Stability study of PP-DPI 2**

Time point (month)	Particle size (nm) <sup>‡</sup>	PDI <sup>‡</sup>	Zeta potential <sup>‡</sup>	% Drug Entrapment <sup>‡</sup>	Percentage drug release in 24 hr <sup>‡</sup>
0	323.3 ± 10	0.321 ± 0.13	6.11 ± 0.11	80.13 ± 0.11	42.51 ± 1.5
1.5	323.8 ± 09	0.319 ± 0.21	6.19 ± 2.7	80.13 ± 0.09	43.15 ± 0.9
3	326.1 ± 05	0.317 ± 0.32	5.9 ± 3.5	80.12 ± 0.12	43.89 ± 3.2
6	331.4 ± 12	0.319 ± 0.47	6.5 ± 2.1	80.12 ± 0.16	48.32 ± 6.4

<sup>‡</sup>Values are mean of three data ± standard deviation

#### 4.3.8. Design of DPI and delivery dose calculation

Mono-dose inhaler and nasal insufflators were obtained as a gift sample from MIAT S. P. A. Milano, Italy for this project. But these devices are helpful for the DPI delivery in human but not for rodent. Hence, the below mentioned modified delivery devices developed as per previous reported article [176].



**Figure 4. 19: Modified design of dry powder inhaler delivery device**

The delivery tube is made of stainless steel that extends 2'' after a 120-degree bend. It was operated with a 5 ml air syringe. This delivery tube was collected from local ENT specialist. Middle reservoir chamber was chosen from the catheter equipped with chamber (left Figure). In Figure 4.19, two different modified delivery devices were developed. One contained the reservoir chamber and the other does not contain the reservoir chamber. In the present study, reservoir chamber containing dry powder inhaler was used for administration of DPI through pulmonary route.

**Table 4. 24: Delivery dose calculation of modified DPI device**

Absorbance	Conc. (µg/ml)	Volume (ml)	Amount in µg	Amount in mg	Dose given (mg)	Dose delivered (mg)	Percentage delivered
0.047	1.84	10	18.4	0.0184	1.6	1.5816	98.85
0.051	2	10	20	0.02		1.58	98.75
0.053	2.08	10	20.8	0.0208		1.5792	98.70
Average <sup>‡</sup>						1.5802 ± 0.001	
Percentage delivered <sup>‡</sup>						98.77 ± 0.076%	

<sup>‡</sup>Values are mean of three data ± standard deviation

Water-methanol (8:2) solvent system was used to calculate the content of PTH as mentioned in section 4.2.2. Percentage delivery dose of prepared DPI was calculated and found as 98.77 ± 0.076 % (Table 4. 24). During drug administration, this percentage delivery was considered to calculate the delivery dose.

### 4.3.9. *In-vivo* study

*In vitro* drug release was carried out and found  $43.52 \pm 0.81\%$  PTH release in 24 hr. Although *in vitro* release of drug was less, but also the DPI produced sustain release for more than 24 hr. Animal experiment was carried out with this optimized DPI (PP DPI 2) to check the effectiveness of the prepared DPI *in vivo*. Institutional animal ethical committee meeting was conducted at Bengal College of Pharmaceutical Sciences and Research, Durgapur, West Bengal (BCPSR/IAEC/04-16) (Appendix A). Based on recommendation and guideline all the animal experiments were conducted.

#### 4.3.9.1. Dose calculation and its administration

Gently pulled the tongue outside and sprayed DPIs through the device by placing it in trachea region [205]. In each time period, three animals were selected to obtain statistical significant data. Dose equivalent nanoparticles and corresponding DPI was calculated. Depending upon body weight the dose was administered and the data is given in Table 4. 25.

**Table 4. 25: Dose administration of Optimized DPI (PP-DPI2) in rat**

Animal treated with DPI Study 1 (S1)				Animal treated with DPI Study 2 (S2)				Animal treated with DPI Study 3 (S3)			
Animal code <sup>†</sup>	Rat Weight (Kg)	Dose of PTH (mg)	Equ. wt. of DPI (mg)	Animal code <sup>†</sup>	Rat Weight (Kg)	Dose of PTH (mg)	Equ. wt. of DPI (mg)	Animal code <sup>†</sup>	Rat Weight (Kg)	Dose of PTH (mg)	Equ. wt. of DPI (mg)
F1	0.248	1.9096	61.14	M1	0.237	1.8249	58.43	M1	0.229	1.7633	56.45
M2	0.236	1.8172	58.18	M2	0.232	1.7864	57.19	F2	0.236	1.8172	58.18
M3	0.251	1.9327	61.88	F3	0.225	1.7325	55.47	F3	0.242	1.8634	59.66
M6	0.224	1.7248	55.22	M6	0.22	1.694	54.23	F6	0.232	1.7864	57.19
F12	0.239	1.8403	58.92	F12	0.243	1.8711	59.90	M12	0.231	1.7787	56.95
F24	0.221	1.7017	54.48	F24	0.238	1.8326	58.67	M24	0.236	1.8172	58.18

<sup>†</sup> Animal code was divided in two parts: First digit stand for the sex of rat, last numerical digit denote the time of sacrificing after dose administration

In study period 1, the first rat (S1F1) weight was 0.248 kg. Equivalent dose of PTH calculated was 1.9096 mg (section 3.5.5.3). Prepared nanoparticles for the animal study contained 60.06 mg of PTH in 949.6 mg of nanoparticles.

So, 1.9096 mg PTH equivalent nanoparticles is  $(949.6 * 1.9096)/60.06 = 30.1924$  mg of nanoparticles.

On the other hand, optimized DPI (PP-DPI2) contained nanoparticles-lactose proportion was 1:1. So total equivalent amount of DPI is  $= 30.1924 * 2 = 60.384$  mg.

But modified delivery device was able to deliver  $98.77 \pm 0.076$  % of its content.

Hence, the corrected DPI amount is  $(100 * 60.384)/98.77 = 61.1368 \approx 61.14$  mg. Similar calculation was followed for rest of the animals (Table 4.25).

On the other hand, PTH dose was calculated as mentioned previously and DPI was prepared by the physical mixture of pure PTH with inhalable grade lactose. Optimum DPI found for the pure PTH- lactose (PL-DPI 4) in the ratio of 1:4. Hence, Equivalent weight of DPI was calculated by multiplying 5 with dose of Prothionamide.

**Table 4. 26: Dose administration of DPI containing pure PTH (PL-DPI 4) in rat**

Animal treated with DPI Study 1 (S1)				Animal treated with DPI Study 2 (S2)				Animal treated with DPI Study 3 (S3)			
Animal Code	Rat Weight (Kg)	Dose of PTH (mg)	Equ. wt. of DPI (mg)	Animal Code	Rat Weight (Kg)	Dose of PTH (mg)	Equ. wt. of DPI (mg)	Animal Code	Rat Weight (Kg)	Dose of PTH (mg)	Equ. wt. of DPI (mg)
M1	0.236	1.8172	9.20	M1	0.232	1.7864	9.04	F1	0.234	1.8018	9.12
F2	0.231	1.7787	9.00	F2	0.243	1.8711	9.47	F2	0.232	1.7864	9.04
M3	0.228	1.7556	8.89	F3	0.236	1.8172	9.20	M3	0.223	1.7171	8.69
M6	0.226	1.7402	8.81	F6	0.224	1.7248	8.73	M6	0.238	1.8326	9.28
F12	0.237	1.8249	9.24	M12	0.225	1.7325	8.77	M12	0.243	1.8711	9.47
F24	0.232	1.7864	9.04	M24	0.22	1.694	8.58	F24	0.238	1.8326	9.28

<sup>a</sup>Animal code was divided in two parts: First digit stand for the sex of rat, last numerical digit denote the time of sacrificing after dose administration

As for example, the 0.236 kg weight rat (Table 4. 26 – S1M1) corresponding PTH weight is 1.8172 mg. Equivalent weight of DPI for the same is  $1.8172 \times 5 = 9.086 \approx 9.09$  mg.

As delivery device is able to deliver  $98.77 \pm 0.076$  % of its content. Hence, corrected dose is  $(100 \times 9.086) / 98.77 = 9.1991 \approx 9.20$  mg. Table 4. 26 shows body weight equivalent dose and respective DPI for individual rat.

#### 4.3.9.2. Pharmacokinetic analysis

Two different studies were carried out to determine as lungs tissue distribution and bio-distribution of Prothionamide (Table 4. 27).

**Table 4. 27: Lungs tissue and plasma distribution of PTH from DPI**

Lung's tissue distribution study				
Time of study (hr)	DPI containing PTH-PLGA nanoparticles (PP-DPI 2)		DPI containing pure PTH (PL-DPI 4)	
	PTH amount in lung's tissue <sup>‡</sup> (µg)	PTH conc. <sup>‡</sup> (µg/ml)	PTH amount in lungs tissue <sup>‡</sup> (µg)	PTH conc. <sup>‡</sup> (µg/ml)
1	19.86 ± 0.24	2.31 ± 0.03	39.28 ± 2.66	4.56 ± 0.31
2	17.81 ± 0.08	2.07 ± 0.01	17.61 ± 0.86	2.05 ± 0.09
3	17.43 ± 0.12	2.03 ± 0.01	6.22 ± 0.48	0.72 ± 0.06
6	5.58 ± 0.33	0.65 ± 0.04	1.55 ± 0.24	0.18 ± 0.03
12	2.37 ± 0.24	0.28 ± 0.03	---	---
24	1.89 ± 0.16	0.22 ± 0.02	--	---
Plasma distribution study				
Time (hr)	DPI containing PTH-PLGA nanoparticles (PP-DPI 2)		DPI containing pure PTH (PL-DPI 4)	
	PTH amount in plasma <sup>‡</sup> (µg)	PTH conc. <sup>‡</sup> (µg/ml)	PTH amount in plasma <sup>‡</sup> (µg)	PTH conc. <sup>‡</sup> (µg/ml)
1	22.70 ± 0.85	0.09 ± 0.005	87.18 ± 8.71	0.42 ± 0.03
2	21.60 ± 0.38	0.096 ± 0.0003	29.18 ± 1.42	0.14 ± 0.01
3	18.52 ± 0.94	0.079 ± 0.005	16.94 ± 1.35	0.08 ± 0.01
6	15.46 ± 0.23	0.074 ± 0.003	0.15 ± 0.12	0.001 ± 0.001
12	6.44 ± 0.43	0.028 ± 0.005	---	---
24	5.44 ± 0.20	0.025 ± 0.001	---	---

<sup>‡</sup>Values are mean of three data ± standard deviation



DPI containing PTH nanoparticles (PP-DPI 2) maintained drug concentration above the MIC for the period of 6 hr in lungs, but pure PTH loaded DPI could able to maintain the same only for 3 hr. Concentration attained by PTH nanoparticles was  $0.22 \pm 0.02 \mu\text{g/ml}$  at 24 hr. PTH detected after 24 hr, when given in the form of nanoparticles that signified prolong drug residency of DPI in lungs. AUC increased significantly when PTH was given in the form of nanoparticles (Table 4. 28). Concentration maximum reached at lungs was  $2.31 \pm 0.03 \mu\text{g/ml}$  at 1 hr from PP DPI 2. Whereas maximum concentration reached by pure PTH loaded DPI (PL-DPI4) was  $4.57 \pm 0.31 \mu\text{g/ml}$  at  $T_{\text{max}}$  of 1 hr.

As PTH reached plasma very slowly from PTH nanoparticles, AUC was relatively less of  $1.16 \pm 0.02 \mu\text{g/ml}$  in comparison to lungs. Hence, drugs concentrate more in lungs rather than plasma (Figure 4. 20).

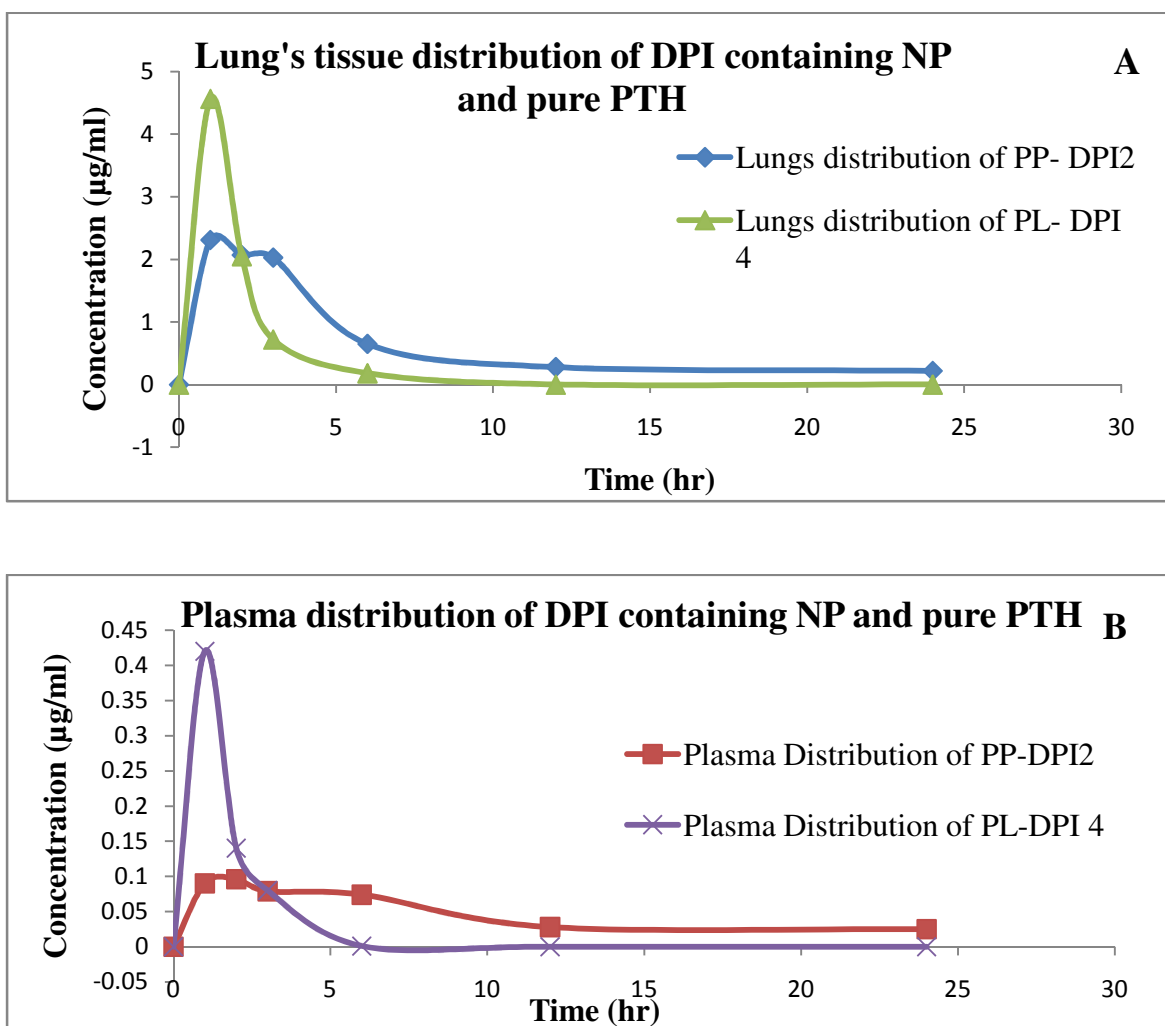


**Figure 4. 20: Lung's tissue (A) & Plasma (B) distribution of PP-DPI2 and PL-DPI 4**

**Table 4. 28: Pharmacokinetic parameters of PTH in plasma and lungs**

Pharmacokinetic parameters of PTH in lung's tissue			
DPI containing	$C_{\max}^{\ddagger}$ ( $\mu\text{g/ml}$ )	$T_{\max}^{\ddagger}$ (hr)	$AUC^{\ddagger}$ ( $\mu\text{g hr/ml}$ )
Nanoparticles (PP-DPI2)	$2.31 \pm 0.03$	1	$15.79 \pm 0.20$
Pure PTH (PL-DPI 4)	$4.57 \pm 0.31$	1	$10.08 \pm 2.31$
Pharmacokinetic parameters of PTH in plasma			
DPI containing	$C_{\max}^{\ddagger}$ ( $\mu\text{g/ml}$ )	$T_{\max}^{\ddagger}$ (hr)	$AUC^{\ddagger}$ ( $\mu\text{g hr/ml}$ )
Nanoparticles (PP- DPI 2)	$0.098 \pm 0.005$	1	$1.16 \pm 0.02$
Pure PTH (PL-DPI 4)	$0.416 \pm 0.024$	1	$0.728 \pm 0.009$

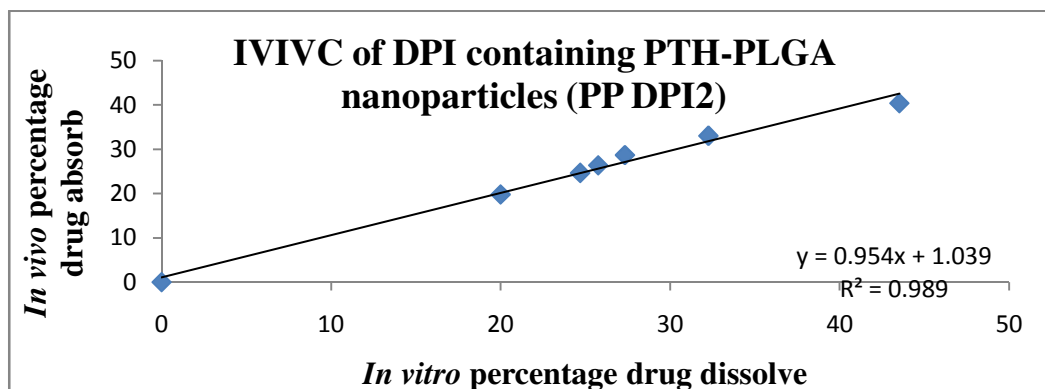
<sup>‡</sup>Values are mean of three data  $\pm$  standard deviation

#### 4.3.9.3. *In vitro*- *In vivo* correlation of DPI containing PP-DPI 2

*In vitro* drug release and *in vivo* drug diffusion are plotted in graph, where *in vitro* release represented in the X-axis and *in vivo* drug diffusion study into Y-axis (Table 4. 29). A good correlation coefficient was established as the  $R^2$  values came 0.989 (Figure 4. 21).

**Table 4. 29: Comparison between *in-vitro* release and *in-vivo* diffusion**

Time (hr)	<i>In-vitro</i> drug release	<i>In-vivo</i> drug diffusion
1	20.00	19.77
2	24.69	24.65
3	25.75	26.37
6	27.33	28.67
12	32.26	33.02
24	43.52	40.36

**Figure 4. 21: IVIVC of DPI containing PP-DPI 2**

#### 4.3. 10. *In-vitro* anti tubercular activity

The intensity of the dissolved formazan crystals (purple colour) was determined at 590 nm. Average value of three data was presented in table 4. 30. Based on the literature survey, PTH concentration selected for the study was 0.4-0.7 µg/ml. The drug PTH showed the MIC of 0.5 µg/ml, whereas nanoparticles containing PTH showed 0.6 µg/ml (Table 4. 30).

**Table 4. 30: Absorbance and cell viability of Pure Prothionamide and Prothionamide-PLGA nanoparticles in MTT assay**

<b>Pure Prothionamide</b>				
<b>Conc. (µg/ml)</b>	<b>0.4</b>	<b>0.5</b>	<b>0.6</b>	<b>0.7</b>
<b>Average absorbance</b>	0.2509	0.0874	0.081067	---
<b>SD</b>	0.016795	0.015894	0.004155	---
<b>% Viability</b>	13.28965	-0.15903	-0.67997	---
<b>SD</b>	1.381466	1.307335	0.221019	---
<b>Prothionamide-PLGA nanoparticles</b>				
<b>Conc. (µg/ml)</b>	<b>0.4</b>	<b>0.5</b>	<b>0.6</b>	<b>0.7</b>
<b>Average absorbance</b>	0.619967	0.2467	0.0759	0.069
<b>SD</b>	0.118059	0.022257	0.004957	0.00811
<b>% Viability</b>	43.64718	12.94418	-1.104957	-1.67252
<b>SD</b>	9.710962	1.830776	0.407722	0.667076

SD- Standard deviation; %- Percentage

#### 4.4. Formulation and characterization of DPI containing Prothionamide nanoparticles prepared by Chitosan

##### 4.4.1. Compatibility study

FTIR spectra (Figure 4. 22 a: pure PTH & b: physical mixture) confirmed the absence of chemical interaction whereby confirming the chemical compatibility by maintaining the integrity of principle peaks.

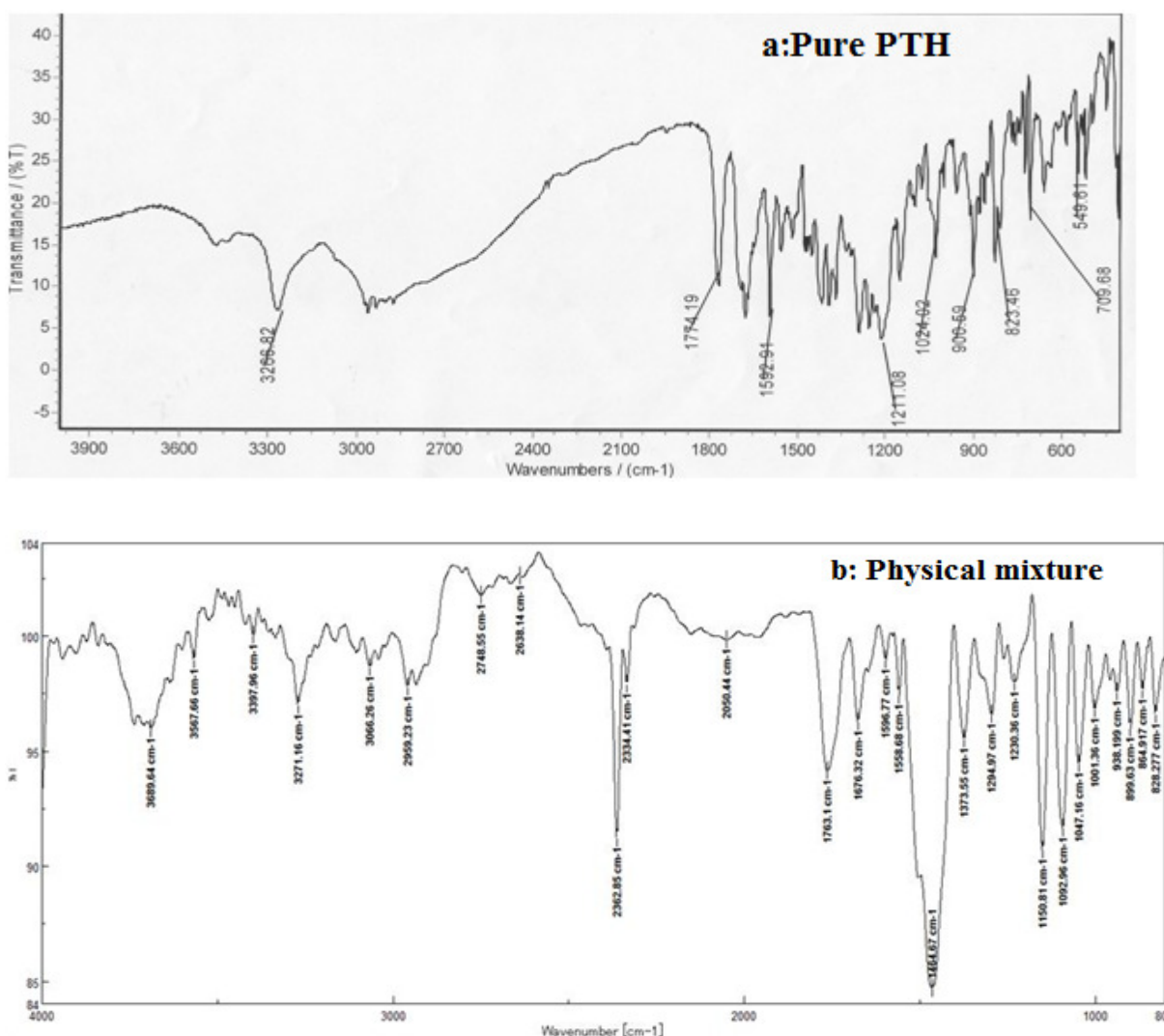


**Figure 4. 22: FTIR of pure PTH (a) and physical mixture of PTH, Chitosan, Inhalable grade lactose (b)**

N-H wag peak found in pure PTH was at 823.46 cm<sup>-1</sup>, whereas this peak was detected at 828.277 cm<sup>-1</sup> in physical mixture. =C-H bending was detected for pure PTH and mixture at 900.59 cm<sup>-1</sup> & 899.63 cm<sup>-1</sup> respectively. C-C=C stretch in ring, N-H stretch and C=S

stretching peak also showed at  $1592.91\text{ cm}^{-1}$ ,  $3266.82\text{ cm}^{-1}$  and  $1024.02\text{ cm}^{-1}$  respectively with narrow diffraction range which signified the compatibility of PTH with Chitosan and Lactose. FTIR data of pure PTH and physical mixture is given in Table 4. 31.

**Table 4. 31: Comparison of FTIR date between pure PTH with physical mixture**

Principle Peak( $\text{cm}^{-1}$ ) Pure Drug/ Physical Mixture	Functional Group	Principle Peak ( $\text{cm}^{-1}$ ) Pure Drug/ Physical Mixture	Functional Group
823.46/828.277	N-H wag	1211.08/1230.36	C-N stretching
900.59/899.63	=C-H bending	1592.91/1596.77	C-C=C stretch in ring
1024.02/1047.16	C=S Stretching	3266.82/3271.16	N-H stretch

#### 4.4.2. Characterization of Chitosan nanoparticles

Chitosan is insoluble in water, but the presence of amino groups causes its solubility in acidic solutions below pH of 6.5 [102]. Hence, Chitosan was dissolved in 1 % acetic acid solution. As PTH also dissolves in acetic acid, it was incorporated in the Chitosan solution. Chitosan nanoparticles were prepared by gelation technique. Cross linking occurred instantly upon addition of Chitosan-PTH solution into the TPP solution. Several step by step optimizations applied to prepare the suitable nanoparticles for dry powder inhaler.

##### 4.4.2.1. Effect of stirring time

Initially, percentage drug entrapment (PDE) values increased with increasing the stirring time but PDI value decreased on further increasing the stirring time. On the other hand, average particle sizes were decreased with increasing stirring time. Dynamic light scattering (DLS) results are often expressed in terms of the Z-average value which is intensity based harmonic mean. The PDI or polydispersity index is an indication of how narrow a Gaussian size distribution would be that could represent the fitted DLS data [206]. There was a significant gap between Z-average value and average particle size due to high PDI (Table 4. 32). Formulation C2 showed highest PDE of  $63.5 \pm 0.56\%$  in comparison to other formulation and its zeta potential value was  $30.22 \pm 1.88\text{ mV}$ . Most of the cases, values are not statistical significant. So, further modification was carried out on C2 formulation.

**Table 4. 32: Effect of stirring time on Chitosan-PTH nanoparticles (1:1)**

Code with respect to stirring time	Stirring time (min)	Z average value (nm) <sup>‡</sup>	Average particle size (nm) <sup>‡</sup>	PDI	Zeta potential (mV) <sup>‡</sup>	Entrapment efficiency (%) <sup>‡</sup>
C1	15	7921±174 <sup>#</sup>	553.9±45.2	0.995 ± 0.007	31.67 ± 2.52	52.31 ± 1.85
C2	30	3238±102 <sup>#</sup>	456.9±33.04	0.963 ± 0.031	30.22 ± 1.88	63.5 ± 0.56
C3	45	1687±55	161.5±35.4 <sup>#</sup>	0.993 ± 0.01	18.47 ± 3.81	46.99 ± 1.8
C4	60	5545±97	235.37±52.18 <sup>#</sup>	0.991 ± 0.015	26.17 ± 1.97	55.69 ± 2.16

<sup>‡</sup>Values are mean of three data ± standard deviation, <sup>#</sup>*p* value less than 0.05

#### 4.4.2.2. Effect of Chitosan-TPP ratio

Keeping the stirring time of 30 min (C2), four new batches were prepared using different Chitosan/TPP ratio and compared with the formulation C2 (Table 4. 33). There was no significant difference between the C2 and CT2 based on the average particle size but the PDI was improved in CT2 of 0.671±0.006 in comparison with C2. Hence, CT2 had narrow distribution in comparison with C2 and resulted in Z average value of 1065.67 ± 41.1 nm. Initially average particle size was decreased but this value again increased while increasing the TPP (negative charge ion) amount.

**Table 4. 33: Effect of Chitosan & TPP ratio on nanoparticles**

Coding with respect to Chitosan:TPP	Chitosan: TPP (W/W)	Z average value (nm) <sup>‡</sup>	Average particle size (nm) <sup>‡</sup>	PDI <sup>‡</sup>	Zeta potential (mV) <sup>‡</sup>	Drug entrapment (%) <sup>‡</sup>
C2	6:1	3238 ± 120.0 <sup>#</sup>	456.9 ± 33.04	0.963 ± 0.031	30.22 ± 1.88	63.50 ± 0.56
CT 2	5:1	1065.67 ± 41.1	470.93 ± 93.01	0.671 ± 0.006 <sup>#</sup>	17.71 ± 2.93	69.42 ± 1.96
CT 3	4:1	1635.33 ± 53.53	236.57 ± 28.97	0.703 ± 0.009 <sup>#</sup>	-9.41 ± 2.14	66.37 ± 2.53
CT 4	3:1	5448 ± 125.74	428.7 ± 28.97	0.697 ± 0.009 <sup>#</sup>	1.78 ± 1.03	42.38 ± 1.31
CT 5	2:1	2569.3 ± 133.25	443.73 ± 31.01	0.732 ± 0.01 <sup>#</sup>	19.49 ± 2.19	42.16 ± 0.77 <sup>#</sup>

<sup>‡</sup>Values are mean of three data ± standard deviation; <sup>#</sup>*p* value less than 0.05

On the other hand, Zeta potential value was decreased due to increase of negative charge of TPP amount. In CT3 average particles size was  $236.57 \pm 28.97$  nm and significant correlation was established with Z average due to low PDI value. Its zeta potential reached  $-9.41 \pm 2.14$  mV, which had more tendencies to coagulate in solution form rather than CT2. Statistical significant found in terms of PDI and in some values of percentage drug entrapment.

#### 4.4.2.3. Effect of PTH-Chitosan ratio

Further modification was carried out on CT2 batch. PTH amount was constant in all the formulation, whereas Chitosan amount was increased gradually up to 90 mg in 10 ml of 1 % acetic acid solution and Chitosan-TPP ratio was maintained as 5:1. PTH entrapment was increased significantly with increase of chitosan amount. No significant correlation was established between average particle size and z-average in DC6-DC9 due to high PDI. Average particle size, percentage drug entrapment and zeta potential were under consideration for optimization. DC 6 contained least average particles size but PDE was less in comparison to DC 8. Hence, DC 8 (contain 80 mg of Chitosan) was selected as optimized batch due to smaller particle size and highest PDE (Table 4. 34). In all the cases, the PDI was near to 1.000, hence no correlation was established between average particle size and Z average value.

**Table 4. 34: Effect of PTH:Chitosan ratio on nanoparticles**

Coding with respect to PTH: Chitosan	PTH: Chitosan (mg)	Z average value (nm) <sup>‡</sup>	Average particle size (nm) <sup>‡</sup>	PDI <sup>‡</sup>	Zeta potential (mV) <sup>‡</sup>	Drug entrapment (%) <sup>‡</sup>
CT 2	50:50	$1069 \pm 54$	$462.2 \pm 89.2$	$0.666 \pm 0.11$	$15.5 \pm 5.6$	$69.69 \pm 2.32$
DC 6	50:60	$2792.33 \pm 39.50$	$187.07 \pm 23.92$	$0.992 \pm 0.12$	$35.9 \pm 0.79$	$70.9 \pm 0.45$
DC 7	50:70	$2874.33 \pm 60.14$	$256.13 \pm 26.5$	$0.997 \pm 0.004^{\#}$	$21.6 \pm 1.9$	$73.65 \pm 0.5$
DC 8	50:80	$2978.67 \pm 29.91$	$236.3 \pm 10.58$	$0.975 \pm 0.029$	$31.37 \pm 1.96$	$78.8 \pm 0.36^{\#}$
DC 9	50:90	$2882 \pm 56.22$	$333.5 \pm 23.19$	$0.999 \pm 0.001^{\#}$	$27.4 \pm 2.11$	$74.78 \pm 0.23$

\*Values are mean of three data  $\pm$  standard deviation; <sup>#</sup>p value less than 0.05

#### 4.4.2.4. Optimization of TPP solution volume

Significant changes occurred in z-average and PDI value, when TPP solution volume rose up to 10 ml with constant TPP amount of 16 mg. This was the final step for optimization of PTH-chitosan nanoparticles. Optimized batch (OPB) contains 50 mg of PTH, 80 mg of Chitosan and 16 mg of TPP in 10 ml of aqueous solution. Stirring time was maintained for 30min. OPB batch showed Z-average value of  $314.37 \pm 3.68$  nm which was significantly correlated with average particle size of  $303.77 \pm 7.38$  nm. PDE, Zeta potential of the optimized batch was found to be  $80.65 \pm 0.4$  % and  $32.4 \pm 1.04$  mV respectively. Drug entrapment, PDI and Z- average values of OPB batch were found to be statistically significant. Due to higher zeta potential, optimized nanoparticles had lesser affinity to coagulate during storage and in solution form (Table 4. 35).

**Table 4. 35: Effect of TPP solution volume contain 16 mg TPP**

Formula code	TPP solution volume (ml)	Z average value (nm) <sup>‡</sup>	Avg. particle size (nm) <sup>‡</sup>	PDI <sup>‡</sup>	Zeta potential (mV) <sup>‡</sup>	Drug entrapment (%) <sup>‡</sup>
DC 8	5	$2978.67 \pm 29.91$	$236.3 \pm 10.58$	$0.975 \pm 0.029^{\#}$	$31.37 \pm 1.96$	$78.8 \pm 0.36^{\#}$
OPB	10	$314.37 \pm 3.68$	$303.77 \pm 7.38$	$0.412 \pm 0.016^{\#}$	$32.4 \pm 1.04$	$80.65 \pm 0.4^{\#}$

<sup>‡</sup>Values are mean of three data  $\pm$  standard deviation; <sup>#</sup>p value less than 0.05

#### 4.4.2.5. Scanning electron microscopy (SEM)

SEM images of optimized formulation (OPB) showed that the nanoparticles were spherical in shape (Figure 4. 23). Most of the particle size was of 301.9 nm, which are suitable for the inhalation formulation. In rest of the cases, aggregation occurred due to moisture entrapment during handling.

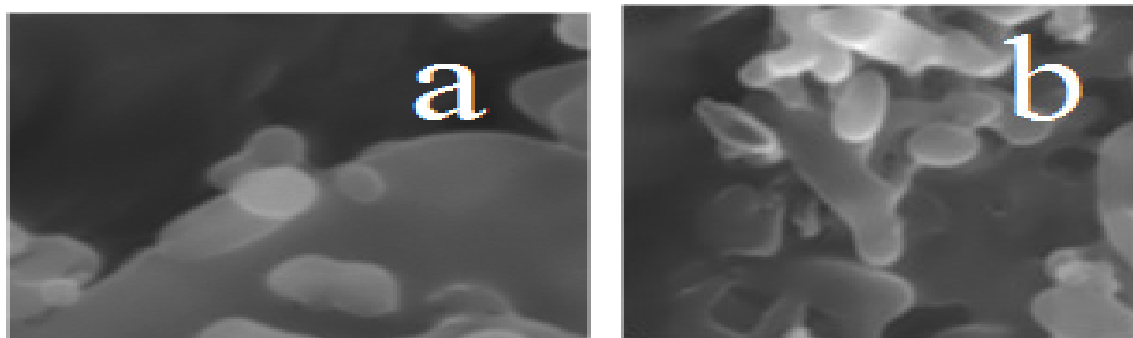


**Figure 4. 23: SEM image of Chitosan-PTH nanoparticles (OPB)**



#### 4.4.2.6. Differential scanning calorimetry (DSC)

DSC is very useful in the investigation of the thermal properties of drug delivery carriers, providing both qualitative and quantitative information about the physiochemical state of drug inside the delivery system [207]. DSC thermograph of Prothionamide, Chitosan and optimized Chitosan-PTH nanoparticles are shown in Figure 4.24. Pure PTH (Figure 4.24-a) gives a sharp peak at 143.05°C with an onset at 139.09°C indicating its crystalline structure, which correspond to its melting point [208]. Thermograph of Chitosan (Figure 4. 24-b) showed a broad peak at 88.03°C. This peak observed due to amorphous nature of Chitosan and water evaporates below 100°C. This water is associated with hydrophilic groups in the amorphous Chitosan [209]. PTH loaded Chitosan nanoparticles (OPB) (4. 24-c) showed all the characteristic peak of PTH and Chitosan. PTH peak in nanoparticles was little wide due to change in the physical state from crystalline to amorphous form.

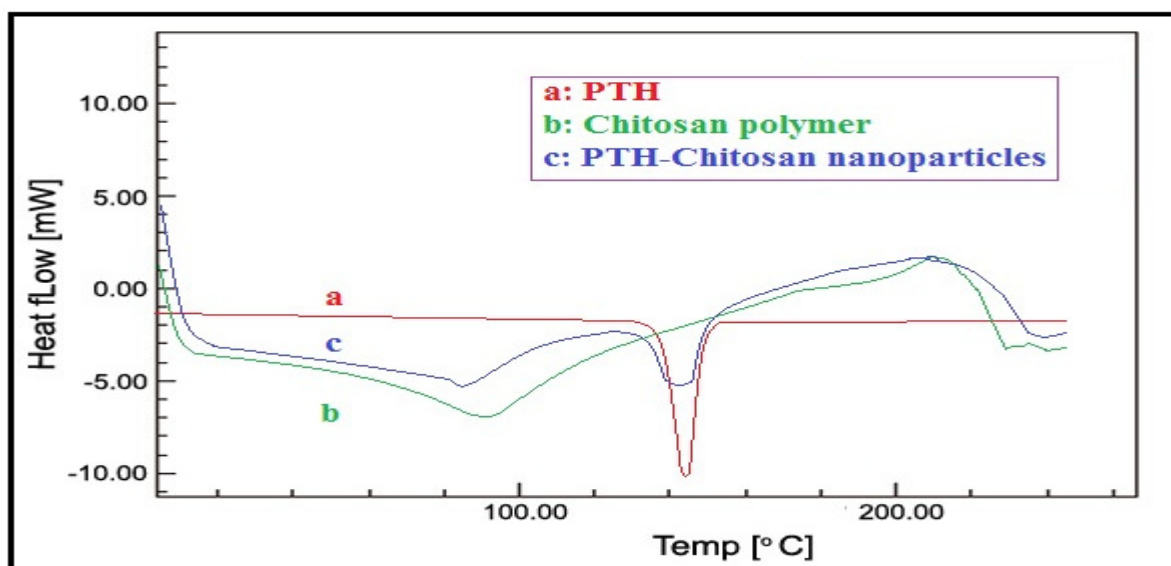


**Figure 4. 24: DSC thermogram of (a) PTH, (b) Chitosan polymer, (c) PTH-Chitosan nanoparticles (OPB)**

#### 4.4.3. Formulation and characterization of dry powder inhaler

The development of an adequate carrier system has become a prerequisite for deep lung delivery, and its choice for pulmonary delivery of NPs is still challenging. Apart from the necessary safety regarding contact with lung tissue, the carrier should provide drug stability, ease of handling during filling and processing, adequate aerodynamic properties for proper lung deposition, as well as improved powder flowability which aids in drug dispersion from

the inhaler device [95]. Prepared freeze dried nanoparticles were the fluffy mass with fair flow property. These nanoparticles showed angle of repose, Carr's index and Hausner ratio as 37.32°, 17.43 % and 1.21 respectively. Hence, special inhalable grade lactose was used to increase the bulk and flow property of nanoparticles. Due to fine particles of this special grade lactose, flow property was increased significantly. Initially, different proportion of anhydrous lactose was added to the optimized Prothionamide nanoparticles (OPB) by physical geometric mixture. In each addition of anhydrous lactose, the values of angle of repose, Carr's index and Hausner ratio were determined (Table 4. 36). Lactose-PTH nanoparticles (PC-DPI4) in ratio 1:2 showed the values as 29.31±0.91°, 09.60±0.13 % and 1.11±0.001 respectively.

**Table 4. 36: Optimization of dry powder inhaler**

Formulation code	Nanoparticles: Anhydrous lactose	Angle of repose <sup>‡</sup>	Carr's index <sup>‡</sup>	Hausner ratio <sup>‡</sup>
PC-DPI 1	1.0:0.5	31.31 ± 0.60	11.21 ± 0.18	1.13 ± 0.002
PC-DPI 2	1.0:1.0	30.85 ± 0.54	10.41 ± 2.46	1.12 ± 0.03
PC-DPI 3	1.0:1.5	30.23 ± 1.78	12.00 ± 2.39	1.13 ± 0.03
PC-DPI 4	1.0:2.0	29.31 ± 0.91	9.60 ± 0.13	1.11 ± 0.001
PC-DPI 5	1.0:3.0	32.37 ± 0.64	14.89 ± 1.26	1.17 ± 0.02

<sup>‡</sup>Values are mean of three data ± standard deviation

#### 4.4.3.1. Determination of MMAD and geometric standard deviation

Mass median aerodynamic diameter (MMAD) particle size is the main parameter that determines their deposition in the different parts of lungs. Particle size with 0.5-5 µm can reach to the small airways and alveoli [142]. Deposition of PC-DPI4 was observed in each stage of the chamber (Table 4. 37). With higher concentration of carrier, the better dispersion was seen [210]. Maximum fine particle fraction, extra fine particle fraction and emitted dose were found as 81.19 %, 18.91 % and 82.37 % respectively. Maximum deposition of DPI was seen in stage 5 followed by 4 and 6, hence aerodynamic particle size obtained 1.76 µm with geometric standard deviation of 1.96 (Figure 4. 25). A relatively low MMAD coupled with a low GSD is indicative of a tight size distribution centred on a fine particle size, a potentially beneficial combination for efficient delivery [211]. That signifies that the prepared DPI can reach deeply to lungs.

**Table 4. 37: Amount of drug determination in different stage in cascade impactor**

Stage	micron	Absorbance	Conc. (µg/ml)	dilution factor	amount(µg)	amount(mg)	Percentage deposition
0	9	0.159	6.28	1	6.28	0.00628	0.0628
1	5.8	0.561	22.36	5	111.8	0.1118	1.118
2	4.7	0.673	26.84	10	268.4	0.2684	2.684
3	3.3	0.209	8.28	100	828	0.828	8.28
4	2.1	0.476	18.96	100	1896	1.896	18.96
5	1.1	0.711	28.36	100	2836	2.836	32.36
6	0.7	0.469	18.68	100	1868	1.868	18.68
7	0.4	0.345	13.72	1	13.72	0.01372	0.1372
Filter	n/a	0.231	9.16	1	9.16	0.00916	0.0916

Flow Rate:		28.3 L/min
Cut off Diameter		
Impactor Stage	(microns)	Drug Collected
Stage 0	9	0.0063
Stage 1	5.8	0.1118
Stage 2	4.7	0.2684
Stage 3	3.3	0.8280
Stage 4	2.1	1.8960
Stage 5	1.1	2.8360
Stage 6	0.7	1.8680
Stage 7	0.4	0.0137
Filter	n/a	0.0092
MMAD:	1.76	microns
GSD:	1.96	

**Figure 4. 25: Snapshot of aerodynamic determination from web site****4.4.3.2. In-vitro release study**

Prepared DPI loaded with Prothionamide nanoparticles (PC-DPI4) was subjected for *in-vitro* drug release behaviour. Simulated lung fluid of pH 7.4 was used as dissolution medium for evaluation of release pattern of Prothionamide from Chitosan nanoparticles [172]. Prepared Prothionamide-Chitosan nanoparticles showed initial burst release of  $22.04 \pm 1.94$  % and released up to  $96.91 \pm 0.91$  % in 24 hr (Figure 4. 26). This initial burst release would help to reach the desired plasma concentration in lungs, and the sustained release would help them to maintain the drug concentration for prolong period of time. The model that best fits the

release data is selected based on the correlation coefficient value of various models. Initially significant difference observed but latter most of the cases  $p$  values observed significant. The *in-vitro* release data was analyzed through zero order, Higuchi, Korsmeyer-Peppas models and obtained correlation co-efficient ( $r^2$ ) were found to be 0.886, 0.961, and 0.976 respectively (Table 4. 38).

**Table 4. 38: Release study of PTH from chitosan nanoparticles loaded DPI (PC-DPI 4)**

Zero order		Higuchi Model		Peppas Model	
Time (Hr)	% CDR <sup>‡</sup>	Square route of time	% CDR <sup>‡</sup>	Log time	log % CDR <sup>‡</sup>
1	22.04 ± 1.94	1	22.04 ± 1.94	0	1.34
2	27.31 ± 2.56	1.41	27.31 ± 2.56	0.30	1.43
3	32.6 ± 2.20	1.73	32.6 ± 2.20	0.48	1.51
4	37.92 ± 3.38	2	37.92 ± 3.38	0.60	1.58
5	44.74 ± 3.24	2.24	44.74 ± 3.24	0.69	1.65
6	50.13 ± 2.70	2.45	50.13 ± 2.70	0.78	1.70
7	56.28 ± 4.51	2.65	56.28 ± 4.51	0.85	1.75
8	62.47 ± 6.67	2.83	62.47 ± 6.67	0.90	1.79
9	67.95 ± 3.77	3	67.95 ± 3.77	0.95	1.83
10	73.45 ± 2.78	3.16	73.45 ± 2.78	1	1.87
11	76.79 ± 3.07	3.32	76.79 ± 3.07	1.04	1.89
12	81.61 ± 3.50	3.46	81.61 ± 3.50	1.08	1.91
13	84.99 ± 3.52	3.60	84.99 ± 3.52	1.11	1.93
14	86.91 ± 3.53	3.74	86.91 ± 3.53	1.15	1.94
15	89.58 ± 0.60	3.87	89.58 ± 0.60	1.18	1.95
16	92.99 ± 1.63	4	92.99 ± 1.63	1.20	1.97
20	94.21 ± 1.63	4.47	94.21 ± 1.63	1.30	1.97
24	96.91 ± 0.91	4.89	96.91 ± 0.91	1.38	1.99
Zero order		Higuchi Model		Peppa's Model	
$R^2 = 0.886$		$R^2 = 0.961$		$y = 0.544x + 1.294$ $R^2 = 0.976$	

<sup>‡</sup>Values are mean of three data ± standard deviation

The release best fitted with Korsmeyer-Peppas model based on higher  $R^2$  value and release exponent “n” of this kinetic model describes drug release mechanism. Values of “n” was 0.544 signifies the release followed both combination of erosion and diffusion mechanism.

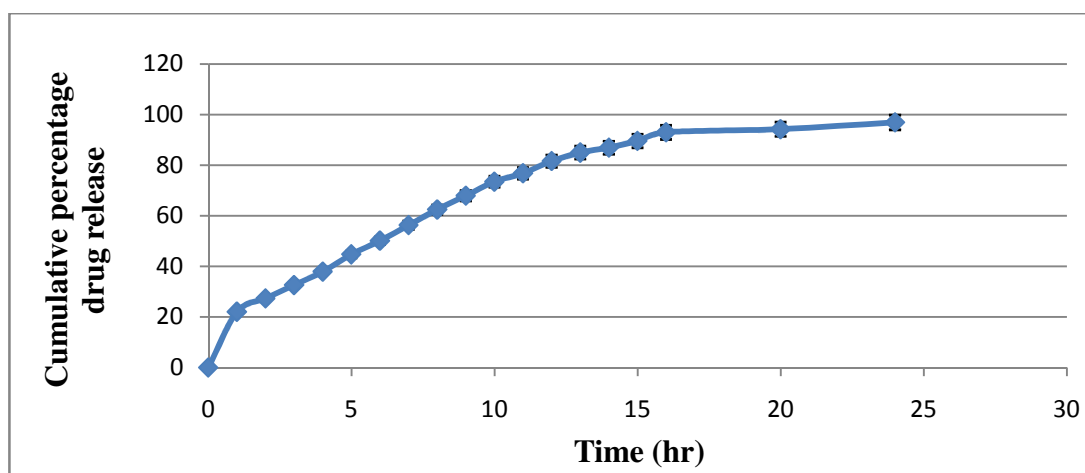


**Figure 4. 26: *In-vitro* dissolution profile of CP-DPI 4**

#### 4.4.3.3. Stability study

Stability of NPs was determined in terms of z-average particle size, zeta potential, drug entrapment and release profile. Zeta size, zeta potential, PDI, and drug release demonstrated the conservation of dry powder inhaler during stress testing. There was no significant changes occurred in PDI, zeta potential, PDE and percentage drug release. Particle sizes were changed in narrow range but it did not create any significant effect on the release of PTH from Chitosan nanoparticles (Table 4. 39). Data represented as mean  $\pm$  SD with  $p$  values.

**Table 4. 39: Stability study of PC-DPI4**

Time point (month)	Z-average (nm) <sup>‡</sup>	PDI <sup>‡</sup>	Zeta potential <sup>‡</sup>	% Drug Entrapment <sup>‡</sup>	% drug release in 24 hr <sup>‡</sup>
0	323.3 $\pm$ 10	0.411 $\pm$ 0.13	28.3 $\pm$ 3.6	79.75 $\pm$ 0.11 <sup>#</sup>	96.91 $\pm$ 1.5
1.5	326.7 $\pm$ 09	0.429 $\pm$ 0.21	28.6 $\pm$ 2.7	79.50 $\pm$ 0.09 <sup>#</sup>	98.86 $\pm$ 0.9 <sup>#</sup>
3	351.3 $\pm$ 05	0.426 $\pm$ 0.32	28.4 $\pm$ 3.5	78.33 $\pm$ 0.12 <sup>#</sup>	97.71 $\pm$ 3.2
6	361.4 $\pm$ 12	0.428 $\pm$ 0.47	29.5 $\pm$ 2.1	78.12 $\pm$ 0.16 <sup>#</sup>	98.32 $\pm$ 6.4

<sup>‡</sup>Values are mean of three data  $\pm$  standard deviation; <sup>#</sup> $p$  value less than 0.05

#### 4.4.3.4. Delivery dose calculation using modified device

38.96 mg of PC-DPI4 containing 1.6 mg of PTH was sprayed in three divided form. Content remaining in the needle and syringe was dissolved in water-methanol in the ratio of 8:2. PTH content was determined under UV-Spectrophotometer at 287.40 nm. Equation used to estimate PTH was mentioned in the section 4.2.2. Percentage drug delivered was calculated

and found as  $98.78 \pm 0.052 \%$  (Table 4. 40). This value was considered to calculate the delivery dose of PTH using modified delivery device.

**Table 4. 40: Delivery dose of PC-DPI4 calculation of modified DPI device**

Absorbance	Conc. (µg/ml)	Volume (ml)	Amount in µg	Amount in mg	Dose given (mg)	Dose delivered (mg)	Percentage delivered
0.048	1.88	10	18.8	0.0188	1.6	1.5812	98.825
0.049	1.92	10	19.2	0.0192		1.5808	98.800
0.052	2.04	10	20.4	0.0204		1.5796	98.725
Average <sup>‡</sup>						1.5805 ± 0.001	
Percentage delivered <sup>‡</sup>						98.78 ± 0.052%	

<sup>‡</sup>Values are mean of three data  $\pm$  standard deviation

#### 4.4.4. *In-vivo* study

All the guidelines of institutional animal ethical committee of Bengal College of Pharmaceutical Sciences and Research, Durgapur, West Bengal are followed throughout the animal experiments (BCPSR/IAEC/04-16) (Appendix A).

##### 4.4.4.1. Dose, DPI calculation and administration

Prothionamide dose calculation was done as depicted previously. Study 1 of Table 4. 41: First rat (S1M1) weight was 0.228 kg. Hence, equivalent PTH dose is 1.756 mg. Optimized batch of chitosan nanoparticles contained 39.67 mg PTH in 322 mg of nanoparticles.

So, 1.756 mg equivalent nanoparticles were  $(322 * 1.756)/39.67 = 14.25$  mg. PC-DPI 4 contained the proportion of nanoparticles:lactose =1:2.

Hence, equivalent DPI was  $14.25 * 3 = 42.75$  mg. As modified DPI delivery device able to deliver 98.78 % of its content, corrected delivery DPI dose was  $(42.75 * 100)/98.78 = 43.2779 \approx 43.28$  mg.

Similar calculation was followed for rest of rats and the data is represented in Table 4. 41. Whereas, animal treated with PDI containing pure PTH (PL-DPI 4) are given in Table 4. 26. Calculated dose of Prothionamide was administered by pulling the tongue of rat out of mouth with a spatula and sprayed the equivalent DPI in this region.

**Table 4. 41: Dose and equivalent DPI calculation**

Animal treated with DPI Study 1 (S1)				Animal treated with DPI Study 2 (S2)				Animal treated with DPI Study 3 (S3)			
Animal code	Rat Weight (Kg)	Dose of PTH (mg)	Equ. wt. of DPI (mg)	Animal code	Rat Weight (Kg)	Dose of PTH (mg)	Equ. wt. of DPI (mg)	Animal code	Rat weight (Kg)	Dose of PTH (mg)	Equ. wt. of DPI (mg)
M1	0.228	1.756	43.28	M1	0.22	1.694	41.76	F1	0.23	1.771	43.66
M2	0.226	1.740	42.90	F2	0.223	1.717	42.33	M2	0.221	1.701	41.95
F3	0.221	1.701	41.95	M3	0.226	1.740	42.90	F3	0.223	1.717	42.33
M6	0.22	1.694	41.76	M6	0.226	1.740	42.90	F6	0.218	1.678	41.38
F12	0.227	1.748	43.09	F12	0.222	1.709	42.14	M12	0.231	1.779	43.85
F24	0.226	1.740	42.90	F24	0.221	1.701	41.95	M24	0.227	1.748	43.09

† Animal code was divided in two parts: First digit stand for the sex of rat, last numerical digit denote the time of sacrificing after dose administration

#### 4.4.4.2. Pharmacokinetic study

Two different studies were carried out to demonstrate lungs tissue distribution and bio-distribution of Prothionamide at specific time interval. DPI of PTH nanoparticles maintained plasma concentration above the MIC for the period more than 12 hr, whereas pure PTH could maintain up to 3 hr. PTH nanoparticles gave the concentration of  $0.3893 \pm 0.06 \mu\text{g/ml}$  at 24 hr (Table 4.42).

**Table 4. 42: Lung's tissue and plasma distribution of PC-DPI4 and PL-DPI4**

Lungs distribution study				
Time of study (hr)	PC-DPI 4 containing PTH nanoparticles		PL-DPI4 containing pure PTH	
	PTH amount in lung's tissue <sup>‡</sup> ( $\mu\text{g}$ )	PTH concentration <sup>‡</sup> ( $\mu\text{g/ml}$ )	PTH amount in lung's tissue <sup>‡</sup> ( $\mu\text{g}$ )	PTH concentration <sup>‡</sup> ( $\mu\text{g/ml}$ )
1	$18.65 \pm 2.33$	$2.1684 \pm 0.27$	$39.28 \pm 2.66$	$4.56 \pm 0.31$
2	$23.05 \pm 1.99$	$2.6801 \pm 0.23$	$17.61 \pm 0.86$	$2.05 \pm 0.09$
3	$24.97 \pm 2.39$	$2.9029 \pm 0.28$	$6.22 \pm 0.48$	$0.72 \pm 0.06$
6	$14.32 \pm 0.79$	$1.6647 \pm 0.09$	$1.55 \pm 0.24$	$0.18 \pm 0.03$
12	$8.04 \pm 1.15$	$0.9347 \pm 0.13$	---	---
24	$2.53 \pm 0.36$	$0.3893 \pm 0.06$	---	---

Plasma distribution study				
Time of study (hr)	PC-DPI 4 containing PTH nanoparticles		PL-DPI4 containing pure PTH	
	PTH amount in plasma <sup>‡</sup> (µg)	PTH concentration <sup>‡</sup> (µg/ml)	PTH amount in plasma <sup>‡</sup> (µg)	PTH concentration <sup>‡</sup> (µg/ml)
1	18.96 ± 1.34	0.0905 ± 0.002	87.18 ± 8.71	0.42 ± 0.03
2	27.69 ± 2.92	0.1355 ± 0.014	29.18 ± 1.42	0.14 ± 0.01
3	32.14 ± 2.32	0.1572 ± 0.009	16.94 ± 1.35	0.08 ± 0.01
6	5.63 ± 0.24	0.0281 ± 0.001	0.15 ± 0.12	0.001 ± 0.001
12	4.25 ± 1.46	0.0203 ± 0.007	---	---
24	0.99 ± 0.381	0.0049 ± 0.002	---	---

<sup>‡</sup>Values are mean of three data ± standard deviation

AUC increased significantly when PTH was given in the form of nanoparticles. There was no significant difference between the AUC of PTH nanoparticles and pure PTH administration in plasma (Table 4. 43). As PTH reached very slowly to plasma from PTH nanoparticles, AUC achieved relatively less in comparison to lungs tissue revealed from Figure 4. 27. So, prepared formulation should be used once every day to maintain the plasma concentration above MIC for the period of 24 hr. Due to short half life, PTH is prescribed 250 mg for 2 times a day in oral route. This animal study confirmed PTH maintained concentration above MIC with reduced dose. In terms of concentration of PTH in blood, AUC of plasma and some other parameters values found to be statistical significant as *p* value is less than 0.05.

**Table 4. 43: Pharmacokinetic evaluation**

Pharmacokinetic parameters of PTH in lung's tissue			
DPI containing	C <sub>max</sub> (µg/ml)	T <sub>max</sub> (hr)	AUC (µg hr/ml)
PTH –Chitosan nanoparticles (PC-DPI 4)	2.90 ± 0.28	3	29.17 ± 1.96
Pure PTH (PL-DPI4)	4.57 ± 0.31	1	10.08 ± 2.31
Pharmacokinetic parameters of PTH in plasma			
DPI containing	C <sub>max</sub> (µg/ml)	T <sub>max</sub> (hr)	AUC (µg hr/ml)
PTH –Chitosan nanoparticles (PC-DPI 4)	0.157 ± 0.009 <sup>#</sup>	3	0.893 ± 0.085 <sup>#</sup>
Pure PTH (PL-DPI4)	0.416 ± 0.024 <sup>#</sup>	1	0.728 ± 0.009 <sup>#</sup>

\*\* Values are mean of three data ± standard deviation; <sup>#</sup> *p* value less than 0.05



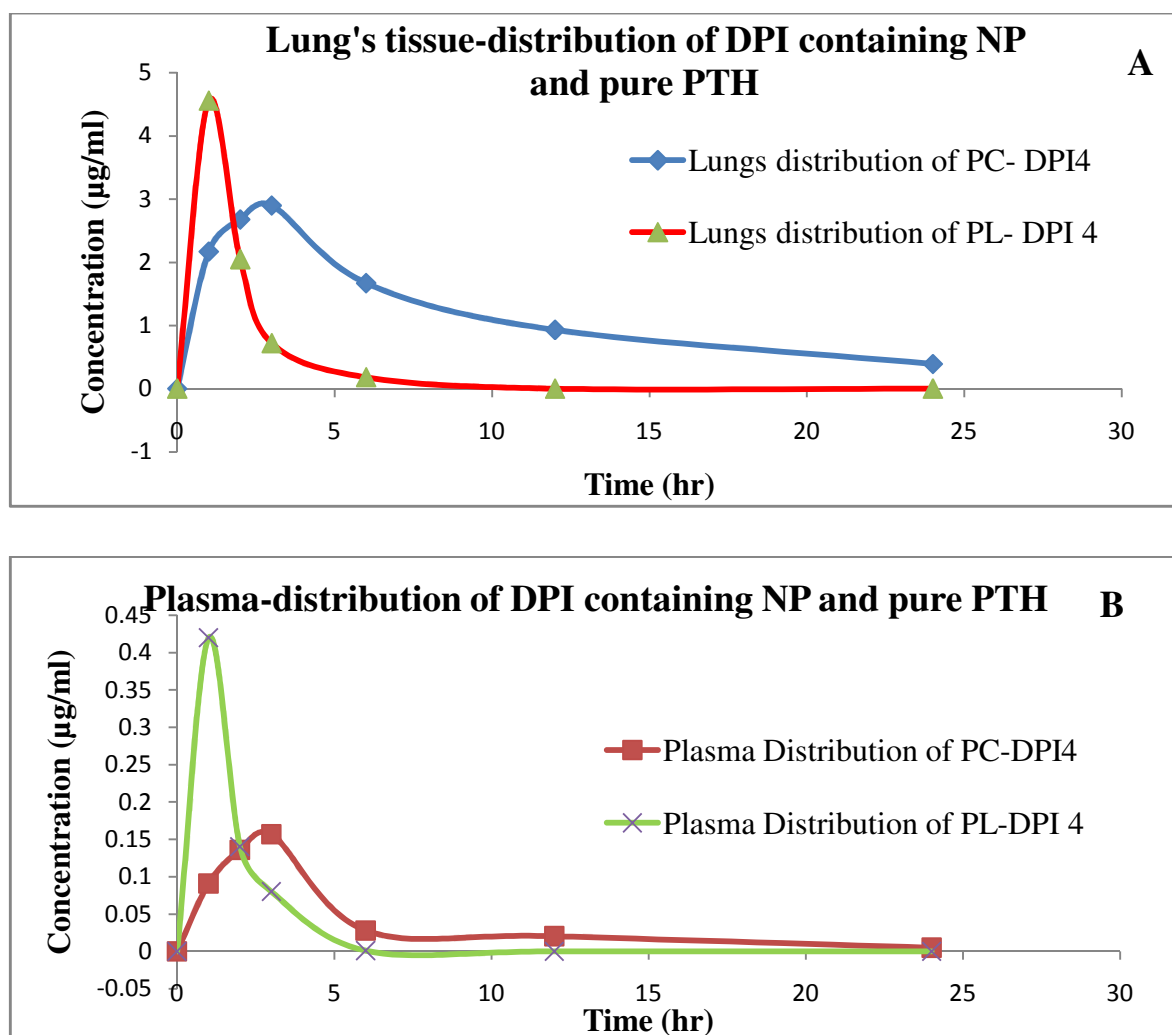


**Figure 4. 27: Lungs (A) & Plasma (B) distribution of PC-DPI 4 & PL-DPI4**

#### 4.4.4.3. IVIVC of DPI containing PTH-Chitosan nanoparticles

IVIVC was carried out between *in vitro* percentage drugs released with percentage drugs absorbed for PC- DPI4 (Table 4. 44). Good correlation coefficient of 0.988 was obtained when plotted the graph between *in-vitro* drugs released at X-axis and *in-vivo* drug absorbed in Y-axis (Figure 4. 28).

**Table 4. 44: Comparison between *in vitro* release and *in vivo* drug diffusion for PC-DPI4**

Time (hr)	<i>In vitro</i> percentage drug release	<i>In vivo</i> percentage drug diffusion
1	22.04	14.68
2	27.31	23.57
3	32.6	30.54
6	50.13	50.4

12	81.61	72.65
24	96.91	97.8

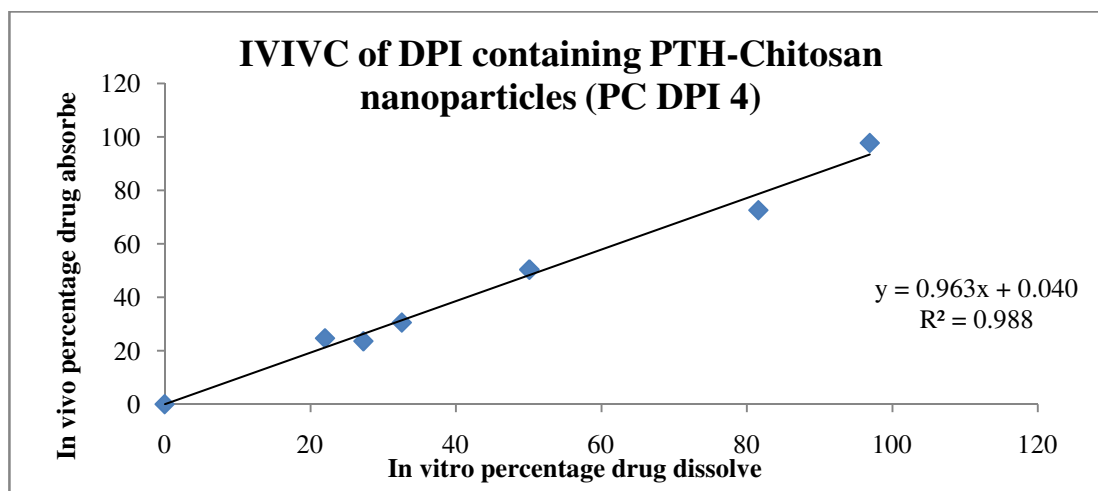


**Figure 4. 28: IVIVC of PC-DPI4**

#### 4.4.5. *In-vitro* anti-tubercular activity

As mentioned earlier, anti-tubercular activity was carried out using MTT assay. Comparison between pure drugs with nanoparticles loaded drug was represented in table 4. 45. PTH loaded chitosan nanoparticles showed MIC value of 0.6 µg/ml in comparison with pure PTH of 0.5 µg/ml.

**Table 4. 45: Absorbance and cell viability of pure Prothionamide and Prothionamide-Chitosan nanoparticles in MTT assay**

Pure Prothionamide				
Conc. (µg/ml)	0.4	0.5	0.6	0.7
Average absorbance	0.2509	0.0874	0.081067	---
SD	0.016795	0.015894	0.004155	---
% Viability	13.28965	-0.15903	-0.67997	---
SD	1.381466	1.307335	0.221019	---
Pure PTH loaded chitosan nanoparticles				
Conc. (µg/ml)	0.4	0.5	0.6	0.7
Average absorbance	0.732033	0.296533	0.08387	0.076233
SD	0.103999	0.059537	0.006038	0.003153
% viability	52.86521	17.04321	-0.44966	-1.309
SD	8.55443	4.897201	0.496695	0.259375

## **CHAPTER 5: Method Pertaining to Ethionamide**

### **5.1. Identification of drugs**

Prior to start the product development, identification test was performed for the procured drug to verify and ensure its purity. Identification test like appearance, melting point and infrared absorptivity and chemical test were performed on the drug sample.

#### **5.1.1. Appearance**

The procured drug sample was physically examined for its state, colour and was compared with the reported description of drug.

#### **5.1.2. Melting point**

Melting point is another prerequisite identification test for solid substance. Usually, each and every solid drug has spiky or narrow range of melting point. Therefore, it was determined by capillary method using melting point apparatus (Sunsim, India). After sealing one side, small amount of sample was filled in the capillary tube and placed in the melting point apparatus. Temperature was raised gradually and observed visually the range over which the drug melts. Replication was made for three times.

#### **5.1.3. Chemical test**

10 mg ETH was placed in a conical flask and dissolved in 5 ml of methanol. 5 ml of 0.1 M silver nitrate was added in that solution and observed for the change in colour (IP 2007, 486).

#### **5.1.4. Infrared absorption**

The qualitative aspects of infrared spectroscopy are one of the most powerful attributes of this diverse and versatile analytical technique [153]. It is an important complementary tool for the solid-state characterization of pharmaceutical solids. The drugs were directly placed on sample disc in the sample compartment. Sample was scanned at transmission mode in the range of 400 to 4000  $\text{cm}^{-1}$ . IR spectrum obtained was compared with standard spectrum of pure drug.

### **5.2. Analytical method**

#### **5.2.1. Estimation of Ethionamide using UV-Spectrophotometric method and its method validation**

##### **5.2.1.1. Preparation of stock solution**

1000  $\mu\text{g/ml}$  (S5) of stock solution was prepared by dissolving 100 mg of Ethionamide in sufficient quantity of pH 7.4 Phosphate buffer (method of preparation mentioned in chapter-3) to produce 100 ml. 1 ml of the above solution was further diluted with same solvent to prepare 100  $\mu\text{g/ml}$  stock solutions (S6).

##### **5.2.1.2. Determination of wavelength of maximum absorbance ( $\lambda_{\text{max}}$ )**

S6 stock solution (100  $\mu\text{g/ml}$ ) was further diluted to 10 ml with pH 7.4 Phosphate buffer to obtained different concentration of Ethionamide solution. An UV spectroscopic scanning (200–400 nm) was carried out with these diluted solutions to determine the maximum absorptivity of Ethionamide against pH 7.4 Phosphate buffer as blank.

##### **5.2.1.3. Linearity and range**

For linearity study, five different concentrations (6, 9, 12, 15 & 18  $\mu\text{g/ml}$ ) were prepared after withdrawing five different aliquots from the S6 stock solution and diluted up to 10 ml with pH 7.4 Phosphate buffer. Data obtained from above these solutions were used for construction of linearity curve by plotting concentration of Ethionamide on X-axis and absorbance on Y-axis. Regression equation was computed. The LOD and LOQ were also calculated as described previously.

**5.2.1.4. Assay of Ethionamide in marketed tablet**

Ethionamide marketed tablets (Ethomid, Macleods Pharmaceuticals Ltd.) were analyzed using this newly developed method. Initially weighed 20 tablets and triturated to form fine powder. 10 mg of Ethionamide equivalent powder was taken in 100 ml of volumetric flask and the volume was made up to 100 ml with pH 7.4 phosphate buffer. The content was stirred under magnetic stirrer followed by sonication for 20 min to solubilise ETH. After filtration (Whatman filter paper No. 41), 0.8, 1.2 and 1.6 ml of this tablet powder solution diluted to 10ml with pH 7.4 Phosphate buffer to make 8, 12 & 16 µg/ml solution respectively. These samples were used to calculate the content of Ethionamide at 288 nm.

**5.2.1.5. Accuracy**

The accuracy of the proposed methods was assessed by recovery study. The recovery experiments were performed by adding known amounts of ETH containing powdered tablets to standard drug solution [199]. Three different levels (80 %, 100 % and 120 %) were selected for this study [158]. For this measurement, nine determinations [157] was carried out at lower, intermediate and higher concentration level.

**5.2.1.6. Precision**

The precision of analytical procedure expresses closeness of agreement (degree of scatter) between a series of measurements obtained from multiple sampling of the same homogenous sample under prescribed conditions [156]. Intermediate precision was checked by assay the sample solution on same day (Intra-day precision) and on three different days (inter-day precision). Three different working stock solution in triplicates (5, 10, 15 µg/ml) were prepared from standard stock solution (S6). These solutions were studied for three different times in a day (intraday; n=9) and continued up to 3<sup>rd</sup> day (inter-day; n=15). The relative standard deviation (RSD) was taken as precision.

**5.2.2. Estimation of ETH in water-methanol system**

UV-spectrophotometric method for the estimation of ETH at pH 7.4 phosphate buffer is able to detect the un-entrapped/ free ETH concentration in solution. When ETH was coated with polymer, estimation of entrapped drug was found difficult. Here, estimation of drug is time consuming using the pH 7.4 phosphate buffer as lots of time will be taken to extract the ETH

from nanoparticles. Therefore, alternate method was needed to extract drug from polymer coated nanoparticles.

#### **5.2.2.1. Preparation of stock solution**

Solvent system was prepared with water-methanol in the ratio of 9:1. 10 mg of ETH was transferred into 100 ml volumetric flask. ETH was dissolved in 10 ml of methanol and finally the volume made up to 100 ml with water (S7) (100 µg/ml).

#### **5.2.2.2. Detection of maximum absorptivity**

From the stock solution (100 µg/ml) (S7), 1.0 ml of ETH solution was transferred to 10 ml volumetric flask and the volume was adjusted to the mark with same solvent to obtain 10 µg/ml. The wavelength of maximum absorptivity of ETH in specific media (water-methanol in 9:1 ratio) was determined by scanning the diluted solutions in the range of 200-400 nm.

#### **5.2.2.3. Construction of standard curve**

1, 1.5, 2, 2.5, 3, 3.5 and 4 ml of the above stock solution (S7) (100 µg/ml) were transferred into 10 ml volumetric flask. The volume was made up to mark with combination solvent of water-methanol in the ratio of 9:1 to prepare 10, 15, 20, 25, 30, 35, 40 µg/ml solutions. These seven solutions were used to construct standard curve. Replication was made for three times.

### **5.2.3. Estimation of Ethionamide in rat plasma using HPLC method**

#### **5.2.3.1. Chromatography system and condition**

Analysis was performed with a Shimadzu (Japan) RP HPLC equipped with an SPD-10A UV-visible detector, Phenomenex ODS analytical column (250mm × 4 mm internal diameter, 5 µm Particles) as mentioned in the determination of Prothionamide. The mobile phase was composed of water and Acetonitrile in the ratio of 70:30 (v/v). The flow rate was 1.0 ml/min and all the spectrums were monitored at 290 nm using Prothionamide as internal standard[55].

#### **5.2.3.2 Preparation of standard curve in rat plasma**

Weighed accurately 10 mg of Ethionamide and transferred into 100 ml volumetric flask. 30 ml of HPLC grade Acetonitrile was added, and the mixture was sonicated to dissolve the

drug. Finally volume of this solution was made up with HPLC grade water (100 µg/ml) (S8). Prepared stock solution was filtered through 0.22 µm nylon membrane filter and then sonicated for degassing [155]. The stock solution was stored at 4°C and protected from light [160]. The details of plasma collection, selection of detection wavelength and construction of calibration curve mentioned in section 3.4.3.

### **5.3. Formulation and characterization of DPI containing Ethionamide nanoparticles prepared by PLGA (50:50)**

#### **5.3.1. Compatibility**

Fourier transform infrared spectroscopy (FTIR) analysis was performed to check the chemical interaction between the ingredients using Perkin Elmer (Massachusetts, USA). Two samples were prepared separately: one for pure ETH and another for physical mixture of ETH, inhalable grade anhydrous lactose and PLGA (50:50). These samples (without KBr) were placed on the sample disc and scanned in the range of 400 to 4000 cm<sup>-1</sup>.

#### **5.3.2. Preparation of nanoparticles**

Nanoparticles were prepared by emulsion solvent evaporation technique as reported previously with minor modification [117]. While formulating nanoparticles of PTH using PLGA 75:25, we found the percentage of release was not as required at the end of 24 hr. This may be due to the less amount of glycolic acid in 75:25 compared to PLGA 50:50. Our result coincided with previous report of Vij N et al (2010) [21] and Hamilla SM et al (2011) [212]. Hence, in preparing Ethionamide nanoparticles PLGA 50:50 was used instead of 75:25. Briefly, PLGA (50:50) were dissolved in sufficient volume of Dichloromethane (DCM) and Acetone to obtain low viscous clear solution. The resulting solution (organic phase) was added slowly to the aqueous phase containing Polyvinyl alcohol (PVA) solution followed by vortexing for 5 min. Immediately, resulting solution was probe sonicated (Bandelin Electronics, Germany) for 5 min over ice bath to form nano-emulsion. This nano-emulsion was kept under stirring for complete evaporation of organic solvent. Nanoparticles were separated by centrifuging the suspension at 18,000 rpm at -4 °C for 30 min using Remi C-24 plus with rotar R-244M and relative centrifugal force was 31150 g.

### **5.3.3. Optimization and characterization of nanoparticles**

After centrifugation, the amount of free ETH in the supernatant was measured by UV-Spectrophotometer at 288 nm as reported previously. From it, percentage drug entrapment (PDE) was determined. Zeta size, zeta potential and Poly Dispersibility Index (PDI) were determined using Zetasizer (Malvern, UK). Influences of different experimental parameters such as polymer to drug ratio, surfactant concentration and organic phase composition on the encapsulation efficacy of ETH in the nanoparticles were evaluated.

#### **5.3.3.1. Effect of ETH-PLGA ratio**

Polymer amounts play important role in the drug entrapment. Initially, PVA concentration was chosen as 0.25 % w/v (critical micelle concentration of PVA). After preliminary trials, DCM, Acetone volume was selected as 2 and 1.5 ml respectively to dissolve both PLGA and ETH. Five batches were prepared with different proportion of PLGA and by keeping the ETH amount same.

#### **5.3.3.2. Effect of surfactant concentration**

Modification was done on the selected batch with specific ratio of ETH and PLGA. Concentration of PVA solution increased with constant volume of aqueous phase and studied its influence on the characterization of nanoparticles.

#### **5.3.3.3. Effect of organic phase composition**

Nanoparticles were further prepared by changing the amount of organic phase. Addition of Acetone causes perturbation resulting in a larger interface area between the organic and aqueous medium, creates extremely fine nano droplets which result in the formation of small sized nanoparticles [114]. So, Acetone volume was raised by constant volume of DCM.

#### **5.3.3.4. Scanning electron microscopy**

The morphology of the optimized Ethionamide nanoparticles was examined by Scanning Electron Microscopy (SEM) (Karl Zesis with SE detector, EVO-18). The samples were sputter-coated with gold and observed for morphology at an acceleration voltage of 7.0 kV with highest magnification of 19.99 KX.



#### **5.3.3.5. Differential scanning calorimetry (DSC)**

Differential scanning calorimetry (DSC) is one of the most powerful analytical techniques, which offers the possibility of detecting chemical interaction [213]. Initially, 5 mg ETH was weighed very accurately. The temperature was controlled within the range of 20-250 °C, with a heating rate was 20 °C/min and similar procedure was followed for PLGA (50:50) and ETH-PLGA nanoparticles as mentioned in 3.5.3.5.

#### **5.3.3.6. Residual solvent analysis**

In the formulation of Ethionamide nanoparticles, acetone and dichloromethane were used to dissolve Ethionamide and PLGA. Hence, residual solvent study was conducted to check the absence of these solvents as a residue in the final optimized nanoparticles. Pure DCM and acetone were spiked separately followed by nanoparticles as mentioned in section 3.5.3.4 using GC-head space.

#### **5.3.4. Formulation of dry powder inhaler and its characterization**

Optimized nano-suspension was further freeze dried with Mannitol (2 % w/v) as cryoprotectant. Thereafter, freeze dried nanoparticles and anhydrous inhalable grade lactose were mixed manually using geometrical dilution process. Flow property (angle of repose, bulk density and tap density) was carried out in each stage of lactose addition. Optimized dry powder inhaler was chosen on the basis of excellent flow property. Optimized formulation was further characterized for zeta size and potential to check the changes of nanoparticles in the form of DPI. On the other hand DPI of pure Ethionamide was also prepared by blending pure Ethionamide with inhalable grade lactose.

##### **5.3.4.1. Determination of mass median aerodynamic diameter**

Mass median aerodynamic diameter (MMAD) of the optimized dry powder inhaler was determined using an eight stage cascade impactor [9]. After deposition of DPI in each chamber, ETH content was determined by UV-spectrophotometric method. Estimated drug content in each chamber were inserted into the “MMAD CALCULATOR” to obtain MMAD and geometric standard deviation (GSD). Fine particle fraction, extra fine particle and emitted dose were calculated as mentioned as previously (section 3.5.4.1).

**5.3.4.2. *In-vitro* release study**

5 mg ETH equivalent dry powder inhaler was dispersed in 2 ml of simulated lung fluid (SLF) [11] and filled in dialysis bag (HiMedia labs, Mumbai, 12,000 molecular weight cut off). To avoid floating, the drug filled bag was tied over the glass plate and kept at the bottom of the dissolution chamber. In vitro release study was carried out in 1 litre SLF and maintained temperature at  $37 \pm 0.5$  °C with a paddle speed of 100 rpm [12]. 10 ml of dissolution fluid was withdrawn at specific time interval up to 24 hr and replaced with fresh SLF.

**5.3.4.3. Delivery dose calculation**

Calculated content of optimized DPI sprayed through the modified DPI that was described in section 3.5.4.4. After spray, the needle and syringe was cleaned with the water-methanol solvent in the ratio of 9:1. After filtration, Ethionamide content in this solution was estimated using UV-Spectrophotometric method (section 5.4.2).

**5.3.4.4. Stability study**

Stability study was carried out as per ICH guideline Q1A (R2). Paraffin tape was used to seal cryoprotectant vials, containing freshly prepared dry powder inhaler of Ethionamide nanoparticles. These vials were kept in stability chamber and maintained temperature, relative humidity at  $25 \pm 2$  °C and  $60 \pm 5$  % respectively. The nanoparticles were analyzed for six months with a frequency of 1.5 months for first 3 months and next at the end of 6<sup>th</sup> month [13;14]. Zeta size, zeta potential, PDI, drug entrapment and drug release were carried out to check the stability of Ethionamide nanoparticles in the form of dry powder inhaler.

**5.3.5. *In-vivo* study**

Ethical approval was already taken prior to animal handling from institutional animal ethical committee of Bengal College of Pharmaceutical Sciences and Research, Durgapur, West Bengal (Registration No:1799/PO/Ere/15/S/CPCSEA under CPCSEA, India). A total of 36 Wistar rats (4-6 months old & average weight 200-250 gm) either sex were used for this study design. The rats were housed in 12 hr light/dark cycle with sufficient food and water. Human lungs volume (4.341 litre) [15] and elimination half life of 2.5 hr were used to calculate the human dose of Ethionamide for pulmonary administration. Targeted concentration was chosen as 2 µg/ml to maintain the plasma concentration above minimum inhibitory concentration (MIC) for the period of 24 hr. Dose was divided as loading and maintenance

dose as explained in section 3.5.5.3. Equivalent dose calculation for rat had been carried out from the human dose. Dose calculation for rat was carried out with equivalent surface and weight with no observed adverse effect with 6.4 mg/kg body weight [16; 17]. Previously designed dry powder inhaler delivery device was used to administer the calculated drug through pulmonary route [132]. Rats were divided into two groups [19] one treated with DPI of Ethionamide-PLGA nanoparticles and another was treated with pure ETH loaded DPI. Animals were anesthetized by intra-peritoneal administration of Ketamine (80 mg/Kg) and Xylazine (10 mg/kg). Gently pulled the tongue outside and sprayed DPIs through the device by placing it in trachea region. In each time period, three animals were chosen to obtain statistical significant data. Rest of the procedure was followed as mentioned in section 3.5.5.4.

#### **5.3.6. *In vitro* anti-tubercular activity**

*In-vitro* anti-tubercular activity was carried out as mentioned as earlier (section 3.5.6). Based on the literature the MIC of Ethionamide is 0.5 µg/ml. Hence, the concentration of pure ETH for MTT assay was carried out in the range of 0.4-0.6 µg/ml and ETH loaded nanoparticles concentration in the range of 0.4-0.7 µg/ml.

#### **5.3.7. Statistical analysis**

All the experiments were conducted in triplicate with data reported as mean ± standard error. The analysis of variance (ANOVA) and standard error of mean were used to analyze the stability study and pharmacokinetic properties. The significant level (*P*) was set as 0.05.

## CHAPTER 6: Result and Discussion Pertaining to Ethionamide

### 6.1. Identification of drug

➤ The identification tests and the inferences for the drug sample based on its appearance, and melting point determination are summarized in Table 6.1.

**Table 6. 1: Test for physical properties of Ethionamide**

Parameters	Observations <sup>‡</sup>	Reported	Inference
Appearance	Yellow powder	Yellow, crystalline powder [77]	Complies
Melting point	160 ± 1° C	158-164°C [76]	Complies

<sup>‡</sup> values show in mean ± standard deviation

➤ Ethionamide solution was prepared by dissolving 10 mg of Ethionamide in 5 ml of methanol. 5 ml silver nitrate solution was added to this above solution and formed a dark brown precipitate which confirmed the official identification test of Ethionamide according to USP.

➤ Various functional groups present in the powder drug sample were determined by Fourier-transform infrared (FT-IR) spectroscopic and compared with the standard spectra of Ethionamide for confirmation. The observed and reported IR spectra of Ethionamide are shown in Figure 6.1. The major IR peaks observed and reported for Ethionamide molecule is summarized in Table 6.2. Strong peak of C=S peak was detected at 1020.70 cm<sup>-1</sup>. Another strong peak of C=N stretching was detected at 1513.42 cm<sup>-1</sup>. Peak at 3256.68 cm<sup>-1</sup> is due to N-H stretch. Rest all the peaks match as the compound of Ethionamide with reference standard [194].

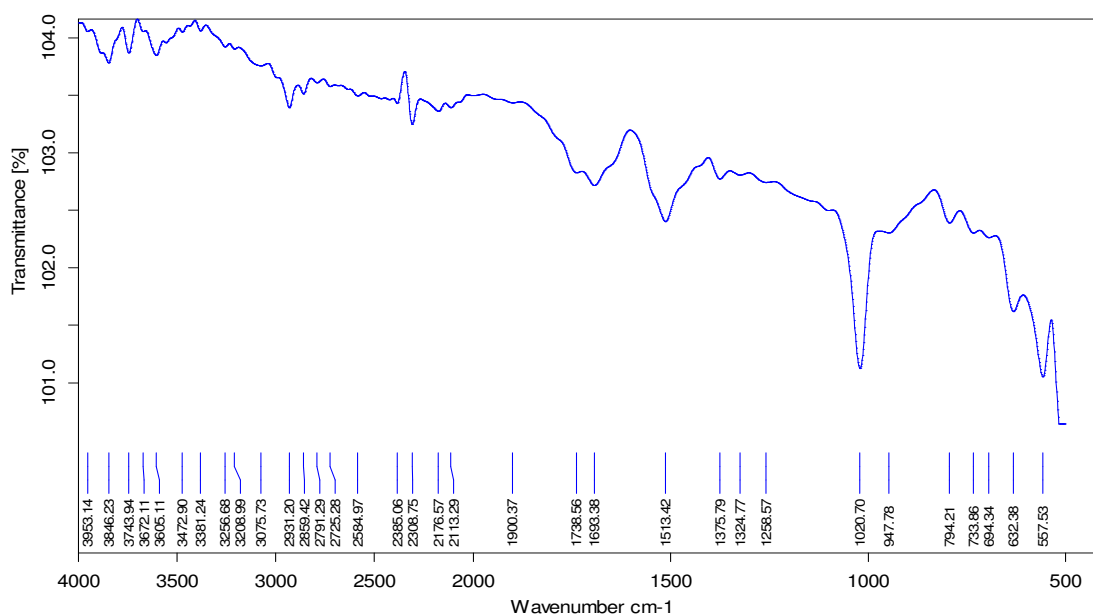


**Figure 6. 1: FTIR of Pure Ethionamide**

**Table 6. 2: Major peaks observed and reported for Ethionamide in IR spectra**

Principle Peak (cm <sup>-1</sup> ) Pure Drug	Functional Group	Principle Peak (cm <sup>-1</sup> ) Pure Drug	Functional Group
794.21	C-H out plane bending	1693.38	C=C stretching Pyridine ring
1020.70	C=S stretching	2859.42	C-H stretching
1258.57	C-N stretching	3208.99	N-H Stretching
1324.77	C-H out plane bending	3256.68	N-H stretching
1375.79	C- N stretching in ring	3381.24	Primary amide
1513.42	C=N stretching /C-C stretching/N-H bend		

Based on physical properties, IR spectra and UV- Spectrophotometric data, it was confirmed that the procured powder sample was Ethionamide and the sample can be used for further process.

## 6.2. Analytical methods

### 6.2.1. Estimation of Ethionamide using UV-Spectrophotometry and its method validation

Some HPLC estimation methods [1],[72],[74] & column chromatographic-mass spectrometric technique [5], Voltammetric Determination [196], catalytic kinetic spectrophotometric method [215] were reported by different authors. But most of the cases, methods neither validated nor provide sufficient information for estimation of Ethionamide. Some of the cases used hazardous chemicals.

#### 6.2.1.1. Determination of wavelength of maximum absorbance ( $\lambda_{\max}$ )

Different diluted solution of Ethionamide scanned in the range of 200-400 nm. The overlay spectra of PTH at different concentrations are shown in Figure 6.2. The maximum absorptivity found at 288 nm.

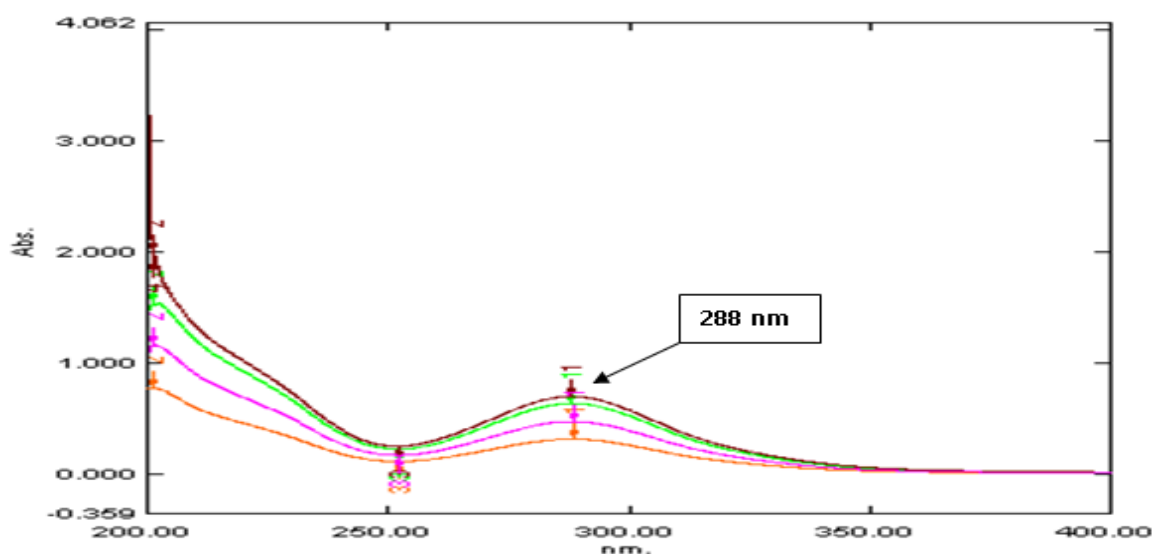


**Figure 6. 2: Determination of  $\lambda_{\max}$  for Ethionamide in pH 7.4**

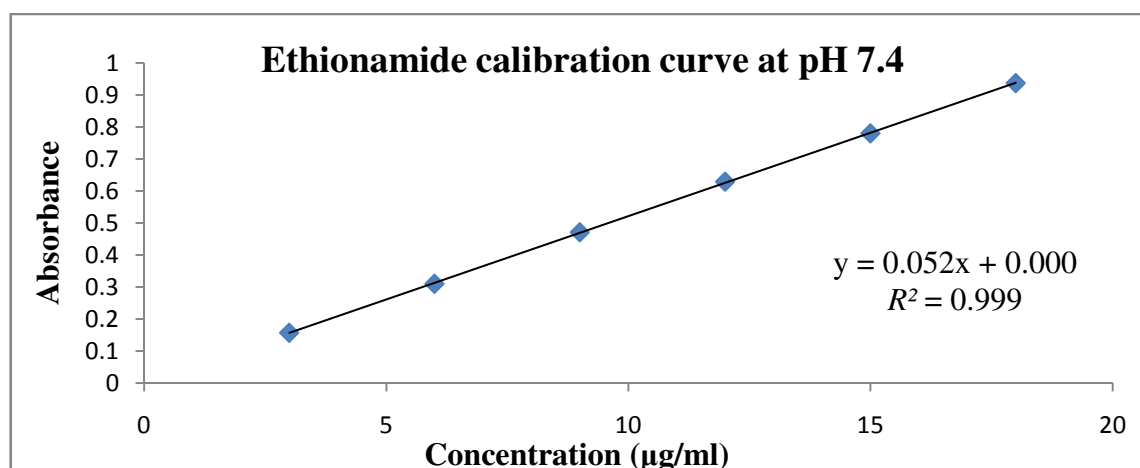
#### 6.2.1.2. Linearity and range

To determine Ethionamide content, five Point calibration curve data was constructed in the range of 6 to 18  $\mu\text{g/ml}$ , using UV-spectrophotometer (UV-1800, Shimadzu). The data obtained for calibration curve is shown in Table 6.3 and calibration curve is shown in Figure 6.3.

**Table 6. 3: Absorbance of different concentration of ETH in pH 7.4**

Conc. ( $\mu\text{g/ml}$ )	Absorbance ( $\lambda_{\text{max}}=288 \text{ nm}$ )			
	Trial 1	Trial 2	Trial 3	Mean absorbance <sup>‡</sup>
6	0.31	0.311	0.31	0.310 $\pm$ 0.003
9	0.471	0.47	0.472	0.471 $\pm$ 0.001
12	0.626	0.632	0.629	0.629 $\pm$ 0.001
15	0.779	0.781	0.781	0.780 $\pm$ 0.001
18	0.942	0.933	0.936	0.937 $\pm$ 0.004
Parameter				
With out Zero interpretation	$y = 0.052x - 0.003$	$y = 0.051x + 0.003$	$y = 0.052x + 0.001$	$y = 0.52x + 0.000$
	0.999	0.999	0.999	0.999
With Zero interpretation	$y = 0.052x$	$y = 0.052x$	$y = 0.052x$	$y = 0.052x$
	0.999	0.999	0.999	0.999

<sup>‡</sup>Values are mean of three data  $\pm$  standard deviation

**Figure 6. 3: Calibration curve of Ethionamide at pH 7.4.**

The linear regression equation obtained by the proposed method using three authentic calibration curves was,  $y = 0.052x + 0.000$ , where “y” represents the absorbance, and “x” represents Ethionamide concentration in  $\mu\text{g/ml}$ . Calibration curve exhibit good correlation co-efficient ( $R^2 = 0.999$ ). The intercepts value is zero that confirmed the good linearity of the method. Ethionamide proved linear in the range of 6 to 18  $\mu\text{g/ml}$ .

LOD and LOQ were estimated for Ethionamide as per the previous adopted method and are found to be 0.076 µg/ml and 0.2301 µg/ml respectively, which indicate that the proposed UV method is highly sensitive (Table 6. 4). The results of LOD and LOQ supported the sensitivity of the developed method.

**Table 6. 4: Determination of limit of detection and limit of quantification**

y-intercept				S	LOD (µg/ml)	LOQ (µg/ml)
Trial 1	Trial 2	Trial 3	SD			
0.003	0.003	0.001	0.0012	0.052	0.076	0.2301

#### 6.2.1.3. Assay of Ethionamide in marketed tablet

The method developed in this study was used for determination of Ethionamide content from Ethomid (Macleods Pharmaceutical Ltd.). Assay result from three replicate analyses of Ethomid tablets showed the recovery of 99.47±0.12 % with RSD of 0.123 %. In content uniformity experiment, Ethionamide content in tablets was examined and found in the range of 99.20±0.14 to 99.84±0.07 % with RSD of 0.070-0.161 (Table 6. 5). In the estimation of Ethionamide, no interference of excipients was observed. This indicates that the distribution of drug in tablet was uniform without significant variation.

**Table 6. 5: Assay of marketed tablet for Ethionamide**

Prepared conc. (µg/ml)	Absorbance	Conc. recovered (µg/ml)	Percentage Label claim	Average percentage label claim <sup>‡</sup>	RSD
8	0.413	7.942	99.28	99.20±0.14	0.140
	0.412	7.923	99.04		
	0.413	7.9423	99.28		
12	0.621	11.942	99.52	99.36±0.16	0.161
	0.619	11.904	99.20		
	0.620	11.923	99.36		
16	0.831	15.981	99.88	99.84±0.07	0.070
	0.831	15.981	99.88		
	0.830	15.962	99.76		
Over all mean percentage label claim				99.47±0.12	0.123

<sup>‡</sup>Values are mean of three data ± standard deviation



#### 6.2.1.4. Accuracy

This method demonstrated excellent mean recovery of  $99.80 \pm 0.53$  % (Table 6. 6). All the estimated parameters were found to be statistically significant due to low RSD values ( $RSD < 2$ ).

**Table 6. 6: Recovery studies on marketed formulations**

Conc. level	Sl. No	Drug	Formulation	Amount added (µg/ml)	Amt recovered	Percentage recovery	Mean Recovery <sup>‡</sup> (n=3)	% RSD
80%	1	10ml of 15 µg/ml	10 ml of 12µg/ml	13.5	13.46	99.72	99.76±0.22	0.22
	2				13.44	99.57		
	3				13.50	100.0		
100%	1		10 ml of 15µg/ml	15	14.92	99.49	99.79±0.27	0.27
	2				15.00	100.0		
	3				14.98	99.87		
120%	1		10 ml of 18µg/ml	16.5	16.50	100.0	99.85±0.18	0.18
	2				16.44	99.65		
	3				16.48	99.88		
Mean recovery							99.80±0.53	0.22

<sup>‡</sup>Values are mean of three data  $\pm$  standard deviation

#### 6.2.1.5. Precision

Three different working stock solution in triplicates (5, 10, 15  $\mu\text{g/ml}$ ) were prepared and studied for three different times in a day (intraday;  $n=9$ ) and continued up to 3<sup>rd</sup> day (inter-day;  $n=15$ ). Relative standard deviation (RSD) value varies from 0.017-0.668 % in case of intra-day precision and 0.666-1.703 % for inter-day precision. In all the cases the values were within the permitted limit (Table 6. 7).

**Table 6. 7: Intra-day & Inter-day precision for three different concentrations of ETH**

Conc. ( $\mu\text{g/ml}$ )	Intra Day						Inter Day	
	DAY-1		DAY-2		DAY-3		Inter Day	
	Repeatability <sup>‡</sup> (n=9)	% RSD	Repeatability <sup>‡</sup> (n=3)	% RSD	Repeatability <sup>‡</sup> (n=3)	% RSD	Repeatability <sup>‡</sup> (n=15)	% RSD
5	$4.99 \pm 0.017$	0.334	$4.93 \pm 0.017$	0.344	$4.79 \pm 0.032$	0.668	$4.91 \pm 0.083$	1.703
10	$9.99 \pm 0.013$	0.128	$9.95 \pm 0.014$	0.137	$9.79 \pm 0.029$	0.295	$9.91 \pm 0.089$	0.899
15	$14.97 \pm 0.017$	0.017	$14.88 \pm 0.029$	0.194	$14.75 \pm 0.055$	0.371	$14.87 \pm 0.099$	0.666

<sup>‡</sup>Values are mean  $\pm$  standard deviation; n=No of sample analysed

UV-Spectroscopic method was developed with commonly known chemicals, which can be used for the routine analysis of Ethionamide in bulk and pharmaceutical dosage forms. Although different chemicals were used in tablet form of ETH, no significant shifting of  $\lambda_{\max}$  was detected. So, this validated method can precisely estimate the ETH in bulk and formulation without the interference of solvent effect.

### 6.2.2. Preparation of standard curve of ETH in water-methanol system

As like of Prothionamide, similar standard curve for Ethionamide was prepared in water-methanol (9:1) system. Ethionamide showed maximum absorptivity at 288.60 nm in this solvent. Different concentrations of stock solutions were prepared and took the absorbance three times (Table 6. 8).

**Table 6. 8: Standard curve of ETH in water-methanol (9:1)**

Conc. μg/ml)	Absorbance			
	Trial 1	Trial 2	Trial 3	Average <sup>‡</sup>
10	0.237	0.239	0.239	0.238±0.001
15	0.355	0.354	0.351	0.353±0.002
20	0.461	0.462	0.462	0.462±0.001
25	0.58	0.581	0.581	0.581± 0.001
30	0.694	0.699	0.699	0.697±0.003
35	0.816	0.813	0.814	0.814±0.002
40	0.93	0.933	0.931	0.931±0.002
Regression equation	y=0.023x+0.004	y =0.023x+0.005	y=0.023x+0.004	y = 0.023x + 0.004
$R^2$	0.999	0.999	0.999	0.999

<sup>‡</sup>Values are mean of three data ± standard deviation

Individually, all the curves were analysed and found the regression value as 0.999. These values signified the suitability and accurate determination of Ethionamide in a solvent of water-methanol (9:1).

Average absorbance value of each concentration was used to construct the standard curve (Figure 6. 4) of Ethionamide in water-methanol system. The regression equation of standard curve is  $y = 0.023x + 0.004$  with  $R^2$  value of 0.999.

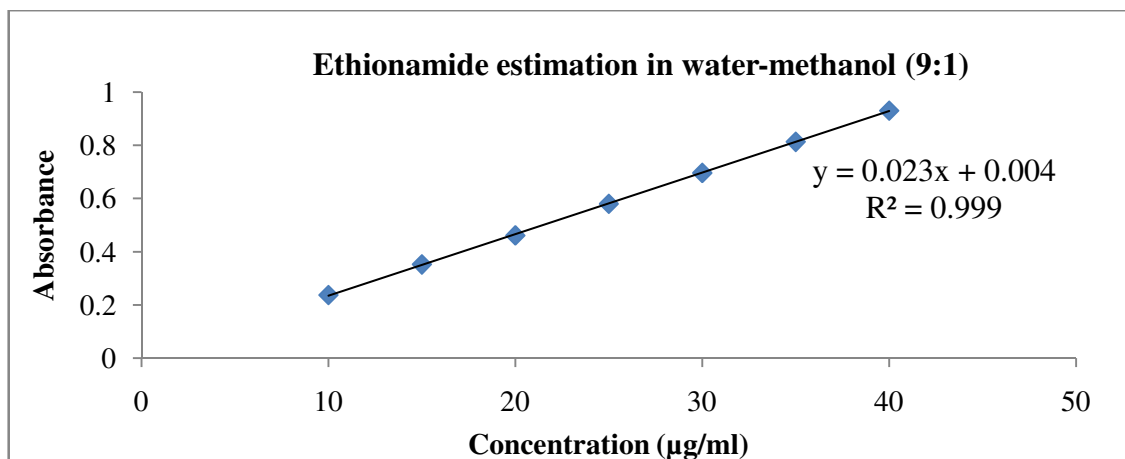


**Figure 6. 4: Standard curve of Ethionamide in water-methanol system**

### 6.2.3. Estimation of Ethionamide in rat plasma using HPLC method

Mobile phase composed of HPLC grade water and acetonitrile in the ratio of 70:30 (v/v) with a flow rate of 1 ml/min. ETH showed the maximum absorptivity at 290 nm in the mobile phase. Diluted ETH solutions injected in HPLC and the responses (peak area) were recorded at that  $\lambda_{\max}$ . C18-Phenomenex (250 mm  $\times$  4mm i.d., 5  $\mu$ m particles) was used for the same [88]. The data of regression analysis of the calibration curve was shown in Table 6. 9.

**Table 6. 9: Calibration data of ETH using HPLC**

ETH Conc. ( $\mu$ g/ml)	Trial 1	Trial 2	Trial 3	Average <sup>‡</sup>
	Area [mV.s]	Area [mV.s]	Area [mV.s]	Area [mV.s]
0.1	11.227	25.262	25.1	20.53 $\pm$ 8.06
0.5	86.227	100.422	100.06	95.569 $\pm$ 8.09
1	180.158	194.372	193.76	189.43 $\pm$ 8.04
5	956.359	974.359	983.856	971.525 $\pm$ 13.97
10	1864.248	1882.858	1866.745	1871.284 $\pm$ 1.10
15	2748.343	2763.530	2749.891	2753.921 $\pm$ 8.36
20	3761.674	3789.621	3768.942	3773.412 $\pm$ 14.50
25	4695.589	4720.469	4717.953	4711.337 $\pm$ 13.69
Regression Equation	$y=187.5x-7.484$	$y=187.9x+6.439$	$y=187.4x+6.356$	$y=187.6x+1.770$
$R^2$	0.999	0.999	0.999	0.999

<sup>‡</sup>Values are mean of three data  $\pm$  standard deviation

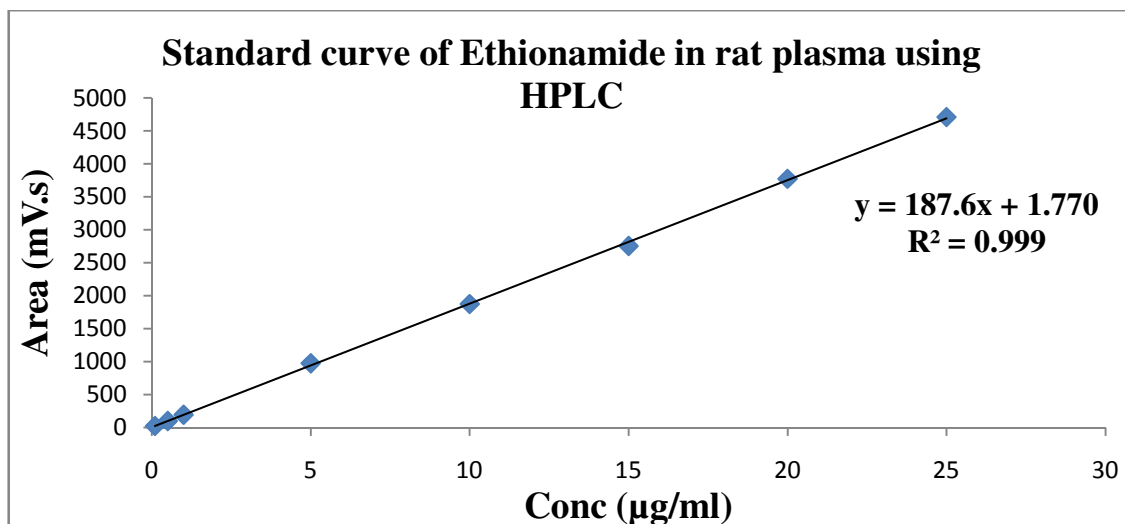


**Figure 6. 5: Linear curve of Ethionamide using HPLC**

The calibration curve (Figure 6. 5) for Ethionamide was obtained by plotting the peak area versus the concentration of Ethionamide over the range of 0.1-25 µg/ml, and it was found to be linear with  $R^2=0.999$ . The regression equation of ETH concentration over its area was found to be  $y=187.6x + 1.770$ , where “x” is the concentration of ETH and “y” is the respective peak area. The chromatogram of working standard of Ethionamide solution was shown in Figure 4.6 in section 4.2.3.

The retention time for ETH was found to be 4.90 min, whereas internal standard of Prothionamide was detected at 9.5. No interference from mobile phase or baseline disturbance observed in the chromatogram.

### 6.3. Formulation and Characterization of DPI containing Ethionamide nanoparticles prepared by PLGA (50:50)

#### 6.3.1. Compatibility study

FTIR spectra of pure Ethionamide and physical mixture were shown in Figure 6. 6. C=S stretching at  $1020.70\text{ cm}^{-1}$  in pure ETH, that peak was obtained at  $1021.63\text{ cm}^{-1}$  in physical mixture. C-N stretching in pure ETH and mixture was detected at  $1375.79$  and  $1375.68\text{ cm}^{-1}$  respectively.

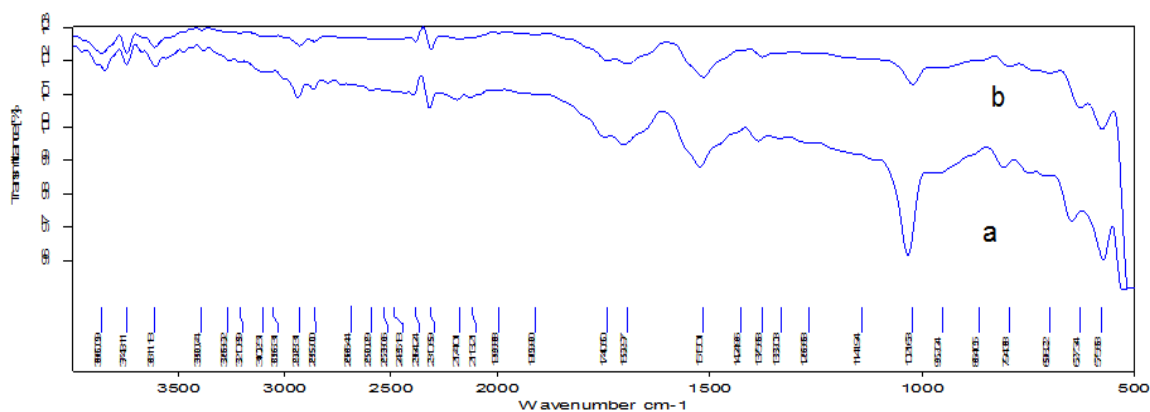


**Figure 6. 6: FTIR of pure ETH (a) and physical mixture of ETH, PLGA (50:50),  
Inhalable grade lactose (b)**

**Table 6. 10: Comparison of principle peaks between pure ETH with physical mixture**

Peak (cm <sup>-1</sup> ) Pure Drug/ Physical Mixture	Functional Group	Peak (cm <sup>-1</sup> ) Pure Drug/ Physical Mixture	Functional Group
794.21/794.38	C-H out plane bending	1693.38/1692.67	C=C stretching Pyridine ring
1020.70/1021.63	C=S stretching	2859.42/2859.00	C-H stretching
1258.57/1266.68	C-N stretching	3208.99/3210.89	N-H Stretching
1324.77/1332.03	C-H out plane bending	3256.68/3268.92	N-H stretching
1375.79/1375.68	C- N stretching in ring	3381.24/3390.74	Primary amide
1513.42/1515.01	C=N stretching /C-C stretching/N-H bend		

All other major peaks like C-H stretching, C-N stretching, C=N stretching are obtained in the narrow range with similar intensity are mentioned in Table 6. 10. Hence, FTIR confirmed the absence of chemical interaction between drug and excipients.

### 6.3.2. Optimization and characterization of ETH nanoparticles

Ethionamide nanoparticles were prepared by solvent evaporation method. Several process parameters like surfactant concentration, ETH-PLGA ratio, and organic phase composition

were optimized to find suitable nanoparticles for the formulation of DPI. Values reported are the mean diameter with standard deviation for three replicate samples.

### 6.3.2.1. Effect of ETH-PLGA ratio

Five batches were prepared with varying proportion of PLGA. Particle size and percentage drug entrapment were increased with increasing the amount of PLGA. EP4 showed least PDI and higher zeta potential rather than the rest of batch (Table 6. 11). Polymer amount was more in EP5 in comparison with EP4, but also showed very little rise in drug entrapment. PLGA carries negative charge, hence zeta potential value reduced to  $-1.8 \pm 1.2$  mV in EP5. Particles in EP5 had more tendencies to be coagulating each other that influences in rise in PDI and z-average value. Hence EP4 was selected for further modification.

**Table 6. 11: Influence of ETH-PLGA ratio on nanoparticles**

Formula code	ETH : PLGA	Z average value (nm) <sup>‡</sup>	PDI <sup>‡</sup>	Zeta potential (mV) <sup>‡</sup>	PDE <sup>‡</sup>
EP1	1:1	$412.9 \pm 6.4$	$0.360 \pm 0.013^{\#}$	$-2.3 \pm 1.6$	$78.32 \pm 0.38$
EP2	1:2	$415.7 \pm 7.8$	$0.393 \pm 0.037^{\#}$	$-3.9 \pm 2.3$	$81.38 \pm 0.59$
EP3	1:3	$469.0 \pm 11.5$	$0.621 \pm 0.071^{\#}$	$-3.2 \pm 2.1$	$80.25 \pm 0.11^{\#}$
EP4	1:4	$488.4 \pm 7.2$	$0.394 \pm 0.014^{\#}$	$-5.7 \pm 0.3^{\#}$	$83.62 \pm 0.97$
EP5	1:5	$523.0 \pm 5.9$	$0.878 \pm 0.074^{\#}$	$-1.8 \pm 1.2$	$84.01 \pm 0.54$

<sup>‡</sup>Values are mean of three data  $\pm$  standard deviation; <sup>#</sup>P value less than 0.05.

### 6.3.2.2. Effect of surfactant concentration

Further modification was done in EP4 by changing PVA concentration. Four new batches were prepared and compared with EP4 (Table 6. 12). High concentrations of PVA lead to reduction in particles size. Concurrently, it also observed that distribution of nanoparticles became narrow with increasing the PVA amount. Insufficient concentration of emulsifier would fail to stabilize all the nanoparticles [21] and thus aggregation was more in EP4 rather than rest of batch in Table 6. 12. PVA amount plays vital role in emulsification process and protection of globules by preventing coagulation. But, increasing the concentration of PVA, drug entrapment efficiency was decreased significantly. Here, EPS1 with 0.5 % w/v PVA was selected due to higher PDE of  $89.02 \pm 0.43$  % and zeta potential of  $-8.1 \pm 0.8$  mV with lesser PDI value of  $0.241 \pm 0.032$ .

**Table 6. 12: Effect of surfactant concentration on nanoparticles**

Formula code	PVA conc. (% w/v)	Z average value (nm) <sup>‡</sup>	PDI <sup>‡</sup>	Zeta potential (mV) <sup>‡</sup>	PDE <sup>‡</sup>
EP4	0.25	488.4 ± 7.2	0.394 ± 0.014 <sup>#</sup>	-5.7 ± 0.3 <sup>#</sup>	83.62 ± 0.97
EPS1	0.50	329.5 ± 6.3	0.241 ± 0.032 <sup>#</sup>	-8.1 ± 0.8 <sup>#</sup>	89.02 ± 0.43 <sup>#</sup>
EPS2	0.75	308.9 ± 12.8	0.578 ± 0.041 <sup>#</sup>	-1.9 ± 1.7	85.62 ± 1.10
EPS3	1.00	257.1 ± 10.7	0.598 ± 0.011 <sup>#</sup>	-3.8 ± 1.1	82.89 ± 0.76
EPS4	1.25	231.0 ± 23.8	0.574 ± 0.086	-4.3 ± 2.1	77.71 ± 0.98

<sup>‡</sup>Values are mean of three data ± standard deviation; <sup>#</sup>P value less than 0.05.

### 6.3.2.3. Effect of organic phase composition

Oil phase solvent mixture composition plays important role in particle size as emulsion fabrication is the most critical step during the nanoparticles preparation, where emulsion droplets directly relevant to final nanoparticles size [114]. In order to verify the effect of organic phase composition on the particle size and drug entrapment three new batches were prepared. Further modification in EPS1 was made by changing acetone amount. Particle size was decreased with increasing the acetone volume (Table 6. 13), but concurrently zeta potential value was decreased significantly resulting in more prominent chance of particles coagulation.

**Table 6. 13: Effect of DCM-acetone ratio on the nanoparticles**

Formula code	DCM(ml): Acetone(ml)	Z average value (nm) <sup>‡</sup>	PDI <sup>‡</sup>	Zeta potential (mV) <sup>‡</sup>	PDE <sup>‡</sup>
EPS1	2:1.5	329.5 ± 6.3	0.241 ± 0.032 <sup>#</sup>	-8.10 ± 0.8 <sup>#</sup>	89.28 ± 0.43 <sup>#</sup>
EPV1	2:2.0	317.3 ± 9.4	0.559 ± 0.062 <sup>#</sup>	-7.60 ± 0.23	85.46 ± 0.76
EPV2	2:2.5	268.3 ± 8.3	0.481 ± 0.048 <sup>#</sup>	-1.02 ± 0.34	82.33 ± 0.11 <sup>#</sup>
EPV3	2:3.0	543.1 ± 5.8	0.480 ± 0.076 <sup>#</sup>	-2.81 ± 1.01	79.07 ± 1.32

<sup>‡</sup>Values are mean of three data ± standard deviation; <sup>#</sup>P value less than 0.05.

In this regards, EPS1 showed zeta potential of -8.10 ± 0.8 mV, which had less chance of aggregation in comparison with other formulation. Hence, EPS1 was considered to be suitable candidate for the dry powder inhaler.

### 6.3.2.4. SEM analysis

Shape and surface morphology of prepared lyophilized nanoparticles (EPS1) were evaluated by SEM. The study revealed that most of the nanoparticles were spherical in

shape and confirmed that the particle size was in the nano-meter range [108]. The surface of the particles showed a characteristic smoothness (Figure 6. 7). Polydispersibility index of the optimized batch was within 0.5 indicates less chances of aggregation of particles [216].

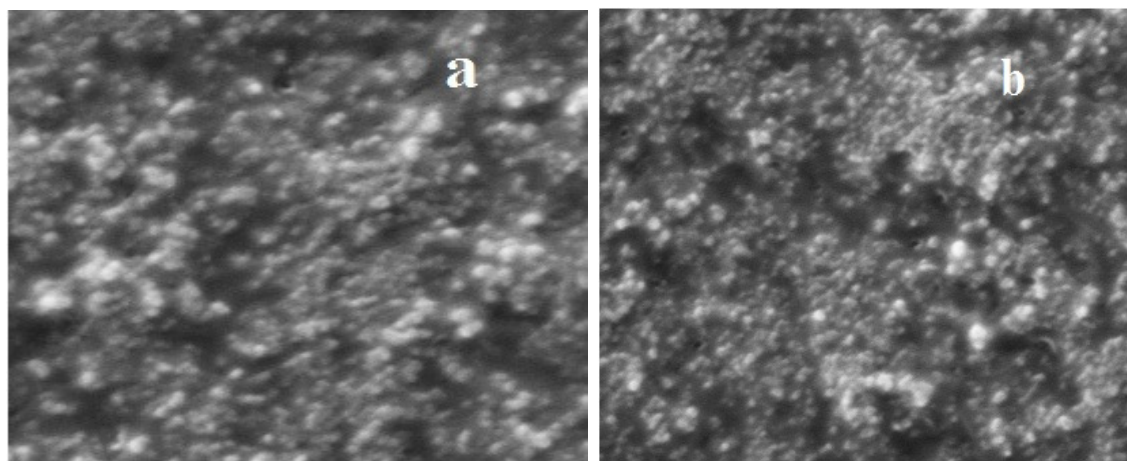


**Figure 6. 7: SEM image of optimized freeze dried nanoparticles (EPS1) at 19.99KX**

#### 6.3.2.5. Differential scanning calorimetry (DSC)

DSC gives information regarding the physical properties like crystalline or amorphous nature of the samples [213]. DSC thermo gram of pure Ethionamide showed melting point at 161.31°C (Figure 6.8-a). This sharp peak confirmed that the Ethionamide present in crystalline form. The another dip peak at 212.52 °C be due to decomposition of ETH at higher temperature [217]. PLGA was amorphous which showed glass transition state at 63.21 °C (Figure 6.8- b).

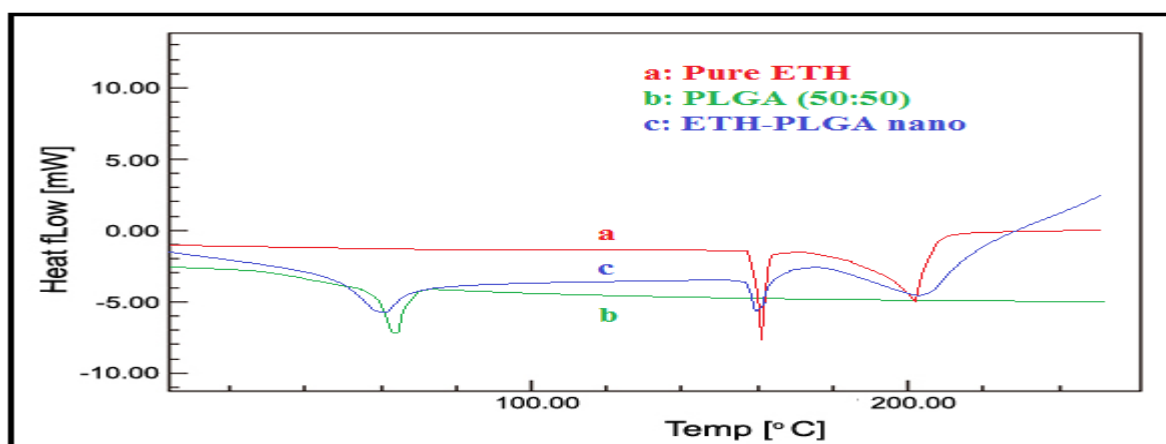


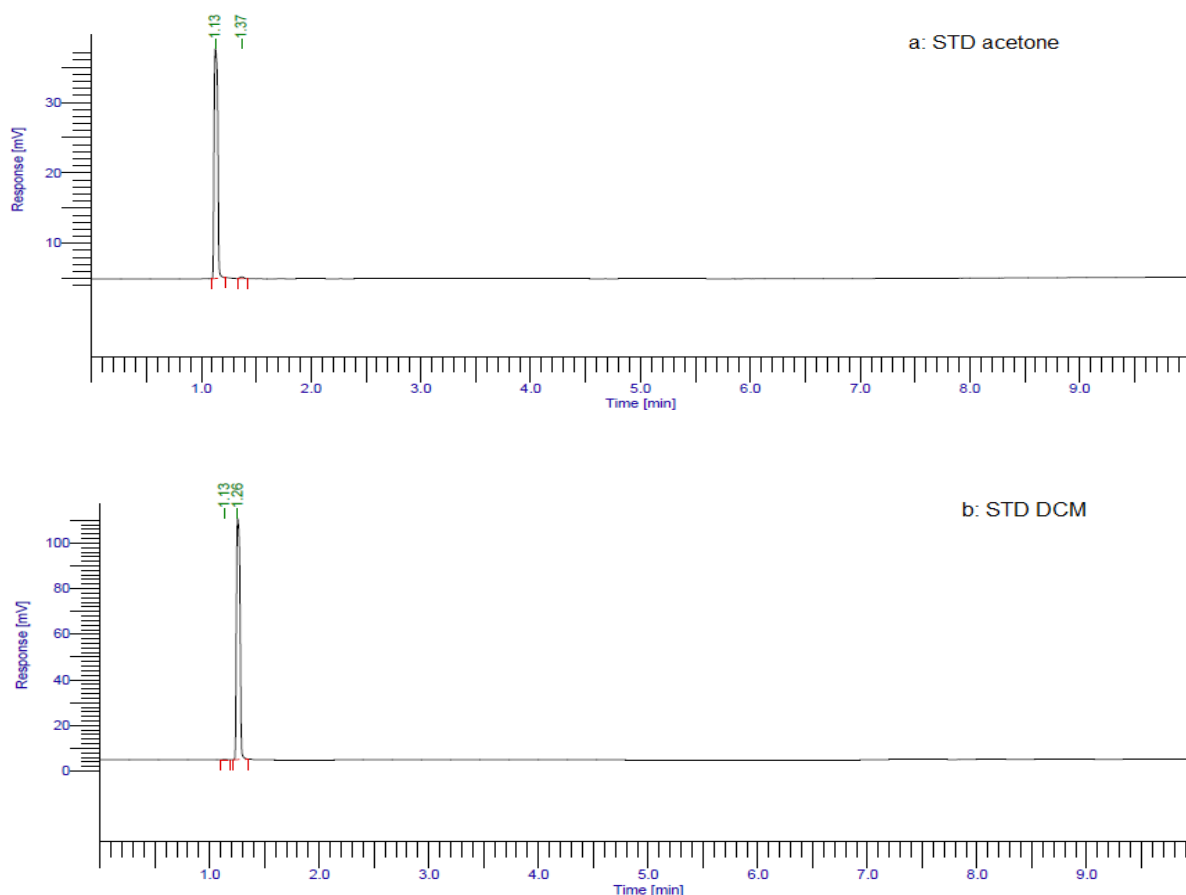
**Figure 6. 8: DSC thermogram of pure ETH (a), PLGA (50:50) (b), optimized nanoparticles of ETH-PLGA (EPS1) (c)**



In drug loaded nanoparticles, glass transition state slightly decreased and shown at 60.23°C. The endothermic peak of Ethionamide was broadened and shifted to lower temperature of 160.36 °C (Figure 6.8-c) due to incorporation of PVA as an impurity or conversion of crystalline form to amorphous form in the optimized batch of ETH-PLGA (EPS1).

### 6.3.2.6. Residual solvent analysis

DCM is listed under class II solvent which means non-genotoxic animal carcinogens or possible causative agents of other irreversible toxicity such as neurotoxicity or teratogenicity. Use of this solvent should be limited within 6 ppm [218]. DCM showed characteristic peak at 1.26 min (Figure 6.9-b) but was not detected in the final freeze dried nanoparticles (EPS1) (Figure 6.9-c). On the other side, Acetone, another volatile solvent, listed in class III solvents means that solvent is of low toxic to human; No health-based exposure limit is needed [121]. Pure acetone showed characteristic peak at 1.13 min (Figure 6.9-a) and same peak is detected in nanoparticles (EPS1) (Figure 6.9-c). Acetone was found to be 0.65 ppm (Appendix C) and this amount is non toxic for human.



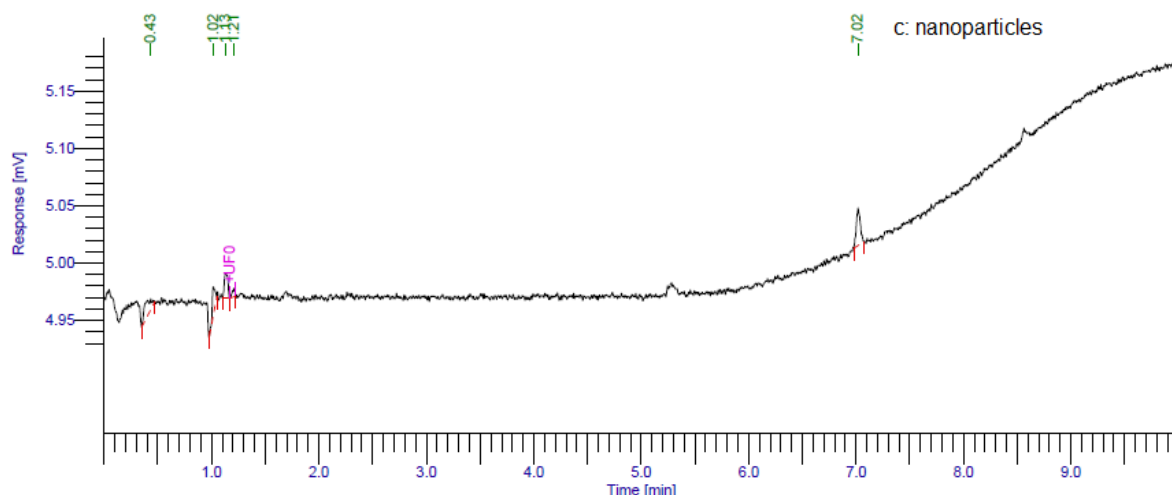


**Figure 6. 9: GC chromatograms of (a) pure Acetone, (b) pure DCM and (c) optimized PLGA-ETH nanoparticles (EPS1)**

### 6.3.3. Formulation and characterization of dry powder inhaler

MMAD represents aerodynamic diameter below which 50 % particles remain. Aerodynamic diameter of a particle controls its deposition in different region of pulmonary tract. Different proportion of anhydrous lactose was added to Optimized ETH-PLGA nanoparticles (EPS1) by physical geometric mixture. At 1:1 ratio of EPS1-lactose (EP-DPI2), DPI showed good flow property with angle of repose of  $29.05 \pm 0.45^\circ$  (Table 6.14). Carr's index and Hausner ratio were found to be  $10.00 \pm 0.33\%$  and  $1.11 \pm 0.01$  respectively. Optimized DPI tested for the zeta size, potential and PDI were found to be  $225.7 \pm 4.56$  nm,  $-6.9 \pm 2.59$  mV and  $0.216 \pm 0.015$  respectively. DPI containing freeze dried ETH nanoparticles showed better PDI and Z average value.

**Table 6. 14: Flow property analysis of different composition of DPI**

Formulation code	Nanoparticles: Anhydrous lactose	Angle of repose <sup>‡</sup>	Carr's index <sup>‡</sup>	Hausner ratio <sup>‡</sup>
EP-DPI 1	1.0:0.5	$32.91 \pm 1.33$	$10.43 \pm 3.33$	$1.12 \pm 0.04$
EP- DPI 2	1.0:1.0	$29.05 \pm 0.45$	$10.00 \pm 0.33$	$1.11 \pm 0.01$
EP- DPI 3	1.0:1.5	$32.01 \pm 0.65$	$11.83 \pm 1.86$	$1.14 \pm 0.02$
EP-DPI 4	1.0:2.0	$34.51 \pm 0.76$	$12.34 \pm 2.89$	$1.14 \pm 0.04$

<sup>‡</sup>Values are mean of three data  $\pm$  standard deviation

Similarly, DPI of pure Ethionamide was prepared by blending ETH with inhalable grade lactose. Pure ETH- inhalable lactose in the ratio of 1:5 (EL-DPI5) showed the excellent flow property and considered as optimized DPI of pure Ethionamide.

### 6.3.3.1. Determination of MMAD and geometric standard deviation

Depending upon the particle size, deposition of ETH loaded DPI in the different chamber of cascade impactor was determined using UV-spectrophotometric method. Parameters like particles size and shape determine their deposition in the different parts of trachea and lungs. Particle size was in the range of 0.5-5  $\mu\text{m}$ , which can reach deeper to alveoli [22].

**Table 6. 15: Deposition of drug in different chamber of cascade impactor for EP-DPI 2**

Stage	Size (micron)	Absorbance	Conc. ( $\mu\text{g/ml}$ )	Dilution factor	Amount ( $\mu\text{g}$ )	Amount (mg)	Percentage deposition
0	9	0.119	5	1	5	0.005	0.05
1	5.8	0.761	32.9130	2	65.8261	0.0658	0.66
2	4.7	0.494	21.3043	10	213.0434	0.2130	2.13
3	3.3	0.232	9.9130	100	991.3043	0.9913	9.91
4	2.1	0.568	24.52173	100	2452.1739	2.4522	24.52
5	1.1	0.973	42.1304	100	4213.0435	4.2130	42.13
6	0.7	0.369	15.8696	100	1586.9565	1.5869	15.87
7	0.4	0.415	17.8696	10	178.6956	0.1786	1.79
Filter	n/a	0.381	16.3913	1	16.3913	0.0164	0.16

Flow Rate:			28.3 L/min
Cut off Diameter			
Impactor Stage	(microns)	Drug Collected	
Stage 0	9	0.0050	
Stage 1	5.8	0.0658	
Stage 2	4.7	0.2130	
Stage 3	3.3	0.9913	
Stage 4	2.1	2.4522	
Stage 5	1.1	1.5869	
Stage 6	0.7	0.1787	
Stage 7	0.4	0.0164	
Filter	n/a		
MMAD:	1.79	microns	
GSD:	1.71		

**Figure 6. 10: Snapshot of aerodynamic determination from web site**

Deposition of drug in different chamber is shown in Table 6.15. Fine particle fraction, extra fine particle fraction and emitted dose were found as 94.38 %, 17.82 % and 97.22 % respectively. Optimized DPI (EP-DPI 2) showed aerodynamic particles size of 1.79  $\mu\text{m}$  with geometric standard deviation of 1.71 (Figure 6.10). Hence, Prepared DPI can penetrate deep to lungs.

### 6.3.3.2. *In-vitro* release study

Prepared DPI was further characterized for the *in-vitro* release study in simulated lungs fluid. Optimized DPI showed initial burst release of  $9.23 \pm 1.15$  % in first 1 hr, which attributed to the drug release from adsorbed surface which might have got desorbed upon contact with the dissolution medium [110]. This burst releases will help to reach the drug concentration above MIC and continue to release up to  $95.17 \pm 3.59$  % in 24 hr (Table 6. 16). ETH coated with PLGA (50:50) degraded rapidly due to more amount of glycolic acid unit in the copolymer [23]. Hence, more than 95 % release achieved in 24 hr. Different models like zero order, Higuchi and Peppas models were applied to check the release patterns. Percentage drug release-time profile of zero order kinetic showed highest correlation co-efficient ( $R^2$ ) of 0.992 in comparison of Higuchi, Peppas's models with  $R^2$  of 0.930 and 0.949 respectively. Hence the release best fitted with zero order mechanism.

**Table 6. 16: *In-vitro* release profile of EP- DPI 2**

Zero order		Higuchi model		Peppas's model	
Time (hr)	Cumulative % drug release <sup>‡</sup>	Square route of time (hr)	Cumulative % drug release <sup>‡</sup>	Log time (hr)	log % CDR
1	$9.23 \pm 1.15$	1	$9.23 \pm 1.15$	0	0.97
2	$12.02 \pm 1.69$	1.41	$12.02 \pm 1.69$	0.30	1.08
3	$14.06 \pm 1.70$	1.73	$14.06 \pm 1.70$	0.48	1.15
4	$16.89 \pm 1.43$	2	$16.89 \pm 1.43$	0.60	1.23
5	$19.36 \pm 2.38$	2.24	$19.36 \pm 2.38$	0.69	1.29
6	$22.24 \pm 2.10$	2.45	$22.24 \pm 2.10$	0.78	1.35
7	$31.30 \pm 3.10$	2.65	$31.30 \pm 3.10$	0.85	1.49
8	$33.15 \pm 1.85$	2.83	$33.15 \pm 1.85$	0.90	1.52
9	$38.47 \pm 1.80$	3	$38.47 \pm 1.80$	0.96	1.59
10	$41.53 \pm 2.43$	3.16	$41.53 \pm 2.43$	1	1.62
11	$46.54 \pm 1.49$	3.32	$46.54 \pm 1.49$	1.04	1.67
12	$52.37 \pm 1.72$	3.46	$52.37 \pm 1.72$	1.08	1.72

24	95.17 ± 3.59	4.89	95.17 ± 2.10	1.38	1.98
Zero order		Higuchi Model		Peppas's Model	
$R^2 = 0.9928$		$R^2 = 0.930$		$R^2 = 0.949$	

<sup>‡</sup>Values are mean of three data ± standard deviation

### 6.3.3.3. Delivery dose calculation

Whole content of EP-DPI 2 was sprayed in three divided form and the non-delivered Ethionamide was determined using UV-Spectrophotometric method at 288.60 nm. Water-methanol 9:1 was used for this analysis. Equation used for this estimation was mentioned in section 6.2.2. The device was able to deliver  $98.25 \pm 0.14\%$  of its content (Table 6. 17). This value was considered in final dose calculation for rat using modified DPI delivery device.

**Table 6. 17: Delivery dose for EP- DPI 2**

Sr. No	Absorbance	Conc. (µg/ml)	Volume (ml)	Amount (µg)	Amount (mg)	Dose given (mg)	Dose delivered (mg)	Percentage delivered (%)
1	0.051	2.1304	10	21.3043	0.0213	1.3	1.2787	98.36
2	0.053	2.2173	10	22.1739	0.0222		1.2778	98.29
3	0.059	2.4783	10	24.7826	0.0248		1.2752	98.09
Average <sup>‡</sup>							1.2772 ± 0.002	
Average percentage delivered <sup>‡</sup>							98.25 ± 0.14%	

<sup>‡</sup>Values are mean of three data ± standard deviation

### 6.3.3.4. Stability study

Optimized DPI was packed in different vials and maintained humidity and temperature for the period of 6 months in humidity control chamber. No significant aggregation of particles and physical properties of nanoparticles were occurred during the storage period (Table 6.18).

**Table 6. 18: Stability study of DPI**

Time point (month)	Particle size (nm) <sup>‡</sup>	PDI <sup>‡</sup>	Zeta potential <sup>‡</sup>	PDE <sup>‡</sup>	% drug release in 24hr <sup>‡</sup>
0	225.7 ± 6.4	0.216 ± 0.011 <sup>#</sup>	-6.9 ± 1.24 <sup>#</sup>	88.80 ± 1.64	95.17 ± 3.23
1.5	240.7 ± 7.3	0.229 ± 0.019 <sup>#</sup>	-5.6 ± 1.43 <sup>#</sup>	85.69 ± 2.57	97.90 ± 1.34
3	272.3 ± 4.6	0.226 ± 0.005 <sup>#</sup>	-6.4 ± 2.12	83.52 ± 4.35	99.43 ± 0.21
6	286.6 ± 5.4	0.219 ± 0.050	-6.6 ± 1.56	83.21 ± 4.76	98.97 ± 0.71

<sup>‡</sup>Values are mean of three data ± standard deviation, <sup>#</sup>P value less than 0.05.

Particle sizes were changed in the narrow range but it would not create any significant effect on the release profile of ETH from DPI.

#### 6.3.4. *In-vivo* study

As mentioned previously, animal experiment was conducted with prior permission (BCPSR/IAEC/04-16) (Appendix A) and all the guidelines of institutional animal ethical committee of Bengal College of Pharmaceutical Sciences and Research, Durgapur, West Bengal are followed throughout the experiments.

##### 6.3.4.1. Dose, DPI calculation and administration

Dose equivalents DPI of individual rats are shown in Table 6. 19. First rat in study 1 of Table 6.19: Rat weight (S1F1) was 0.235 kg. Hence, equivalent ETH dose is 1.503 mg (as calculated in section 3.5.5.3).

Optimized batch of PLGA-ETH nanoparticles contained 44.26 mg ETH in 446.1 mg of nanoparticles.

So, 1.50 mg equivalent nanoparticles were  $(446.1 \times 1.5) / 44.26 = 15.1542$  mg.

EP-DPI 2 contained the proportion of nanoparticles-lactose =1:1. Hence, equivalent DPI was  $15.1542 \times 2 = 30.31$  mg.

As modified DPI delivery device was able to deliver 98.25 % of its content, corrected delivery DPI dose was  $(30.31 \times 100) / 98.25 = 30.84824 \approx 30.85$  mg. Similar calculation was followed in rest of rat and the data is given in Table 6.19.

**Table 6. 19: Dose administration of EP-DPI2 in rat**

Animal treated with DPI Study 1 (S1)				Animal treated with DPI Study 2 (S2)				Animal treated with DPI Study 3 (S3)			
Animal code	Rat Weight (Kg)	Dose of ETH (mg)	Equi. Weight of DPI (mg)	Animal code	Rat Weight (Kg)	Dose of ETH (mg)	Equi. Weight of DPI (mg)	Animal code	Rat Weight (Kg)	Dose of ETH (mg)	Equi. Weight of DPI (mg)
F1	0.235	1.503	30.85	M1	0.23	1.472	30.19	F1	0.231	1.478	30.32
M2	0.22	1.408	28.88	M2	0.226	1.445	29.67	F2	0.223	1.426	29.27
F3	0.224	1.433	29.40	M3	0.228	1.458	29.93	M3	0.226	1.445	29.67
F6	0.227	1.452	29.80	F6	0.22	1.408	28.88	M6	0.22	1.408	28.88
M12	0.224	1.433	29.40	F12	0.222	1.420	29.14	M12	0.232	1.484	30.45

M24	0.226	1.445	29.67	F24	0.231	1.477	30.32	M24	0.231	1.478	30.32
-----	-------	-------	-------	-----	-------	-------	-------	-----	-------	-------	-------

<sup>a</sup>Animal code was divided in two parts: First digit stand for the sex of rat, last numerical digit denote the time of sacrificing after dose administration

Similar calculation was done for the rats those treated with DPI containing pure ETH. Dose equivalents of DPI for individual rats are shown in Table 6.20.

Considering rat weight (S1M1) as 0.234 kg, the equivalent ETH dose is 1.497 mg. Optimized DPI batch of pure ETH contained drug-Lactose ratio of 1:5 (EL-DPI5).

Hence, equivalent DPI was  $1.497 \times 6 = 8.983$  mg.

As modified DPI delivery device was able to deliver 98.25 % of its content, corrected delivery DPI dose was  $(8.983 \times 100) / 98.25 = 9.14$  mg. Similar calculation was followed in rest of rat and the data is given in Table 6.20.

**Table 6. 20: Dose administration of EL-DPI5 containing pure ETH in rat**

Animal treated with DPI Study 1 (S1)				Animal treated with DPI Study 2 (S2)				Animal treated with DPI Study 3 (S3)			
Animal code	Rat Weight (Kg)	Dose of ETH (mg)	Equi. Weight of DPI (mg)	Animal code	Rat Weight (Kg)	Dose of ETH (mg)	Equi. Weight of DPI (mg)	Animal code	Rat Weight (Kg)	Dose of ETH (mg)	Equi. Weight of DPI (mg)
M1	0.234	1.497	9.14	F1	0.23	1.471	8.99	F1	0.234	1.497	9.14
M2	0.238	1.523	9.30	M2	0.236	1.509	9.22	F2	0.243	1.554	9.49
F3	0.244	1.561	9.53	M3	0.228	1.458	8.91	F3	0.229	1.465	8.95
F6	0.227	1.452	8.87	M6	0.239	1.529	9.34	M6	0.239	1.529	9.34
M12	0.229	1.465	8.95	F12	0.242	1.548	9.46	M12	0.231	1.478	9.03
F24	0.236	1.509	9.22	F24	0.232	1.484	9.06	M24	0.236	1.509	9.22

#### 6.3.4.2. Pharmacokinetic analysis

A novel delivery of DPI containing ETH nanoparticles to the rat's lungs by pulmonary administration was studied. Two different studies were carried out to demonstrate lung's tissue distribution and bio-distribution of Ethionamide at specific time interval. ETH concentration reached  $4.621 \pm 0.36$   $\mu\text{g/ml}$  ( $C_{\text{max}}$ ) at  $T_{\text{max}}$  of 1 hr in lungs tissue when given in pure form (EL-DPI 5). Maximum concentration reached by EP-DPI2 was  $2.64 \pm 0.07$   $\mu\text{g/ml}$  ( $C_{\text{max}}$ ) at  $T_{\text{max}}$  1 hr in lung's tissue (Table 6. 21).

**Table 6. 21: Lung's tissue and plasma distribution of ETH from DPI**

Lung's tissue distribution study				
Time (hr)	EP-DPI 2 containing ETH nanoparticles		EL-DPI 5 containing pure ETH	
	ETH amount in lung's tissue <sup>‡</sup> (µg)	ETH concentration <sup>‡</sup> (µg/ml)	ETH amount in lung's tissue <sup>‡</sup> (µg)	ETH concentration <sup>‡</sup> (µg/ml)
1	22.7002 ± 0.62	2.64 ± 0.07	39.75 ± 3.12	4.62 ± 0.36
2	19.8784 ± 1.18	2.31 ± 0.14	18.68 ± 0.78	2.17 ± 0.09
3	17.2603 ± 0.29	2.01 ± 0.03	5.91 ± 0.53	0.69 ± 0.06
6	13.8837 ± 0.42	1.61 ± 0.05	1.40 ± 0.23	0.16 ± 0.03
12	08.2751 ± 0.47	0.96 ± 0.05	-	-
24	03.3517 ± 0.67	0.39 ± 0.08	-	-
Plasma distribution study				
Time (hr)	EP-DPI 2 containing ETH nanoparticles		EL-DPI 5 containing pure ETH	
	ETH amount in plasma <sup>‡</sup> (µg)	ETH concentration <sup>‡</sup> (µg/ml)	ETH amount in plasma <sup>‡</sup> (µg)	ETH concentration <sup>‡</sup> (µg/ml)
1	11.43 ± 0.365	0.0518 ± 0.0005	79.166 ± 2.28	0.36 ± 0.003
2	11.15 ± 0.865	0.0548 ± 0.0056	24.300 ± 0.67	0.12 ± 0.001
3	11.13 ± 0.195	0.0532 ± 0.0016	7.549 ± 0.63	0.04 ± 0.004
6	10.80 ± 0.431	0.05344 ± 0.0039	0.429 ± 0.17	0.002 ± 0.001
12	10.74 ± 0.389	0.0514 ± 0.0020	-	-
24	2.78 ± 0.617	0.0129 ± 0.0027	-	-

<sup>‡</sup>Values are mean of three data ± standard deviation

AUC<sub>0-∞</sub> was high when ETH was administered in nanoparticles form. Similarly in plasma, residency of ETH was high in the nanoparticles form. No ETH was detected in lungs and plasma after 6 hr of administration of ETH in free form (Table 6. 22).

**Table 6. 22: Pharmacokinetic evaluation**

Pharmacokinetic parameters of ETH in lung's tissue			
DPI containing	C <sub>max</sub> (µg/ml)	T <sub>max</sub> (hr)	AUC (µg hr/ml)
ETH –PLGA nanoparticles	2.639±0.07	1	28.634±0.58
Pure ETH	4.621±0.36	1	9.00±0.48
Pharmacokinetic parameters of ETH in plasma			
DPI containing	C <sub>max</sub> (µg/ml)	T <sub>max</sub> (hr)	AUC (µg hr/ml)
ETH nanoparticles	0.055 ± 0.006	2	1.039 ± 0.031
Pure ETH	0.36 ± 0.003	1	0.497 ± 0.106



Area under the concentration-time curve from zero to infinity time ( $AUC_{0-\infty}$ ) signifies the prolong residency of ETH in body compartment, when given in the nanoparticles form (Figure 6. 11).

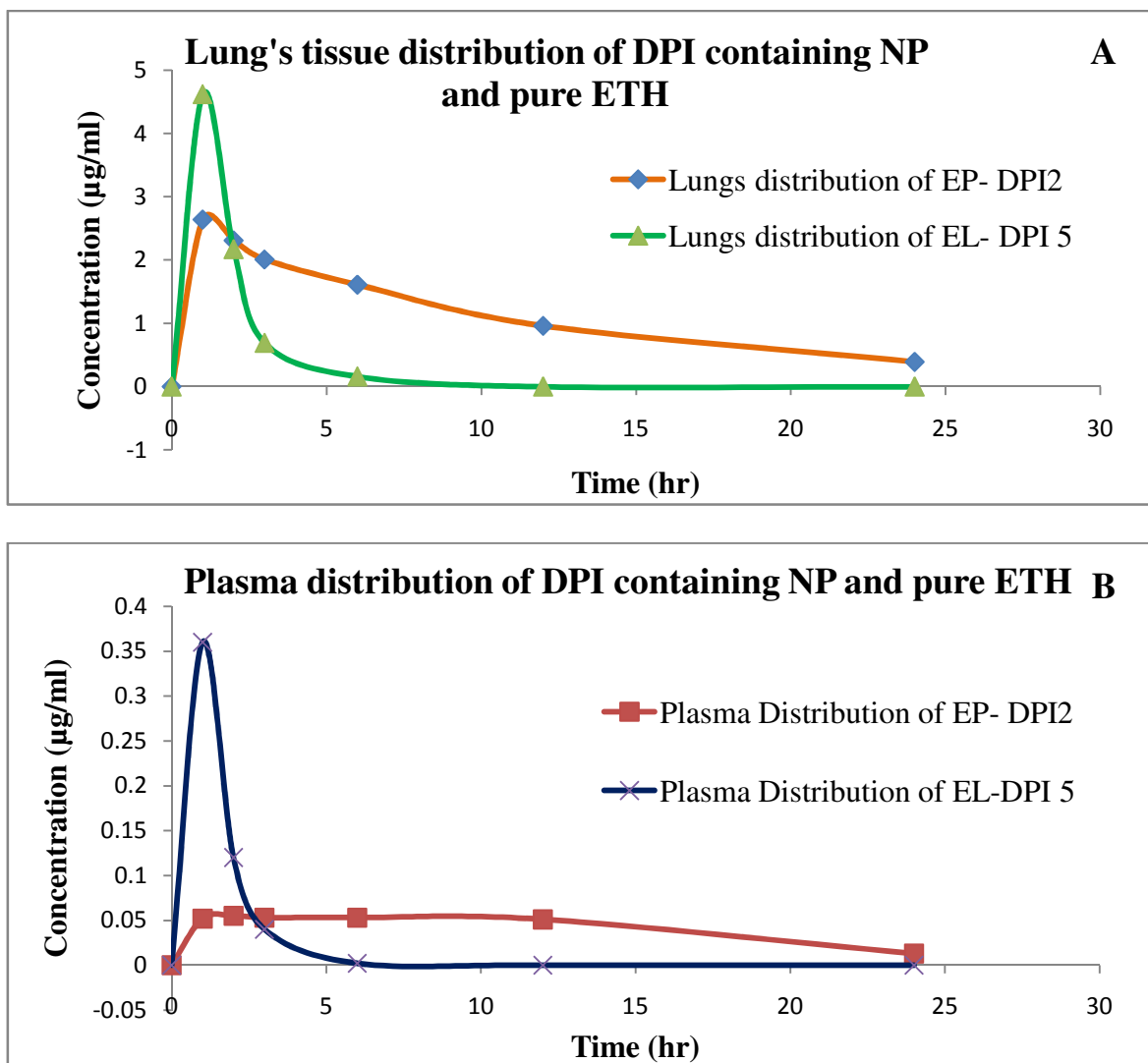


**Figure 6. 11: Lungs (A) & plasma (B) distribution of EP-DPI2 & EL-DPI5**

One way ANOVA was applied here to meet the statistical significance and found  $p$  value less than 0.05 in case of ETH nanoparticles administration. Standard error mean values in all the cases were found to be in the acceptable range except *in-vivo* percentage drug release. This mainly happened due to varying dose administration according to body weight of rats. ETH concentration in lungs at 24 hr was  $0.39 \pm 0.08$   $\mu\text{g/ml}$ . Although this concentration did not reach the MIC, daily dose administration will help to maintain the concentration of ETH above MIC in lungs. Generally 250 mg of ETH tablet for 2 times a day maintain the plasma concentration above MIC for 12 hr. Whereas, EP-DPI2 maintained ETH concentration above MIC for more than 12 hr with lesser than single

dose. Also, the data suggested the localization of ETH in the lung's tissue and prevent its distribution in the plasma. This will be helpful to treat the pulmonary tuberculosis more efficiently. In previous reported article, Ethionamide nanoparticles were administered through the oral route [8]. Hence gastrointestinal side effect cannot be overcome using this formulation.

#### 6.3.4.3. *In-vivo-in vitro* correlation of EP-DPI2

*In vitro* drug release was compared with *in vivo* drug absorbed for EP-DPI2 to establish the IVIVC. *In vitro* percentage drug release was kept in the X-axis and *in vivo* drug absorption was kept in the Y-axis (table 6. 23). Good correlation coefficient of 0.999 was established (Figure 6. 12)

**Table 6. 23: IVIVC of DPI containing ETH-PLGA (50:50) nanoparticles**

Time (hr)	<i>In vitro</i> percentage drug release	<i>In vivo</i> percentage drug absorbed
1	9.23	9.25
2	12.02	11.68
3	14.06	15.84
6	22.24	23.74
12	52.37	53.83
24	95.17	98.45

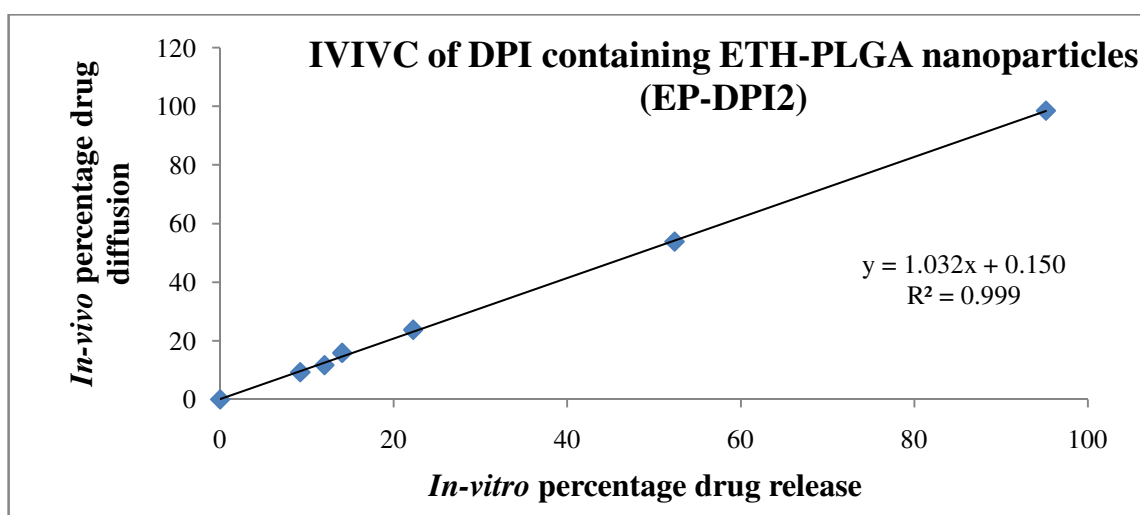


**Figure 6. 12: IVIVC of EP-DPI2**

**6.3.5. *In-vitro* anti tubercular activity**

Absorbance and percentage cell viability are shown in table 6.24. Pure Ethionamide showed the MIC value of 0.5 µg/ml, whereas ETH loaded nanoparticles showed 0.6 µg/ml. Hence, in the form of nanoparticles, drug showed anti-tubercular activity.

**Table 6. 24: Absorbance and cell viability of Ethionamide in MTT assay**

<b>Pure Ethionamide</b>				
<b>Conc. (µg/ml)</b>	<b>0.4</b>	<b>0.5</b>	<b>0.6</b>	<b>0.7</b>
<b>Average absorbance</b>	0.104033	0.077333	0.0736	---
<b>SD</b>	0.021076	0.004726	0.005597	---
<b>% Viability</b>	1.209147	-0.98706	-1.29414	---
<b>SD</b>	1.733615	0.388721	0.460407	---
<b>ETH loaded nanoparticles</b>				
<b>Conc. (µg/ml)</b>	<b>0.4</b>	<b>0.5</b>	<b>0.6</b>	<b>0.7</b>
<b>Average absorbance</b>	0.294867	0.098467	0.0786	0.072867
<b>SD</b>	0.03996	0.015179	0.002848	0.005284
<b>% Viability</b>	16.90612	0.751261	-0.88287	-1.35446
<b>SD</b>	3.286927	1.24855	0.234246	0.434656

## **CHAPTER 7: Summary and Conclusion**

### **7.1. Summary of the work**

Tuberculosis can attack any organ system in the body. While pulmonary tuberculosis is the most common one [219]. In recorded history, Hippocrates writes about patients with wasting away associated with chest pain and coughing, frequently with blood in sputum. These symptoms allowed Hippocrates to diagnose TB, which at that time was called “consumption”. The frequency of descriptions of patients with these symptoms indicated that the disease was already well entrenched in ancient times [45]. In the treatment of tuberculosis, first line and second line drugs are available in the market. Drugs like Kanamycin, Amikacin, Capreomycin and different types of fluoroquinolones are available in injectable form and rest of other second line ATDs are available for oral administration. The treatment of tuberculosis continues for several months to years. Hence, patient incompliance rises with injectable drug in long term therapy [9]. Along with, only a small fraction of the anti-tubercular drugs reach alveoli from oral administration in the treatment of pulmonary tuberculosis. Concurrently, this small fraction is cleared rapidly due to short biological half life. On the other hand, drug resistance cases are the ultimate challenge of clinician due to patient incompliance, missed up dose etc. In that situation first line drugs fail to treat this disease and further treatment continues with second line anti-tubercular drug.

The aims of the present investigations were to design and develop of nanoparticles of second line anti-tubercular drug to sustain the release of drug from nanoparticles and target the nanoparticles in the form of dry powder inhaler to lungs through pulmonary route.

#### **7.1.1. With respect to PP-DPI 2 contained PTH-PLGA nanoparticles**

FTIR study confirmed no interaction between the drug and other ingredients in their physical mixture. Prothionamide loaded PLGA nanoparticles optimized through Box

Behnken Design and optimized nanoparticles contained 25 mg of PTH, 125 mg of PLGA, 0.36 % PVA and 2 ml of DCM volume. Particle size and percentage drug entrapment influenced significantly with the changes of particle size, organic phase volume, and surfactant concentration. Optimized nanoparticles showed spherical shape particle size of 205.6 nm under Scanning Electron Microscopy. Residual solvent study was conducted and found to be 0.11 ppm of DCM in optimized nanoparticles; That confirmed the nanoparticles are safe for human as per ICH guideline [193]. DSC thermograph showed the change in physical form of PTH without changing the melting point. Optimized nanoparticles were modified into dry powder inhaler (PP-DPI 2) to make suitable for pulmonary administration. PP-DPI 2 showed MMAD value of 1.69  $\mu\text{m}$  with geometric standard deviation of 1.95. *In-vitro* release study in simulated lungs fluids showed  $43.52 \pm 0.81$  % release in 24 hr and followed zero order kinetics. Stability study revealed no clumping or aggregation of particles for 6 months. Modified DPI delivery device [132] was able to deliver  $98.77 \pm 0.076$  % DPI. After considering this value, DPI dose of individual rat was calculated and administered to pre-anaesthetized rat [178]. Drug retention in lungs and plasma was increased (more than 24 hr) in the form of nanoparticles (PP-DPI 2) in comparison with pure Prothionamide. PP-DPI 2 was able to maintain PTH concentration above MIC for 6 hr, whereas pure PTH was able to maintain for 3 hr. No PTH was detected at lungs after 12 hr of PL-DPI4 (DPI contained pure PTH) administration.

#### 7.1.2. With respect to PC-DPI 4 contained PTH-Chitosan nanoparticles

To maintain the PTH concentration for more than 6 hr at lungs, new nano-formulation of PTH was prepared using alternate biodegradable polymer like Chitosan. Optimized Chitosan nanoparticles of PTH showed more or less spherical shape. In DSC analysis, PTH melting point peak was detected in nanoparticles but shifted to lower temperature due to conversion of amorphous form. Optimized DPI (PC-DPI 4) showed MMAD value of 1.76  $\mu\text{m}$  with geometric standard deviation of 1.96. *In-vitro* release of PC-DPI 4 showed initial burst release of  $22.04 \pm 1.94$  % in 1 hr followed Korsmeyer-Peppas kinetic release of  $96.91 \pm 0.91$  % in 24 hr. By *In-vivo*; PC-DPI 4 gave sustain release and showed  $C_{\text{max}}$  of  $4.56 \pm 0.31 \mu\text{g/ml}$  at  $T_{\text{max}}$  of 1 hr in lungs. AUC was increased significantly, when PTH was given in the form of nanoparticles due to prolong residency of PTH at lungs. PC-DPI4 maintained plasma concentration above the MIC for more than 12hr, whereas pure PTH could maintain up to 3hr.

### 7.1.3. With respect to EP-DPI 2 contained ETH-PLGA (50:50) nanoparticles

Ethionamide nanoparticles were prepared using PLGA (50:50) by emulsion solvent evaporation technique. Optimized PLGA-ETH nanoparticles (EPS1) were prepared with 1:4 ratio of ETH-PLGA (50:50), 0.5 % w/v PVA. Optimized nanoparticles showed z-average value, zeta potential and PDI as  $225.7 \pm 6.4$  nm,  $-6.9 \pm 1.24$  mV, and  $0.216 \pm 0.011$  respectively. Residual solvent analysis study showed the presence of acetone in the concentration of 0.65 ppm in EPS1, but this amount will not create any problem in human. Second solvent DCM is not detected in this study which confirmed complete removal of DCM in the preparation of nanoparticles. Endothermic peak of Ethionamide (DSC) was broadened and shifted to lower temperature due to incorporation of PVA. This Optimized nanoparticles were further modified into DPI. Optimized DPI (EP-DPI2) showed aerodynamic particles size of  $1.79 \mu\text{m}$  with geometric standard deviation of 1.71. *In-vitro* drug release-time profile of this DPI followed zero order kinetic with highest correlation co-efficient ( $R^2$ ) of 0.992 in comparison to Higuchi, Peppas models with  $R^2$  of 0.930 and 0.949 respectively. There were no significant changes occurred in the physical properties of nanoparticles during 6 month storage period as per ICH guideline. In the form of DPI, nanoparticles showed initial burst release of  $9.23 \pm 1.15\%$  in first 1 hr and continued to release up to  $95.17 \pm 3.59\%$  in 24 hr. This initial burst release helped to reach the ETH concentration ( $C_{\text{max}}$ ) to  $2.639 \pm 0.07 \mu\text{g/ml}$  at 1 hr ( $T_{\text{max}}$ ) in lungs. ETH residency detected at 24 hr in lungs and plasma.

## 7.2. Achievements with respect to the objectives

Different excipients, process, surfactant etc. were screened and statistically analyzed for proper selection. By selecting pulmonary route, drug targeting to lungs was achieved and also overcome the problems associated with oral administered drugs. By the use of biodegradable polymer like PLGA (75:25), PLGA (50:50) and Chitosan drug release of Prothionamide and Ethionamide were controlled. This polymer successfully targeted the drug to lungs in the form of dry powder inhaler and sustained the drug release for prolong period of time at lungs. Here, PLGA (50:50) and Chitosan delivered more than 95 % of its content in 24 hr. Optimized DPIs (PP-DPI 4 & EP-DPI 2) are able to maintain the drug concentration above MIC for more than 12 hr. Thus it could be concluded that the developed formulation has the potential to reach the target site of lungs in the form of DPI

and increase the drug retention at lungs for more than 24 hr. Not only drug retention, DPIs are able to maintain the drug concentration above MIC for more than 12 hr.

### **7.3. Major contribution and practical implications of the work to society**

Tuberculosis is a deadly disease that has been around for thousands of years. It is a bacterial disease that infects the lungs and may spread to other parts of the body. It has been plaguing humankind for thousands of years and still is one of the lethal infectious diseases in the world [220].

Extensive literature review was done to identify the challenges associated with the management of tuberculosis. Many researchers have worked on development of modified dosage form of anti-tubercular drugs. But drug resistance, multi-drug resistance makes the treatment regimen more complicated. This resistance mainly occur in the first line ATD. In this situation, second line drugs are the only possible medicine to treat tuberculosis. But due to short biological half life, these drugs get eliminated rapidly from systemic circulation resulting in repeated administration with high dose. Apart from this, high dose of ATD increase the chances of drug induce liver injury, systemic toxicity and excessive GI problems. These problems increase the chances of patient incompliance, missed up dose etc. Due to these problems, idea was taken to develop nanoparticles of second line anti-tubercular drugs like Prothionamide and Ethionamide and target them in the form of dry powder inhaler to lungs through pulmonary route for sustained effect. Moreover, the formulations reduce the dose and dosing frequency and are convenient to administer in DPI form. These DPI formulations are cost effective and patient compliance as it is non-invasive delivery. Formulation techniques adopted here are feasible for industrial scale. These developed formulation demand good scope for commercialization after go through of clinical trials and fulfilment of other regulatory requirements. PTH and ETH are not listed in first line drug due to their severe side effect like metabolic taste and abdominal pain. With the help of this modified dosage form, these drugs can be proposed as first line drug to WHO.

### **7.4. Recommendation for future research**

The present investigation on development of Nanoparticulate drug delivery for pulmonary administration involves the use of single anti-tubercular drug. Optimized dosage form

maintained drug concentration above minimum inhibitory concentration for more than 12 hr. This work carried out on rats. In future, work can be clinical trialled with help of CRO centre.

### **7.5. Conclusion**

With the present investigation, it may be concluded that nanoparticles of Prothionamide were successfully developed using chitosan nanoparticles using ionic gelation technique and Ethionamide nanoparticles were prepared by emulsion solvent evaporation method using PLGA (50:50). Optimized nanoparticles were further modified into dry powder inhaler. Pulmonary administration of the optimized DPI showed efficiency to target the drug in lungs. This DPI would able to maintain drug concentration above MIC for more than 12 hr. Twice a day or daily basis administration may maintain the drug concentration above MIC for 24 hr. Along with, it also can be concluded that the developed formulation has the potency to increase drug residency in lungs for more than 24 hr. These formulations reduce dose and dosing frequency, concurrently increase the patient compliance. Hence, these developed formulations have the promising potential to manage tuberculosis that can be confirmed through clinical trials.



## References

1. Vannelli TA, Dykman A, Montellano O, Paul R, (2002) Enzyme catalysis and regulation: The antituberculosis drug ethionamide is activated by a flavoprotein monooxygenase. *J Biol Chem.* 277(15),12824–9.
2. WHO, (2015) Tuberculosis control in the south east asia region annual TB report 2014 [Internet]. World Health Organization. 2015. p. 1–198.
3. Medina G, Chapman PT, (1965) Treatment with Ethionamide in various drug combination. *Drug Resist Pulm Tuberc.* 47(2),146–52.
4. Hallbauer UM, Schaaf HS, (2011) Ethionamide-induced hypothyroidism in children. *South Afr J Epidemiol Infect.* 26(3),161–3.
5. Conte JE, Golden JA, Quitty MMC, Kipps J, Lin ET, Zurlinden E, (2000) Effects of AIDS and gender on steady-state plasma and intrapulmonary Ethionamide concentrations. *Antimicrob Agents Chemother.* 44(5),1337–41.
6. Bijev A, Georgieva M, (2010) The development of new tuberculostatics addressing the return of tuberculosis: Current status and trends. *J Univ Chem Technol Metall.* 45(2),111–26.
7. Hari BNV, Chitra KP, Bhimavarapu R, Karunakaran P, Muthukrishnan N, Rani BS, (2010) Novel technologies: A weapon against tuberculosis. *Indian J Pharmacol.* 42(6),338–44.
8. Kumar G, Sharma S, Shafiq N, Pandhi P, Khuller GK, Malhotra S, (2011) Pharmacokinetics and tissue distribution studies of orally administered nanoparticles encapsulated ethionamide used as potential drug delivery system in management of multi-drug resistant tuberculosis. *Drug Deliv.* 18(1),65–73.
9. Lee JK, Cho WH, Bae JW, Kim YU, Park G Bin, Yuk SH, Lee D, Khang G, (2012) Improvement of Prothionamide dissolution by solid dispersion with complex polymer. *Int J Tissue Regen.* 3(1),28–33.
10. Venkatesan K, (1989) Clinical pharmacokinetic considerations in the treatment of patients with leprosy. *Clin Pharmacokinet.* 16,365–86.
11. Kshirsagar N, Kirodian B, (2002) Liposomal drug delivery systme from laboratory to patiensts: Our experience. *Proc Indian Natl Sci Acad.* 68(4),333–48.
12. Vij N, Min T, Marasigan R, Belcher CN, Mazur S, Ding H, Yong K, Roy I, (2010) Development of PEGylated PLGA nanoparticle for controlled and sustained drug delivery in cystic fibrosis. *J Nanobiotechnology.* 8(22),1–18.
13. Dim N, (2011) Nanomedicine for tuberculosis : Insights from animal models. *Int J Nano Dimens.* 2(1),67–84.
14. Pandey R, Khuller GK, (2005) Antitubercular inhaled therapy: opportunities, progress and challenges. *J Antimicrob Chemother.* 55(4),430–5.
15. Kaur S, Rao R, Hussain A, Khatkar S, (2011) Preparation and characterization of Rivastigmine loaded Chitosan nanoparticles. *J Pharm Sci Res.* 3(5),1227–32.
16. Anbarasan B, Menon V V, Niranjana VA, Ramaprabhu S, (2013) Optimization of the formulation and in-vitro evaluation of Chloroquine loaded chitosan nanoparticles using ionic gelation method. *J Chem Pharm Sci.* 6(2),106–12.

17. Ilyas A, Islam M, Asghar W, Menon J, Wadajkar AS, Nguyen KT, Iqbal SM, Member S, Poly A, (2013) Salt-Leaching synthesis of porous PLGA nanoparticles. *Nanotechnology*. 12(6),1082–8.
18. Semete B, Booysen L, Lemmer Y, Kalombo L, Katata L, Verschoor J, Swai HS, (2010) In vivo evaluation of the biodistribution and safety of PLGA nanoparticles as drug delivery systems. *Nanomedicine Nanotechnology, Biol Med*. 6(5),662–71.
19. Stevanovi M, Uskokovi D, (2009) Poly(lactide-co-glycolide ) based micro and nanoparticles for the controlled drug delivery of vitamins. *Curr Nanosci*. 5(1),1–15.
20. Ivanova EP, Kateryna B, Roy JC, (2014) Natural polymer biomaterials: advanced applications. In: *New Functional Biomaterials for Medicine and Healthcare*. 2014. p. 32–70.
21. Patel B, Chakraborty S, (2013) Biodegradable polymers: Emerging excipients for the pharmaceutical and medical device industries . *J Exp Food Chem*. 4(4),126–57.
22. Fattahi P, Borhan A, Abidian MR, (2013) Characterization of the size, shape, and drug encapsulation efficiency of PLGA microcapsules produced via electrojetting for drug delivery to brain tumors. In: *6th annual international IEEE EMBS conference on neural engineering*. 2013. p. 953–6.
23. Danhier F, Ansorena E, Silva JM, Coco R, Le A, Préat V, (2012) PLGA-based nanoparticles: An overview of biomedical applications. *J Control Release*. 30(1),1–18.
24. Soni A, Gadad A, Dandagi P, Mastiholmath V, (2011) Simvastatin-loaded PLGA nanoparticles for improved oral bioavailability and sustained release: Effect of formulation variables. *Asian J Pharm*. 2,57–64.
25. Muthu M, (2009) Nanoparticles based on PLGA and its co-Polymer: An overview. *Asian J Pharm*. 3(4),266–73.
26. Mainardes RM, Evangelista RC, (2005) PLGA nanoparticles containing praziquantel: Effect of formulation variables on size distribution. *Int J Pharm*. 290,137–44.
27. Wang YJ, Strohm EM, Kolios MC, Pfh AP, Preparation P, (2014) In vitro study of PLGA / PFH particles loaded with gold nanoparticles as theranostic agents for photoacoustic imaging and cancer therapy. In: *IEEE International Ultrasonics Symposium Processing*. 2014. p. 1658–61.
28. Tan Q, Liu W, Guo C, Zhai G, (2011) Preparation and evaluation of quercetin-loaded lecithin-chitosan nanoparticles for topical delivery. *Int J Nanomedicine*. 6,1621–30.
29. Agnihotri SA, Mallikarjuna NN, Aminabhavi TM, (2004) Recent advances on chitosan-based micro and nanoparticles in drug delivery. *J Control Release*. 100,5–28.
30. Morris GA, Kok MS, Harding SE, Adams GG, (2010) Polysaccharide drug delivery systems based on pectin and chitosan. *Biotechnol Genet Eng Rev*. 27,257–84.
31. Subbiah R, Ramalingam P, Ramasundaram S, Yang D, Park K, Ramasamy MK, Jin K, (2012) N, N, N-Trimethyl chitosan nanoparticles for controlled intranasal delivery of HBV surface antigen. *Carbohydr Polym*. 89(4),1289–97.
32. Hao C, Wang W, Wang S, Zhang L, Guo Y, (2017) An overview of the protective effects of chitosan and acetylated chitosan oligosaccharides against neuronal disorders. *Mar Drugs*. 15(89),1–15.
33. KaswanDeepak, Kumar MS, Mahadevan N, (2012) Thiolated chitosan: Modified advanced generation of mucoadhesive polymer. *Int J Recent Adv Pharm Res*. 2(3),31–41.
34. Sharma S, Khuller GK, Garg SK, (2003) Alginate-based oral drug delivery system for tuberculosis: Pharmacokinetics and therapeutic effects. *J Antimicrob Chemother*. 51,931–8.
35. Kumar N, Kumar P, Kumar P, Kumar M, Kumar R, (2011) Nanotechnology: A focus on treatment of

- tuberculosis. *Int J Drug Deliv.* 3(1),25–42.
36. Zhang P-R, Xie Y, Li M, (2011) Preparation and characterization of budesonide-loaded solid lipid nanoparticles for pulmonary delivery. *J Chinese Pharm Sci.* 20(4),390–6.
  37. Umaretiya, M G, Patel RP, Patel KJ, (2011) Formulation and Characterization of solid lipid nanoparticles dry powder inhaler containing Triamcinolone acetonide. *Int J Res Pharm Chem.* 1(3),662–73.
  38. Nasiruddin M, Neyaz MK, Das S, (2017) Nanotechnology-Based approach in tuberculosis treatment. *Tuberc Res Treat.* 2017(1),1–12.
  39. Shegokar R, Al SL, Mitri K, (2011) Present status tuberculosis of nanoparticle for treatment of tuberculosis. *J Pharmacepy Pharm Sci.* 14(1),100–16.
  40. Lemmer Y, Semete B, Booysen L, Kalombo L, Jones AT, Khati M, Swai HS, Verschoor JA, (2010) Targeted nanodrug delivery systems for the treatment of tuberculosis. *Drug Discov Today.* 15(23),1098.
  41. Pandey R, Khuller GK, (2006) Nanotechnology based drug delivery system(s) for the management of tuberculosis. *Indian J Exp Biol.* 44(5),357–66.
  42. Burkitt HG, Quick CRG, Reed JB, (2007) Essential surgery: Problems, diagnosis and management. Churchill Livingstone Elsevier; 2007. 793 p.
  43. Symptoms of TB | Tiredness, losing weight, fever, cough [Internet]. Tbfacts.org.
  44. (2010) Tuberculosis [Internet]. Wikipedia. 2010. p. 1–9.
  45. Jordao L, Vieira O V, (2011) Tuberculosis: New aspects of an old disease. *Int J Cell Biol.* 1(1),1–13.
  46. Madsen MP, (2012) Development of biodegradable nanoparticle-based therapies against tuberculosis in a zebrafish model. 2012.
  47. Van Boogaard J Den, Kibiki GS, Kisanga ER, Boeree MJ, Aarnoutse RE, (2009) New drugs against tuberculosis: Problems, progress, and evaluation of agents in clinical development. *Antimicrob Agents Chemother.* 53(3),849–62.
  48. Haj K, Ebrahim M, Kobarfard F, Azerang P, (2013) Synthesis and antimycobacterial activity of symmetric Thiocarbohydrazone derivatives against Mycobacterium bovis BCG. *Iran J Pharm Res.* 12(6),331–46.
  49. Calligaro GL, Dheda K, (2013) Drug-resistant tuberculosis. *Contin Med Educ.* 31(9),344–6.
  50. Ongaya VA, Githui WA, Heme H, Kiiyukia C, Juma E, (2012) High Ethionamide resistance in Mycobacterium tuberculosis strains isolated in Kenya. *Afr J Health Sci.* 20(1),37–41.
  51. Mohan A, Kumar PD, Harikrishna J, (2012) Therapeutics. In: Newer anti-TB drugs and drug delivery systems. 2012. p. 388–92.
  52. Tripathi KD, (2008) Essentials of Medical Pharmacology. 6th ed. Tripathi KD, editor. New Delhi, India: Jaypee Brothers Medical Publishers Pvt Ltd; 2008.
  53. Harrison AC, (2003) M . Tuberculosis, TB medicines and monitoring. In: Guidelines for Tuberculosis Control in New Zealand. Auckland; 2003. p. 1–47.
  54. Bartels H, Bartels R, (1998) Simple, rapid and sensitive determination of Protionamide in human serum by high-performance liquid chromatography. *J Chromatogr B.* 707,338–41.
  55. Lee HW, Kim DW, Park JH, Kim S, Lim M, Phapale PB, Kim E, Park SK, Yoon Y, (2009)

- Pharmacokinetics of Prothionamide in patients with multidrug-resistant tuberculosis. *Int J Tuberc Lungs Dis.* 13(9),1161–6.
56. Garcia-prats PAJ, Donald PR, Hesselning AC, Schaaf HS, (2013) Second-line antituberculosis drugs in children : A commissioned review for the World Health Organization 19th expert committee on the selection and use of essential medicines. WHO. 2013. p. 1–105.
  57. Shim TS, Jo KW, (2013) Medical treatment of pulmonary multidrug-resistant tuberculosis. *Infect Chemother.* 45(4),367–74.
  58. Kumar PM, Sreeramulu J, (2011) Development and validation of a stability- indicating reversed-phase high performance liquid chromatography method for assay of Prothionamide in pure and pharmaceutical dosage form. *Int J ChemTech Res.* 3(1),321–8.
  59. Chemwatch, (2010) Prothionamide- Chemical product and company identification [Internet]. 2010. p. 1–7.
  60. Pharmacopoeia J, (2014) Prothionamide [Internet]. 17th ed. Tokyo, Japan: Japanese Pharmacopoeia; 2014. 720 p.
  61. Chemicalize, (2014) Basic properties of Prothionamide [Internet]. 2014. p. 1.
  62. Drugupdate, (2014) Prothionamide drug information from drugs update [Internet]. Solution of Health Care Professional. 2014. p. 1–8.
  63. Trivedi V, Upadhyay V, Shah G, Yadav M, Shrivastav PS, Sanyal M, (2013) Ex vivo conversion of prodrug prothionamide to its metabolite prothionamide sulfoxide with different extraction techniques and their estimation in human plasma by LC-MS/MS. *Bioanalysis.* 5(2),185–200.
  64. Druginfosystem, (2014) Prothionamide: Drug monograph from drug Info Sys.com [Internet]. System Drug Information. 2014. p. 1–4.
  65. Zhang Z, Sun Z, Wang Z, Hu H, Wen Z, Song Y, Zhao J, Wang H, Guo X, (2012) Identification and pathogenicity analysis of a novel non-tuberculous mycobacterium clinical isolate with nine-antibiotic resistance. *Clin Microbiol Infect.* 19,91–6.
  66. Pattyn S, Loo G, (1980) Combined chemotherapy against Mycobacterium leprae in the mouse. *Ann Soc Belg Med Trop (1920).* 60,291–5.
  67. Matsuo Y, Tatsukawa H, Murray JF, Peters JH, (1981) Prothionamide and Prothionamide-S-Oxide in experimental leprosy. *Int J Lepr.* 49(3),302–6.
  68. Farmaceutici Italia, (1972) 2-ethyl and 2-propyl isonicotinonitrile - intermediates for Ethionamide and Prothionamide [Internet]. France; FR2091338 (A5), 1972. p. 1–8.
  69. Cherenko Svitlana Oleksandrivna, (2012) Method for treating tuberculosis of lungs with the advanced resistance of mycobacteria towards antituberculous drugs within intensive phase of chemotherapy [Internet]. European Patent Office; 2012. p. 1.
  70. European Patent Office, Espacenet - Prothionamide [Internet].
  71. Arbex MA, Varella MCL, Siqueira HR, Mello FAF, (2010) Antituberculosis drugs: Drug interactions, adverse effects, and use in special situations. Part2: Second-line drugs. *J Bras Pneumol.* 36(5),641–56.
  72. Ahmad M, Madni AU, Usman M, (2009) In-vitro release and pharmacokinetics of anti-tubercle drug Ethionamide in healthy male subjects. *J Bioanal Biomed.* 1(1),46–9.
  73. Goel A, Singh S, Sati J, Tewari U, (2011) Pharmacokinetic, solubility and dissolution profile of leprotic drug. *Int J Pharma Prof Res.* 2(1),242–6.

- 
74. Auclair B, Nix DE, Adam RD, James GT, Peloquin CA, (2001) Pharmacokinetics of Ethionamide administered under fasting conditions or with orange juice, food, or antacids. *Antimicrob Agents Chemother.* 45(3),810–4.
75. Neurolex, (2014) Ethionamide [Internet]. The Neuroscience Neurol. 2014. p. 1–6.
76. Pharmacopoeia E, (2005) Ethionamidum. 5th ed. Strasbourg, France: European Pharmacopoeia; 2005. 1551 p.
77. Inchem, (2015) Ethionamide (PIM 224) [Internet]. 2015. p. 1–3.
78. Chemicalize, (2011) Ethionamide [Internet]. 2011. p. 1–6.
79. MSDS, Ethionamide [Internet]. National Library of Medicine HSDB Database.
80. (2013) Ethionamide (DB00609) [Internet]. Drug Bank. 2013. p. 3–7.
81. Palmer AL, Leykam VL, Larkin A, Krueger SK, Phillips IR, Shephard E a, Williams DE, (2012) Metabolism and pharmacokinetics of the anti-tuberculosis drug ethionamide in a flavin-containing monooxygenase null mouse. *Pharmaceuticals (Basel)*. 5(11),1147–59.
82. Somaraju V, (2003) Drugs used in tuberculosis and leprosy. In: Modern Pharmacology with Clinical application. 2003. p. 557–66.
83. Index M, (2008) Ethionamide. *Tuberculosis*. 88(2),106–8.
84. Vannelli TA, Dykman A, Montellano PRO De, (2002) The antituberculosis drug Ethionamide ss activated by a flavoprotein monooxygenase. *J Biol Chem*. 277(15),12824–9.
85. Organization WH, (2007) Quality assurance of pharmaceuticals [Internet]. Vol. 2, WHO Expert Committee on Specifications for Pharmaceutical Preparations. Thirty-sixth report. Geneva. 2007. 17-57 p.
86. United State, (2010) USP monographs: Ethionamide [Internet]. Rockville, USA: United State Pharmacopoeia; 2010. p. 711.
87. Walash MI, Metwally MES, Abdelal AA, (2004) Fluorimetric determination of Ethionamide in pharmaceutical preparations and biological fluids. *J Chinese Chem Soc*. 51,1059–64.
88. Peloquin CA, (1991) Improved high-performance liquid chromatographic assay for the determination of Ethionamide in serum. *J Chromatogr*. 563,472–5.
89. Mykhailovych PV, Oleksandrivn CS, Mykhailivn Tsyhankova Liudmyla, Vitaliina PM, (2006) Method for treating patients with cronic tuberculosis of lungs. Ukraine: Ukraine; UA76005 (C2), 2006. p. 1–8.
90. Timmins G, Masters S, Deretic VP, (2013) Rationally improved Isoniazid and Ethionamide derivatives and activity through selective isotopic substitution. United State; US2013150415 (A1), 2013.
91. Deprez B, Willand N, Dirié B, Toto P, Villeret V, Loch C, Baulard A, (2008) Compounds having a potentiating effect on the activity of ethionamide and uses thereof. United State; US2011136823 (A1), 2008. p. 168.
92. Baulard A, Engohang NJ, Frenois F, (2005) Selecting compounds that inhibit the mycobacterial EthR repressor, useful in treatment of tuberculosis and leprosy, improve efficiency of conversion of Ethionamide to its active form [Internet]. France; FR20040004636 20040430, 2005. p. 1–8.
93. Agnihotri J, Saraf S, Khale A, (2011) Targeting: New potential carriers for targetted drug delivery system. *Int J Pharm Sci Rev Res*. 8(2),117–23.
-

94. Singh A, Deep A, (2011) Formulation and evaluation of nanoparticles containing Losartan Potassium. *Int J Pharm Res Technol.* 1(1),17–20.
95. Qadi S Al, Grenha A, Carrion DR, Seijo B, Remunan CL, (2012) Microencapsulated chitosan nanoparticles for pulmonary protein delivery : In vivo evaluation of insulin-loaded formulations. *J Control Release.* 157(3),383–90.
96. Vaculikova E, Grunwaldova V, Kral V, Dohnal J, Jampilek J, (2012) Preparation of Candesartan and Atorvastatin nanoparticles by solvent evaporation. *Molecules.* 17,13221–34.
97. Marin E, Briceno MI, George CC, (2013) Critical evaluation of biodegradable polymers used in nanodrugs. *Int J Nanomedicine.* 8,3071–91.
98. Elmizadeh H, Khanmohammadi M, Ghasemi K, (2013) Preparation and optimization of chitosan nanoparticles and magnetic chitosan nanoparticles as delivery systems using Box – Behnken statistical design. *J Pharm Biomed Anal.* 80,141–6.
99. Ting C, Hao C, Yung Y, Fung M, Lin J, Huang K, (2011) Kinetic study of acid depolymerization of chitosan and effects of low molecular weight chitosan on erythrocyte rouleaux formation. *Carbohydr Res.* 346(1),94–102.
100. Fan W, Yan W, Xu Z, Ni H, (2012) Erythrocytes load of low molecular weight chitosan nanoparticles as a potential vascular drug delivery system. *Colloids Surfaces B Biointerfaces.* 95,258–65.
101. Nadesh R, Narayanan D, Sreerekha PR, Vadakumpully S, Mony U, Koyakkutty M, Nair S V, Menon D, (2013) Hematotoxicological analysis of surface-modified and unmodified chitosan nanoparticles. *J Biomed Mater Res.* A,1–10.
102. Pospiskova K, Safarik I, (2013) Low-cost, easy-to-prepare magnetic chitosan microparticles for enzymes immobilization. *Carbohydr Polym.* 96(2),545–8.
103. Fernandez-carballido A, Barcia E, Cordoba-diaz D, Cordoba-diaz M, (2014) Lisinopril-loaded chitosan nanoparticles and Indapamide in hard gelatine capsules: Simultaneous HPLC quantification. *Curr Pharm Anal.* 10(1),10–9.
104. Nesalin JAJ, Smith AA, (2012) Preparation and evaluation of chitosan nanoparticles containing zidovudine. *Asian J Pharm Sci.* 7(1),80–4.
105. Shan C, Yang H, Han D, Zhang Q, Ivaska A, Niu L, (2010) Graphene/AuNPs/chitosan nanocomposites film for glucose biosensing. *Biosensors Bioelectron.* 25,1070–4.
106. Deng Q, Zhou C, Luo B, (2006) Preparation and characterization of chitosan nanoparticles containing lysozyme. *Pharm Biol.* 44(5),336–42.
107. Zheng Y, Wu YAN, Yang W, Wang C, Fu S, Shen X, (2006) Preparation, characterization, and drug release in vitro of Chitosan-Glycyrrhetic acid nanoparticles. *J Pharm Sci.* 95(1),181–91.
108. Morales-cruz M, Figueroa CM, Gonzalez-robles T, Delgado Y, Molina A, Mendez J, Morales M, Griebenow K, (2014) Activation of caspase-dependent apoptosis by intracellular delivery of cytochrome c-based nanoparticles. *J Nanobiotechnology.* 12(33),1–11.
109. Pirooznia N, Hasannia S, Lotfi AS, Ghanei M, (2012) Encapsulation of Alpha-1 antitrypsin in PLGA nanoparticles: In vitro characterization as an effective aerosol formulation in pulmonary diseases. *J Nanobiotechnology.* 10(20),1–15.
110. Sharma D, Maheshwari D, Philip G, Rana R, Bhatia S, Singh M, et al., (2014) Formulation and optimization of polymeric nanoparticles for intranasal delivery of Lorazepam using Box-Behnken design:in vitro and in vivo evaluation. *Biomed Res Int.* 1,1–14.

111. Chan JM, Zhang L, Yuet KP, Liao G, Rhee J, Langer R, Farokhzad OC, (2009) Biomaterials PLGA–lecithin–PEG core–shell nanoparticles for controlled drug delivery. *Biomaterials*. 30(8),1627–34.
112. Jain DS, Athawale RB, Bajaj AN, Shrikhande SS, Goel PN, Nikam Y, (2014) Unraveling the cytotoxic potential of Temozolomide loaded into PLGA nanoparticles. *DARU J Pharm Sci*. 22(18),1–9.
113. Mozafari M, (2014) Synthesis and characterisation of poly(lactide-co-glycolide) nanospheres using vitamin E emulsifier prepared through one-step oil-in-water emulsion and solvent evaporation techniques. *IET Nanobiotechnol*. 8(4),257–62.
114. Manoochchri S, Darvishi B, Kamalinia G, Amini M, Fallah M, Ostad SN, (2013) Surface modification of PLGA nanoparticles via human serum albumin conjugation for controlled delivery of docetaxel. *DARU J Pharm Sci*. 21(58),1–10.
115. Bhatnagar P, Gupta KC, (2013) Oral administration of Eudragit coated Bromelain encapsulated PLGA nanoparticles for effective delivery of Bromelain for chemotherapy in vivo. In: 2013 29th Southern Biomedical Engineering Conference. Ieee; 2013. p. 47–8.
116. Hussein AS, Ahmadun F-R, Abdullah N, (2013) In vitro degradation of poly (D, L-lactide-co-glycolide) nanoparticles loaded with linamarin. *IET Nanobiotechnology*. 7(2),33–41.
117. Averineni RK, Shavi G V, Gurram AK, Deshpande PB, Arumugam K, Maliyakkal N, Meka SR, Nayanabhirama U, (2012) PLGA 50:50 nanoparticles of paclitaxel: Development, in vitro anti-tumor activity in BT-549 cells and in vivo evaluation. *Bull Mater Sci*. 35(3),319–26.
118. Derakhshandeh K, Hochhaus G, Dadashzadeh S, (2011) In-vitro cellular uptake and transport study of 9-nitrocamptothecin PLGA nanoparticles across caco-2 cell monolayer model. *Iran J Pharm Res*. 10(3),425–34.
119. Bojat V, Balabanyan V, Alyautdin R, (2011) The entrapment of Paclitaxel in PLGA nanoparticles increases its cytotoxicity against multiresistant cell line. *Br J Med Med Res*. 1(4),306–19.
120. Jain S, Mittal A, Jain AK, Mahajan RR, Singh D, (2010) Cyclosporin a loaded PLGA nanoparticle: Preparation, optimization, in-vitro characterization and stability Studies. *Curr Nanosci*. 6(1),422–31.
121. Ramos CS, (2013) Development and validation of a headspace gas chromatographic method for determination of residual solvents in five drug substances. *Int J Pharm Sci Invent*. 2(3),36–41.
122. Manwar J, Mahadik K, Paradkar A, Patil S, Yorkshire-bd W, (2013) Gas chromatography method for the determination of non-ethanol volatile compounds in herbal formulation. *Int J Anal Bioanal Chem*. 3(1),12–7.
123. International, Conferance, Of, Harmonisation, (2011) Impurities: Guideline for residual solvents. Requirements for registration of pharmaceuticals for human use. (October 2002),1–25.
124. Chen J, Yeh M, Chiang C, (2004) Dichloromethane evaporative behavior during the solidifying process of Ovalbumin-Loaded poly (DL lactic-co-glycolic acid ) microparticles. *J Food Drug Anal*. 12(4),291–8.
125. Kim H, Kim D, Yang JS, Kim C, (2006) Sample preparation for headspace GC analysis of residual solvents in Hyaluronic acid derivative fiber. *Bull Korean Chem Soc*. 27(2),302–4.
126. Zhang X, Liu Q, Hu J, Xu L, Tan W, (2014) An aerosol formulation of R-salbutamol sulfate for pulmonary inhalation. *Acta Pharm Sin B*. 4(1),79–85.
127. Telko JM, Hickey AJ, (2005) Dry powder inhaler formulation. *Respir Care*. 50(9),1209–27.
128. Bhavya M V, Gowda D V, Srivastava A, S ARA, Osmani RAM, (2016) Development and Characterization of Ethionamide loaded microparticles as Dry Powder Inhalers for Multi-drug

- Resistant Tuberculosis. *Der Pharm Lett.* 8(8),273–9.
129. Wang Y-B, Watts AB, Peters JI, Liu S, Batra A, Williams RO, (2014) In vitro and in vivo performance of dry powder inhalation formulations: comparison of particles prepared by thin film freezing and micronization. *AAPS PharmSciTech.* 15(4),981–93.
  130. Kumaresan C, Subramanian N, Antoniraj MG, Ruckmani K, (2012) Dry powder inhaler-Formulation aspects. *Pharma Times.* 44(10),14–8.
  131. Lee SL, Adams WP, Li B V, Conner DP, Chowdhury B a, Yu LX, (2009) In vitro considerations to support bioequivalence of locally acting drugs in dry powder inhalers for lung diseases. *Am Assoc Pharm Sci J.* 11(3),414–23.
  132. Okuda T, Suzuki Y, Kobayashi Y, Ishii T, Uchida S, Itaka K, Kataoka K, Okamoto H, (2015) Development of biodegradable polycation-based inhalable dry gene powders by spray freeze drying. *Pharmaceutics.* 7(3),233–54.
  133. Lindert S, Below A, Breitzkreutz J, (2014) Performance of dry powder inhalers with single dosed capsules in preschool children and adults using improved upper airway models. *Pharmaceutics.* 6(1),36–51.
  134. Pascal D, Paul H, Anne DBH, Henderik FW, (2014) The clinical relevance of dry powder inhaler performance for drug delivery. *Respir Med.* 108(8),1195–203.
  135. Sinha B, Mukherjee B, Pattnaik G, (2013) Poly-lactide-co-glycolide nanoparticles containing voriconazole for pulmonary delivery: in vitro and in vivo study. *Nanomedicine.* 9(1),94–104.
  136. Sinha B, Mukherjee B, (2012) Development of an inhalation chamber and a dry powder inhaler device for administration of pulmonary medication in animal model. *Drug Dev Ind Pharm.* 38(2),171–9.
  137. Geller DE, Weers J, Heuerding S, (2011) Development of an inhaled dry-powder formulation of Tobramycin using Pulmosphere technology. *J Aerosol Med Pulm Drug Deliv.* 24(4),175–82.
  138. Westerman EM, Boer AH De, Brun PPH Le, Touw DJ, Roldaan AC, (2007) Dry powder inhalation of colistin in cystic fibrosis patients: A single dose pilot study. *J Cyst Fibros.* 6,284–92.
  139. Muttill P, Kaur J, Kumar K, Yadav AB, Sharma R, (2007) Inhalable microparticles containing large payload of anti-tuberculosis drugs. *Eur J Pharm Sci.* 32,140–50.
  140. Grenha A, Grainger CI, Dailey AL, Seijo B, Martin GP, Lopez CR, Forbes B, (2007) Chitosan nanoparticles are compatible with respiratory epithelial cells in vitro. *Eur J Pharm Sci.* 31,73–84.
  141. Gelperina S, Kisich K, Iseman MD, Heifets L, (2005) Pulmonary perspective the potential advantages of nanoparticle drug delivery systems in chemotherapy of tuberculosis. *Am J Respir Crit Care Med.* 172,1487–90.
  142. Fernandez Tena A, Casan Clara P, (2012) Deposition of inhaled particles in the lungs. *Arch Bronconeumol.* 48(7),240–6.
  143. Paranjpe M, Müller-Goymann CC, (2014) Nanoparticle-mediated pulmonary drug delivery: A review. *Int J Mol Sci.* 15(4),5852–73.
  144. Sung JC, Garcia-contreras L, Jarod L, Peloquin CA, Elbert KJ, Hickey AJ, Edwards DA, Verberkmoes JL, (2009) Dry powder Nitroimidazopyran antibiotic PA-824 aerosol for inhalation. *Antimicrob Agents Chemother.* 53(4),1338–43.
  145. Mansour HM, Rhee Y, Wu X, (2009) Nanomedicine in pulmonary delivery. *Int J Nanomedicine.* 4(1),299–319.



146. Van Putte BP, Huisman A, Hendriks JMH, Van Schil PEY, Van Boven WJ, Schramel F, Nijkamp F, Folkerts G, (2005) Pulmonary intravascular volume can be used for dose calculation in isolated lung perfusion. *Eur J cardio-thoracic Surg.* 28(4),594–8.
147. Smith A, Perelman M, Hinchcliffe M, (2014) Chitosan: A promising safe and immune-enhancing adjuvant for intranasal vaccines. *Hum Vaccin Immunother.* 10(3),797–807.
148. Louis Pasteur, (1986) Note sur le sucre de lait. *Comptes rendus.* 42,347–51.
149. Astete CE, Sabliov CM, (2006) Synthesis and characterization of PLGA nanoparticles. *J Biomater Sci Polym Ed.* 17(3),247–89.
150. Polysciences I, (2013) PLGA ( Poly Lactic co-Glycolic Acid ) uniform dry microspheres. Vol. 1. 2013. p. 18976.
151. MSDS, (2015) Safety data sheet: PEO-block-PLGA. *Mater Saf Data Sheet.* 4(1),1–5.
152. Gadad AP, Vannuruswamy G, P SC, Dandagi PM, Mastiholmath VS, (2012) Study of different properties and applications of Poly Lactic-Co-Glycolic Acid (PLGA) nanotechnology: An overview. *Indian Drugs.* 49(12),5–22.
153. Coates J, (2000) Interpretation of infrared spectra, a practical approach. In: Meyers R, editor. *Encyclopedia of Analytical Chemistry.* 1st ed. John Wiley & Sons Ltd, Chichester; 2000. p. 10815–37.
154. Viana ODS, Patricia F, Medeiros M, Grangeiro-junior S, Muniz M, Felts M, Roca L, Soares-sobrinho JL, Darlene L, (2011) Development and validation of a HPLC analytical assay method for efavirenz tablets: A medicine for HIV infections. *Brazilian J Pharm Sci.* 47(1),97–102.
155. Ravisankar P, Rao GD, (2013) Development and validation of RP-HPLC method for determination of Levamisole in bulk and dosage form. *Asian J Pharm Clin Res.* 6(3),6–10.
156. Zinjad S, Pawar D, Warad S, Jasud S, Jagdale G, (2014) Analytical UV spectroscopic method development and validation for the estimation of Ritonavir. *World J Pharm Pharm Sci.* 2(6),5473–90.
157. Kavathia A, Misra M, (2013) Development and validation of RP-HPLC and UV-spectrophotometric methods for rapid simultaneous estimation of amlodipine and benazepril in pure and fixed dose combination. *Arab J Chem.* 30,1–8.
158. Jain R, Jain N, Kumar D, Kumar V, (2013) Novel UV spectrophotometer methods for quantitative estimation of metronidazole and furazolidone using mixed hydrotropy solubilization. *Arab J Chem.* 30,1–6.
159. Swamivelmanickam M, Manavalan R, Reddy PG, (2009) Determination and validation of UV spectrophotometric method for estimation of Bicalutamide tablet. *Int J ChemTech Res.* 1(4),1189–93.
160. Sivakumar T, Manavalan R, Valliappan K, (2007) Development and validation of a reversed-phase HPLC method for simultaneous determination of Domperidone and Pantoprazole in pharmaceutical dosage forms. *ACTA Chromatogr.* 18(1),130–42.
161. Kambham V, Kothapalli Bonnoth C, (2016) Development of stavudine sustained release tablets: In-vitro studies. *Futur J Pharm Sci.* 2(2),37–42.
162. Shaikh J, Ankola DD, Beniwal V, Singh D, Kumar MNVR, (2009) Nanoparticle encapsulation improves oral bioavailability of curcumin by at least 9-fold when compared to curcumin administered with piperine as absorption enhancer. *Eur J Pharm Sci.* 37(3),223–30.
163. Kumar S, Talegaonkar S, Negi LM, Khan ZI, Design and Development of Ciclopirox Topical Nanoemulsion Gel for the Treatment of Subungual Onychomycosis. ,303–11.

- 
164. Gazori T, Reza M, Azizi E, Yazdizade P, (2009) Evaluation of Alginate / Chitosan nanoparticles as antisense delivery vector : Formulation , optimization and in vitro characterization. 77,599–606.
  165. Rora SA, Upta SG, Arang RKN, Udhiraja RDB, (2011) Sci Pharm Amoxicillin Loaded Chitosan – Alginate Polyelectrolyte Complex Nanoparticles as Mucopenetrating Delivery System for H . Pylori.
  166. Emami J, Boushehri MSS, Varshosaz J, (2014) Preparation , characterization and optimization of glipizide controlled release nanoparticles. 9(388520),301–14.
  167. Zhou Y, (2011) Development and optimization of solid lipid nanoparticle formulation for ophthalmic delivery of chloramphenicol using a Box-Behnken design. ,683–92.
  168. Nimbalkar UA, Dhoka M V, Sonawane PA, (2011) Formulation and Optimization of Cefpodoxime Proxetil Loaded Solid Lipid Nanoparticles by Box-Behnken Design. *Int J Res Ayurveda Pharm.* 2(6),1779–85.
  169. Cook DL, David J, Griffiths GD, (2007) Retrospective identification of ricin in animal tissues following administration by pulmonary and oral routes. *Natootan Organ.* 149,1–16.
  170. Pandey S, Pandey P, Kumar R, Singh NP, (2011) Residual solvent determination by head space gas chromatography with flame ionization detector in omeprazole API. *Brazilian J Pharm Sci.* 47(2),379–84.
  171. Commission IP, (2007) Indian Pharmacopoeia. Vol. 1. Ghaziabad, India: The Indian Pharmacopoeia Commission; 2007. p. 1–383.
  172. Marques MRC, Loebenberg R, Almukainzi M, (2011) Simulated biological fluids with possible application in dissolution testing. *Dissolution Technol.* 18(3),15–28.
  173. May S, Jensen B, Wolkenhauer M, Schneider M, Lehr CM, (2012) Dissolution techniques for in vitro testing of dry powders for inhalation. *Pharm Res.* 29(8),2157–66.
  174. Fernandes CA, Vanbever R, (2009) Preclinical models for pulmonary drug delivery. *Expert Opin Drug Deliv.* 6(11),1231–45.
  175. Chougule M, Padhi B, Misra A, (2007) Nano-liposomal dry powder inhaler of tacrolimus: Preparation, characterization, and pulmonary pharmacokinetics. *Int J Nanomedicine.* 2(4),675–88.
  176. Century P, (2015) Dry powder insufflator<sup>TM</sup>- Model DP-4 and model DP-4M instructions for use [Internet]. "Penn- Century. Inc. Wyndmoor, PA. 2015. p. 1–11.
  177. Bosquillon C, Pr  at V, Vanbever R, (2004) Pulmonary delivery of growth hormone using dry powders and visualization of its local fate in rats. *J Control Release.* 96(2),233–44.
  178. Center for Drug Evaluation and Research, (2005) Guidance for industry: Estimating the maximum safe starting dose in initial clinical trials for therapeutics in adult healthy volunteers [Internet]. US Department of Health and Human Services. 2005.
  179. NCI, (2012) Equivalent surface area dosage conversion factors [Internet]. Vol. 50, The Frederick National Lab Animal Care and Use Committee. 2012. p. 1–2.
  180. Vanbever R, Lombry C, Bosquillon C, (2002) Confocal imaging of rat lungs following intratracheal delivery of dry powders or solutions of fluorescent probes. 83,331–41.
  181. Mativandlela SPN, Meyer JJM, Hussein AA, Lall N, (2007) Antitubercular activity of compounds isolated from Pelargonium sidoides. *Pharm Biol.* 45(8),645–50.
  182. Saha P, Goyal AK, Rath G, (2010) Formulation and evaluation of chitosan-based Ampicillin Trihydrate nanoparticles. *Trop J Pharm Res.* 9(5),483–8.

183. Grenha A, Gomes ME, Rodrigues M, Santo VE, Mano JF, Neves NM, Reis RL, (2009) Development of new chitosan/carrageenan nanoparticles for drug delivery applications. *J Biomed Mater Res.* A(1),1265–72.
184. Kundawala AJ, Patel VA, Patel H V, Choudhary D, (2011) Isoniazid loaded chitosan microspheres for pulmonary delivery : Preparation and characterization. *Pelagia Res Libr.* 2(5),88–97.
185. Rajan M, Raj V, (2012) Encapsulation, characterisation and in-vitro release of anti-tuberculosis drug using Chitosan-Poly Ethylene Glycol nanoparticles. *Int J Pharm Pharm Sci.* 4(4),255–9.
186. Luo Y, Zhang B, Cheng W, Wang Q, (2010) Preparation, characterization and evaluation of selenite-loaded chitosan/TPP nanoparticles with or without zein coating. *Carbohydr Polym.* 82(3),942–51.
187. Dadras OG, Sadeghi MA, Mohammad, Farhangi N, (2013) Preparation, characterization and in vitro studies of chitosan nanoparticles containing Androctonus Crassicauda scorpion venom. *J Appl Chem Res.* 7(3),35–46.
188. Othayoth R, Karthik V, Kumar SK, (2013) Development and characterization of chitosan - pluronic nanoparticles for Tamoxifen delivery and cytotoxicity to MCF -7 cells. In: International Conference on Advanced Nanomaterials & Emerging Engineering Technologie. 2013. p. 394–401.
189. Rezaei MA, Alonso MJ, (2006) Preparation and evaluation of chitosan nanoparticles containing Diphtheria toxoid as new carriers for nasal vaccine delivery in mice. *Arch Razi Inst.* 61(1),13–25.
190. Zhao Z, Xie M, Li Y, Chen A, Li G, Zhang J, Hu H, Wang X, Li S, (2015) Formation of curcumin nanoparticles via solution-enhanced dispersion by supercritical CO<sub>2</sub>. *Int J Nanomedicine.* 10(1),3171–81.
191. Pilicheva B, Katsarov P, Kassarova M, (2014) Flowability evaluation of dry powder inhalation formulations intended for nasal delivery of Betahistine Dihydrochloride. *Sikk Manipal Univ Med J.* 2(1),77–90.
192. Hao J, Fang X, Zhou Y, Wang J, Guo F, Li F, Peng X, (2011) Development and optimization of solid lipid nanoparticle formulation for ophthalmic delivery of chloramphenicol using a Box-Behnken design. *Int J Nanomedicine.* 6,683–92.
193. ICH Expert Working Group, (2003) ICH guideline Q1A(R2) stability testing of new drug substances and products. In: International Conference on Harmonization. 2003. p. 24.
194. Abdelghany S, Alkhalwaldeh M, AlKhatib HS, (2017) Carrageenan-stabilized chitosan alginate nanoparticles loaded with ethionamide for the treatment of tuberculosis. *J Drug Deliv Sci Technol.* 39(1),442–9.
195. Jahnke R, Dwornik K, Rubeau V, Phanouvong S, (2010) Thin layer chromatographic tests. In: A Concise quality control guide on essential drugs and other medicines. The Global Pharma Health Fund, Merck Darmstadt, Germany; 2010. p. 1–40.
196. Ferraz BRL, Leite FRF, Batista BL, (2016) Voltammetric determination of Ethionamide in pharmaceutical formulations and human urine using a Boron-Doped diamond electrode. *J Brazilian Chem Soc.* 27(4),677–84.
197. Ramachandran G, (2014) Simple and rapid high pressure liquid chromatography method for estimation of Ethionamide in plasma. *Asian J Biomed Pharm Sci.* 4(38),1–5.
198. Nijhu RS, Akhter DT, Jhanker YM, (2011) Development and validation of UV spectrophotometric method for quantitative estimation of nitroglycerin in pharmaceutical dosage form. *Int Curr Pharm J.* 1(1),1–5.
199. Garg RK, Singhvi I, (2015) UV Spectrophotometric method development and validation for quantitative estimation of Nizatidine. *J Innov Pharm Biol Sci.* 2(3),333–6.

- 
200. Agarry SE, Ogunleye OO, (2012) Box-Behnken design application to study enhanced bioremediation of soil artificially contaminated with spent engine oil using biostimulation strategy. *Int J Energy Environ Eng.* 3(31),1–14.
201. Sahoo BK, Chakraborty U, Mukherjee J, Pal TK, (2010) Optimization and validation of modulated release formulation of Ranitidine HCl by response surface methodology. *J Biomed Sci Res.* 2(2),76–85.
202. Pandya VM, Patel JK, Patel DJ, (2011) Formulation and optimization of nanosuspensions for enhancing Simvastatin dissolution using central composite design. *Dissolution Technol.* 18(3),40–5.
203. Mainardes RM, Gremiao MPD, Evangelista RC, (2006) Thermoanalytical study of praziquantel-loaded PLGA nanoparticles. *Rev Bras Ciencias Farm.* 42(4),523–30.
204. Yu K, Zhao J, Yu C, Sun F, Liu Y, Zhang Y, Lee RJ, Teng L, Li Y, (2016) Role of four different kinds of polyethylenimines (PEIs) in preparation of polymeric lipid nanoparticles and their anticancer activity study. *J Cancer.* 7(7),872–82.
205. Gonzalez-Juarrero M, Woolhiser LK, Brooks E, DeGroote MA, Lenaerts AJ, (2012) Mouse model for efficacy testing of antituberculosis agents via intrapulmonary delivery. *Antimicrob Agents Chemother.* 56(7),3957–9.
206. Nobbmann U, (2014) What is the significance of Z-average in dynamic light scattering [Internet]. Research Gate. 2014. p. 1.
207. Thagele R, Mishta A, Pathak A, (2011) Formulation and characterization of Clarithromycin based nanoparticulate drug delivery system. *Int J Pharm Life Sciences.* 2(1),510–5.
208. Patil P, Bhoskar M, (2014) Optimization and evaluation of spray dried chitosan nanoparticles containing Doxorubicin. *Int J Curr Pharm Res.* 6(2),7–15.
209. Mardiyanto S, (2013) Investigation of nanoparticulate formulation intended for caffeine delivery to hair follicles. Universitat des Saarlandes; 2013.
210. Desai TR, Hancock RE, Finlay WH, (2003) Delivery of liposomes in dry powder form: aerodynamic dispersion properties. *Eur J Pharm Sci.* 20,459–67.
211. Lewis D, Copley M, (2011) Inhaled product characterization calculating particle-size distribution metrics. *Pharm Technol.* 11,33–7.
212. Hamilla SM, Michael H, Ashley M, (2011) Microparticle drug delivery syringe. In: 2011 IEEE 37th Annual Northeast Bioengineering Conference. 2011. p. 1–2.
213. Bhosale U, Kusum D V, Jain N, (2011) Formulation and optimization of mucoadhesive nanodrug delivery system of acyclovir. *J Young Pharm.* 3(4),275–83.
214. Mahajan HS, Gundare SA, (2014) Preparation, characterization and pulmonary pharmacokinetics of xyloglucan microspheres as dry powder inhalation. *Carbohydr Polym.* 102(1),529–36.
215. Walash MI, Metwally MS, Abdelal AA, (2004) Spectrophotometric and kinetic determination of some sulphur containing drugs in bulk and drug formulations. *Bull Korean Chem Soc.* 25(4),517–24.
216. Tripathi A, Gupta R, Saraf SA, (2010) PLGA nanoparticles of anti tubercular drug: Drug loading and release studies of a water in soluble drug. *Int J Pharmatech Res.* 2(3),2116–23.
217. Kumar G, Malhotra S, Shafiq N, Pandhil P, Khuller GK, Sharma S, (2011) In vitro physicochemical characterization and short term in vivo tolerability study of ethionamide loaded PLGA nanoparticles: potentially effective agent for multidrug resistant tuberculosis. *J Microencapsul.* 28(8),717–28.
218. Siddiqui MR, Singh R, Bhatnagar A, Kumar J, Chaudhaary M, (2017) Determination of residual

- solvents in Docetaxel by headspace gas chromatography. *Arab J Chem.* 10(1),2479–84.
219. Golden MP, Vikram HR, (2005) Extrapulmonary tuberculosis: An overview. *Am Fam Physician.* 72(9),1761–8.
220. Rodriguez D, (2016) What is tuberculosis [Internet]. Everyday Health. 2016.

## Bibliography

- ❖ Abdelwahed W, Degobert G, Stainmesse S, Fessi H. (2006) Freeze-drying of nanoparticles: Formulation, process and storage considerations. *Adv Drug Deli Rev.* 58,1688-1713.
- ❖ Acharya VK, Mandyam CV, Rudrapatnam NT. (2007) Low molecular weight Chitosan-preparation with the aid of pepsin, characterization and its bactericidal activity. *Biomacromolecules.* 8,566-72.
- ❖ Adhikari L, Mishra US, Murthy PN. (2013) Spectrophotometric estimation and statistical correlation for Rosiglitazone in rat and human plasma. *Asian J Pharma Clini Res.* 6(3),138-141.
- ❖ Agnihotri J, Saraf S, Khale A. (2011) Targeting: New potential carriers for targeted drug delivery system. *Int J Pharmaceut Sci Rev Res.* 8(2),117-123.
- ❖ Ahmad M, Madni AU, Usman M. (2009) *In-vitro* release and pharmacokinetics of anti-tubercle drug Ethionamide in healthy male subjects. *J Bioana Biomed.* 1(1),46-49.
- ❖ Ahmad Z, Pandey R, Sharma S, Khuller GK. (2006) Alginate nanoparticles as antituberculosis drug carriers: Formulation development, pharmacokinetics and therapeutic potential. *Ind J Chest Dis All Sci.* 48,171-76.
- ❖ Ain Q, Sharma S, Khuller GK, Garg SK. (2003) Alginate based oral drug delivery for tuberculosis: pharmacokinetics and therapeutic effects. *J Antimicro Chemothe.* 51,931-38.
- ❖ Anbarasan B, Vennya VM, Niranjanan VA, Ramaprabhu S. (2013) Optimization of the formulation and *in-vitro* evaluation of Chloroquine loaded Chitosan nanoparticles using ionic gelation method. *J Chem Pharmaceut Sci.* 6(2),106-112.
- ❖ Andrews LM. (2001) Determination of minimum inhibitory concentrations. *J Antimicro Chemothera.* 48(S1), 5-16.
- ❖ Aqil M, Ali A, Ahad A, sultana Y, Najmi AK, Saha N. (2007) A validated HPLC method for estimation of Metoprolol in human plasma. *ACTA Chromato.* 19,130-140.
- ❖ Arany S, Benoit DSW, Dewhurst S and Ovitt CE. (2013) Nanoparticle-mediated gene silencing confers radioprotection to salivary glands *in vivo*. *Molecular Therapy.* 21(6),1182-1194.
- ❖ Avery EE, Morch ET, Benson DW. (1956) Critically crushed chests. A new method of treatment with continuous mechanical hyperventilation to produce alkalotic apnea and internal pneumatic stabilization. *J Thoracic Surg.* 32,291-309.
- ❖ Awari VP, Meyyanathan SN, Karthik Y, Jawahar N. (2014) HPLC method development and validation of Rizatriptan in rabbit plasma. *J Pharm Sci Res.* 6(1),24-26.
- ❖ Balcerzak J, Mucha M. (2012) Analysis of model drug release kinetics from complex matrices of polylactide-chitosan. *Prog Chem Applic Chit.* 15,117-126.
- ❖ Bosquillon C, Preat V, Vanbever R. (2004) Pulmonary delivery of growth hormone using dry powders and visualization of its local fate in rats. *J Control Release.* 96,233-44.
- ❖ Bozdag S, Dillen K, Vandervoort J, Ludwig A. (2005) The effect of freeze-drying with different cryoprotectants and gamma-irradiation sterilization on the characteristics of Ciprofloxacin HCl-loaded poly(D,L-lactide-glycolide) nanoparticles. *J Pharm Pharmacol.* 57(6),699-707.

- ❖ Center for drug evaluation and research, U. S Department of health and human services. Guidance for industry chronic obstructive pulmonary disease: Developing drugs for treatment. 2007: 1-14 available in <http://www.fda.gov/cder/guidance/index.htm> accessed on 03<sup>rd</sup> March, 2015
- ❖ Center for Drug Evaluation and Research, U.S. Department of Health and Human Services, Food and Drug Administration. Estimating the maximum safe starting dose in initial clinical trials for therapeutics in adult healthy volunteers. 2005.1-27.
- ❖ Chen JL, Yeh MK, Chiang CH. (2004) Dichloromethane evaporative behaviour during the solidifying process of Ovalbumin-loaded poly (DL lactic-co-glycolic acid) microparticles. *J Food Drug Ana.* 12(4),291-98.
- ❖ Chime SA, Onunkwo GC, Onyishi II. (2013) Kinetics and mechanisms of drug release from swellable and non swellable matrices: A review. *Res J Pharma Bio Chem.* 4(2),97-103.
- ❖ Chimote G, Banerjee R. (2009) Evaluation of antitubercular drug-loaded surfactant as inhalable drug delivery systems for pulmonary tuberculosis. *J Biomed Mater Res A.* 89(2),281-92.
- ❖ Chrystyn H. (2001) Methods to identify drug deposition in the lungs following inhalation. *Br J Clin Pharmacol.* 51,289-299.
- ❖ Contreiras LG, Sethuraman V, Kazantseva M, Godfrey V, Hickey AJ. (2006) Evaluation of dosing regimen of respirable Rifampicin biodegradable microspheres in the treatment of tuberculosis in the guinea pig. *J Antimicro Chemothera.* 58,980-86.
- ❖ Constan AA, Wong BA, Everitt JJ, Butterworth BE. (2002) Chloroform inhalation exposure conditions necessary to initiate liver toxicity in female B6C3F1 mice. *Toxicolo Sci.* 66,201-208.
- ❖ Cunha RA, Soares TA, Rusu VH, Pontes FJS, Franca EF, Lins RD. The molecular structure and conformational dynamics of Chitosan polymers: An integrated perspective from experiments and computational simulations. *The complex world of Polysaccharides.* Chapter 9:229-56.
- ❖ Dadras OG, Sadeghi AMM, Farhangi N, Forouhar N, Mohammadpour N, Avadi MR. (2013) Preparation, characterization and *in vitro* studies of Chitosan nanoparticles containing *Androctonus crassicauda* scorpion venom. *J App Chem Res.* 7(3),35-46.
- ❖ Dash AK, Singh D, Mishra J, Nirwan S, Pandey SP. (2011) Development and characterization of Chitosan nanoparticles loaded with Amoxycilin. *Int Res J Pharm.* 2(5),145-51.
- ❖ Date PV, Samad A, Devarajan PV. (2010) Freeze thaw: A simple approach for prediction of optimal cryoprotectant for freeze drying. *AAPS Phar Sci Tech.* 11(1),304-313.
- ❖ Demoly P, Hagedoorn P, Boer AH, Frijlink HW. (2004) The clinical relevance of dry powder inhaler performance for drug delivery. *Res Med.* 108,1195-1203.
- ❖ Desai D, Shah M. (2015) A review: Validated analytical methods developed on antitubercular drug, Rifampicin. *J Pharm Sci Biosienti Res.* 5(3),254-65.
- ❖ Desai TR, Hancock REW, Finlay WH. (2003) Delivery of liposome in dry powder form: Aerodynamic dispersion properties. *Euro J Pharma Sci.* 20,459-467.
- ❖ Dharmadhikari AS, Kabadi M, Gerety B, Hickey AJ, Fourie PB, Nardell E. (2013) Phase I, single dose, dose-escalating study of inhaled dry powder Capreomycin: a new approach to therapy of drug resistant tuberculosis. *Antimicrob Agen Chemo.* 57(6),2613-2619.

- ❖ Dharmalingam SR, Ramamurthy S, Chidamnaram K, Nadaraju S. (2014) A simple HPLC bioanalytical method for the determination of Doxorubicin hydrochloride in rat plasma: Application to pharmacokinetic studies. *Topi J Pharma Res.* 13(3),409-415.
- ❖ Ding J, Na L, Mao S. (2012) Chitosan and its derivatives as the carrier for intranasal drug delivery. *Asian J Pharmaceut Sci.* 7(6),349-61.
- ❖ Ditte MKJ, Dongmei C, Morten JM, Sven F, Hanne MN, Camilla F. (2010) Spray drying of siRNA-containing PLGA nanoparticles intended for inhalation. *J Controll Rel.* 142,138-45.
- ❖ Edwards D. (2010) Applications of capsule dosing techniques for use in dry powder inhalers. *Therapeutic Deli.* 1(1),195-201.
- ❖ Elbary AA, Ellaithy M, Tadros MI. (2007) Promising ternary dry powder inhaler formulations of cromolyn sodium: Formulation and *in vitro-in vivo* evaluation. *Arch Pharm Res.* 30(6),785-92.
- ❖ Ferraz BRL, Leite FRF, Batista BL, Malagutti AR. (2016) Voltammetric determination of Ethionamide in pharmaceutical formulation human urine using a Boron-Doped diamond electrode. *J Braz Chem Soc.* 27(4),677-84.
- ❖ Freireich EJ. (1966) Quantitative comparison of toxicity of anticancer agents in mouse, rat, dog, monkey and man. *Cancer Chemother Rep.* 50(4),219-244.
- ❖ Frijlink HW, Boer AHD. (2004) Dry powder inhalers for pulmonary drug delivery. *Expert Opin Drug Deliv.* 1(1),67-86.
- ❖ Geller DE, Weers J, Heuerding S. (2011) Development of an inhalable dry powder formulation of Tobramycin using pulmoSphere technology. *J Aerosol Medi Pulmo drug deliv.* 24(4),175-182.
- ❖ Gelperina S, Kisich K, Iseman MD, Heifets L. (2005) The potential advantages of nanoparticles drug delivery systems in chemotherapy of tuberculosis. *American J Respira Criti Care Med.* 172,1487-90.
- ❖ Grenha A, Gomes ME, Rodrigues M, Santo VE, Mano JF, Neves NM, Reis RL. (2009) Development of new Chitosan/carrageenan nanoparticles for drug delivery applications. *J Biomed Mat Res.* A,1265-72.
- ❖ Guillon A, Montharu J, Vecellio L, Schubnel V, Roseau G, Guillemain J, Diot P, Monte M. (2012) Pulmonary delivery of dry powders to rats: Tolerability limits of an intra-tracheal administration model. *Int J Pharm.* 434,481-487.
- ❖ Gupta H, Aqil M, Khar RK, Ali A, Bhatnagar A, Mittal G. (2010) Sparfloxacin-loaded PLGA nanoparticles for sustained ocular drug delivery. *Nanomed Nanotech Bio Med.* 6,324-33.
- ❖ Gupta M, Sharma V. (2011) Targeted drug delivery system: A review. *Res J Chem Sci.* 1(2),135-38.
- ❖ Gupta V, Jain ADK, Gill NS, Gupta K. (2012) Development and validation of HPLC method- a review. *Int Res J Pharm App Sci.* 2(4),17-25.
- ❖ Guterres SS, Alves MP, Pojlmann AR. (2007) Polymeric nanoparticles, nanospheres and nanocapsules for cutaneous applications. *Drug Tar Insight.* 2,147-57.
- ❖ Hallak MHD, SarfraZ MK, Azarmi S, Rao WH, Finlay W, Lobenberg R. (2011) Pulmonary delivery of inhalable nanoparticles: dry powder inhalers. *Therapeu Deliv.* 2(10),1-12.
- ❖ Hamishehkar H, Rahimpour Y, Javadzades Y. (2001) The role of carrier in dry powder inhaler. Recent advances in novel drug carrier systems. Chapter 3.39-66.
- ❖ Hoff J, Rlatg LVT. (2000) Methods of blood collection in the mouse. *Lab Animal.* 29(10), 47-53.



- ❖ Huang X, Brazel CS. (2001) On the importance and mechanisms of burst release in matrix-controlled drug delivery system. *J Control Relea.* 73,121-136.
- ❖ Hunter G. (1957) A method for deproteinization of blood and other body fluids. *J Clin Path.* 10,161-164.
- ❖ Hussain S, Munjewar RR, Farooqui M. (2012) Development and validation of a simultaneous HPLC method for quantification of Amlodipine Besylate and Metoprolol tartrate in tablet. *J Pharma Sci Tech.* 1(2),1-5.
- ❖ Ibrahim AA, Betigeri SS, Zhang H, Evans BA, Neau SH. (2002) Molecular weight and degree of deacetylation effects on lipase-loaded Chitosan bead characteristics. *Biomaterial.* 23,3637-44.
- ❖ Ingen JV, Boeree MJ, Kusters K, Wieland A, Tortoli E, Dekhuijzen PNR, Soolingen DV. (2009) Proposal to elevate *Mycobacterium avium* complex ITS sequevar MAC-Q to *Mycobacterium vulneris* sp. Nov. *Int J Systema Evolutio Micro.* 59,2277-2282.
- ❖ Jamieson D. (1962) A method for the quantitative estimation of drugs on the isolated intact trachea. *Brit J Pharmacol.* 19,286-294.
- ❖ Jaruszewski KM, Ramakrishnan S, Poduslo JF, Kandimalla KK. (2012) Chitosan enhances the stability and targeting of immuno-nanovehicles to cerebro-vascular deposits of Alzheimer's disease amyloid protein. *Nanomed Nanotech Bio Med.* 8,250-60.
- ❖ Jean M, Almeh M, Jesus DD, Thibault M, Lavertu M, Darras V, Nelea M, Buschmann MD, Merzouki A. (2012) Chitosan based therapeutic nanoparticles for combination gene therapy and gene silencing of *in vitro* cell lines relevant to type 2 diabetes. *European J Pharm Sci.* 45,138-49.
- ❖ Jensen DMK, Cun D, Maltesen MJ, Frokjaer S. (2010) Spray drying of siRNA containing PLGA nanoparticles intended for inhalation. *J Control Rel.* 142,138-145.
- ❖ Juarrero MG, Woolhiser LK, Brooks E, Groote MA, Lenaerts AJ. (2012) Mouse model for efficacy testing of antituberculosis agents via intrapulmonary delivery. *Antimicro Agent Chemother.* 56(7),3957-59.
- ❖ Kannan C, Karunanithi V, Janarthanan S, Dheivasigamani V. (2010) Formulation and *in vitro* evaluation of gastroretentive Rosiglitazone maleate floating tablets. *Int J Chem Pharm Sci.* 1(1),26-32.
- ❖ Kim H, Kim D, Yang JS, Kim CW. (2006) Sample preparation for headspace GC analysis of residual solvent in Hyaluronic acid derivative fiber. *Bull Korean Chem Soc.* 27(2),302-04.
- ❖ Kumar TM, Srikanth G, Rao JV, Rao KRS. (2011) Development and validation of HPLC-UV method for the estimation of Levofloxacin in human plasma. *Int J Pharm Pharma Sci.* 3(2),247-250.
- ❖ Kumaresan C, Subramanian N, Antoniraj MG, Ruckmani K. (2012) Dry powder inhaler- Formulation aspects. *Pharma Times.* 44(10),14-18.
- ❖ Kumirska J, Weinhold Mx, Thoming J, Stepnowski P. (2011) Biomedical activity of chitin/Chitosan based materials-Influence of physicochemical properties apart from molecular weight and degree of N-acetylation. *Polymers.* 3,1875-1901.
- ❖ Kundawala AJ, Patel VA, Patel HV, Choudhary D. (2011) Isoniazid loaded Chitosan microspheres for pulmonary delivery: Preparation and characterization. *Der Pharmacia Sinica.* 2(5),88-97.
- ❖ Kunjachan S, Jose S, Lammers T. (2010) Understanding the mechanism of ionic gelation for synthesis of Chitosan nanoparticles using qualitative techniques. *Asian J Pharm.* 2,148-53.
- ❖ Kuper KM. Intravenous to oral therapy. Conversion from Competence assessment tools for health-system pharmacies. 2008. Chapter 29, 347-359.

- ❖ Larhrib H, Zeng XM, Martin GP, Marriott C, Pritchard J. (1999) The use of different grades of lactose as carrier for aerisilised Salbutamol sulphate. *Int J Pharma.* 191,1-14.
- ❖ Lee SL, Adams WP, Li BV, Conner DP. (2009) *In vitro* considerations to support bioequivalence of locally acting drugs in dry powder inhalers for lung disease. *AAPS J.* 11(4),414-423.
- ❖ Lewis D, Copley M. (2011) Inhaled product characterization: Calculating particle-size distribution metrics. *Pharm Tech.* 33-37.
- ❖ Lindert S, Below A, Breitreutz J. (2014) Performance of dry powder inhalers with single dosed capsules in preschool children and adults using improved upper airway models. *Pharmaceutics.* 6,36-51.
- ❖ Lodha R, Menon PR Kabra SK. (2008) Concerns on the dosing of antitubercular drugs for children in RNTCP. *Ind Pediat.* 45,852-854.
- ❖ Lombry C, Bosquillon C, Preat V, Vanbever R. (2002) Confocal imaging of rat lungs following intratracheal delivery of dry powders or solutions of fluorescent probes. *J Control Relea.* 83,331-41.
- ❖ Luo Y, Zhang B, Cheng WH, Wang Q. (2010) Preparation characterization and evaluation of selenite loaded Chitosan/TPP nanoparticles with or without zein coating. *Carbohydrate Poly.* 82,942-51.
- ❖ Mahajan HS, Gundare SA. (2014) Preparation, characterization and pulmonary pharmacokinetics of Xyloglucan microspheres as dry powder inhalation. *Carbohydrate Poly.* 102,529-36.
- ❖ Malhotra KK. (2003) Treatment of tuberculosis in chronic renal failure maintenance dialysis and renal transplant. *Indian J Nephrol.* 13,69-71.
- ❖ Maleque M, Hasan R, Hossen F, Safi S. (2012) Development and validation of a simple UV spectrophotometric method for the determination of Levofloxacin both in bulk and marketed dosage formulations. *J Pharm Analysis.* 2(6),454-57.
- ❖ Manwar J, Mahadik K, Paradkar An Patil S, Sathiyarayanan L, Manmode R. (2013) Gas chromatography method for the determination of non-ethanol volatile compounds in herbal formulation. *Int J Anal Bioanal Chem.* 3(1),12-17.
- ❖ Marques MRC, Loebenberg R, Almukainzi M. (2011) Simulated geological fluids with possible application in dissolution testing. *Disso Tech.* 1,15-28
- ❖ Massimo M. (2013) Nanoparticles for brain drug delivery. *ISRN Biochem.* 1-18.
- ❖ Mathew TV, Rao KVK. Marshall mix design in Introduction of transportation engineering. Chapter 26. 2006:1-7.
- ❖ Mohanraj VJ, Chen Y. (2006) Nanoparticles- A review. *Trop J Pharmaceut Res.* 5(1),561-73.
- ❖ Mohd AB, Sanka K, Gullapelly R, Diwan PV, Shastri N. (2014) Development and validation of RP-HPLC method for Glimepiride and its application for novel self nanoemulsifying powder (SNEP) formulation analysis and dissolution study. *J Anal Sci Tech.* 5(2),1-8.
- ❖ Moore BB, Lawson WE, Oury TD, Sisson TH, Raghvendra K, Hogaboam CM. (2013) Animal models of fibrotic lung disease. *Ameri J Res Cell Mol Bio.* 49,167-179.
- ❖ Morris GA, Kok MS, Harding SE, Adams GG. (2010) Polysaccharide drug delivery systems based on pectin and Chitosan. *Biotech Gen Eng Rev.* 27,257-84.
- ❖ Murthy TEGK, Bala MVP, Satyanarayana V. (2010) Formulation and evaluation of dry powder inhaler for Tiotropium bromide. *Int J Inno Pharmaceut Res.* 1(1), 14-22.

- ❖ Mustafa C, Mustafa SK, Sacide A, Selma S. (2014) UV spectrophotometric method for determination of the dissolution profile of Rivaroxaban. *Disso Tech.* 1,56-59.
- ❖ Muthu MS. (2009) Nanoparticles based on PLGA and its co-polymer: An overview. *Asian J Pharm.* 4,266-73.
- ❖ Muttill P, Kaur J, Kumar K, Yadav AB, Sharma R, Misra A. (2007) Inhalable microparticles containing large payload of anti-tuberculosis drug. *Eur J Pharma Sci.* 32,140-150.
- ❖ Nagavarma BVN, Yadav HKS, Ayaz A, Vasudha LS, Shivakumar HG. (2012) Different techniques for preparation of polymeric nanoparticles-A review. *Asian J Pharm Cli Res.* 5(3),16-23.
- ❖ Nagpal K, Singh SK, Mishra DN. (2010) Chitosan nanoparticles: A promising system in novel drug delivery. *Chem Pharm Bull.* 58(11),1423-30.
- ❖ Nijhu RS, Akhter DT, Jhanker YM. (2011) Development and validation of UV spectrophotometric method for quantitative estimation of nitroglycerin in pharmaceutical dosage form. *Int Cur Pharm J.* 1(1),1-5.
- ❖ Newman SP, Busse WW. (2002) Evolution of dry powder inhaler design, formulation and performance. *Res Medi.* 96,293-304.
- ❖ Oberdorster G, Oberdorster E, Oberdorster J. (2007) Concepts of nanoparticles dose metric and response metric. *Environment Heal Persp.* 115(6),290-294.
- ❖ Onoue S, Aoki Y, Matsui T, Kojo Y, Misaka S, Mizumoto T, Yamada S. (2011) Formulation design and *in vivo* evaluation of dry powder inhalation system of new vasoactive intestinal peptide derivative ([R<sup>15,20,21</sup>, L<sup>17</sup>, A<sup>24,25</sup>, des-N<sup>28</sup>]-VIP-GRR) in experimental asthma/COPD model rats. *Int J Pharma.* 410,54-60.
- ❖ Othayoth R, Karthik V, Kumar KS. Development and characterization of Chitosan-pluronic nanoparticles for Tamoxifen delivery and cytotoxicity to MCF-7 cells. International conference on advanced nanomaterials and emerging technologies at Chennai, India 2013, 394-401.
- ❖ Pai PNS, Balaphanisekhar B, Rao GK, Pasha K. (2006) Determination of methylene chloride organic volatile impurity in marketed formulations of Ciprofloxacin, Norfloxacin, Pefloxacin and Ofloxacin. *Ind J Pharma Sci.* 3,368-69.
- ❖ Pandey R, Khuller GK. (2006) Nanotechnology based drug delivery system for the management of tuberculosis. *Ind J Exp Bio.* 44,357-66.
- ❖ Pandey R, Sharma S, Khuller GK. (2004) Lung specific stealth liposomes as antitubercular drug carriers in guinea pigs. *Ind J Exp Bio.* 42,562-66.
- ❖ Pandey S, Pandey P, Kumar R, Singh NP. (2011) Residual solvent determination by head space gas chromatography with flame ionization detector in Omeprazole API. *Brazili J Pharma Sci.* 47(2),379-84.
- ❖ Patel MP, Patel RR, Patel JK. (2010) Chitosan mediated targeted drug delivery system: A Review. *J Pharm Pharmaceut Sci.* 13(3),536-557.
- ❖ Patil JS, Devi K, Devi K, Suresh S. (2015) Formulation and evaluation of novel spray-dried alginate microspheres as pulmonary delivery systems of Rifampicin in rats. *Ind J Pharma Edu Res.* 49(4),320-328.
- ❖ Patil P, Bhoskar M. (2014) Optimization and evaluation of spray dried Chitosan nanoparticles containing Doxorubicin. *Int J Curr Pharm Res.* 6(2),7-15.
- ❖ Pelpquin CA. (1991) Improved high performance liquid chromatographic assay for the determination of Ethionamide in serum. *J Chromatogra.* 563,472-75.

- ❖ Peters JH, Hamme KJ, Gordon GR. (1982) Determination of Clofezimine in plasma by high performance liquid chromatography. *J Chromatography*. 229,503-08.
- ❖ Pilicheva B, Katsarov P, Kassarova M. (2015) Flowability evaluation of dry powder inhalation formulations intended for nasal delivery of Betahistine dihydrochloride. *SMU Med J*. 2(1), 77-90.
- ❖ Puranik SB, Sharath S, Pai SPN. (2012) Head space gas chromatography analysis of residual solvents using EC-5 column. *Int J Pharma Chem Res*. 1(1), 22-27.
- ❖ Putte BPV, Huisman A, Hendriks JMH, Schil PEYV, Boven WJV, Schramel F, Nijkamp F, Folkerts G. (2005) Pulmonary intravascular volume can be used for dose calculation in isolated lung perfusion. *Euro J Car Thora Sur*. 28,594-598.
- ❖ Qureshi SA. (2010) *In vitro- In vivo* correlation (IVIVC) and determining drug concentrations in blood from dissolution testing- A simple and practical approach. *Open Drug Deli J*. 4,38-47.
- ❖ Rajalingam D, Loftis C, Xi JJ, Kumar TKS. (2009) Trichloroacetic acid-induced protein precipitation involves the reversible association of a stable partially structured intermediate. *Pro Sci*. 18,980-993.
- ❖ Rajan M, Raj V. (2012) Encapsulation characterisation and *in-vitro* release of anti-tuberculosis drug using Chitosan-poly ethylene glycol nanoparticles. *Int J Pharm Pharmaceut Sci*. 4(4),255-59.
- ❖ Ranjita S, Loaye AS, Khalil M. (2011) Present status of nanoparticles research for treatment of tuberculosis. *J Pharm Pharmaceut Sci*. 14(1),100-16.
- ❖ Ramachandra B, Suguna P, Reddy KS, Naidu NVS. (2015) Development of UV-Visible spectrophotometric method for determination of Dasatinib in pharmaceutical formulation and biological samples. *Int J Pharma Sci Res*. 6(2),293-303.
- ❖ Ramachandran G, Chandrasekaran V, Kumar AKH, Dewan P, Swaminathan S, Thomas A. (2013) Estimation of content of anti-TB drugs supplied at centres of the revised national TB control programme in Tamil Nadu, India. *Trop Med Int Health*. 18(9),1141-44.
- ❖ Ramos CS. (2013) Development and validation of a headspace gas chromatographic method for determination of residual solvents in five drug substance. *Int J Pharma Sci Inven*. 2(3),36-41.
- ❖ Ravichandiran V, Masilamani K, Satheshkumar S, Joseprakash D. (2011) Drug delivery to the lungs. *Int J Pharmaceut Sci Rev Res*. 10(2),85-89.
- ❖ Ravisankar P, Rao GD. (2013) Development and validation of RP-HPLC method for determination of Levamisole in bulk and dosage form. *Asian J Pharma Clin Res*. 6(3),169-73.
- ❖ Rathod BH, Rani SS, Kartheek N, Kumar AA. (2014) UV spectrophotometric method development and validation for the quantitative estimation of Indinavir sulphate in capsules. *Int J Pharmacy Pharma Sci*. 6(6),598-601.
- ❖ Rehman M, Yousuf RI, Shoaib MH. (2014) A stability indicating high performance liquid chromatographic assay for the simultaneous determination of Pyridoxine, Ethionamide and Moxifloxacin in fixed dose combination tablets. *Chromatogra Res Int*. 1, 1-8.
- ❖ Reimer LG, Stratton CW, Reller LB. (1981) Minimum inhibitory and bactericidal concentrations of 44 antimicrobial agents against three standard control strains in broth with and without human serum. *Antimicro Ager Chemothera*. 19(6), 1050-1055.
- ❖ Rezaei MA, Alonso MJ. (2006) Preparation and evaluation of Chitosan nanoparticles containing Diphtheria toxoid as new carriers for nasal vaccine delivery in mice. *Arch Razi Institute*. 61(1),13-25.

- ❖ Rieux AD, Fievez V, Garinot M, Schneider YJ, Preat V. (2006) Nanoparticles as potential oral delivery system of proteins and vaccines: A mechanistic approach. *J Control Rel.* 116,1-27.
- ❖ Riley T, Christopher D, Arp J, Casazza A, Colombani A, Cooper A, Dey M, Mass J, Mitchell J, Reiners M, Sigari N. (2012) Challenges with developing *in vitro* dissolution tests for orally inhaled products. *AAPS Pharm Sci Tech.* 13(3),978-989.
- ❖ Ryrfeldt A, Nilsson E. (1978) Uptake and biotransformation of Ibuprofen and Rerbutaline in isolated perfused rat and guinea pig lungs. *Biochem Pharmacol.* 27,301-305.
- ❖ Saboktakin MR, Rabar NA, Tabatabaie RM, Maharramov A, Ramazanov MA. (2012) Intelligent drug delivery system based on modified Chitosan nanoparticles. *Letters Org Chem.* 9,56-70.
- ❖ Sailaja AK, Amareshwar P, Chakravarty P. (2011) Different techniques used for the preparation of nanoparticles using natural polymers and their application. *Int J Pharm Pharmaceut Sci.* 3(2),45-50.
- ❖ Salama RO, Ladd L, Chan HK, Taini D, Young PM. (2009) Development of an *in vivo* Ovine dry powder inhalation model for the evaluation of conventional and controlled release microparticles. *AAPS J.* 11(3),465-468.
- ❖ Shah N, Kondawar M, Shah R, Shah V. (2011) Sustained release of spray dried combination dry powder inhaler formulation for pulmonary delivery. *Asian J Pharmaceut Clini Res.* 4(4),112-1128.
- ❖ Shaikh HK, Kshirsagar RV, Patil SG. (2015) Mathematical models for drug release characterization: A review. *Wor J Pharm Pharmaceu Sci.* 4(4),324-338.
- ❖ Shaikh S, Nazim S, Khan T, Shaikh A, Zameeruddin M, Quazi A. (2010) Recent advances in pulmonary drug delivery system: A review. *Int J Appli Pharm.* 4(2),27-31.
- ❖ Shailaja M, Diwan PV, Ramakrishna S, Ramesh G, Reddy KH, Rao YM. (2012) Development of Olanzapine nano-emulsion for enhanced brain delivery. *Int J Pharma Sci nanotech.* 5(1), 1648-1659.
- ❖ Sharma K, Agrawal SS, Gupta M. (2012) Development and validation of UV spectrophotometric method for the estimation of Curcumin in bulk drug and pharmaceutical dosage forms. *Int J Drug Dev Res.* 4(2),375-80.
- ❖ Sharma P, Ganta S, Denny WA, Garg S. (2009) Formulation and pharmacokinetics of lipid nanoparticles of a chemically sensitive nitrogen mustard derivative: Chlorambucil. *Int J Pharmaceu.* 367,187-194.
- ❖ Sharma R, Saxena D, Dwivedi AK, Misra A. (2001) Inhalable microparticles containing drug combinations to target alveolar macrophages for treatment of pulmonary tuberculosis. *Pharmaceut Res.* 18(10),1405-10.
- ❖ Sherbiny IM, Baz NM, Ycaoub MH. (2015) Inhaled nano and microparticles for drug delivery. *Global Cardio Sci Prac.* 2,1-14.
- ❖ Singh AV, Nath LKM, Pani NR. (2011) Development and validation of analytical method for the estimation of Lamivudine in rabbit plasma. *J Pharma Ana.* 1(4),251-257.
- ❖ Sinha B, Mukherjee B. (2012) Development of an inhalation chamber and a dry powder inhaler device for administration of pulmonary medication in animal model. *Drug Develop Indus Pharm.* 38(2),171-179.
- ❖ Sivakumar T, Manavalan R, Valliappan. (2007) Development and validation of a reversed phase HPLC method for simultaneous determination of Domperidone and Pantoprazole in pharmaceutical dosage forms. *ACTA Chromatogra.* 18,130-42.

- ❖ Sivasaikiran B, Chowdary YN, Sreelakshmi V, Rao VUM, Pugazhendhy S. (2013) Determination by head space gas chromatography with flame ionization detector in Ropinirole API. *Int J Pharm Biomed Res.* 4(4),227-230.
- ❖ Son YJ, Conville JM. (2010) Dissolution testing for inhaled drugs. *Pharm Tech.* 1, 37-41.
- ❖ Son YJ, Horng M, Copley M, Conville JT. (2010) Optimization of an in vitro dissolution test method for inhalation formulation. *Dissolu Tech.* 1, 6-13.
- ❖ Soni A, Gadad A, Dandagi P, Mastihlimath V. (2011) Simvastatin loaded PLGA nanoparticles for improved oral bioavailability and sustained release: Effect of formulation variables. *Asian J Pharm.* 5,57-64.
- ❖ Stanislaw J, Jacek J, Janina S, Brunon W, Malgorzata S. (2002) The effect of cryoprotectants on the physical propertied of large liposomes containing Sodium Diclofenac. *Acta Poloniae Pharmaceut Drug Res.* 59(3),187-192.
- ❖ Sunitha R, Prabha KS, Prasanna PM. (2011) Drug delivery and its developments for pulmonary system. *Int J Pharmaceu Chem Bio Sci.* 1(1), 66-82.
- ❖ Taylor MD, Robart JR, Hubbs AF, Reaso MJ, Antonini JM. (2002) Quantitative image analysis of drug-induced lung fibrosis using laser scanning confocal microscopy. *Toxicolo Sci.* 67,295-302.
- ❖ Tena AF, Clara PC. (2012) Deposition of inhaled particles in the lungs. *Arch Bronconeumol.* 48(7),240-246.
- ❖ Therapeutic Research Center. Considerations for PO to IV Dose Conversions. Pharmacist's let Prescriber's let. 2010, 26,1-4.
- ❖ Toit LC, Pillay V, Danckwerts MP. (2006) Tuberculosis chemotherapy: Current drug delivery approaches. *Respira Res.* 7(118),1-8.
- ❖ Tomicka HS. (1993) Spectrophotometric determination of Ethionamide and Thionicotinamide with4-(2-Pyridylazo) resorcinol and Canadium. *Chem Anal.* 38,745-51.
- ❖ Toutain PL, Melou AB.(2004) Plasma terminal half life. *J Vet Pharmacol Therap.* 27,427-439.
- ❖ Tsao CT, Chang CH, Lin YY, Wu MF, Han JL, Hsieh KH. (2011) Kinetic study of acid depolymerisation of Chitosan and effects of low molecular weight Chitosan on erythrocyte rouleaux formation. *Carbohydrate Res.* 346,94-102.
- ❖ Uduehi AN, Stammberger U, Frese S, Schmid RA. (2001) Efficiency of non-viral gene delivery systems to rat lungs. *Euro J Cardio thora Surg.* 20,159-63.
- ❖ Vannelli TA, Dykman A, Montellano PR. (2002) The antituberculosis drug Ethionamide is activated by a flavoprotein monooxygenase. *J Bio Chem.* 277(15),12824-829.
- ❖ Vella J, Busuttil F, Bartolo NS, Sammut C, Ferrito V, Inglott AS, Azzopardi LM, Ferla GL. (2015) A simple HPLC-UV method for the determination of Ciprofloxacin in human plasma. *J Chromato B.* 989,80-85.
- ❖ Walash MI, Brashy AME, Metwally MS, Abdelal AA. (2004) Spectrophotometric and kinetic determination of some sulphur containing drugs in bulk and drug formulations. *Bull Korean Chem Soc.* 25(4),517-24.
- ❖ Wang XD, Gu J, Wang T, Zhang ZP, Cul ZQ, Wel HP, Deng JY, Zhang XE. (2011) Comparative analysis of mycobacterial NADH pyrophosphatase isoforms reveals a novel mechanism for Isoniazid and Ethionamide inactivation. *Mol Microbio.* 82(6),1375-91.

- ❖ Wang YB, Watts AB, Peters JI, Liu S, Batra A, Williams RO. (2014) *In vitro* and *in vivo* performance of dry powder inhalation formulations: comparison of particles prepared by thin film freezing and micronization. *AAPS Pharm Sci Tech.* 15(4),981-993.
- ❖ Westerman EM, Boer AH, Brun PPH, Touw DJ, Roldaan AC, Frijlink HW, Heijerman HGM. (2007) Dry powder inhalation of colistin in cystic fibrosis patients: A single dose pilot study. *J Cystic Fibrosis.* 6,284-92.
- ❖ Wongsinsup C, Taesotikul W, Kaewvichit S, Sangsrijan S, Sangsrijan S. (2010) Development of Clozapine in human plasma by high performance liquid chromatography with UV-VIS detector. *CMU. J. Nat. Sci.* 9(1),29-37.
- ❖ Xiao W, Weifen Z, Don H, Heidi MM. (2013) Physicochemical characterization and aerosol dispersion performance of organic solution advanced spray dried cyclosporine A multifunctional particles for dry powder inhalation aerosol delivery. *Int J Nanomed.* 8,1269-1283.
- ❖ Zhang Y, Yew WW. (2009) Mechanism of drug resistance in *Mycobacterium tuberculosis*. *Int J Tuberc Lung Dis.* 13(11),1320-30.
- ❖ Zhu Min, Wag H, Liu J, He H, Hua X, He Q, Zhang L, Ye X, Shi J. (2011) A mesoporous silica nanoparticulate/ $\beta$ -TCP/BG composite drug delivery system for osteoarticular tuberculosis therapy. *Biomaterials.* 32,1986-95.

## Appendix A

### Approval from CPCSEA & IAEC for animal study

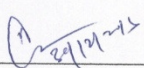
Protocol no: BLP&R/IAEC/04-16

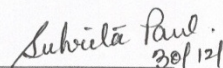
**Certificate**


This is certify that the project title "**Nanoparticulate Drug Delivery System for Tuberculosis**" has been approved by the IAEC committee during the meeting held on 30<sup>th</sup> Dec 2016 ~~30~~.

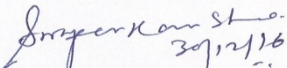
Dr. S. S. Hameed

**Signature with date**

  
(Chairman IAEC)

  
(CPCSEA nominee)  
PROP. SUHRITA PAUL

  
(Capt. R. R. Antti)

  
30/12/16

7 | Page



## Appendix B

### Residual solvent analysis of PLGA-PTH nanoparticles (OP)

**SOPHISTICATED INSTRUMENTATION CENTRE  
FOR APPLIED RESEARCH AND TESTING**  
(Sponsored by Department of Science & Technology, Govt. of India, New Delhi)  
**Sardar Patel Centre for Science & Technology**  
Charutar Vidya Mandal  
Vallabh Vidyanagar – 388120, Dist ANAND, GUJARAT, INDIA  
Phone: +91-2692-234966 FAX +91-2692-238355  
E-mail: [sicart\\_cvm@hotmail.com](mailto:sicart_cvm@hotmail.com) Website: [www.sicart.res.in](http://www.sicart.res.in)



Date: 07-05-15

#### Analysis Report

#### RESIDUAL SOLVENT ANALYSIS DONE ON GC-MS

Sr. No	SAMPLE NAME	DCM (PPM)
1	VB	0.11

## Appendix C

### Residual solvent analysis of PLGA-ETH nanoparticles (EPS1)

SOPHISTICATED INSTRUMENTATION CENTRE  
FOR APPLIED RESEARCH AND TESTING  
(Sponsored by Department of Science & Technology, Govt. of India, New Delhi)  
Sardar Patel Centre for Science & Technology  
Charutar Vidya Mandal  
Vallabh Vidyanagar – 388120, Dist ANAND, GUJARAT, INDIA  
Phone: +91-2692-234966 FAX +91-2692-238355  
E-mail: [sicart\\_cvm@hotmail.com](mailto:sicart_cvm@hotmail.com) Website: [www.sicart.res.in](http://www.sicart.res.in)



Date: 15-11-17

#### Analysis Report

#### RESIDUAL SOLVENT ANALYSIS DONE ON GC-HS

Sr. No	SAMPLE NAME	ACETONE (PPM)	DICHLOROMETHANE (PPM)
1	Nana particulate Drug	0.65	Not Detected

## List of Publications

### Publication from the present research work:

- ❖ **Debnath SK**, Saisivam S, Omri A. (2017) PLGA Ethionamide nanoparticles for pulmonary delivery: Development and *in-vivo* evaluation of dry powder inhaler. *J Pharma Biomed Ana.* 145, 854–859(Elsevier) (**Impact factor-3.255**).
- ❖ **Debnath SK**, Saisivam S, Debnath M, Omri A. (2018) Development and evaluation of Chitosan nanoparticles based dry powder inhalation formulations of Prothionamide. *PLOS One.* 3(1),1-12 (PubMed) (**Impact factor-2.86**).
- ❖ **Debnath SK**, Saisivam S, Debnath M. (2017) Validated UV-Spectrophotometric method for the Ethionamide estimation in bulk, tablet and nanoparticles. *Int J Drug Dev Res.* 9(1), 20-23(Scopus) (**Impact factor-0.5**).
- ❖ **Debnath SK**, Saisivam S and Debnath M. (2017) Development of Dry powder inhaler containing Prothionamide-PLGA nanoparticles optimized through statistical design: *In-vivo* study. *Open Nanomed J.* 04, 30-40 (Scopus).
- ❖ **Debnath SK**, Saisivam S, Dash DK, Debnath M. (2015) Development and validation of UV- spectrophotometric methods for quantitative estimation of Prothionamide in pure and pharmaceutical dosage forms. *Int Curr Pharm J.* 4(7), 402-404 (Saki Publishing Club).

### Papers Presented:

- ❖ Oral presentation on “Formulation and Characterization PLGA nanoparticles using Box-Behnken design in the management of Tuberculosis” in the national conference of “Pharma Innovative & Regulatory Considerations” held on 4th September, 2016 at Gupta College of Technological Sciences, Asansol, West Bengal, India (**ISBN no: 978-93-5267—071-0 hard copy**).